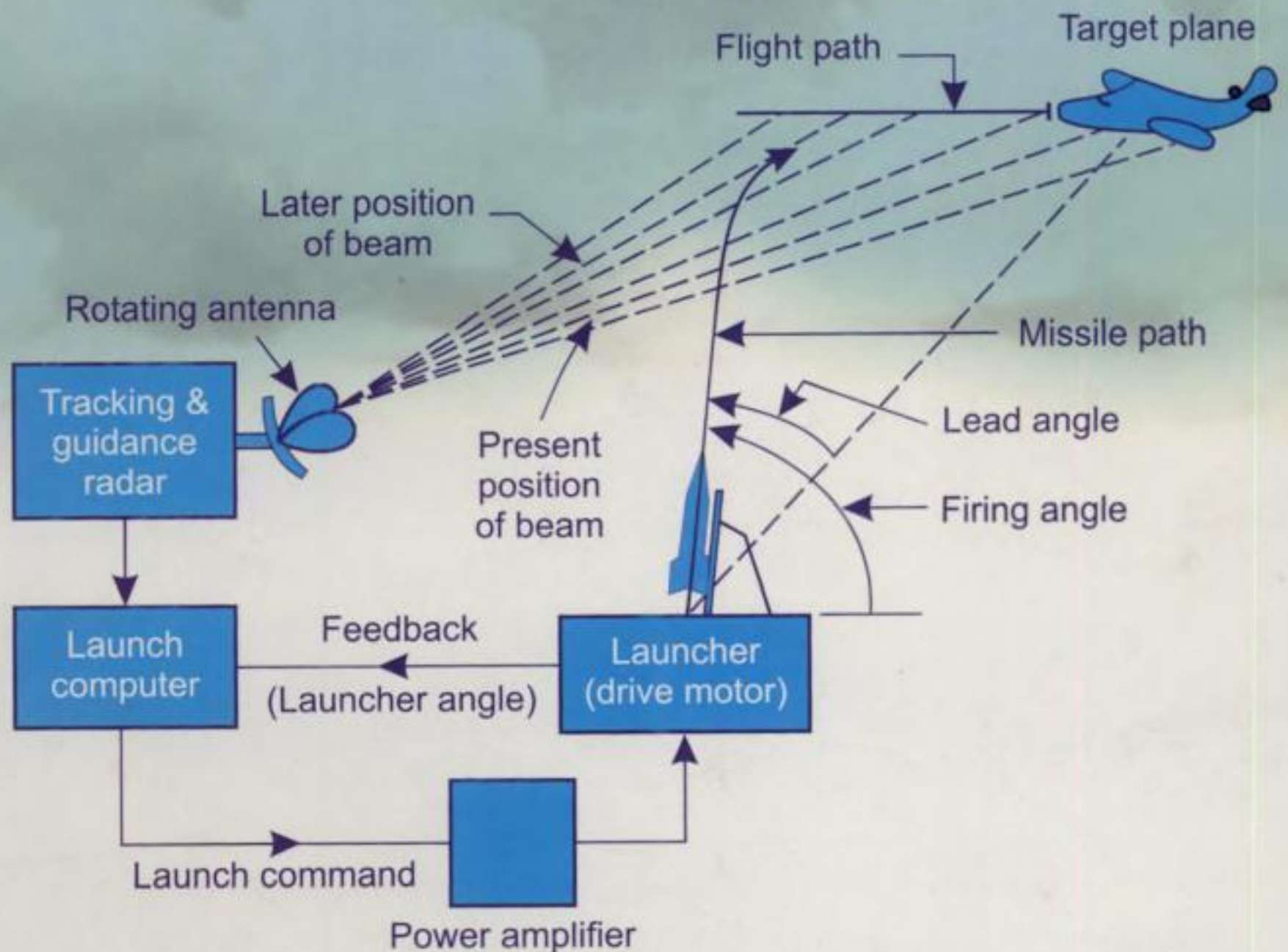


Control Systems Engineering

I.J. NAGRATH • M. GOPAL



NEW AGE INTERNATIONAL PUBLISHERS

Copyright © 2006, 1998, 1982, 1975, New Age International (P) Ltd., Publishers
Published by New Age International (P) Ltd., Publishers
First Edition : 1975
Fourth Edition : 2006

All rights reserved.

No part of this book may be reproduced in any form, by photostat, microfilm, xerography, or any other means, or incorporated into any information retrieval system, electronic or mechanical, without the written permission of the copyright owner.

ISBN : 81-224-1775-2

Rs. 695.00

C-05-07-261

Printed in India at Ajit Printers, Delhi.
Typeset at Goswami Printers, Delhi.

PUBLISHING FOR ONE WORLD

NEW AGE INTERNATIONAL (P) LIMITED, PUBLISHERS

(formerly Wiley Eastern Limited)

4835/24, Ansari Road, Daryaganj, New Delhi - 110002

Visit us at www.newagepublishers.com

CONTENTS

Preface to the Fourth Edition

v

Preface to the Third Edition

vii

1. INTRODUCTION 1-20

- 1.1 The Control System 2
- 1.2 Servomechanisms 6
- 1.3 History and Development of Automatic Control 10
- 1.4 Digital Computer Control 14
- 1.5 Application of Control Theory in Non-engineering Fields 18
- 1.6 The Control Problem 19

2. MATHEMATICAL MODELS OF PHYSICAL SYSTEMS 21-90

- 2.1 Introduction 22
- 2.2 Differential Equations of Physical Systems 24
- 2.3 Dynamics of Robotic Mechanisms 42
- 2.4 Transfer Functions 46
- 2.5 Block Diagram Algebra 54
- 2.6 Signal Flow Graphs 62
- 2.7 Illustrative Examples 72
- Problems 83

3. FEEDBACK CHARACTERISTICS OF CONTROL SYSTEMS 91-129

- 3.1 Feedback and Non-feedback Systems 92
- 3.2 Reduction of Parameter Variations by Use of Feedback 93
- 3.3 Control Over System Dynamics by Use of Feedback 97
- 3.4 Control of the Effects of Disturbance Signals by Use of Feedback 100
- 3.5 Linearizing Effect of Feedback 102
- 3.6 Regenerative Feedback 103
- 3.7 Illustrative Examples 104
- Problems 119

4. CONTROL SYSTEMS AND COMPONENTS 131-192

- 4.1 Introduction 132
- 4.2 Linear Approximation of Nonlinear Systems 133

- 4.3 Controller Components 134
- 4.4 Stepper Motors 154
- 4.5 Hydraulic Systems 163
- 4.6 Pneumatic Systems 177
- Problems 185

5. TIME RESPONSE ANALYSIS, DESIGN SPECIFICATIONS AND PERFORMANCE INDICES **193–268**

- 5.1 Introduction 194
- 5.2 Standard Test Signals 195
- 5.3 Time Response of First-order Systems 197
- 5.4 Time Response of Second-order Systems 199
- 5.5 Steady-state Errors and Error Constants 210
- 5.6 Effect of Adding a Zero to a System 214
- 5.7 Design Specifications of Second-order Systems 215
- 5.8 Design Considerations for Higher-order Systems 221
- 5.9 Performance Indices 223
- 5.10 Illustrative Examples 227
- 5.11 Robotic Control Systems 237
- 5.12 State Variable Analysis—Laplace Transform Technique 245
- 5.13 The Approximation of Higher-order Systems by Lower-order 248
- Problems 261

6. CONCEPTS OF STABILITY AND ALGEBRAIC CRITERIA **269–295**

- 6.1 The Concept of Stability 270
- 6.2 Necessary Conditions for Stability 275
- 6.3 Hurwitz Stability Criterion 277
- 6.4 Routh Stability Criterion 278
- 6.5 Relative Stability Analysis 287
- 6.6 More on the Routh Stability Criterion 290
- 6.7 Stability of Systems Modelled in State Variable Form 291
- Problems 293

7. THE ROOT LOCUS TECHNIQUE **297–343**

- 7.1 Introduction 298
- 7.2 The Root Locus Concepts 299
- 7.3 Construction Foot Loci 302
- 7.4 Root Contours 327
- 7.5 Systems with Transportation Lag 332
- 7.6 Sensitivity of the Roots of the Characteristic Equation 334
- 7.7 MATLAB: Tool for Design and Analysis of Control Systems—Appendix III 340
- Problems 340

8. FREQUENCY RESPONSE ANALYSIS	345–376
8.1 Introduction	346
8.2 Correlation between Time and Frequency Response	347
8.3 Polar Plots	352
8.4 Bode Plots	355
8.5 All-pass and Minimum-phase Systems	366
8.6 Experimental Determination of Transfer Functions	367
8.7 Log-magnitude versus Phase Plots	370
8.8 MATLAB: Tool for Design and Analysis of Control Systems—Appendix III	371
Problems	374
9. STABILITY IN FREQUENCY DOMAIN	377–423
9.1 Introduction	378
9.2 Mathematical Preliminaries	378
9.3 Nyquist Stability Criterion	381
9.4 Assessment of Relative Stability Using Nyquist Criterion	394
9.5 Closed-loop Frequency Response	409
9.6 Sensitivity Analysis in Frequency Domain	417
Problems	420
10. INTRODUCTION TO DESIGN	425–511
10.1 The Design Problem	426
10.2 Preliminary Considerations of Classical Design	428
10.3 Realization of Basic Compensators	435
10.4 Cascade Compensation in Time Domain	440
10.5 Cascade Compensation in Frequency Domain	459
10.6 Tuning of PID Controllers	477
10.7 Feedback Compensation	483
10.8 Robust Control System Design	490
Problems	506
11. DIGITAL CONTROL SYSTEMS	513–568
11.1 Introduction	514
11.2 Spectrum Analysis of Sampling Process	517
11.3 Signal Reconstruction	519
11.4 Difference Equations	519
11.5 The z -transform	521
11.6 The z -transfer Function (Pulse Transfer Function)	531
11.7 The Inverse z -transform and Response of Linear Discrete Systems	535
11.8 The z -transform Analysis of Sampled-data Control Systems	538
11.9 The z - and s -domain Relationship	548

11.10 Stability Analysis 549**11.11 Compensation Techniques 558**
Problems 564**12. STATE VARIABLE ANALYSIS AND DESIGN****569–640****12.1 Introduction 570****12.2 Concepts of State, State Variables and State Model 571****12.3 State Models for Linear Continuous-Time Systems 578****12.4 State Variables and Linear Discrete-Time Systems 596****12.5 Diagonalization 599****12.6 Solution of State Equations 604****12.7 Concepts of Controllability and Observability 617****12.8 Pole Placement by State Feedback 625****12.9 Observer Systems 632**
Problems 634**13. LIAPUNOV'S STABILITY ANALYSIS****641–662****13.1 Introduction 642****13.2 Liapunov's Stability Criterion 646****13.3 The Direct Method of Liapunov and the Linear System 650****13.4 Methods of Constructing Liapunov Functions for Nonlinear Systems 652**
Problems 660**14. OPTIMAL CONTROL SYSTEMS****663–712****14.1 Introduction 664****14.2 Parameter Optimization: Servomechanisms 665****14.3 Optimal Control Problems: Transfer Function Approach 673****14.4 Optimal Control Problems: State Variable Approach 684****14.5 The State Regulator Problem 688****14.6 The Infinite-time Regulator Problem 697****14.7 The Output Regulator and the Tracking Problems 702****14.8 Parameter Optimization: Regulators 704**
Problems 707**15. ADVANCES IN CONTROL SYSTEMS****713–763****15.1 Introduction 714****15.2 Adaptive Control 715****15.3 Fuzzy Logic Control 731****15.4 Neural Networks 749****Problems 760**

APPENDICES

Appendix-I Fourier and Laplace Transforms and Partial Fractions 766

Appendix-II Element of Matrix Analysis 775

Appendix-IV MATLAB : Tool for Design and Analysis of Control Systems 784

Appendix-V Final Value Theorem 796

Appendix-VI Proof of a Transformation 797

Appendix-VII Answers to Problems 800

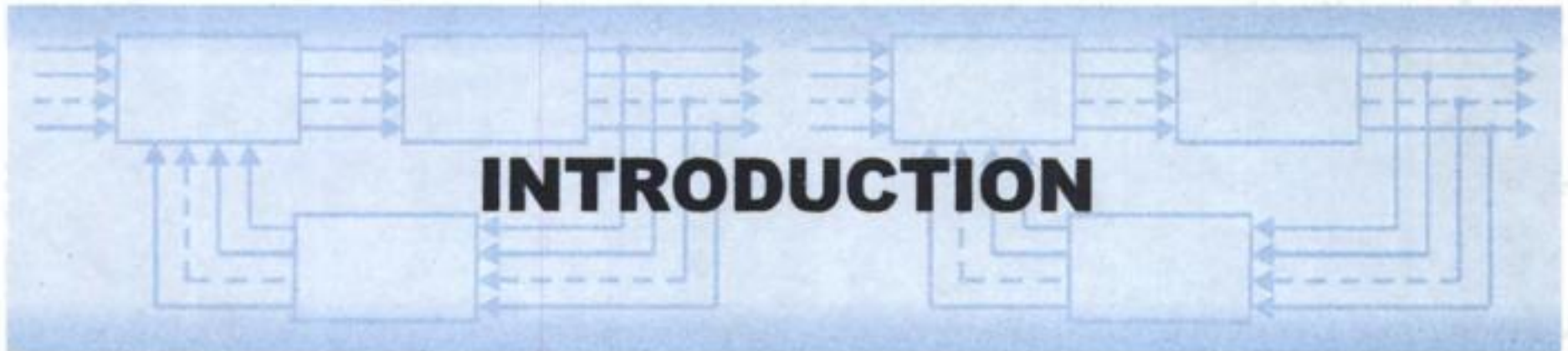
Bibliography 817-833

Index 835-843

1

INTRODUCTION

1



1.1 THE CONTROL SYSTEM

The control system is that means by which any quantity of interest in a machine, mechanism or other equipment is maintained or altered in accordance with a desired manner. Consider, for example, the driving system of an automobile. Speed of the automobile is a function of the position of its accelerator. The desired speed can be maintained (or a desired change in speed can be achieved) by controlling pressure on the accelerator pedal. This automobile driving system (accelerator, carburettor and engine-vehicle) constitutes a control system. Figure 1.1 shows the general diagrammatic representation of a typical control system. For the automobile driving system the input (command) signal is the force on the accelerator pedal which through linkages causes the carburettor valve to open (close) so as to increase or decrease fuel (liquid form) flow to the engine bringing the engine-vehicle speed (controlled variable) to the desired value.

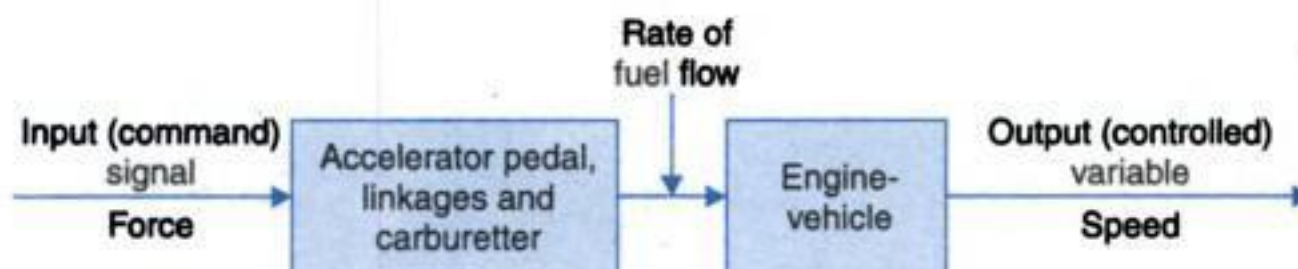


Fig. 1.1. The basic control system.

The diagrammatic representation of Fig. 1.1 is known as *block diagram* representation wherein each block represents an element, a plant, mechanism, device etc., whose inner details are not indicated. Each block has an input and output signal which are linked by a relationship characterizing the block. It may be noted that the signal flow through the block is unidirectional.

Closed-Loop Control

Let us reconsider the automobile driving system. The route, speed and acceleration of the automobile are determined and controlled by the driver by observing traffic and road conditions and by properly manipulating the accelerator, clutch, gear-lever, brakes and steering wheel, etc. Suppose the driver wants to maintain a speed of 50 km per hour (desired output). He accelerates the automobile to this speed with the help of the accelerator and then maintains it by holding the accelerator steady. No error in the speed of the automobile occurs so long as there are no gradients or other disturbances along the road. The actual speed of the automobile is measured by the speedometer and indicated on its dial. The driver reads the speed dial visually and compares the actual speed with the desired one mentally. If there is a deviation of speed from the desired speed, accordingly he takes the decision to increase or decrease the speed. The decision is executed by change in pressure of his foot (through muscular power) on the accelerator pedal.

These operations can be represented in a diagrammatic form as shown in Fig. 1.2. In contrast to the sequence of events in Fig. 1.1, the events in the control sequence of Fig. 1.2 follow a closed-loop, *i.e.*, the information about the instantaneous state of the output is feedback to the input and is used to modify it in such a manner as to achieve the desired output. It is on account of this basic difference that the system of Fig. 1.1 is called an *open-loop system*, while the system of Fig. 1.2 is called a *closed-loop system*.

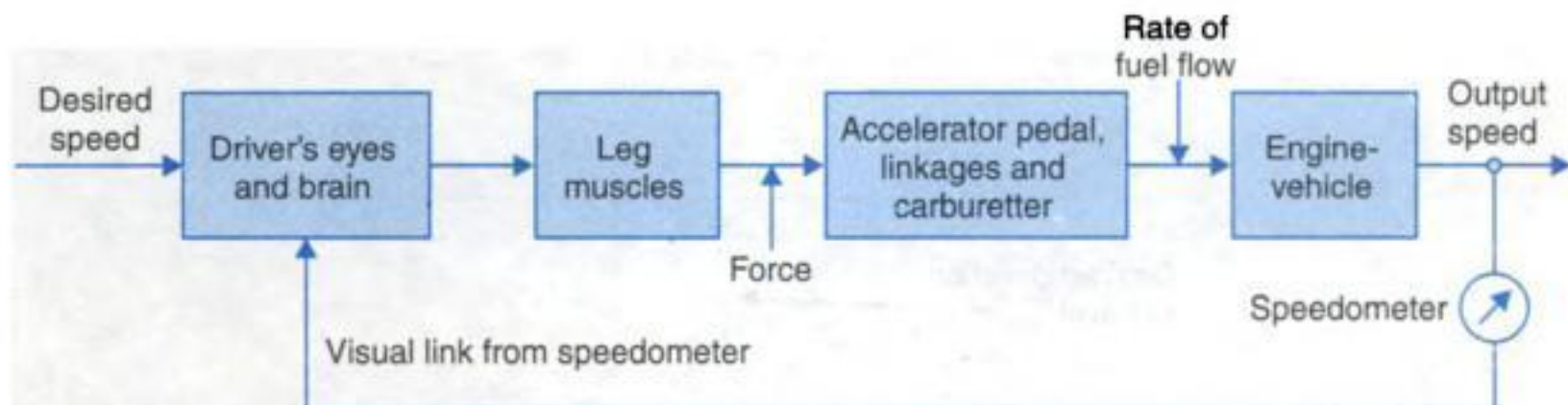


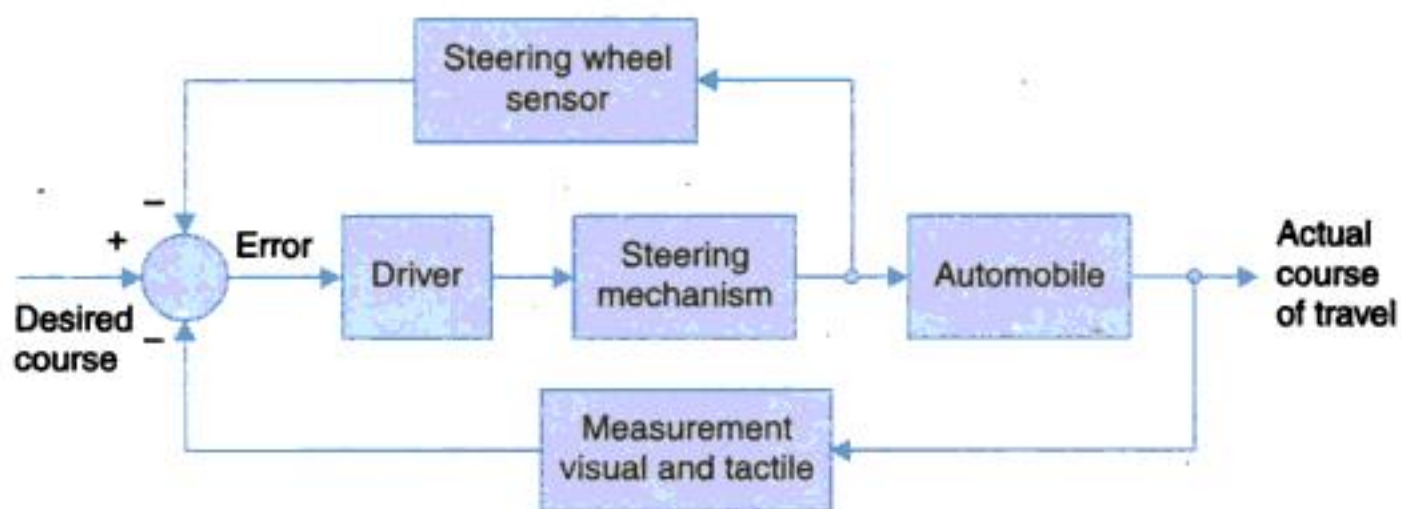
Fig. 1.2. Schematic diagram of a manually controlled closed-loop system.

Let us investigate another control aspect of the above example of an automobile (engine vehicle) say its steering mechanism. A simple block diagram of an automobile steering mechanism is shown in Fig. 1.3(a). The driver senses visually and by tactile means (body movement) the error between the actual and desired directions of the automobile as in Fig. 1.3(b). Additional information is available to the driver from the feel (sensing) of the steering wheel through his hand(s), these informations constitute the feedback signal(s) which are interpreted by driver's brain, who then signals his hand to adjust the steering wheel accordingly. This again is an example of a closed-loop system where human visual and tactile measurements constitute the feedback loop.

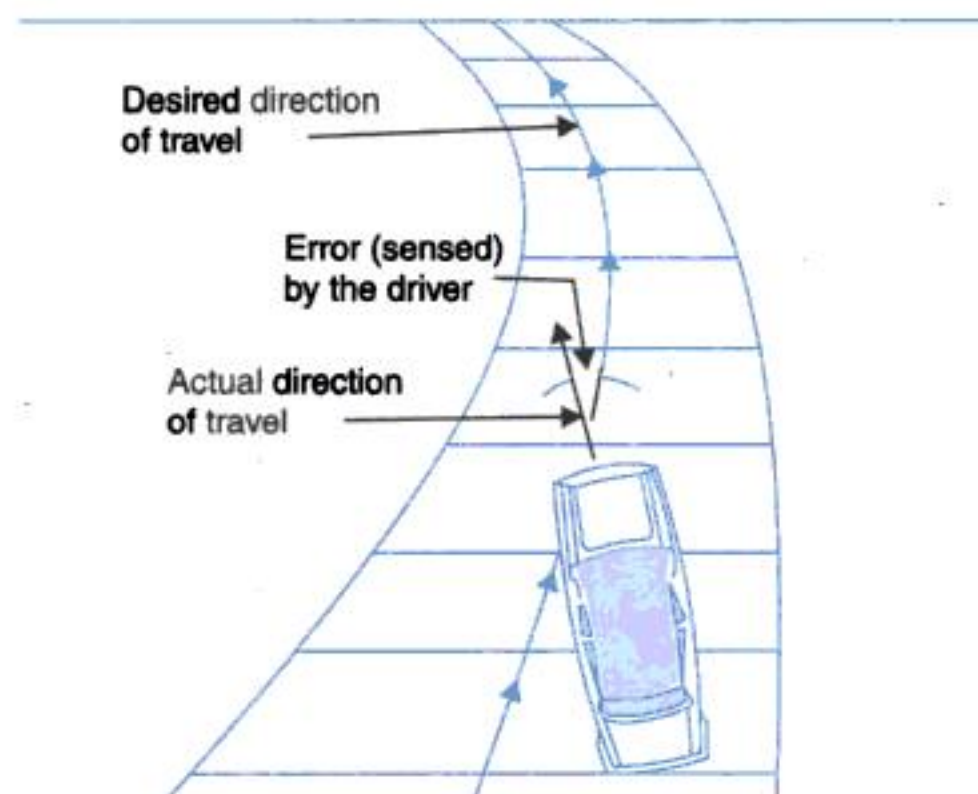
In fact unless human being(s) are not left out of in a control system study practically all control systems are a sort of closed-loop system (with intelligent measurement and sensing loop or there may indeed be several such loops).

Systems of the type represented in Figs. 1.2 and 1.3 involve continuous manual control by a human operator. These are classified as *manually controlled systems*. In many complex

and fast-acting systems, the presence of human element in the control loop is undesirable because the system response may be too rapid for an operator to follow or the demand on operator's skill may be unreasonably high. Furthermore, some of the systems, e.g., missiles, are self-destructive and in such systems human element must be excluded. Even in situations where manual control could be possible, an economic case can often be made out for reduction of human supervision. Thus in most situations the use of some equipment which performs the same intended function as a continuously employed human operator is preferred. A system incorporating such an equipment is known as *automatic control system*. In fact in most situations an automatic control system could be made to perform intended functions better than a human operator, and could further be made to perform such functions as would be impossible for a human operator.



(a)



(b)

Fig. 1.3. (a) Automobile steering control system. (b) The driver uses the difference between the actual and desired direction of travel to adjust the steering wheel accordingly.

The general block diagram of an automatic control system which is characterised by a feedback loop, is shown in Fig. 1.4. An error detector compares a signal obtained through

feedback elements, which is a function of the output response, with the reference input. Any difference between these two signals constitutes an error or actuating signal, which actuates the control elements. The control elements in turn alter the conditions in the plant (controlled member) in such a manner as to reduce the original error.

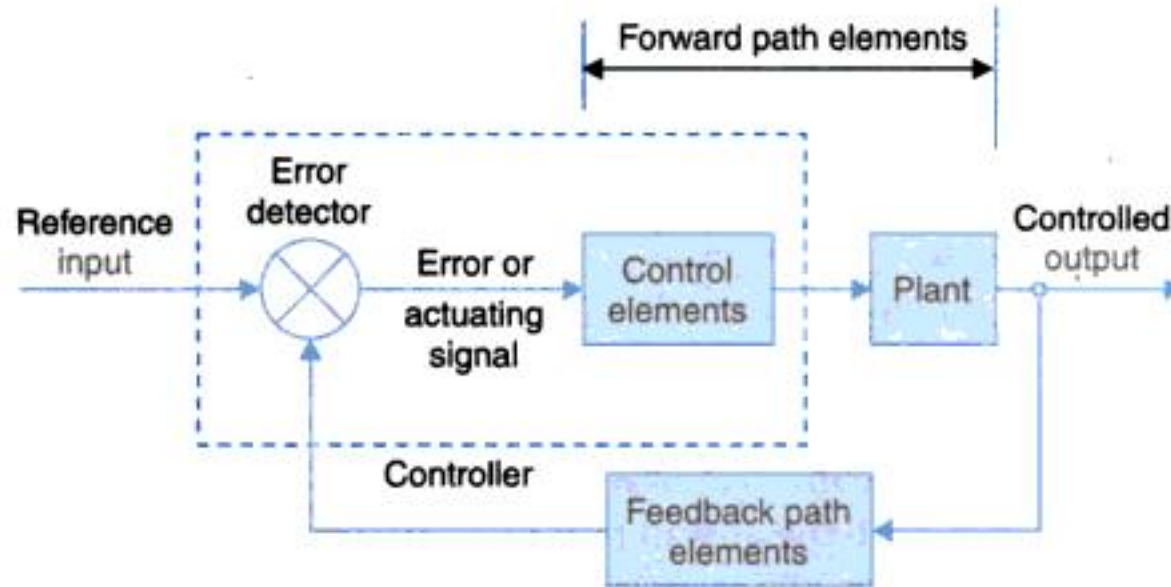


Fig. 1.4. General block diagram of an automatic control system.

In order to gain a better understanding of the interactions of the constituents of a control system, let us discuss a simple tank level control system shown in Fig. 1.5. This control system can maintain the liquid level h (controlled output) of the tank within accurate tolerance of the

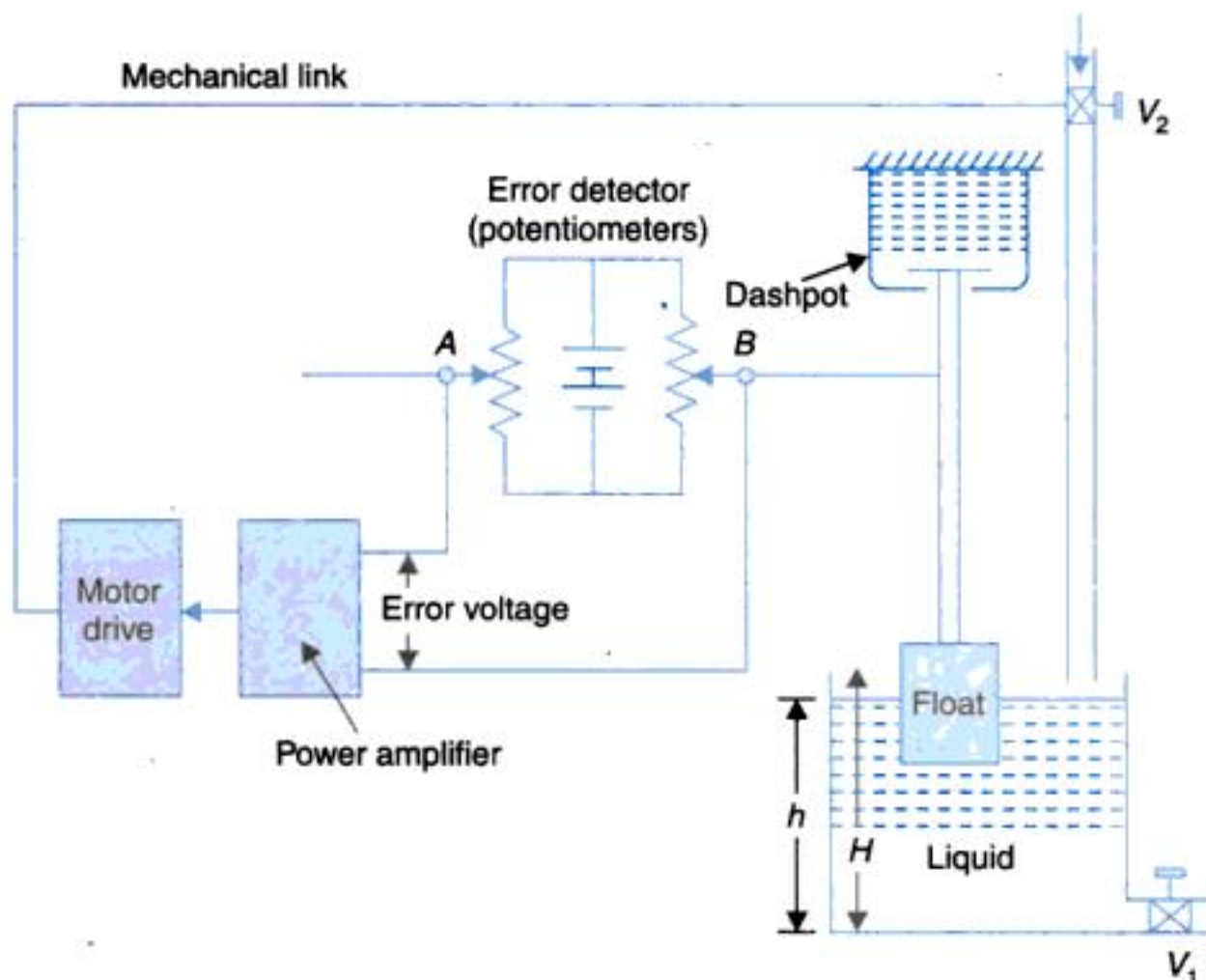


Fig. 1.5. Automatic tank-level control system.

desired liquid level even though the output flow rate through the valve V_1 is varied. The liquid level is sensed by a float (feedback path element), which positions the slider arm B on a

potentiometer. The slider arm A of another potentiometer is positioned corresponding to the desired liquid level H (the reference input). When the liquid level rises or falls, the potentiometers (error detector) give an error voltage (error or actuating signal) proportional to the change in liquid level. The error voltage actuates the motor through a power amplifier (control elements) which in turn conditions the plant (*i.e.*, decreases or increases the opening of the valve V_2) in order to restore the desired liquid level. Thus the control system automatically attempts to correct any deviation between the actual and desired liquid levels in the tank.

Open-Loop Control

As stated already, any physical system which does not automatically correct for variation in its output, is called an open-loop system. Such a system may be represented by the block diagram of Fig. 1.6. In these systems the output remains constant for a constant input signal provided the external conditions remain unaltered. The output may be changed to any desired value by appropriately changing the input signal but variations in external conditions or internal parameters of the system may cause the output to vary from the desired value in an uncontrolled fashion. The open-loop control is, therefore, satisfactory only if such fluctuations can be tolerated or system components are designed and constructed so as to limit parameter variations and environmental conditions are well-controlled.

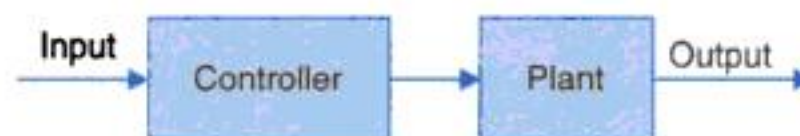


Fig. 1.6. General block diagram of open-loop system.

It is important to note that the fundamental difference between an open and closed-loop control system is that of feedback action. Consider, for example, a traffic control system for regulating the flow of traffic at the crossing of two roads. The system will be termed open-loop if red and green lights are put on by a timer mechanism set for predetermined fixed intervals of time. It is obvious that such an arrangement takes no account of varying rates of traffic flowing to the road crossing from the two directions. If on the other hand a scheme is introduced in which the rates of traffic flow along both directions are measured (some distance ahead of the crossing) and are compared and the difference is used to control the timings of red and green lights, a closed-loop system (feedback control) results. Thus the concept of feedback can be usefully employed to traffic control.

Unfortunately, the feedback which is the underlying principle of most control systems, introduces the possibility of undesirable system oscillations (hunting). Detailed discussion of feedback principle and the linked problem of stability are dealt with later in the book.

1.2 SERVOMECHANISMS

In modern usage the term *servomechanism* or servo is restricted to feedback control systems in which the controlled variable is mechanical position or time derivatives of position, *e.g.*, velocity and acceleration.

A servo system used to position a load shaft is shown in Fig. 1.7 in which the driving motor is geared to the load to be moved. The output (controlled) and desired (reference) positions θ_C and θ_R respectively are measured and compared by a potentiometer pair whose output voltage v_E is proportional to the error in angular position $\theta_E = \theta_R - \theta_C$. The voltage $v_E = K_p \theta_E$ is amplified and is used to control the field current (excitation) of a dc generator which supplies the armature voltage to the drive motor.

To understand the operation of the system assume $K_p = 100$ volts/rad and let the output shaft position be 0.5 rad. Corresponding to this condition, the slider arm B has a voltage of +50 volts. Let the slider arm A be also set at +50 volts. This gives zero actuating signal ($v_E = 0$). Thus the motor has zero output torque so that the load stays stationary at 0.5 rad.

Assume now that the new desired load position is 0.6 rad. To achieve this, the arm A is placed at +60 volts position, while the arm B remains instantaneously at +50 volts position. This creates an actuating signal of +10 volts, which is a measure of lack of correspondence between the actual load position and the commanded position. The actuating signal is amplified and fed to the servo motor which in turn generates an output torque which repositions the load. The system comes to a standstill only when the actuating signal becomes zero, *i.e.*, the arm B and the load reach the position corresponding to 0.6 rad (+60 volts position).

Consider now that a load torque T_L is applied at the output as indicated in Fig. 1.7. This will require a steady value of error voltage v_E which acting through the amplifier, generator, motor and gears will counterbalance the load torque. This would mean that a steady error will exist between the input and output angles. This is unlike the case when there is no load torque and consequently the angle error is zero. In control terminology, such loads are known as load disturbances and system has to be designed to keep the error to these disturbances within specified limits.

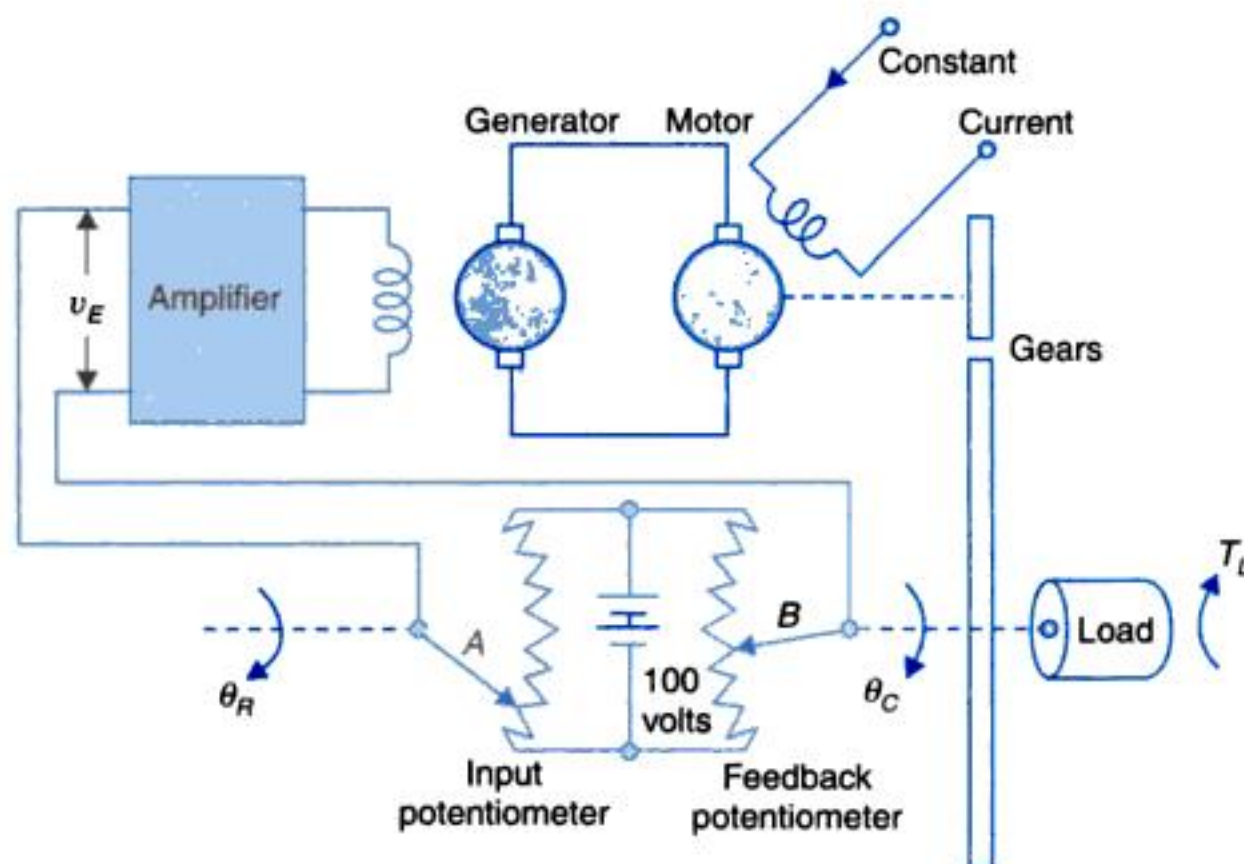


Fig. 1.7. A position control system.

By opening the feedback loop *i.e.*, disconnecting the potentiometer B , the reader can easily verify that any operator acting as part of feedback loop will find it very difficult to adjust θ_c to a desired value and to be able to maintain it. This further demonstrates the power of a negative feedback (hardware) loop.

The position control systems have innumerable applications, namely, machine tool position control, constant-tension control of sheet rolls in paper mills, control of sheet metal thickness in hot rolling mills, radar tracking systems, missile guidance systems, inertial guidance, roll stabilization of ships, etc. Some of these applications will be discussed in this book.

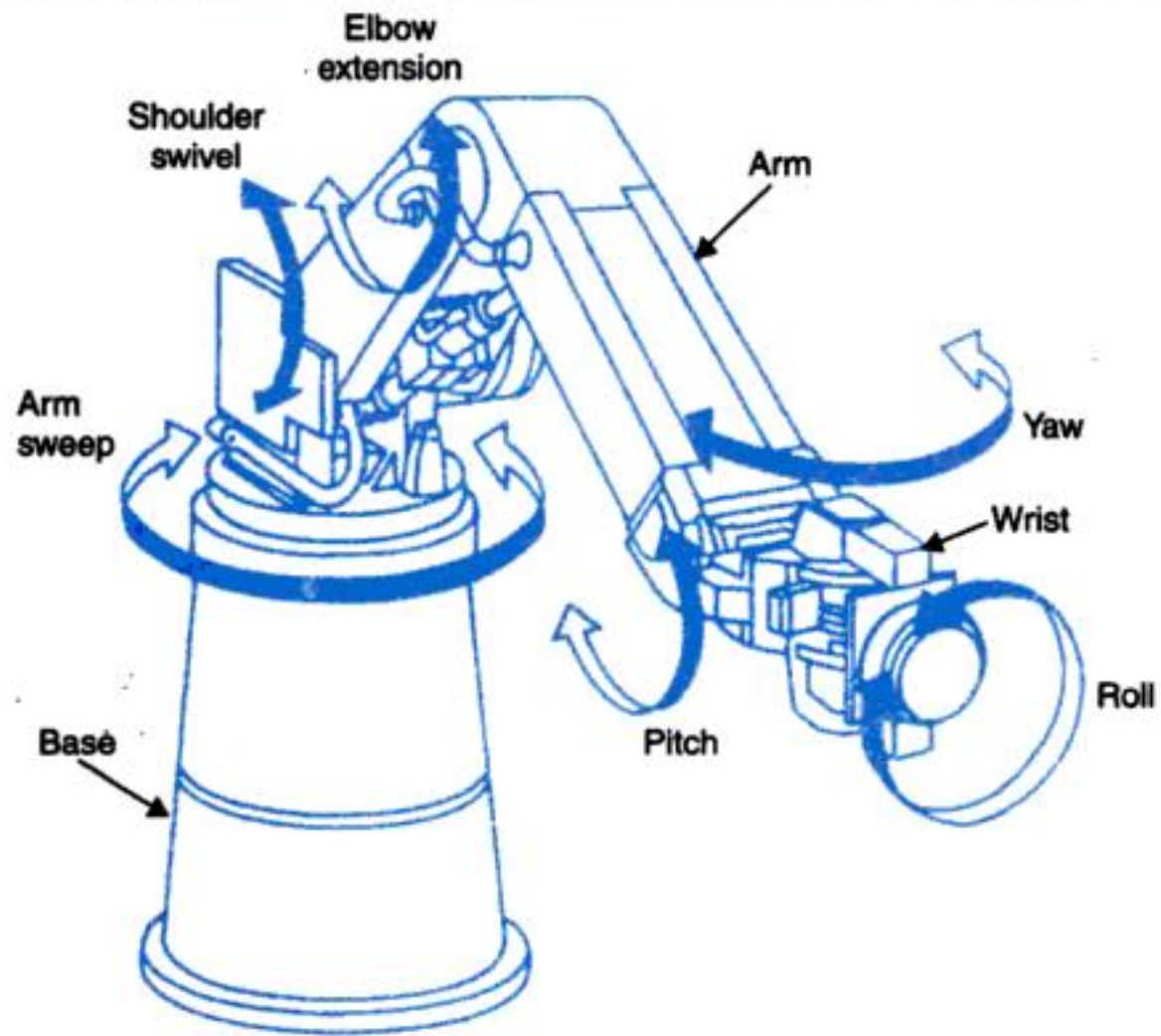
Robotics

Advances in servo mechanism has led to the development of the new field of control and automation, the robots and robotology. A robot is a mechanism devised to perform repetitive tasks which are tiresome for a human being or tasks to be performed in a hazardous environment say in a radioactive area. Robots are as varied as the tasks that can be imagined to be performed by them. Great strides are being made in this field with the explosion in the power of digital computer, interfacing and software tools which have brought to reality the application of vision and artificial intelligent for devising more versatile robots and increased applications of robotology in industrial automation. In fact in replacing a human being for a repetitive and/or hazardous task the robots can perform the task at a greater speed (so increased productivity) and higher precision (better quality and higher reliability of the product or service).

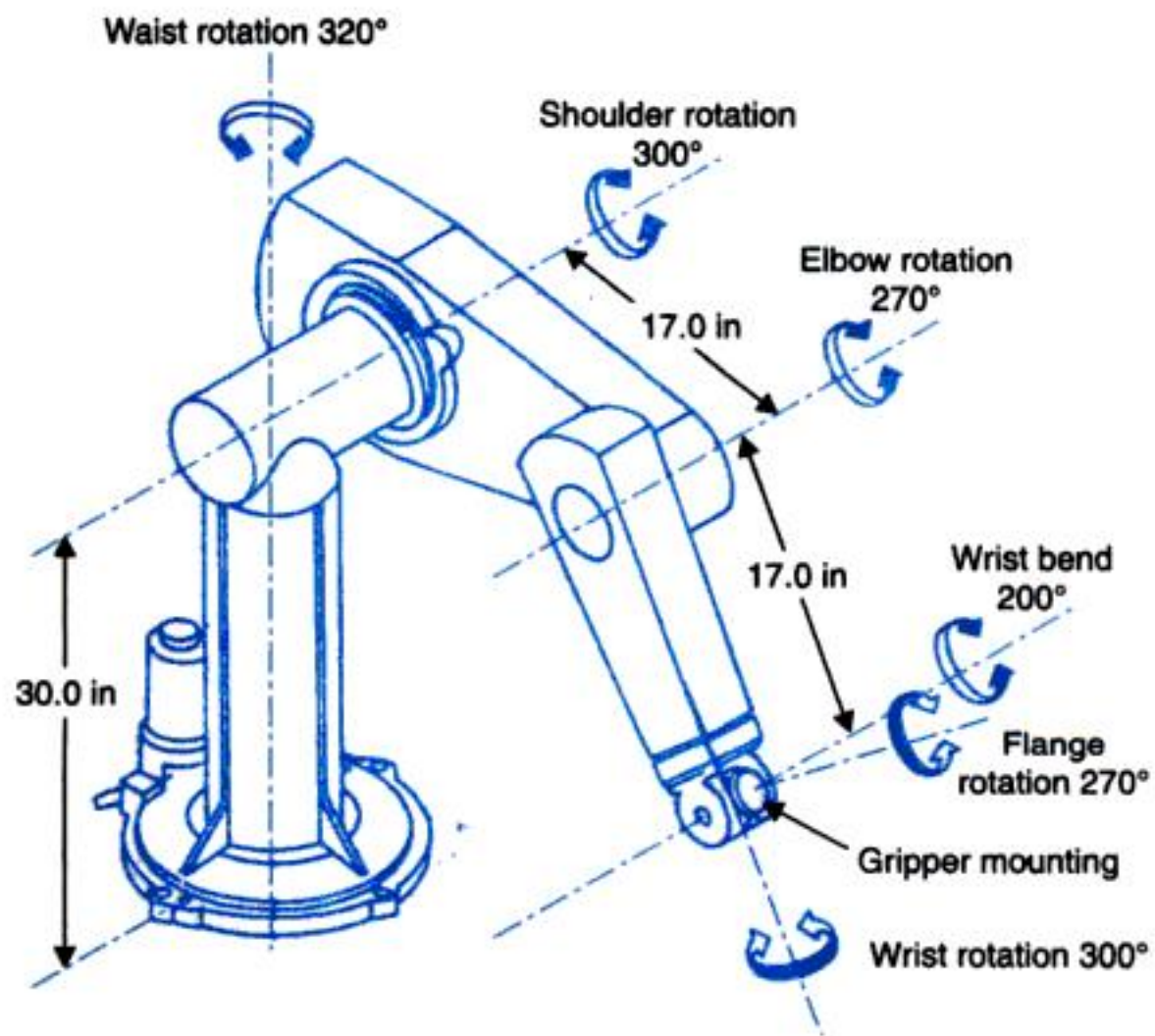
We shall describe here a robot manipulator arm as an example. The arm is devised to preform some of the tasks performed by a human arm (shoulder, elbow and wrist). Imitation of some of the elementary functions of hand is carried out by an end effector with three degrees of freedom in general (roll, yaw and pitch). The robot arm is a set of serial links with the beginning of each link jointed with the end of the preceeding link in form of a revolute joint (for relative rotary motion between the two links) or a prismatic joint (for relative translatory motion). The number of joints determine the degrees of freedom of the arm.

Figures 1.8 (a) and (b) show the schematic diagrams of two kinds of manipulator arms. To reduce joint inertia and gravity loading the drive motors are located in the base and the joints are belt driven. For a programmed trajectory of the manipulator tip, each joint requires not only a controlled angular (or translatory) motion but also controlled velocity, acceleration and torque. Further the mechanism complexity is such that the effective joint inertia may change by as much as 300% during a trajectory traversal. The answer to such control complexity is the computer control. The versatility of high-speed on-line computer further permits the sophistication of control through computer vision, learning of new tasks and other intelligent functions. Manipulators can perform delicate (light) as well as heavy tasks; for example, manipulator can pick up objects weighing hundreds of kilograms and position them with an accuracy of a centimeter or better.

Using robots (specially designed for broken-down tasks) an assembly line in a manufacturing process can be speeded up with added quality and reliability of the end product. Example can be cited of watch industry in Japan where as many as 150 tasks on the assembly are robot executed.



(a)



(b)

Fig. 1.8. (a) Cincinnati Milacron T³ robot arm (b) PUMA 560 series robot arm.

For flexible manufacturing units mobile automations (also called AGV (automated guided vehicle)) have been devised and implemented which are capable of avoiding objects while travelling through a room or industrial plant.

1.3 HISTORY AND DEVELOPMENT OF AUTOMATIC CONTROL

It is instructive to trace brief historical development of automatic control. Automatic control systems did not appear until the middle of eighteenth century. The first automatic control system, the fly-ball governor, to control the speed of steam engines, was invented by James Watt in 1770. This device was usually prone to hunting. It was about hundred years later that Maxwell analyzed the dynamics of the fly-ball governor.

The schematic diagram of a speed control system using a fly-ball governor is shown in Fig. 1.9. The governor is directly geared to the output shaft so that the speed of the fly-balls is proportional to the output speed of the engine. The position of the throttle lever sets the desired speed. The lever pivoted as shown in Fig. 1.9 transmits the centrifugal force from the fly-balls to the bottom of the lower seat of the spring. Under steady conditions, the centrifugal force of the fly-balls balances the spring force* and the opening of flow control valve is just sufficient to maintain the engine speed at the desired value.

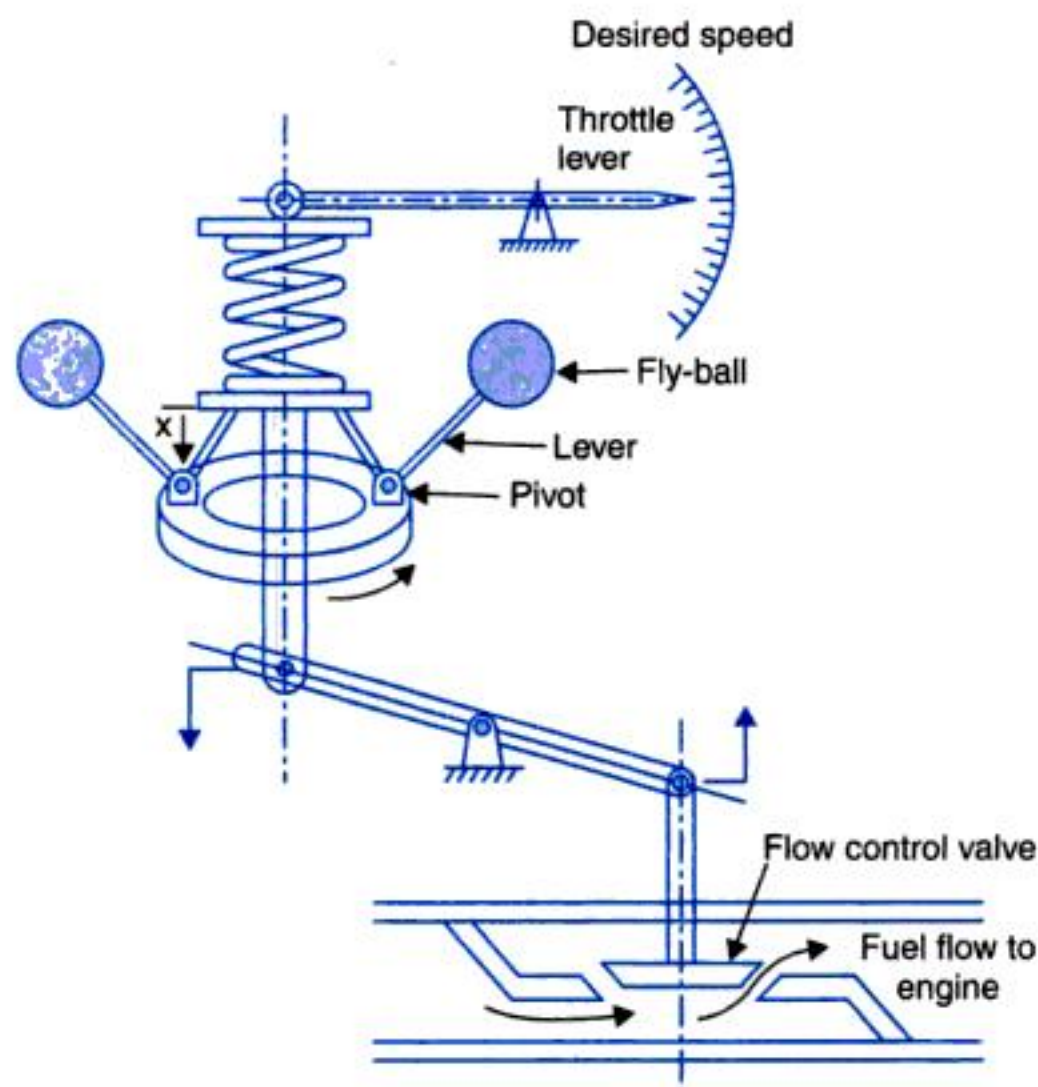


Fig. 1.9. Speed control system.

* The gravitational forces are normally negligible compared to the centrifugal force.

If the engine speed drops below the desired value, the centrifugal force of the fly-balls decreases, thus decreasing the force exerted on the bottom of the spring, causing x to move downward. By lever action, this results in wider opening of the control valve and hence more fuel supply which increases the speed of the engine until equilibrium is restored. If the speed increases, the reverse action takes place.

The change in desired engine speed can be achieved by adjusting the setting of throttle lever. For a higher speed setting, the throttle lever is moved up which in turn causes x to move downward resulting in wider opening of the fuel control valve with consequent increase of speed. The lower speed setting is achieved by reverse action.

The importance of positioning heavy masses like ships and guns quickly and precisely was realized during the World War I. In early 1920, Minorsky performed the classic work on the automatic steering of ships and positioning of guns on the shipboards.

A date of significance in automatic control systems is that of Hazen's work in 1934. His work may possibly be considered as a first struggling attempt to develop some general theory for servomechanisms. The word 'servo' has originated with him.

Prior to 1940 automatic control theory was not much developed and for most cases the design of control systems was indeed an art. During the decade of 1940's, mathematical and analytical methods were developed and practised and control engineering was established as an engineering discipline in its own rights. During the World War II it became necessary to design and construct automatic aeroplane pilots, gun positioning systems, radar tracking systems and other military equipments based on feedback control principle. This gave a great impetus to the automatic control theory.

The missile launching and guidance system of Fig. 1.10 is a sophisticated example of military applications of feedback control. The target plane is sighted by a rotating radar antenna which then locks in and continuously tracks the target. Depending upon the position and velocity of the plane as given by the radar output data, the launch computer calculates the firing angle in terms of a launch command signal, which when amplified through a power amplifier drives the launcher (drive motor). The launcher angular position is feedback to the launch computer and the missile is triggered as soon as the error between the launch command signal and the missile firing angle becomes zero. After being fired the missile enters the radar beam which is tracking the target. The control system contained within the missile now receives a guidance signal from the beam which automatically adjusts the control surface of the missile such that the missile rides along the beam, finally homing on to the target.

It is important to note that the actual missile launching and guidance system is far more complex requiring control of gun's bearing as well as elevation. The simplified case discussed above illustrates the principle of feedback control.

The industrial use of automatic control has tremendously increased since the World War II. Modern industrial processes such as manufacture and treatment of chemicals and metals are now automatically controlled.

A simple example of an automatically controlled industrial process is shown in Fig. 1.11. This is a scheme employed in paper mills for reeling paper sheets. For best results the paper sheet must be pulled on to the wind-up roll at nearly constant tension. A reduction in tension

will produce a loose roll, while an increase in tension may result in tearing of the paper sheet. If reel speed is constant, the linear velocity of paper and hence its tension increases, as the wind-up roll diameter increases. Tension control may be achieved by suitably varying the reel speed.

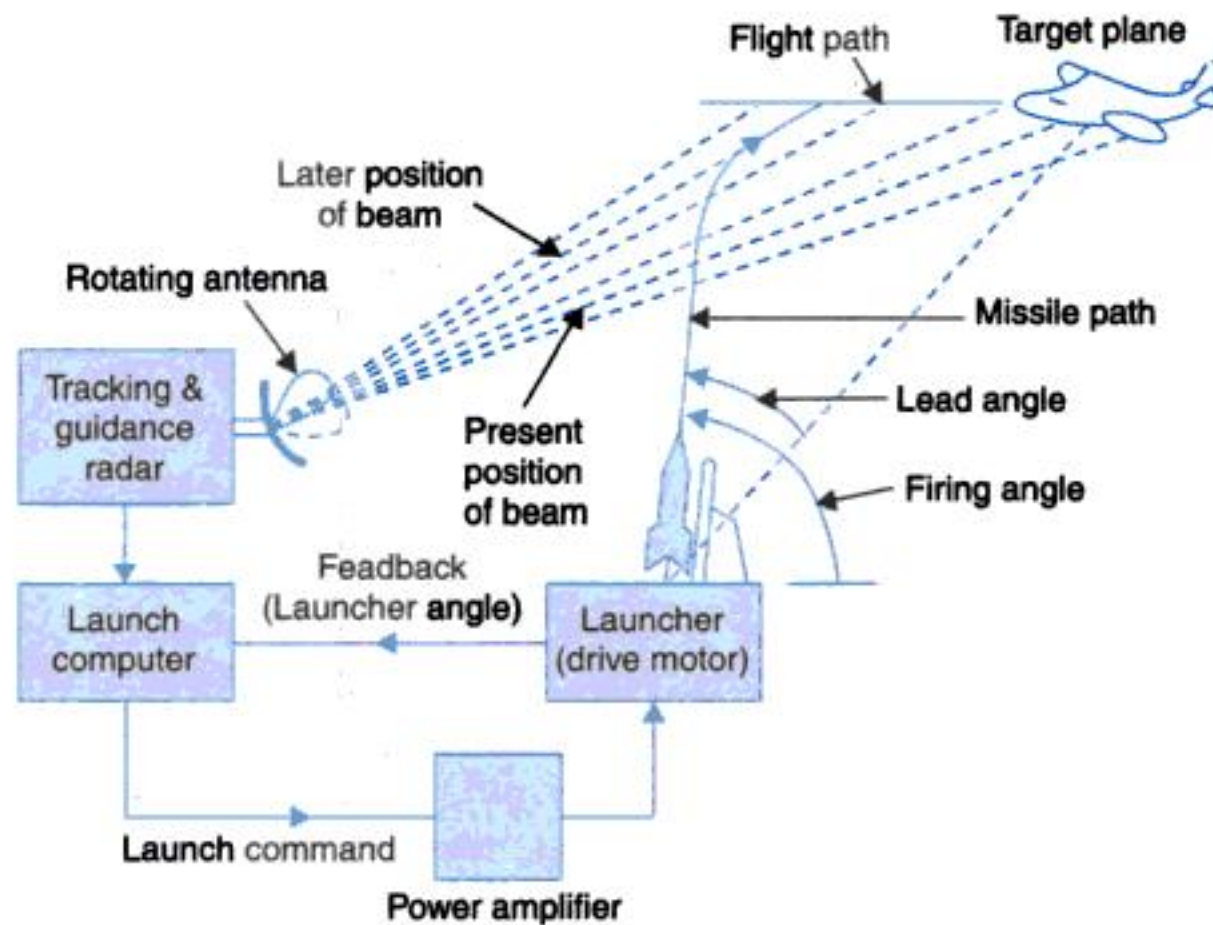


Fig. 1.10. Missile launching and guidance system.

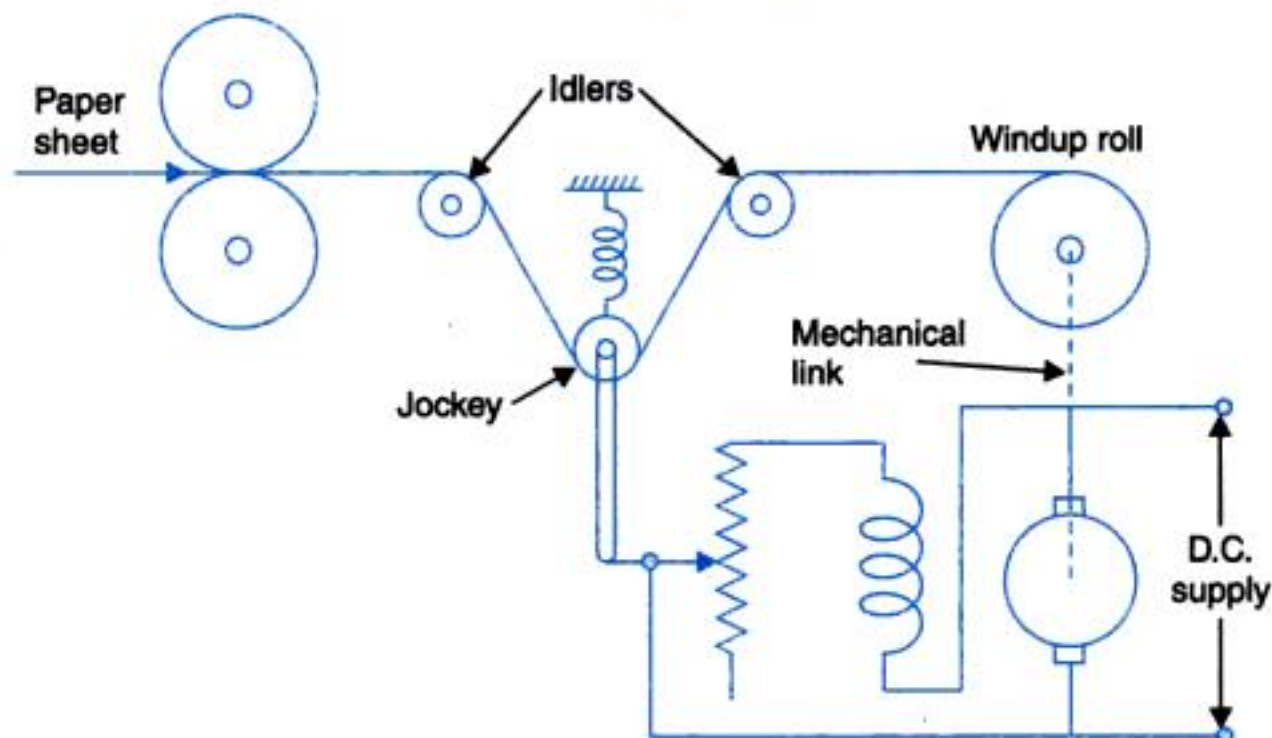


Fig. 1.11. A constant tension reeling system.

In the scheme shown in Fig. 1.11 the paper sheet passes over two idling and one jockey roll. The jockey roll is constrained to vertical motion only with its weight supported by paper tension and spring. Any change in tension moves the jockey in vertical direction, upward for increased tension and downward for decreased tension. The vertical motion of the jockey is used to change the field current of the drive motor and hence the speed of wind-up roll which adjusts the tension.

Another example of controlled industrial processes is a batch chemical reactor shown in Fig. 1.12. The reactants are initially charged into the reaction vessel of the batch reactor and are then agitated for a certain period of time to allow the reaction to take place. Upon completion of the reaction, the products are discharged.

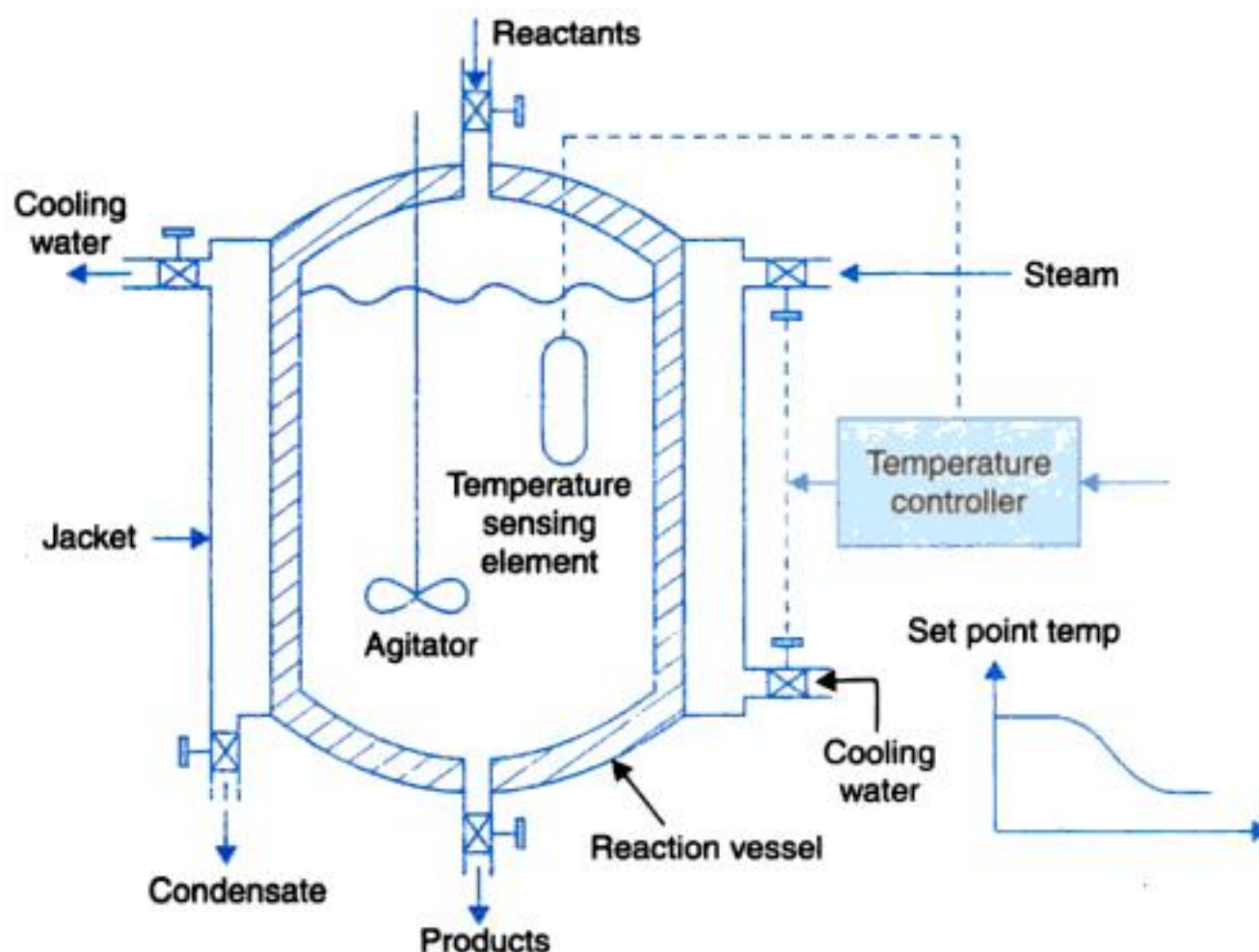


Fig. 1.12. A batch chemical process.

For a specific reaction there is an optimum temperature profile according to which the temperature of the reactor mass should be varied to obtain best results. Automatic temperature control is achieved by providing both steam and cooling water jackets for heating or cooling the reactor mass (cooling is required to remove exothermic heat of reaction during the period the reaction proceeds vigorously). During the heating phase, the controller closes the water inlet valve and opens and controls the steam inlet valve while the condensate valve is kept open. Reverse action takes place during the cooling phase.

Control engineering has enjoyed tremendous growth during the years since 1955. Particularly with the advent of analog and digital computers and with the perfection achieved in computer field, highly sophisticated control schemes have been devised and implemented. Furthermore, computers have opened up vast vistas for applying control concepts to non-engineering fields like business and management. On the technological front fully automated computer control schemes have been introduced for electric utilities and many complex industrial processes with several interacting variables particularly in the chemical and metallurgical processes.

A glorious future lies ahead for automation wherein computer control can run our industries and produce our consumer goods provided we can tackle with equal vigour and success the socio-economic and resource depletion problems associated with such sophisticated degree of automation.

1.4 DIGITAL COMPUTER CONTROL

In some of the examples of control systems of high level of complexity (robot manipulator of Fig. 1.9 and missile launching and guidance system of Fig. 1.11) it is seen that such control systems need a digital computer as a control element to digitally process a number of input signals to generate a number of control signals so as to manipulate several plant variables. In these control systems signals in certain parts of the plant are in analog form *i.e.*, continuous functions of the time variable, while the control computer handles data only in digital (or discrete) form. This requires signal discretization and analog-to-digital interfacing in form of *A/D* and *D/A* converters.

To begin with we will consider a simple form the digital control system known as sampled-data control system. The block diagram of such a system with single feedback loop is illustrated in Fig. 1.13 wherein the sampler samples the error signal $e(t)$ every T seconds. The sampler is an electronic switch whose output is the discretized version of the analog error signal and is a train of pulses of the sampling frequency with the strength of each pulse being that of the error signal at the beginning of the sampling period. The sampled signal is passed through a data hold and is then filtered by a digital filter in accordance with the control algorithm. The smoothed out control signal $u(t)$ is then used to manipulate the plant. The smoothed out control signal $u(t)$ is then used to manipulate the plant.

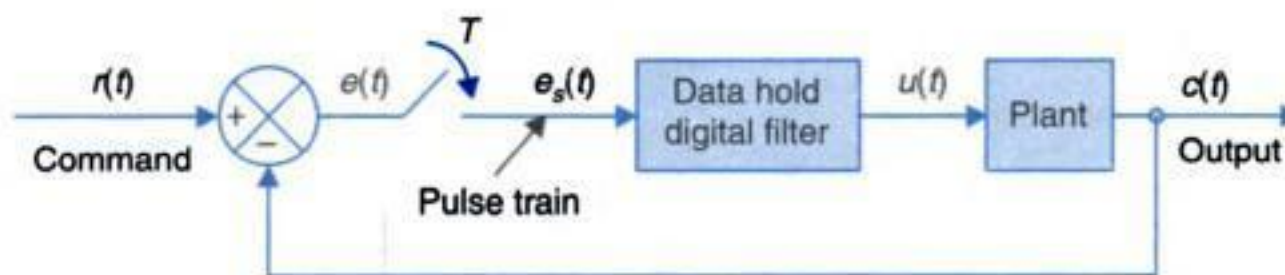


Fig. 1.13. Block diagram of a sampled-data control system.

It is seen above that computer control is needed in large and complex control schemes dealing with a number of input, output variables and feedback channels. This is borne out by the examples of Fig. 1.9 and 1.11. Further in chemical plants, a number of variables like temperatures, pressures and fluid flows have to be controlled after the information on throughput, its quality and its constitutional composition has been analyzed on-line. Such systems are referred to as multivariable control systems whose general block diagram is shown in Fig. 1.14.

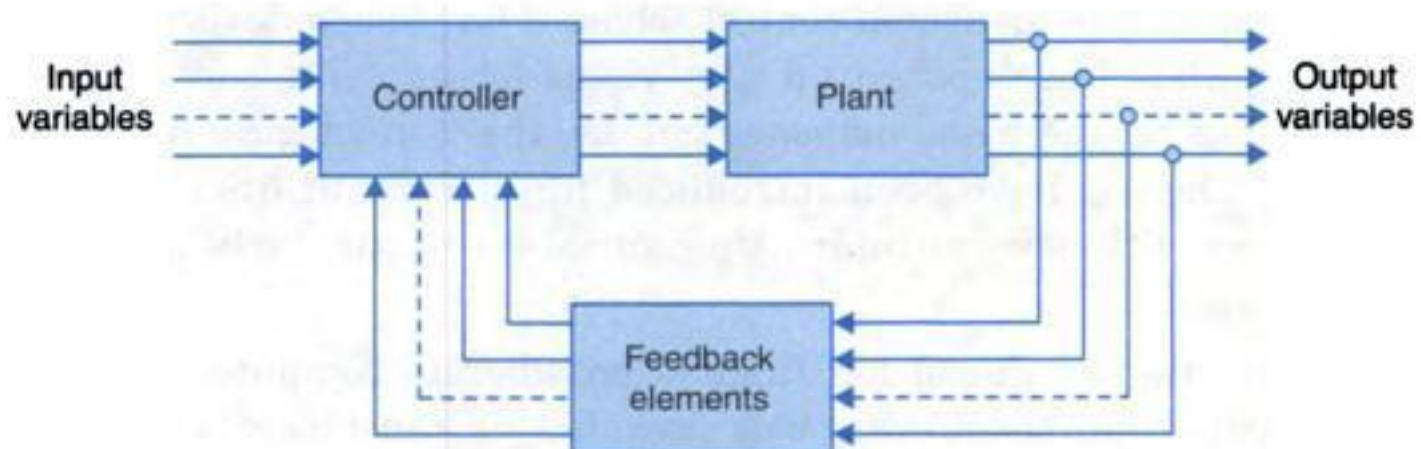


Fig. 1.14. General block diagram of a multivariable control system.

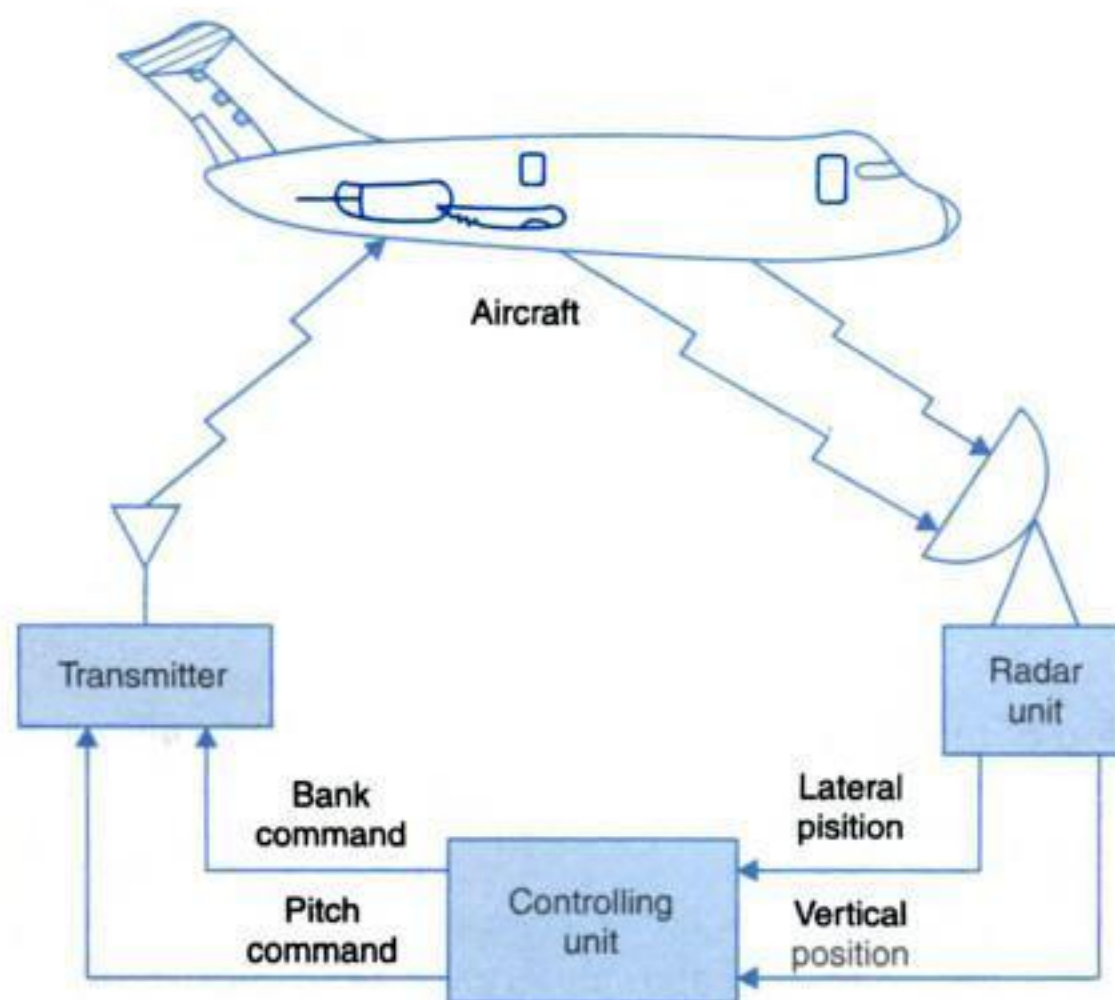
Where a few variable are to be controlled with a limited number of commands and the control algorithm is of moderate complexity and the plant process to be controlled is at a given physical location, a general purpose computer chip, the microprocessor (μP) is commonly employed. Such systems are known as μP -based control systems. Of course at the input/output interfacing A/D and D/A converter chips would be needed.

For large systems a central computer is employed for simultaneous control of several subsystems wherein certain hierarchies are maintained keeping in view the overall system objectives. Additional functions like supervisory control, fault recording, data logging etc, also become possible. We shall advance three examples of central computer control.

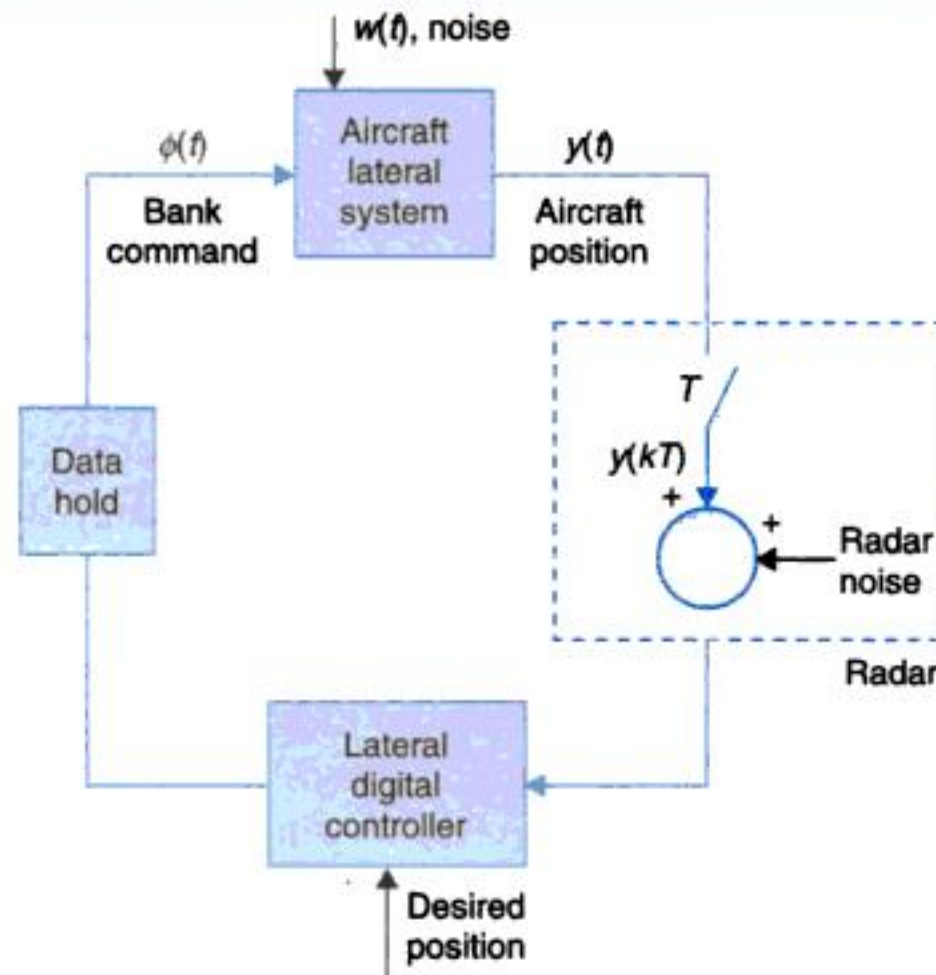
Automatic Aircraft Landing System

The automatic aircraft landing system in a simplified form is depicted in Fig. 1.15(a). The system consists of three basic parts: the aircraft, the radar unit and the controlling unit. The radar unit measures the approximate vertical and lateral positions of the aircraft, which are then transmitted to the controlling unit. From these measurements, the controlling unit calculates appropriate pitch and bank commands. These commands are then transmitted to the aircraft autopilots which in turn cause the aircraft to respond.

Assuming that the lateral control system and the vertical control system are independent (decoupled), we shall consider only the lateral control system whose block diagram is given in Fig. 1.15(b). The aircraft lateral position, $y(t)$, is the lateral distance of the aircraft from the extended centerline of the landing area on the deck of the aircraft carrier. The control system attempts to force $y(t)$ to zero. The radar unit measures $y(kT)$ is the sampled value of $y(t)$, with



(a) Schematic



(b) Lateral landing system.

Fig. 1.15. Automatic aircraft landing system.

$T = 0.05\text{s}$ and $k = 0, 1, 2, 3 \dots$. The digital controller processes these sampled values and generates the discrete bank command constant at the last value received until the next value is received. Thus the bank commands is updated every $t = 0.05\text{s}$, which is called the sampling period. The aircraft responds to the bank command, which changes the lateral position $y(t)$.

It may be noted here that the lateral digital controller must be able to compute the control signal within one sampling period. This is the computational stringency imposed on the central computer in all on-line computer control schemes.

Two unwanted inputs called **disturbances** appear into the system. These are (i) wind gust affecting the position of the aircraft and (ii) radar noise present in measurement of aircraft position. These are labelled as disturbance input in Figure 1.15(b). The system has to be designed to mitigate the effects of disturbance input so that the aircraft lands within acceptable limits of lateral accuracy.

Rocket Autopilot System

As another illustration of computer control, let us discuss an autopilot system which steers a rocket vehicle in response to radioed command. Figure 1.16 shows a simplified block diagram representation of the system.

The state of motion of the vehicle (velocity, acceleration) is fed to the control computer by means of motion sensors (gyros, accelerometers). A position pick-off feeds the computer with the information about rocket engine angle displacement and hence the direction in which the vehicle is heading. In response to heading-commands from the ground, the computer generates a signal which controls the hydraulic actuator and in turn moves the engine.

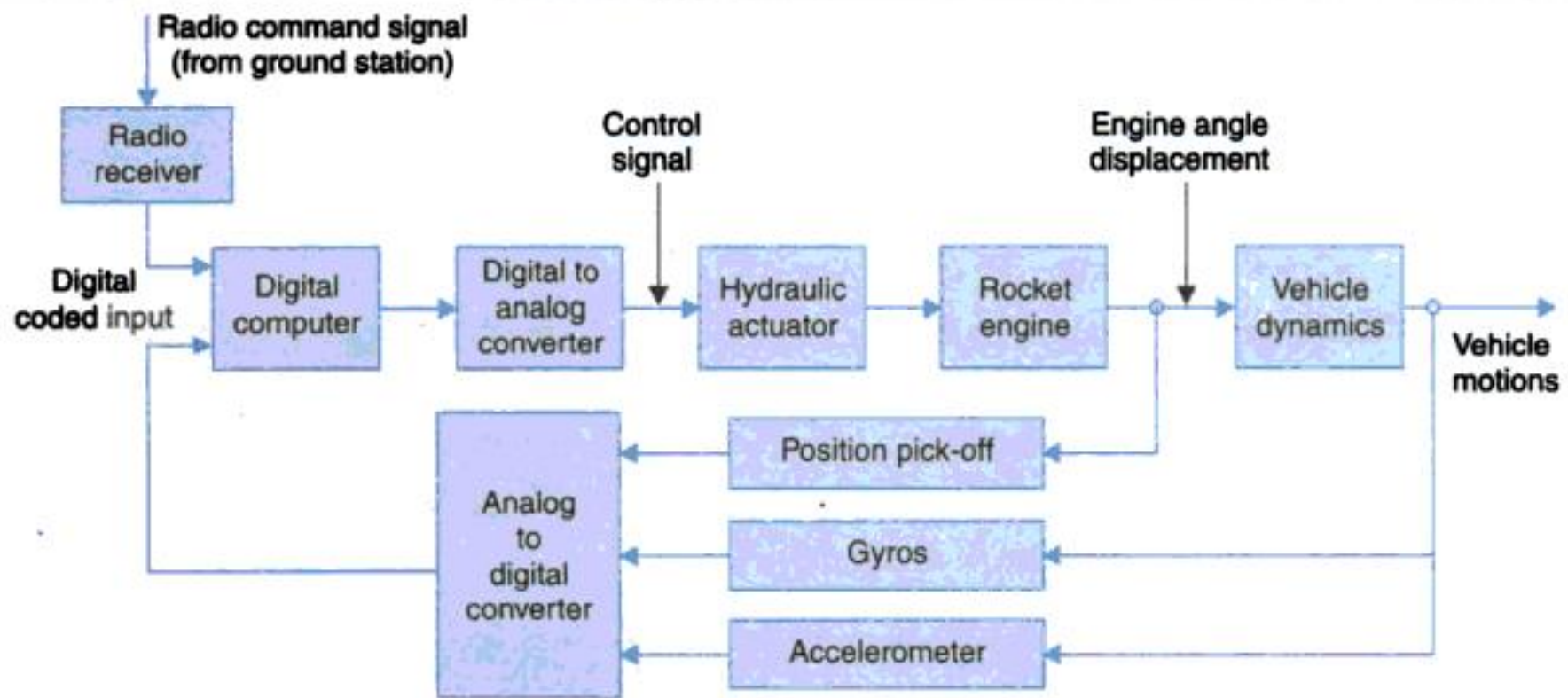


Fig. 1.16. A typical autopilot system.

Coordinated Boiler-Generator Control

Coordinated control system for a boiler-generator unit by a central computer is illustrated by the simplified schematic block diagram of Fig. 1.17. Various signal inputs to the control computer from suitable sensor blocks are:

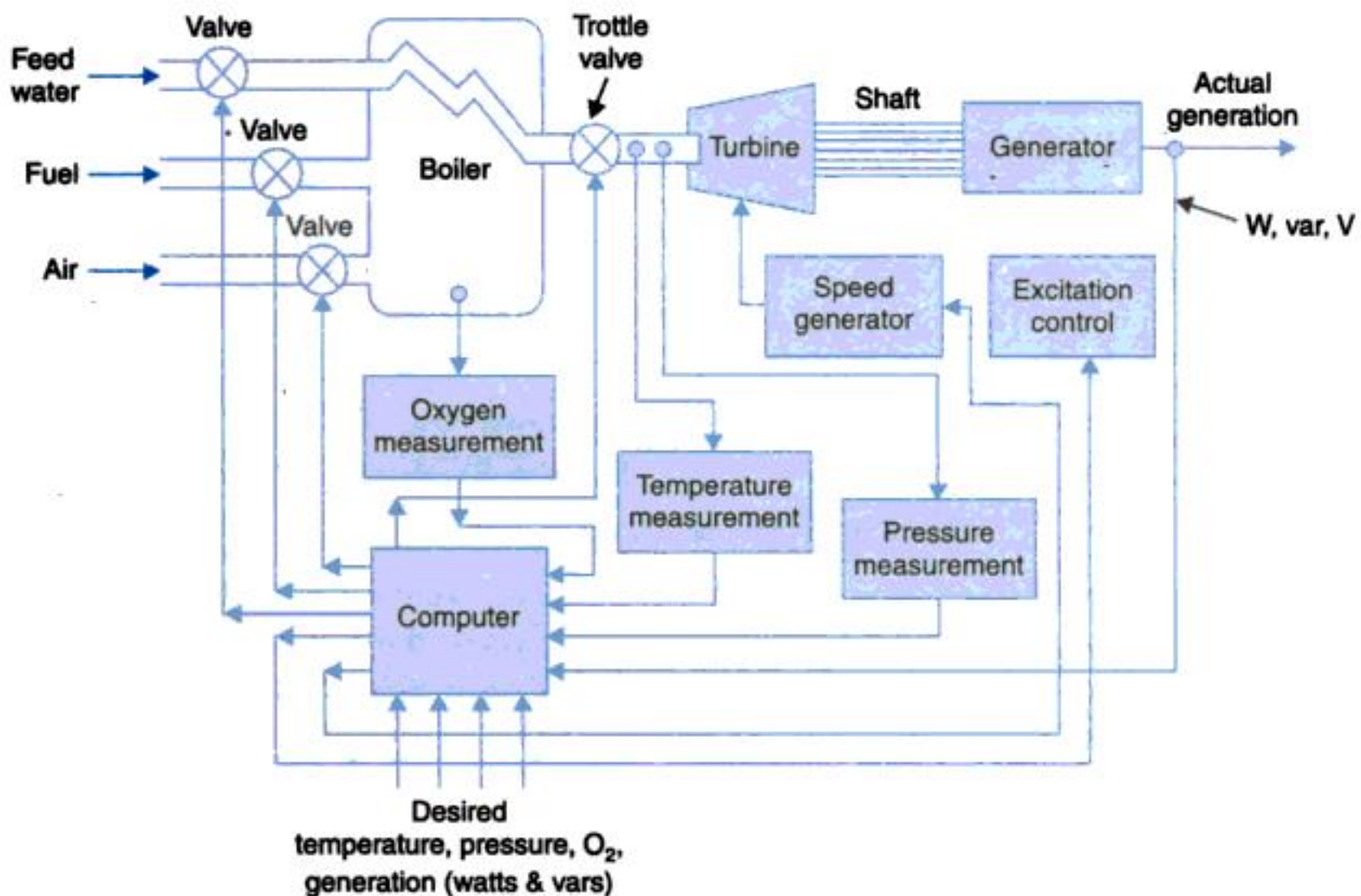


Fig. 1.17. Coordinated control for a boiler-generator.

- Watts, vars, line voltage.
- Temperature and pressure of steam inlet to turbine.
- Oxygen content in furnace air.

These inputs are processed by the control computer by means of a coordinated control algorithm to produce control signals as below:

- Signal to adjust throttle valve. This controls the rate of steam input to turbine and so controls the generator output.
- Signals to adjust fuel, feed water and air in accordance with the throttle valve opening.
- Signals which adjust generator excitation so as to control its var output (which indirectly controls the terminal voltage of the generator).

1.5 APPLICATION OF CONTROL THEORY IN NON-ENGINEERING FIELDS

We have considered in previous sections a number of applications which highlight the potentialities of automatic control to handle various engineering problems. Although control theory originally evolved as an engineering discipline, due to universality of the principles involved it is no longer restricted to engineering confines in the present state of art. In the following paragraphs we shall discuss some examples of control theory as applied to fields like economics, sociology and biology.

Consider an economic inflation problem which is evidenced by continually rising prices. A model of the vicious price-wage inflationary cycle, assuming simple relationship between wages, product costs and cost of living is shown in Fig 1.18. The economic system depicted in this figure is found to be a positive feedback system.

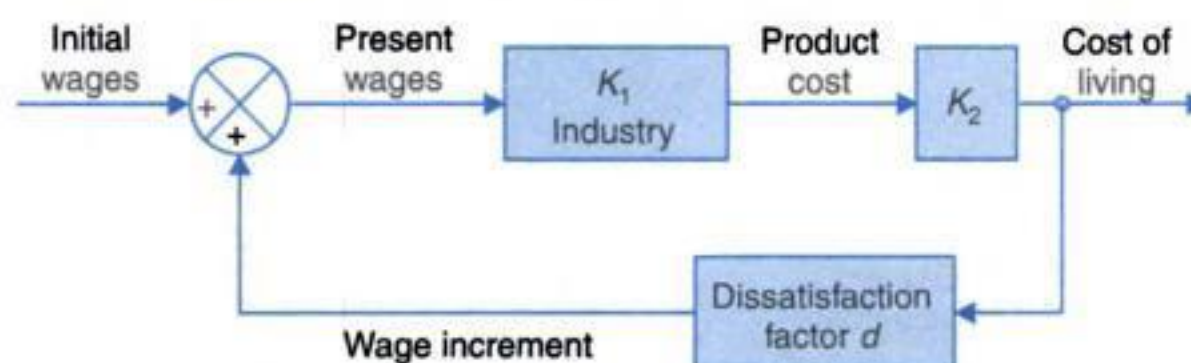


Fig. 1.18. Economic inflation dynamics.

To introduce yet another example of non-engineering application of control principles, let us discuss the dynamics of epidemics in human beings and animals. A normal healthy community has a certain rate of daily contacts C . When an epidemic disease affects this community the social pattern is altered as shown in Fig. 1.19. The factor K_1 contains the

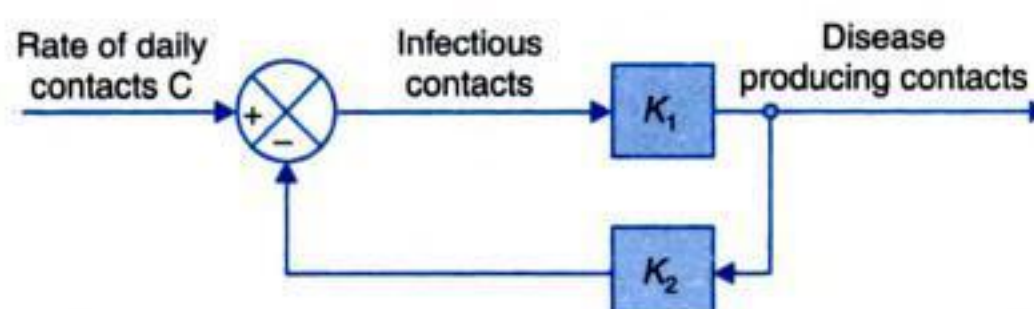


Fig. 1.19. Block diagram representation of epidemic dynamics.

statistical fraction of infectious contacts that actually produce the disease, while the factor K_2 accounts for the isolation of the sick people and medical immunization. Since the isolation and immunization reduce the infectious contacts, the system has a negative feedback loop.

In medical field, control theory has wide applications, such as temperature regulation, neurological, respiratory and cardiovascular controls. A simple example is the automatic anaesthetic control. The degree of anaesthesia of a patient undergoing operation can be measured from encephalograms. Using control principles anaesthetic control can be made completely automatic, thereby freeing the anaesthetist from observing constantly the general condition of the patient and making manual adjustments.

The examples cited above are somewhat over-simplified and are introduced merely to illustrate the universality of control principles. More complex and complete feedback models in various non-engineering fields are now available. This area of control is under rapid development and has a promising future.

1.6 THE CONTROL PROBLEM

In the above account the field of control systems has been surveyed with a wide variety of illustrative examples including those of some nonphysical systems. The basic block diagram of a control system given in Fig. 1.3 is reproduced in Fig. 1.20 wherein certain alternative block and signal nomenclature are introduced.

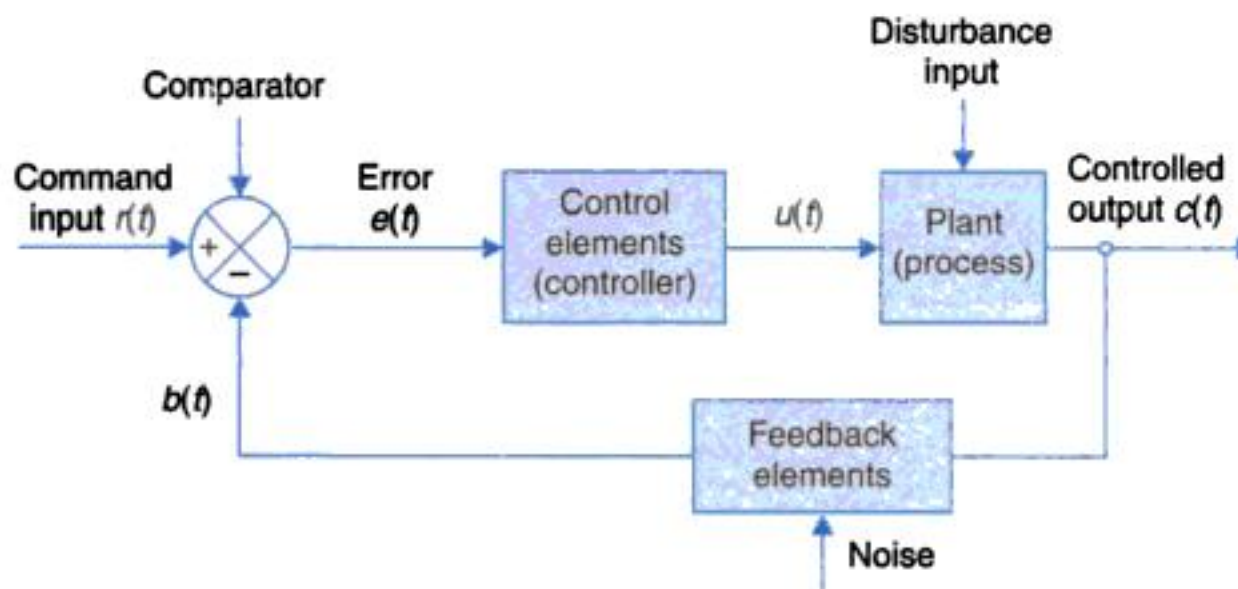


Fig. 1.20. The basic control loop.

Further the figure also indicates the presence of the disturbance input (load disturbance) in the plant and noise input in feedback element (noise enters in the measurement process; see example of automatic aircraft landing system in Fig. 1.15). This basic control loop with negative feedback responds to reduce the error between the command input (desired output) and the controlled output.

Further as we shall see in later chapters that negative feedback has several benefits like reduction in effects of disturbances input, plant nonlinearities and changes in plant parameters. A multivariable control system with several feedback loops essentially follows the same logic. In some mechanical systems and chemical processes a certain signal also is directly

input to the controller elements particularly to counter the effect of load disturbance (not shown in the figure).

Generally, a controller (or a filter) is required to process the error signal such that the overall system satisfies certain criteria specifications. Some of these criteria are:

1. Reduction in effect of disturbance signal.
2. Reduction in steady-state errors.
3. Transient response and frequency response performance.
4. Sensitivity to parameter changes.

Solving the control problem in the light of the above criteria will generally involve following steps:

1. Choice of feedback sensor(s) to get a measure of the controlled output.
2. Choice of actuator to drive (manipulate) the plant like opening or closing a valve, adjusting the excitation or armature voltage of a motor.
3. Developing mathematical models of plant, sensor and actuator.
4. Controller design based on models developed in step 3 and the specified criteria.
5. Simulating system performance and fine tuning.
6. Iterate the above steps, if necessary.
7. Building the system or its prototype and testing.

The criteria and steps involved in system design and implementation and tools of analysis needed of this, form the subject matter of the later chapters.

2

MATHEMATICAL MODELS OF PHYSICAL SYSTEMS

2

MATHEMATICAL MODELS OF PHYSICAL SYSTEMS

2.1 INTRODUCTION

A *physical system* is a collection of physical objects connected together to serve an objective. Examples of a physical system may be cited from laboratory, industrial plant or utility services—an electronic amplifier composed of many components, the governing mechanism of a steam turbine or a communications satellite orbiting the earth are all examples of physical systems. A more general term *system* is used to describe a combination of components which may not all be physical, e.g., biological, economic, socio-economic or management systems. Study in this book will be mainly restricted to physical systems though a few examples of general type systems will also be introduced.

No physical system can be represented in its full physical intricacies and therefore idealizing assumptions are always made for the purpose of analysis and synthesis of systems. An idealized physical system is called a *physical model*. A physical system can be modelled in a number of ways depending upon the specific problem to be dealt with and the desired accuracy. For example, an electronic amplifier may be modelled as an interconnection of linear lumped elements, or some of these may be pictured as nonlinear elements in case the stress is on distortion analysis. A communication satellite may be modelled as a point, a rigid body or a flexible body depending upon the type of study to be carried out. As idealizing assumptions are gradually removed for obtaining a more accurate model, a point of diminishing return is reached, i.e., the gain in accuracy of representation is not commensurate with the increased complexity of the computation required. In fact, beyond a certain point there may indeed be an undetermined loss in accuracy of representation due to flow of errors in the complex computations.

Once a physical model of a physical system is obtained, the next step is to obtain a *mathematical model* which is the mathematical representation of the physical model through

use of appropriate physical laws. Depending upon the choice of variables and the coordinate system, a given physical model may lead to different mathematical models. A network, for example, may be modelled as a set of nodal equations using Kirchhoff's current law or a set of mesh equations using Kirchhoff's voltage law. A control system may be modelled as a scalar differential equation describing the system or state variable vector-matrix differential equation. The particular mathematical model which gives a greater insight into the dynamic behaviour of physical system is selected.

When the mathematical model of a physical system is solved for various input conditions, the result represents the dynamic response of the system. The mathematical model of a system is *linear*, if it obeys the *principle of superposition and homogeneity*. This principle implies that if a system model has responses $y_1(t)$ and $y_2(t)$ to any two inputs $x_1(t)$ and $x_2(t)$ respectively, then the system response to the linear combination of these inputs

$$\alpha_1 x_1(t) + \alpha_2 x_2(t)$$

is given by the linear combination of the individual outputs, i.e.,

$$\alpha_1 y_1(t) + \alpha_2 y_2(t)$$

where α_1 and α_2 are constants.

Mathematical models of most physical systems are characterized by differential equations. A mathematical model is linear, if the differential equation describing it has coefficients, which are either functions only of the independent variable or are constants. If the coefficients of the describing differential equations are functions of time (the independent variable), then the mathematical model is *linear time-varying*. On the other hand, if the coefficients of the describing differential equations are constants, the model is *linear time-invariant*.

The differential equation describing a linear time-invariant system can be reshaped into different forms for the convenience of analysis. For example, for transient response or frequency response analysis of single-input-single-output linear systems, the *transfer function representation* (to be discussed later in this chapter) forms a useful model. On the other hand, when a system has multiple inputs and outputs, the *vector-matrix notation* (discussed in Chapter 12) may be more convenient. The mathematical model of a system having been obtained, the available mathematical tools can then be utilized for analysis or synthesis of the system.

Powerful mathematical tools like the Fourier and Laplace transforms are available for use in linear systems. Unfortunately no physical system in nature is perfectly linear. Therefore certain assumptions must always be made to get a linear model which, as pointed out earlier, is a compromise between the simplicity of the mathematical model and the accuracy of results obtained from it. However, it may not always be possible to obtain a valid linear model, for example, in the presence of a strong nonlinearity or in presence of distributive effects which can not be represented by lumped parameters.

A commonly adopted approach for handling a new problem is: first build a simplified model, linear as far as possible, by ignoring certain nonlinearities and other physical properties which may be present in the system and thereby get an approximate idea of the dynamic response of a system; a more complete model is then built for more complete analysis.

2.2 DIFFERENTIAL EQUATIONS OF PHYSICAL SYSTEMS

This section presents the method of obtaining differential equation models of physical systems by utilizing the physical laws of the process. Depending upon the system well-known physical laws like Newton's laws, Kirchhoff's laws, etc. will be used to build mathematical models.

We shall in first step build the physical model of the system as interconnection of idealized system elements and describe these in form of elemental laws. These idealized elements are sort of building blocks of the system. An ideal element results by making two basic assumptions.

1. Spatial distribution of the element is ignored and it is regarded as a point phenomenon. Thus mass which has physical dimensions, is considered concentrated at a point and temperature in a room which is distributed out into the whole room space is replaced by a representative temperature as if of a single point in the room.

The process of ignoring the spatial dependence by choosing a representative value is called lumping and the corresponding modelling is known as lumped-parameter modelling as distinguished from the distributed parameter modelling which accounts for space distribution.

2. We shall assume that the variables associated with the elements lie in the range that the element can be described by simple linear law of (i) a constant of proportionality or (ii) a first-order derivative or (iii) a first-order integration.

The last two forms are in fact alternatives and can be interconverted by a single differentiation or integration.

To begin with we shall consider ideal elements which have a single-port or two-terminal representation and so have two variables associated with it as shown in Fig. 2.1. These variables are identified as

1. **Through variable V_T** which sort of passes through the element and so has the same value in at one port and out at the other. For example, current through an electrical resistance.
2. **Across variable V_A** which appears across the two terminals of the element. For example, voltage across an electrical resistance.

Another classification of the element variables is

1. **Input variable** or independent variable (V_i)
2. **Output variable** or dependent (response) variable (V_o)

Thus V_i could be V_T or V_A and corresponding V_o would be V_A or V_T . The element is then represented in *block diagram* form (**cause-effect form**) as in Fig. 2.2 wherein the signal V_i flows into the block and flows out of it (V_o) suitably modified by the law represented by the block.

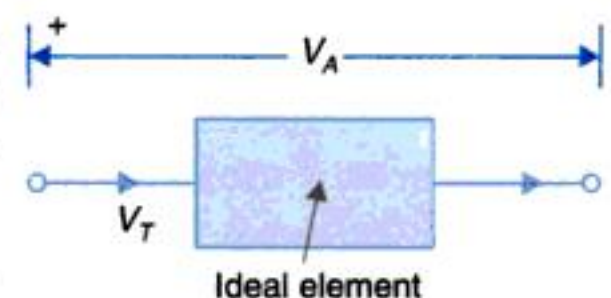


Fig. 2.1

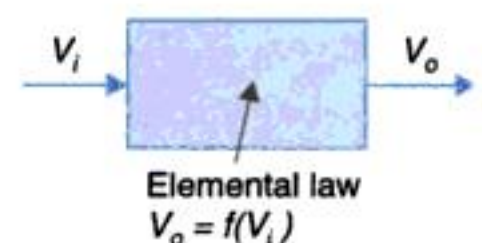


Fig. 2.2. Block diagram of element.

Mechanical Systems

Mechanical systems and devices can be modelled by means of three* ideal translatory and three ideal rotary elements. Their diagrammatic representation and elemental relationships are given in Fig. 2.3. In case of mass/inertia elements it may be noted that one terminal is always the inertial reference frame with respect to which the free terminal moves/rotates.

Through and Across variables for ideal mechanical elements* of Fig. 2.3 are indentified in Table 2.1 along with their units.

Table 2.1. Variables of Mechanical Elements

	<i>Through variable</i>	<i>Integrated through variable</i>	<i>Across variable</i>	<i>Integrated across variable</i>
Translational elements	Force, F $N = \text{kg-m/s}^2$	Translational momentum $p = \int_{-\infty}^t F dt$ ($N\cdot s$)	Velocity difference $v = v_1 - v_2$ (m/s)	Displacement difference $x = x_1 - x_2$ (m)
Rotational elements	Torque, T ($N\cdot m$)	Angular momentum $h = \int_{-\infty}^t T dt$ ($N\cdot ms$)	Angular velocity difference $\omega = \omega_1 - \omega_2$ (rad/s)	Angular Displacement difference $\theta = \theta_1 - \theta_2$ (rad)

Mass/inertia and the two kinds of springs are the energy storage elements where in energy can be stored and retrieved without loss and so these are called conservative elements. Energy stored in these elements in expressed as:

Mass : $E = (1/2) Mv^2 = \text{kinetic energy } (J) ; \text{ motional energy}$

Inertia : $E = (1/2) J\omega^2 = \text{kinetic energy } (J) ; \text{ motional energy}$

Spring (translatory) : $E = 1/2 Kx^2 = \text{potential energy } (J) ; \text{ deformation energy}$

Spring (torsional) : $E = 1/2 K\theta^2 = \text{potential energy } (J) ; \text{ deformation energy}$

Damper is a **dissipative** element and power it consumes (lost in form of heat) is given as

$$P = fv^2 (W)$$

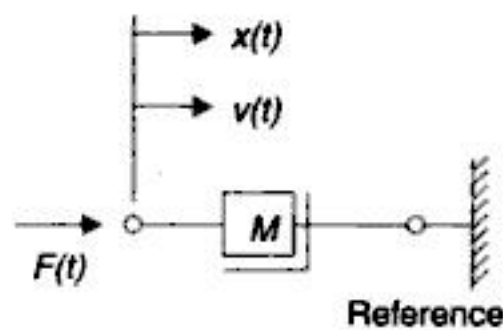
$$= f\omega^2 (W)$$

The elemental relationships in Fig. 2.3 are not expressed in momentum form (which is used mainly in **impulse excitation**). For illustration the relationship of mass can be integrated and expressed as

$$\int_{-\infty}^t F dt = M \int_{-\infty}^t (dv / dt) dt \quad \text{or} \quad p = Mv ; \text{ if } v(-\infty) = 0$$

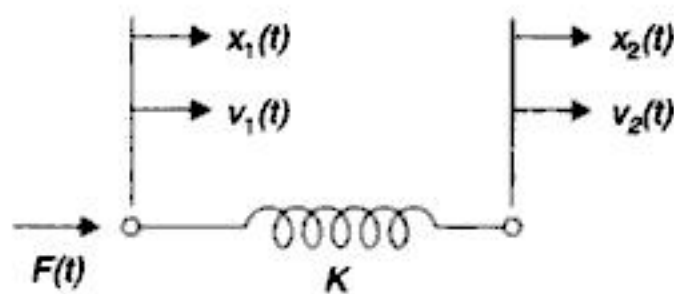
*Another element generally needed is the gear train which will be considered later in this Section.

(1) The mass element



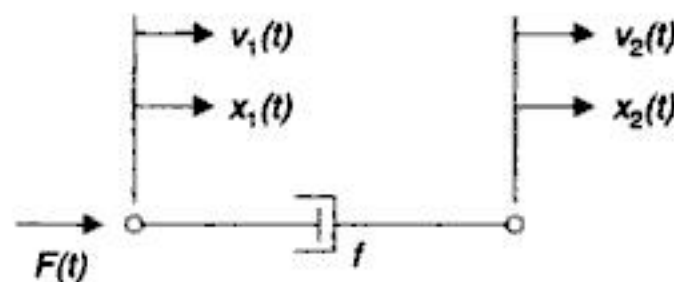
$$F = M \frac{dv}{dt} = M \frac{d^2x}{dt^2}$$

(2) The spring element



$$F = K(x_1 - x_2) = Kx = K \int_{-\infty}^t (v_1 - v_2) dt = K \int_{-\infty}^t v dt$$

(3) The damper element

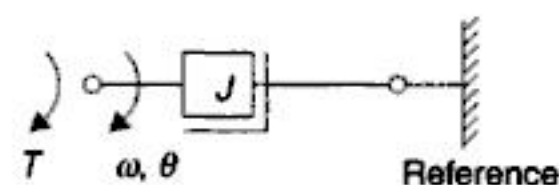


$$F = f(v_1 - v_2) = f v = f(\dot{x}_1 - \dot{x}_2) = f \dot{x}$$

$x(\text{m})$, $v(\text{m/sec})$, $M(\text{kg})$, $F(\text{newton})$, $K(\text{newton/m})$, $f(\text{newton per m/sec})$

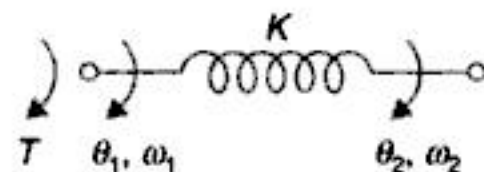
Rotational Elements

(4) The inertia element



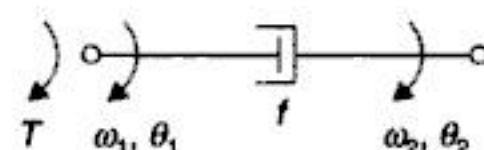
$$T = J \frac{d\omega}{dt} = J \frac{d^2\theta}{dt^2}$$

(5) The torsional spring element



$$T = K(\theta_1 - \theta_2) = K\theta = K \int_{-\infty}^t (\omega_1 - \omega_2) dt = K \int_{-\infty}^t \omega dt$$

(6) The damper element



$$T = f(\omega_1 - \omega_2) = f\omega = f(\dot{\theta}_1 - \dot{\theta}_2) = f\dot{\theta}$$

$\theta(\text{rad})$, $\omega(\text{rad/sec})$, $J(\text{kg-m}^2)$, $T(\text{newton-m})$

$K(\text{newton-m/rad})$, $f(\text{newton-m per rad/sec})$

Fig. 2.3. Ideal elements for mechanical systems.

A mechanical system which is modelled using the three ideal elements presented above would yield a mathematical model which is an ordinary differential equation. Before we advance examples of this type of modelling, we will examine in some detail the friction which has been modelled as a linear element, the damper.

Friction

The friction exists in physical systems whenever mechanical surfaces are operated in sliding contact. The friction encountered in physical systems may be of many types:

- (i) **Coulomb friction force:** The force of sliding friction between dry surfaces. This force is substantially constant.
- (ii) **Viscous friction force:** The force of friction between moving surfaces separated by viscous fluid or the force between a solid body and a fluid medium. This force is approximately linearly proportional to velocity over a certain limited velocity range.
- (iii) **Stiction:** The force required to initiate motion between two contacting surfaces (which is obviously more than the force required to maintain them in relative motion).

In most physical situations of interest, the viscous friction predominates. The ideal relation given in Fig. 2.3 is based on this assumption.

The friction force acts in a direction opposite to that of velocity. However, it should be realised that friction is not always undesirable in physical systems. Sometimes it may even be necessary to introduce friction intentionally to improve the dynamic response of the system (discussed in Chapter 5). Friction may be introduced intentionally in a system by use of a dashpot shown in Fig. 2.4. It consists of a piston and oil filled cylinder with a narrow annular passage between piston and cylinder. Any relative motion between piston and cylinder is resisted by oil with a friction force (fv).

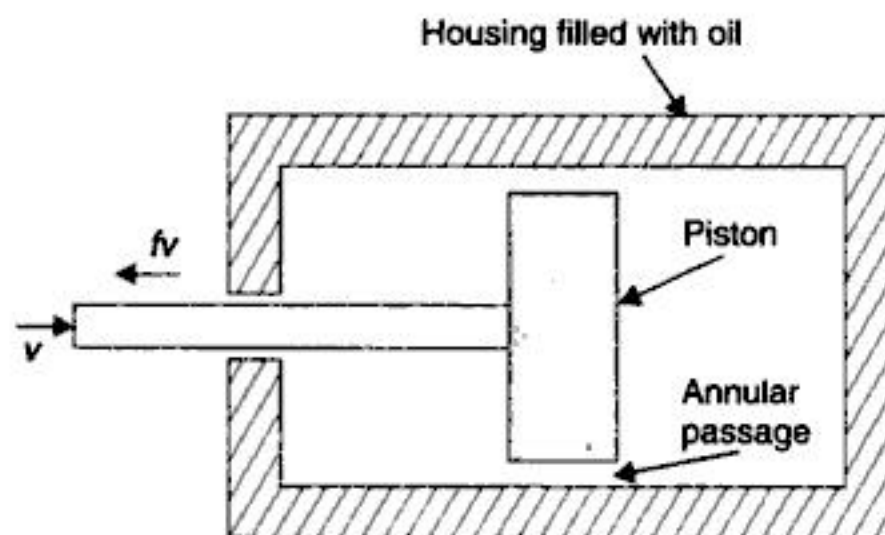


Fig. 2.4. Dashpot construction.

Translational Systems

Let us consider now the mechanical system shown in Fig. 2.5 (a). It is simply a mass M attached to a spring (stiffness K) and a dashpot (viscous friction coefficient f) on which the force F acts. Displacement x is positive in the direction shown. The zero position is taken to be at the point where the spring and mass are in static equilibrium.*

*Note that the gravitational effect is eliminated by this choice of zero position.

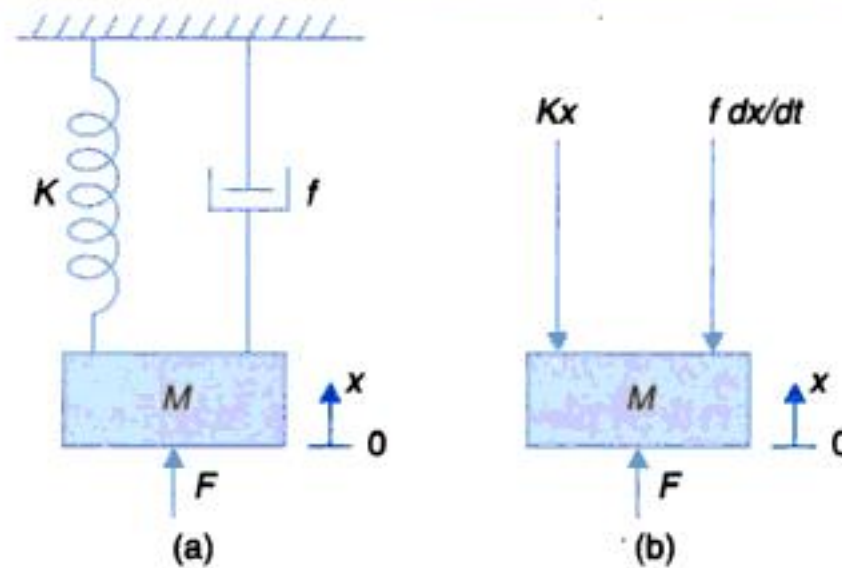


Fig. 2.5. (a) A mass-spring-dashpot system; (b) Free-body diagram.

The systematic way of analyzing such a system is to draw a free-body diagram* as shown in Fig. 2.5 (b). Then by applying Newton's law of motion to the free-body diagram, the force equation can be written as

$$F - f \frac{dx}{dt} - Kx = M \frac{d^2 x}{dt^2} \quad \text{or} \quad F = M \frac{d^2 x}{dt^2} + f \frac{dx}{dt} + Kx \quad \dots(2.1)$$

Equation (2.1) is a linear, constant coefficient differential equation of second-order. Also observe that the system has two storage elements (mass M and spring K).

Mechanical Accelerometer

In this simplest form, an accelerometer consists of a spring-mass-dashpot system shown in Fig. 2.6. The frame of the accelerometer is attached to the moving vehicle.

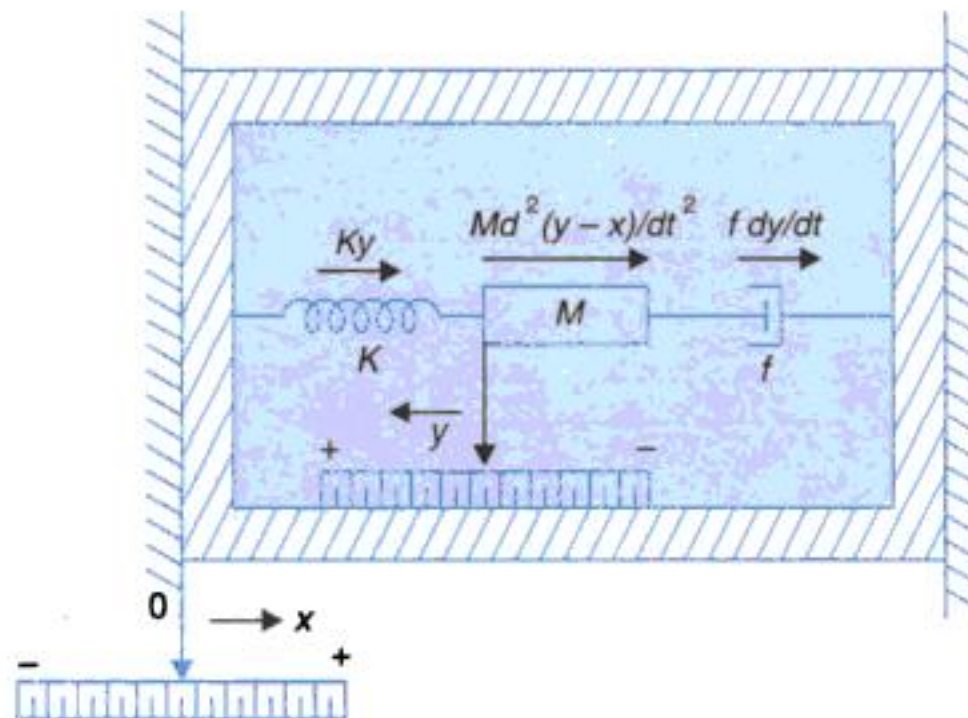


Fig. 2.6. Simplified diagram of an accelerometer.

Whenever the moving vehicle and hence the frame of the accelerometer is accelerated, the spring deflects until it produces enough force to accelerate the mass at the same rate as the

* In example (2.1), we shall see that there is one to one correspondence between free-body diagram approach and nodal method of analysis.

frame. The deflection of the spring which may be measured by a linear-motion potentiometer is a direct measure of acceleration.

Let

x = displacement of the moving vehicle (or frame) with respect to a fixed reference frame.

y = displacement of the mass M with respect to the accelerometer frame.

The positive directions for x and y are indicated on the diagram. Since y is measured with respect to the frame, the force on the mass due to spring is $-Ky$ and due to viscous friction is $-f\frac{dy}{dt}$. The motion of the mass with respect to the fixed reference frame in the positive direction of y is $(y - x)$.

The force equation for the system becomes

$$M\frac{d^2(y - x)}{dt^2} + f\frac{dy}{dt} + Ky = 0$$

$$\text{or} \quad M\frac{d^2y}{dt^2} + f\frac{dy}{dt} + Ky = M\frac{d^2x}{dt^2} = Ma \quad \dots(2.2)$$

where a is the input acceleration.

If a constant acceleration is applied to the accelerometer, the output displacement y becomes constant under steady-state as the derivatives by y become zero, i.e.,

$$Ma = Ky \quad \text{or} \quad a = \left(\frac{K}{M}\right)y$$

The steady-state displacement y is thus a measure of the constant input acceleration. This instrument can also be used for displacement measurements as explained later in Section 2.3.

Nonlinear Spring

No spring is linear over an arbitrary range of extensions—in fact that is true of all physical as well as nonphysical systems. The linear spring elemental law

$$F = Ky$$

is applicable within a limited range of extension y measured beyond the unstretched end of the spring as in Fig. 2.7. Where large extensions are encountered the spring law changes to

$$F = Ky^2 \quad \dots(2.3)$$

which is graphically represented in Fig. 2.8. This law does not obey the principle of superposition as shown below:

$$F_{S_1} = Ky_1 ; y_1 = \text{spring extension in linear range}$$

$$F_{S_2} = Ky_2^2 ; y_2 = \text{spring extension in nonlinear range}$$

$$F_{S_2} = F_{S_1} + F_{S_2}, y = y_1 + y_2 = \text{total spring extension}$$

$$F_S = Ky_1 + Ky_2^2 \neq Ky^2$$

So this behaviour (response) of the spring is not linear (**nonlinear**)

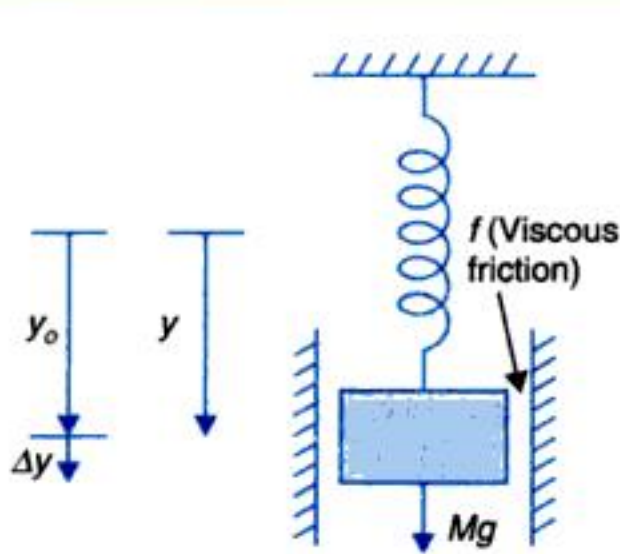


Fig. 2.7

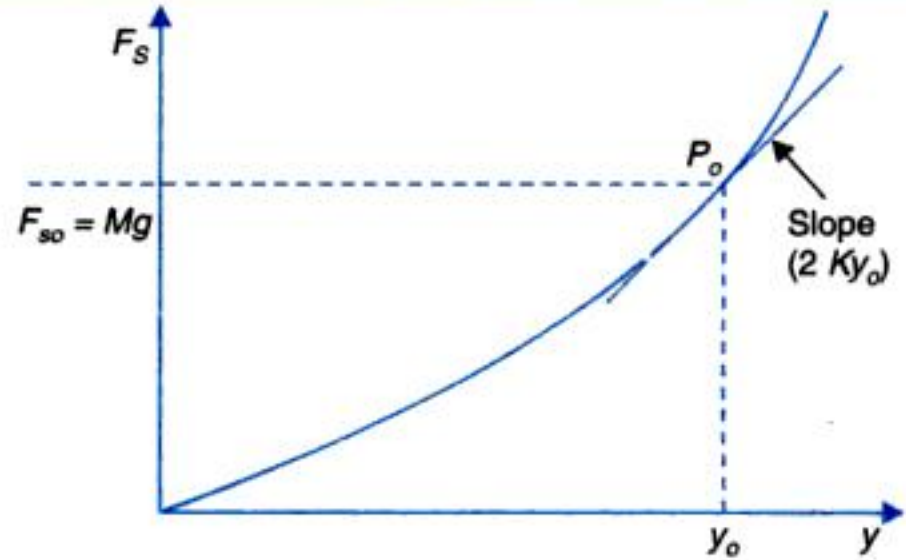


Fig. 2.8

Linearization

Consider the mass-spring system of Fig. 2.7, under gravitational force Mg which when large pushes the spring to nonlinear region of operation. From the freebody diagram we can write the describing equation of the system as

$$Mg = M\ddot{y} + f\dot{y} + Ky^2 \quad \dots(2.4)$$

Under steady condition (rest position of the mass) all derivatives of y are zero. So eqn. (2) gives

$$Mg = Ky_o^2 \text{ or } y_o = \sqrt{Mg/K} \quad \dots(2.5)$$

Consider now that the system moves through a small value Δy about y_o . Equation (2.4) can then be written as

$$Mg = M \frac{d^2}{dt^2} (y_o + \Delta y) + f \frac{d}{dt} (y_o + \Delta y) + K(y_o + \Delta y)^2 \quad \dots(2.6)$$

The nonlinear spring term can be approximated by retaining the first derivative term in Taylor series, i.e.,

$$y = K(y_o + \Delta y)^2 = Ky_o + \left. \frac{d}{dy} (Ky^2) \right|_{y=y_o} \Delta y = Ky_o + (2Ky_o)\Delta y$$

Substituting this approximated value we get

$$Mg = M \frac{d^2}{dt^2} (y_o + \Delta y) + f \frac{d}{dt} (y_o + \Delta y) + Ky_o + (2Ky_o)\Delta y$$

$$\text{or} \quad 0 = M \frac{d^2}{dt^2} (\Delta y) + f \frac{d}{dt} (\Delta y) + (2Ky_o)\Delta y \quad \dots(2.7)$$

It is seen from eqn. (2.7) that the spring behaviour for small movement around $P_o (F_o = Mg, y_o)$ in Fig. 2.8 is linear with spring constant modified to $(2Ky_o)$, the slope of the spring characteristic at the point P_o , called the **operating point**.

If we relabel $x = \Delta y$ and also apply an external force F in positive direction of x (i.e., downwards), eqn. (2.7) becomes

$$F = Mx + fx + K_o x; K_o = 2K/y_o \quad \dots(2.8)$$

The technique of linearization presented above is also known as **small-signal** modelling. This is commonly used in **automatic regulating systems** which operate in a narrow range

around the set point. It will be used in this section in modelling of hydraulic and pneumatic systems which are otherwise nonlinear. The technique of small-signal linearization will be elaborated in Section 2.4 for multivariable components/devices.

Levered Systems

An ideal (mass and friction less) lever is shown in Fig. 2.9 (a) so long as the rotation θ about the axis of the lever is small

$$x = a\theta \text{ and } y = b\theta$$

so that

$$\frac{x}{y} = \frac{a}{b}; \text{ displacement ratio} \quad \dots(2.9a)$$

also

$$aF_1 = bF_2 \quad \dots(2.9b)$$

or

$$\frac{F_1}{F_2} = \frac{b}{a}; \text{ force advantage}$$

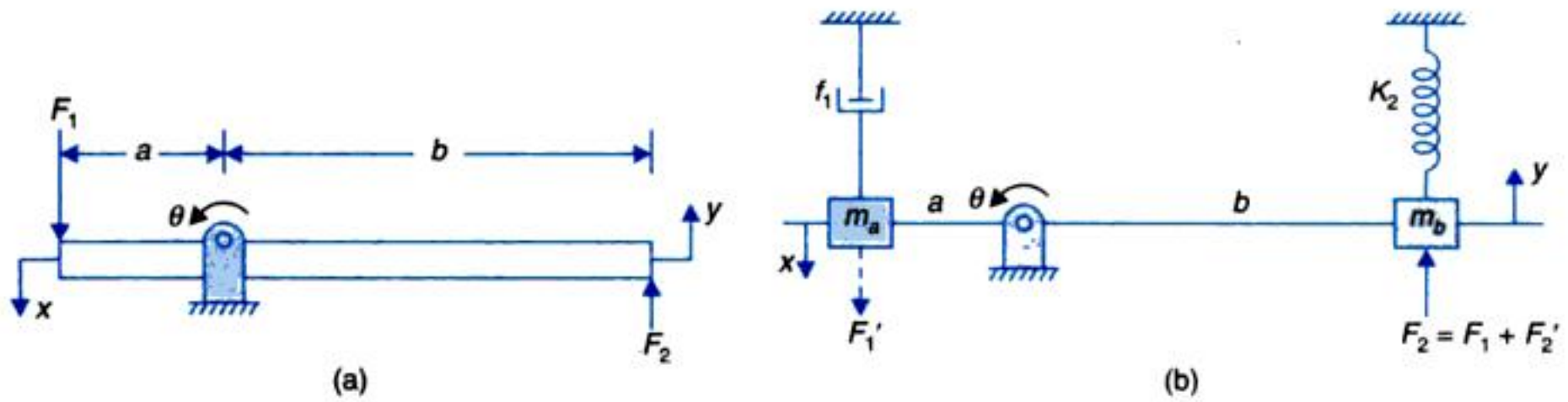


Fig. 2.9. Levered systems.

Consider now the levered system of Fig. 2.9 (b). External force F_2 acting on m_b comprises two components, i.e.,

$$F_2 = F_1 + F_2'$$

F_2' acts on (m_b, K_2) subsystem and F_1' the reflection of F_1 at a -end of the lever acts on (m_a, f_1) subsystem. The dynamical equations for the two systems are written as

$$F_2' = m_b \ddot{y} + K_2 y \quad \dots(2.10a)$$

$$F_1' = m_a \ddot{x} + f_1 \dot{x} \quad \dots(2.10b)$$

But $F_1' = (b/a) F_1$ and $x = (a/b)y$. Substituting in eqn. (2.10b), we get

$$(b/a) F_1 = (a/b) m_a \ddot{y} + (a/b) f_1 \dot{y}$$

or

$$F_1 = (a/b)^2 m_a \ddot{y} + (a/b)^2 f_1 \dot{y} = m_a' \ddot{y} + f_1' \dot{y}. \quad \dots(2.11)$$

where $m_a' = (a/b)^2 m_a$; mass at end 'a' reflected at end 'b' of the lever.

$f_1' = (a/b)^2 f_1$ friction at end 'a' reflected at end 'b' of the lever

Adding eqns. (2.10a) and (2.10b), we have

$$F_2 = F_1 + F_2' = (m_a' + m_b) \ddot{y} + f_1' \dot{y} + K_2 y \quad \dots(2.12)$$

Equation (2.12) can be written down directly by reflecting the parameters from one end of the lever to the other in the inverse square displacement ratio of the lever.

Rotational Systems

Mechanical systems involving fixed-axis rotation occur in the study of machinery of many types and are very important. The modelling procedure is very close to that used in translation. In these systems, the variables of interest are the torque and angular velocity (or displacement). The three basic components for rotational systems are: moment of inertia, torsional spring and viscous friction.

The three ideal rotational elements with their relevant properties and conventions are shown in Fig. 2.3.

Let us consider now, the rotational mechanical system shown in Fig. 2.10 (a) which consists of a rotatable disc of moment of inertia J and a shaft of stiffness K . The disc rotates in a viscous medium with viscous friction coefficient f .

Let T be the applied torque which tends to rotate the disc. The free-body diagram is shown in Fig. 2.10 (b).

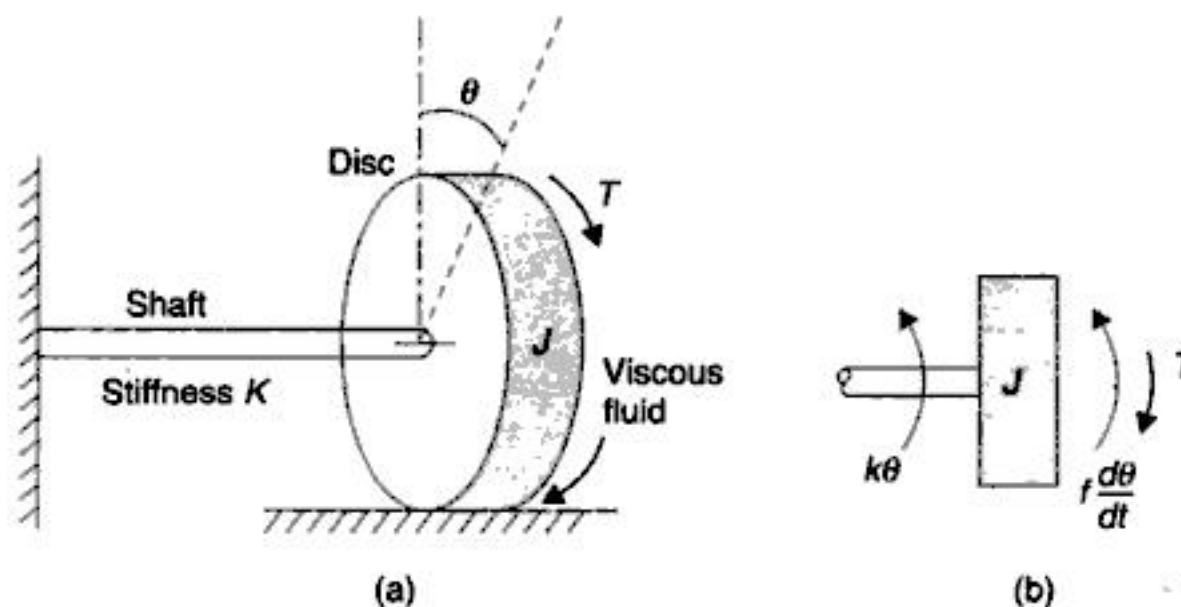


Fig. 2.10. (a) Rotational mechanical system; (b) Free-body diagram.

The torque equation obtained from the free-body diagram is

$$T - f \frac{d\theta}{dt} - K\theta = J \frac{d^2\theta}{dt^2} \quad \text{or} \quad T = J \frac{d^2\theta}{dt^2} + f \frac{d\theta}{dt} + K\theta \quad \dots(2.13)$$

Equation (2.13) is a linear constant coefficient differential equation describing the dynamics of the system shown in Fig. 2.10 (a). Again observe that the system has two storage elements, inertia J and shaft of stiffness K .

Gear Trains

Gear trains are used in control systems to attain the mechanical matching of motor to load. Usually a servomotor operates at high speed but low torque. To drive a load with high torque and low speed by such a motor, the torque magnification and speed reduction are achieved by gear trains. Thus in mechanical systems gear trains act as matching devices like transformers in electrical systems.

Figure 2.11 shows a motor driving a load through a gear train which consists of two gears coupled together. The gear with N_1 teeth is called the primary gear (analogous to primary winding of a transformer) and gear with N_2 teeth is called the secondary gear.

Angular displacements of shafts 1 and 2 are denoted by θ_1 and θ_2 respectively. The moment of inertia and viscous friction of motor and gear 1 are denoted by J_1 and f_1 and those of gear 2 and load are denoted by J_2 and f_2 respectively.

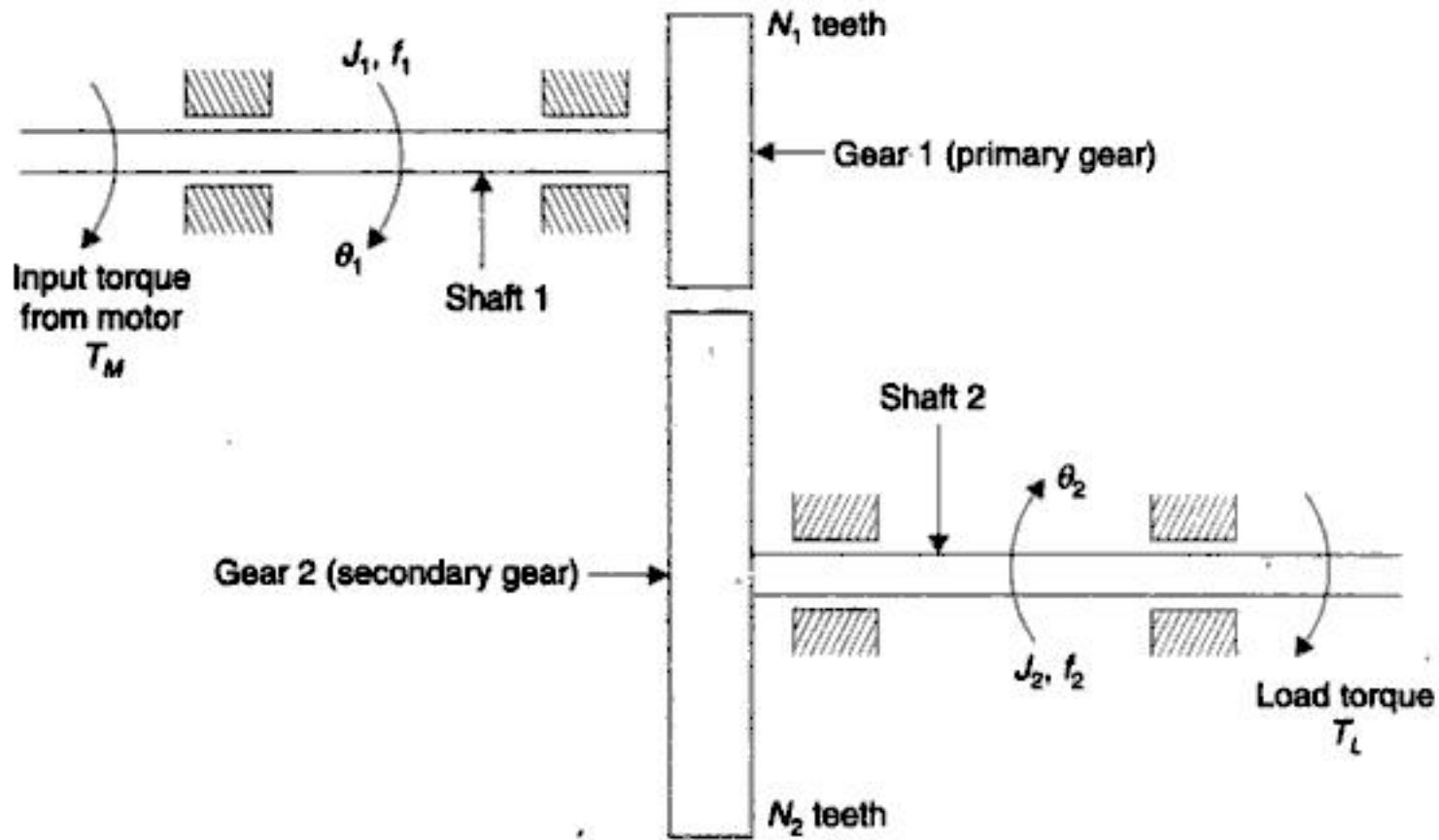


Fig. 2.11. Gear train system.

For the first shaft, the differential equation is

$$J_1 \ddot{\theta}_1 + f_1 \dot{\theta}_1 + T_1 = T_M \quad \dots(2.14)$$

where T_m is the torque developed by the motor and T_1 is the load torque on gear 1 due to the rest of the gear train.

For the second shaft $J_2 \ddot{\theta}_2 + f_2 \dot{\theta}_2 + T_L = T_2 \quad \dots(2.15)$

where T_2 is the torque transmitted to gear 2 and T_L is the load torque.

Let r_1 be the radius of gear 1 and r_2 be that of gear 2. Since the linear distance travelled along the surface of each gear is same, $\theta_1 r_1 = \theta_2 r_2$. The number of teeth on gear surface being proportional to gear radius, we obtain

$$\frac{\theta_2}{\theta_1} = \frac{N_1}{N_2} \quad \dots(2.16)$$

Here the stiffness of the shafts of the gear train is assumed to be infinite. In an ideal case of no loss in power transfer, the work done by gear 1 is equal to that of gear 2. Therefore,

$$T_1 \theta_1 = T_2 \theta_2 \quad \dots(2.17)$$

Combining eqns. (2.16) and (2.17) we have

$$\frac{T_1}{T_2} = \frac{\theta_2}{\theta_1} = \frac{N_1}{N_2} \quad \dots(2.18)$$

Differentiating θ_1 and θ_2 in eqn. (2.18) twice, we have the following relation for speed and acceleration.

$$\frac{\ddot{\theta}_2}{\ddot{\theta}_1} = \frac{\dot{\theta}_2}{\dot{\theta}_1} = \frac{N_1}{N_2} \quad \dots(2.19)$$

Thus if $N_1/N_2 < 1$, from eqns. (2.18) and (2.19) it is found that the gear train reduces the speed and magnifies the torque.

Eliminating T_1 and T_2 from eqns. (2.14) and (2.15) with the help of eqns. (2.18) and (2.19), we obtain

$$J_1 \ddot{\theta}_1 + f_1 \dot{\theta}_1 + \frac{N_1}{N_2} (J_2 \ddot{\theta}_2 + f_2 \dot{\theta}_2 + T_L) = T_M \quad \dots(2.20)$$

Elimination of θ_2 from eqn. (2.20) with the help of eqn. (2.19) yields,

$$\left[J_1 + \left(\frac{N_1}{N_2} \right)^2 J_2 \right] \ddot{\theta}_1 + \left[f_1 + \left(\frac{N_1}{N_2} \right)^2 f_2 \right] \dot{\theta}_1 + \left(\frac{N_1}{N_2} \right) T_L = T_M \quad \dots(2.21)$$

Thus the equivalent moment of inertia and viscous friction of gear train referred to shaft 1 are

$$J_{1eq} = J_1 + \left(\frac{N_1}{N_2} \right)^2 J_2 ; f_{1eq} = f_1 + \left(\frac{N_1}{N_2} \right)^2 f_2$$

In terms of equivalent moment of inertia and friction, eqn. (2.21) may be written as

$$J_{1eq} \ddot{\theta}_1 + f_{1eq} \dot{\theta}_1 + \left(\frac{N_1}{N_2} \right) T_L = T_M$$

Here $(N_1/N_2) T_L$ is the load torque referred to shaft 1.

Similarly, expressing θ_1 in terms of θ_2 in eqn. (2.20) with the help of eqn. (2.19), the equivalent moment of inertia and viscous friction of gear train referred to load shaft are

$$J_{2eq} = J_2 + \left(\frac{N_2}{N_1} \right)^2 J_1 ; f_{2eq} = f_2 + \left(\frac{N_2}{N_1} \right)^2 f_1$$

Torque equation referred to the load shaft may then be expressed as

$$J_{2eq} \ddot{\theta}_2 + f_{2eq} \dot{\theta}_2 + T_L = \left(\frac{N_2}{N_1} \right) T_M$$

It is observed that inertia and friction parameters are referred from one shaft of the gear train to the other in the direct square ratio of the gear teeth. The same will hold for shaft stiffness when present.

Electrical Systems

The resistor, inductor and capacitor are the three basic elements of electrical circuits. These circuits are analyzed by the application of Kirchhoff's voltage and current laws.

Let us analyze the L - R - C series circuit shown in Fig. 2.7 by using Kirchhoff's voltage law. The governing equations of the system are

$$L \frac{di}{dt} + Ri + \frac{1}{C} \int_{-\infty}^t i \, dt = e \quad \dots(2.22)$$

$$\frac{1}{C} \int_{-\infty}^t i \, dt = e_o ; e_o = e_c \quad \dots(2.23)$$

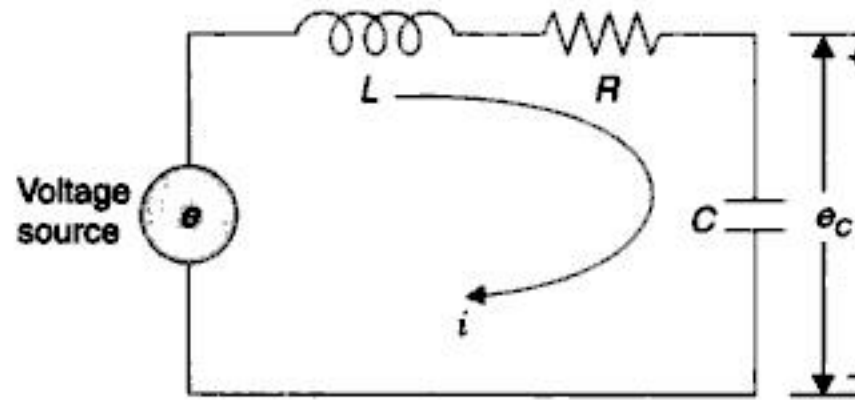


Fig. 2.12. L-R-C series circuit.

Elemental relationships are obvious from these equations. It is also to be noted that inductor and capacitor are the storage elements and resistor is the dissipative element. In terms of electric charge $q = \int i dt$, eqn. (2.12) becomes

$$L \frac{d^2 q}{dt^2} + R \frac{dq}{dt} + \frac{1}{C} q = e \quad \dots(2.24)$$

Similarly, using Kirchhoff's current law, we obtain the following equations for L-R-C parallel circuit shown in Fig. 2.13.

$$C \frac{de}{dt} + \frac{1}{L} \int_{-\infty}^t e dt + \frac{e}{R} = i \quad \dots(2.25)$$

In terms of magnetic flux linkage $\phi = \int e dt$, eqn. (2.25) may be written as

$$C \frac{d^2 \phi}{dt^2} + \frac{1}{R} \frac{d\phi}{dt} + \frac{1}{L} \phi = i \quad \dots(2.26)$$

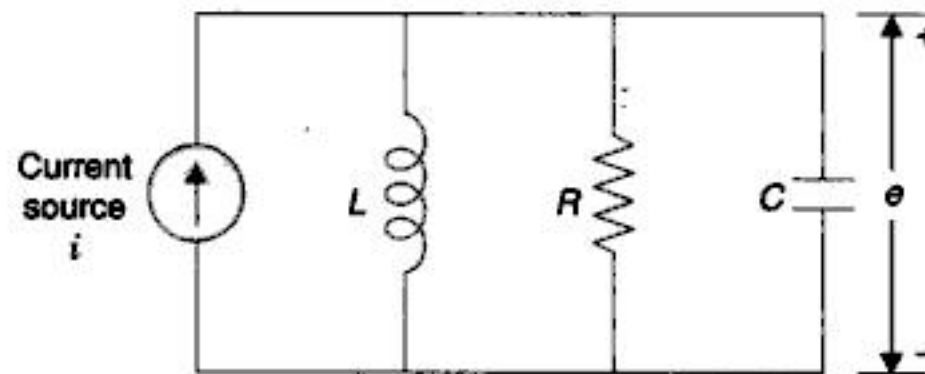


Fig. 2.13. L-R-C parallel circuit.

Analogous System

Comparing eqn. (2.1) for the mechanical translational system shown in Fig. 2.5 (a) or eqn. (2.13) for the mechanical rotational system shown in Fig. 2.10 (a) and eqn. (2.24) for the electrical system shown in Fig. 2.11, it is seen that they are of identical form. Such systems whose differential equations are of identical form are called *analogous systems*. The force F (torque T) and voltage e are the analogous variables here. This is called the Force (Torque)-Voltage analogy. A list of analogous variables in this analogy is given in Table 2.2.

Table 2.2. Analogous Quantities In Force (Torque)-Voltage Analogy

<i>Mechanical translational systems</i>	<i>Mechanical rotational systems</i>	<i>Electrical systems</i>
Force F	Torque T	Voltage e
Mass M	Moment of inertia J	Inductance L
Viscous friction coefficient f	Viscous friction coefficient f	Resistance R
Spring stiffness K	Torsional spring stiffness K	Reciprocal of capacitance $1/C$
Displacement x	Angular displacement θ	Charge q
Velocity \dot{x}	Angular velocity $\dot{\theta}$	Current i

Similarly eqns. (2.1) and (2.3) referred above and eqn. (2.26) for the electrical system shown in Fig. 2.13 are also identical. In this case force F (torque T) and current i are the analogous variables. This is called the Force (Torque)-Current analogy. A list of analogous quantities in this analogy is given in Table 2.3.

Table 2.3. Analogous Quantities In Force (Torque)-current Analogy

<i>Mechanical translational systems</i>	<i>Mechanical rotational systems</i>	<i>Electrical systems</i>
Force F	Torque T	Voltage i
Mass M	Moment of inertia J	Capacitance C
Viscous friction coefficient f	Viscous friction coefficient f	Reciprocal of resistance $1/R$
Spring stiffness K	Torsional spring stiffness K	Reciprocal of inductance $1/L$
Displacement x	Angular displacement θ	Magnetic flux linkage λ
Velocity \dot{x}	Angular velocity $\dot{\theta}$	Voltage e

The concept of analogous system is a useful technique for the study of various systems like electrical, mechanical, thermal, liquid-level, etc. If the solution of one system is obtained, it can be extended to all other systems analogous to it. Generally it is convenient to study a non-electrical system in terms of its electrical analog as electrical systems are more easily amenable to experimental study.

Thermal Systems

The basic requirement for the representation of thermal systems by linear models is that the temperature of the medium be uniform which is generally not the case. Thus for precise analysis a distributed parameter model must be used. Here, however, in order to simplify the analysis, uniformity of temperature is assumed and thereby the system is represented by a lumped parameter model.

Consider the simple thermal system shown in Fig. 2.14. Assume that the tank is insulated to eliminate heat loss to the surrounding air, there is no heat storage in the insulation and liquid in the tank is kept at uniform temperature by perfect mixing with the help of a stirrer. Thus a single temperature may be used to describe the thermal state of the entire liquid. (If complete mixing is not present, there is a complex temperature distribution throughout the liquid and the problem becomes one of the distributed parameters, requiring the use of partial differential equations). Assume that the steady-state temperature of the inflowing liquid is θ_i and that of the outflowing liquid is θ . The steady-state heat input rate from the heater is H . The liquid flow rate is of course assumed constant. To obtain a linear model we shall use small-signal analysis already illustrated for a nonlinear spring.

Let ΔH (J/min) be a small increase in the heat input rate from its steady-state value. This increase in heat input rate will result in increase of the heat outflow rate by an amount ΔH_1 and a heat storage rate of the liquid in the tank by an amount ΔH_2 . Consequently the temperature of the liquid in the tank and therefore of the outflowing liquid rises by $\Delta\theta$ (°C). Since the insulation has been regarded as perfect, the increase in heat outflow rate is only due to the rise in temperature of the outflowing liquid and is given by

$$\Delta H_1 = Qs \Delta\theta$$

where Q = steady liquid flow rate in kg/min; and s = specific heat of the liquid in J/kg °C.

The above relationship can be written in the form

$$\Delta H_1 = \Delta\theta/R \quad \dots(2.27)$$

where $R = 1/Qs$, is defined as the *thermal resistance* and has the units of °C/J/min.

The rate of heat storage in the tank is given by

$$\Delta H_2 = Ms \frac{d(\Delta\theta)}{dt}$$

where M = mass of liquid in the tank in kg; and $\frac{d(\Delta\theta)}{dt}$ = rate of rise of temperature in the tank.

The above equation can be expressed in the form

$$\Delta H_2 = C \frac{d(\Delta\theta)}{dt} \quad \dots(2.28)$$

where $C = Ms$, is defined as the *thermal capacitance* and has the units of J/°C. For the system of Fig. 2.14, the heat flow balance equation is

$$\Delta H = \Delta H_1 + \Delta H_2 = \frac{\Delta\theta}{R} + C \frac{d(\Delta\theta)}{dt}$$

$$\text{or} \quad RC \frac{d(\Delta\theta)}{dt} + \Delta\theta = R(\Delta H) \quad \dots(2.29)$$

Equation (2.29) describes the dynamics of the thermal system with the assumption that the temperature of the inflowing liquid is constant.

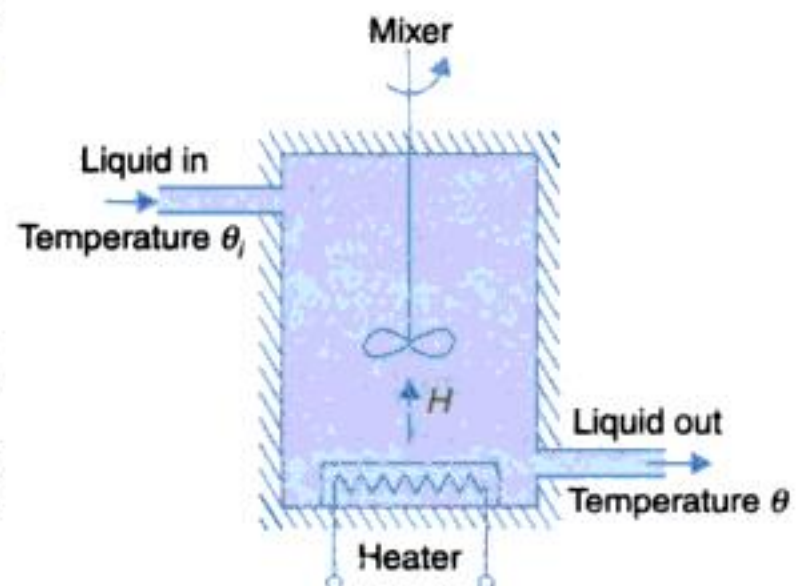


Fig. 2.14. Thermal system.

In practice, the temperature of the inflowing liquid fluctuates. Thus along with a heat input signal from the heater, there is an additional signal due to change in the temperature of the inflowing liquid which is known as the *disturbance signal*.

Let $\Delta\theta_i$ be change in the temperature of the inflowing liquid from its steady-state value. Now in addition to the change in heat input from the heater, there is a change in heat carried by the inflowing liquid. The heat flow equation, therefore, becomes

$$\Delta H + \frac{\Delta\theta_i}{R} = \frac{\Delta\theta}{R} + C \frac{d}{dt}(\Delta\theta)$$

or
$$RC \frac{d}{dt}(\Delta\theta) + \Delta\theta = \Delta\theta_i + R(\Delta H) \quad \dots(2.30)$$

Let us now relax the assumption that the tank insulation is perfect. As the liquid temperature increases by $\Delta\theta$, the rate of heat flow through the tank walls to the ambient medium increases by

$$\Delta H_3 = \frac{\Delta\theta}{R_t}$$

where R_t is the thermal resistance of the tank walls. Equation (2.30) is then modified to

$$\Delta H + \frac{\Delta\theta_i}{R} = \left(\frac{\Delta\theta}{R} + \frac{\Delta\theta}{R_t} \right) + C \frac{d}{dt}(\Delta\theta)$$

or
$$RC \frac{d}{dt}(\Delta\theta) + \Delta\theta = \left(\frac{R'}{R} \right) \Delta\theta_i + R'(\Delta H)$$

where $R' = \frac{RR_t}{R + R_t}$ = effective thermal resistance due to liquid outflow and tank walls (it is a parallel combination of R and R_t).

It is still being assumed above that there is no heat storage in the tank walls. Relaxing this assumption will simply add to the thermal capacitance C .

Fluid Systems

The dynamics of the fluid systems can be represented by ordinary linear differential equations only if the fluid is incompressible and fluid flow is laminar. Industrial processes often involve fluid flow through connecting pipes and tanks where the flow is usually turbulent resulting in nonlinear equations describing the system.

Velocity of sound is a key parameter in fluid flow to determine the compressibility property. If the fluid velocity is much less than the velocity of sound, compressibility effects are usually small. As the velocity of sound in liquids is about 1500 m/s, compressibility* effects are rarely of importance in liquids and the treatment of compressibility is generally restricted to gases, where the velocity of sound is about 350 m/s.

Another important fluid property is the type of fluid flow-laminar or turbulent. Laminar flow is characterized by smooth motion of one laminar of fluid past another, while turbulent flow is characterized by an irregular and nearly random motion superimposed on the main

*The tendency of so-called incompressible fluids to compress slightly under pressure is called *fluid compliance*. This type of effect is accounted for in hydraulic pumps and motors discussed in Section 4.5.

motion of fluid. The transition from laminar to turbulent flow was first investigated by Osborne Reynolds, who after experimentation found that for pipe flow the transition conditions could be correlated by a dimensionless group which is now known as *Reynolds number*, Re .

From his experiments, Reynolds found that pipe flow will be laminar for Re less than 2,000 and turbulent for Re greater than 3,000. When Re is between 2,000 and 3,000, the type of flow is unpredictable and often changes back and forth between the laminar and turbulent states because of flow disturbances and pipe vibrations.

The pressure drop across a pipe section is given by

$$P = \frac{128l\mu}{\pi D^4} Q ; \text{ for laminar flow} \quad \dots(2.31a)$$

$$= RQ$$

$$P = \frac{8K_t\rho l}{\pi^2 D^5} Q^2 ; \text{ for turbulent flow} \quad \dots(2.31b)$$

$$= K_T Q^2$$

where l = length of pipe section (m); D = diameter of pipe (m); μ = viscosity (Ns/m²); Q = volumetric flow rate (m³/s); K_t = a constant (to be determined experimentally); and ρ = mass density (kg/m³).

Equation (2.31a) representing laminar flow is linear, i.e.,

$$P = RQ$$

where $R = \frac{128l\mu}{\pi D^4} \left(\frac{N/m^2}{m^3/s} \right)$ is the *fluid resistance*.

Equation (2.31b) representing turbulent flow is nonlinear, i.e.,

$$P = K_T Q^2$$

where $K_T = \frac{8K_t\rho l}{\pi^2 D^5}$.

This equation can be linearized about the operating point (P_o, Q_o) by techniques discussed earlier in this section (See Nonlinear Spring). At the operating point,

$$P_o = K_T Q_o^2$$

Expanding the turbulent flow equation (2.31b) in Taylor series about the operating point and retaining first-order term only, we have

$$P = P_o + \left. \frac{dP}{dQ} \right|_{(P_o, Q_o)} (Q - Q_o)$$

It follows that $P - P_o = 2K_T Q_o (Q - Q_o)$

or $\Delta P = R \Delta Q \quad \dots(2.32)$

where $R = 2K_T Q_o$ is the *turbulent flow resistance*.

Equation (2.32) relates the incremental fluid flow to incremental pressure around the operating point in the case of turbulent flow.

Large pipes even when long offer small resistance while short devices that contain some contractions (orifices, nozzles, valves, etc.) offer large resistance to fluid flow. For these dissipation devices, head loss

$$P = \frac{8K\rho}{\pi^2 D^4} Q^2$$

where K is a constant. Experimentally determined values of K for various dissipation devices can be found in handbooks. This equation is analogous to eqn. (2.31b) and can be linearized about the operating point to obtain resistance offered by a dissipation device.

The other ideal element used in modelling fluid systems is the *fluid capacitance*. Consider a tank with cross-sectional area $= A(m^2)$.

$$\text{The rate of fluid storage in the tank} = A \frac{dH}{dt} = \frac{A}{\rho g} \frac{dP}{dt} = C \frac{dP}{dt} \quad \dots(2.33)$$

where H = fluid head in the tank (m); $P = \rho g H$ (N/m^2) = pressure at tank bottom; and

$$C = \frac{A}{\rho g} \left(\frac{m^3}{N/m^2} \right) = \text{capacitance of the tank.}$$

Inertial effect of fluid in a pipe line is modelled as *inertance* defined below.

$$\Delta P = L \frac{dQ}{dt}$$

where ΔP = pressure drop as on the pipe

Q = rate of fluid flow through pipe

$$L = \frac{\rho l}{A} = \text{inertance (Ns}^2/\text{m}^5\text{)}.$$

For small fluid accelerations, the inertance effect is usually neglected to obtain a simple mathematical model of the system. This is really true of hydraulic components used in control systems.

Liquid Level Systems

In terms of head $H(m)$, the fluid pressure is given by

$$P = \rho g H$$

The pressure-flow rate relations given by eqns. (2.32a) and (2.32b) may be expressed as the following head-flow rate relations:

$$H = RQ; \text{ for laminar flow} \quad (2.34a)$$

$$\text{where } R = \frac{128lu}{\pi D^2 \rho g}$$

$$\Delta H = R \Delta Q; \text{ for turbulent flow} \quad (2.34b)$$

$$\text{where } R = \frac{2K_T Q_o}{\rho g}$$

The parameter R in eqns. (2.34) is referred to as *hydraulic resistance*.

$$\text{The rate of fluid storage in a tank} = A \frac{dH}{dt} = C \frac{dH}{dt}$$

where $C = A (m^2) = \text{hydraulic capacitance of the tank.}$

Consider a simple liquid-level system shown in Fig. 2.15 where a tank is supplying liquid through an outlet. Under steady conditions, let Q_i be the liquid flow rate into the tank and Q_o be the outflow rate, while H_o is the steady liquid head in the tank. Obviously $Q_i = Q_o$.

Let ΔQ_i be a small increase in the liquid inflow rate from its steady-state value. This increase in liquid inflow rate causes increase of head of the liquid in the tank by ΔH , resulting in increase of liquid outflow rate by

$$\Delta Q_o = \Delta H/R$$

The system dynamics is described by the liquid flow rate balance equation:

Rate of liquid storage in the tank = rate of liquid inflow-rate of liquid outflow

Therefore

$$C \frac{d(\Delta H)}{dt} = \Delta Q_i - \frac{\Delta H}{R}$$

or

$$RC \frac{d(\Delta H)}{dt} + \Delta H = R(\Delta Q_i) \quad (2.35)$$

where C is the capacitance of the tank and R is the total resistance offered by the tank outlet and pipe.

Pneumatic Systems

We shall assume in our discussion that velocities of gases are a small fraction of the velocity of sound, which is true in a number of engineering applications. With this assumption, we treat pneumatic flow also as nearly incompressible. Therefore, the results presented earlier are directly applicable to this class of pneumatic systems.

Consider a simple pneumatic system shown in Fig. 2.16. A pneumatic source is supplying air to the pressure vessel through a pipe line.

Let us define:

P_i = air pressure of the source at steady-state (N/m^2).

P_o = air pressure in the vessel at steady-state (N/m^2).

ΔP_i = small change in air pressure of the source from its steady-state value.

ΔP_o = small change in air pressure of the vessel from its steady-state value.

System dynamics is described by the equation:

Rate of gas storage in vessel = rate of gas inflow

or

$$C \frac{d(\Delta P_o)}{dt} = \frac{\Delta P}{R} = \frac{\Delta P_i - \Delta P_o}{R}$$

or

$$RC \frac{d(\Delta P_o)}{dt} + \Delta P_o = \Delta P_i \quad \dots(2.36)$$

Table 2.4 summarizes the variables and parameters of the thermal, liquid level and pneumatic systems which are analogous to those of electrical systems.

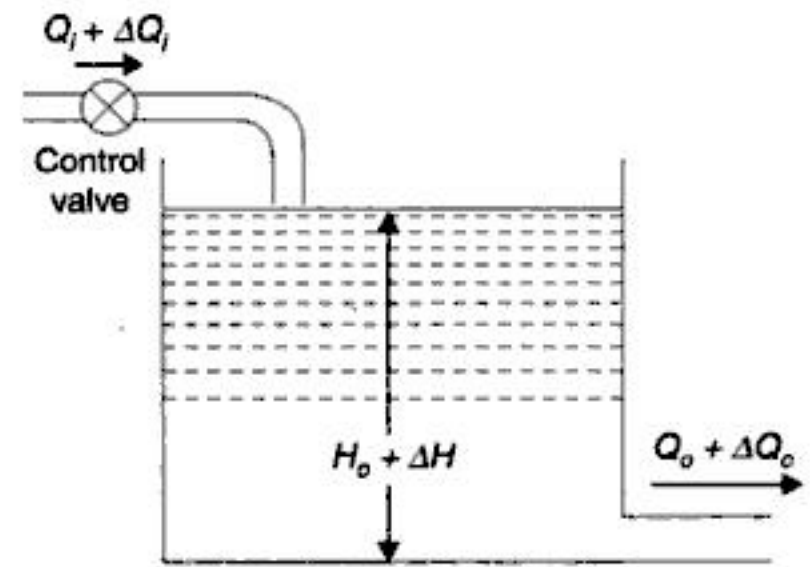


Fig. 2.15. Liquid-level system.



Fig. 2.16. Simple pneumatic system.

Table 2.4. Analogous Quantities

Electrical systems	Thermal systems	Liquid-level systems	Pneumatic systems
Charge, q	Heat flow, J	Liquid flow, m^3	Air flow, m^3
Current, A	Heat flow rate, J/min	Liquid flow rate, m^3/min	Air flow rate, m^3/min
Voltage, V	Temperature, $^{\circ}C$	Head, m	Pressure, N/m^2
Resistance, Ω	Resistance, $\frac{^{\circ}C}{J/min}$	Resistance, $\frac{N/m^2}{m^3/min}$	Resistance, $\frac{N/m^2}{m^3/min}$
Capacitance, C	Capacitance, $J/^{\circ}C$	Capacitance, m^2	Capacitance, $\frac{m^3}{N/m^2}$

2.3 DYNAMICS OF ROBOTIC MECHANISMS

Dynamical equations for robotic serial links will be illustrated here by means of two simple examples of two-link mechanisms.

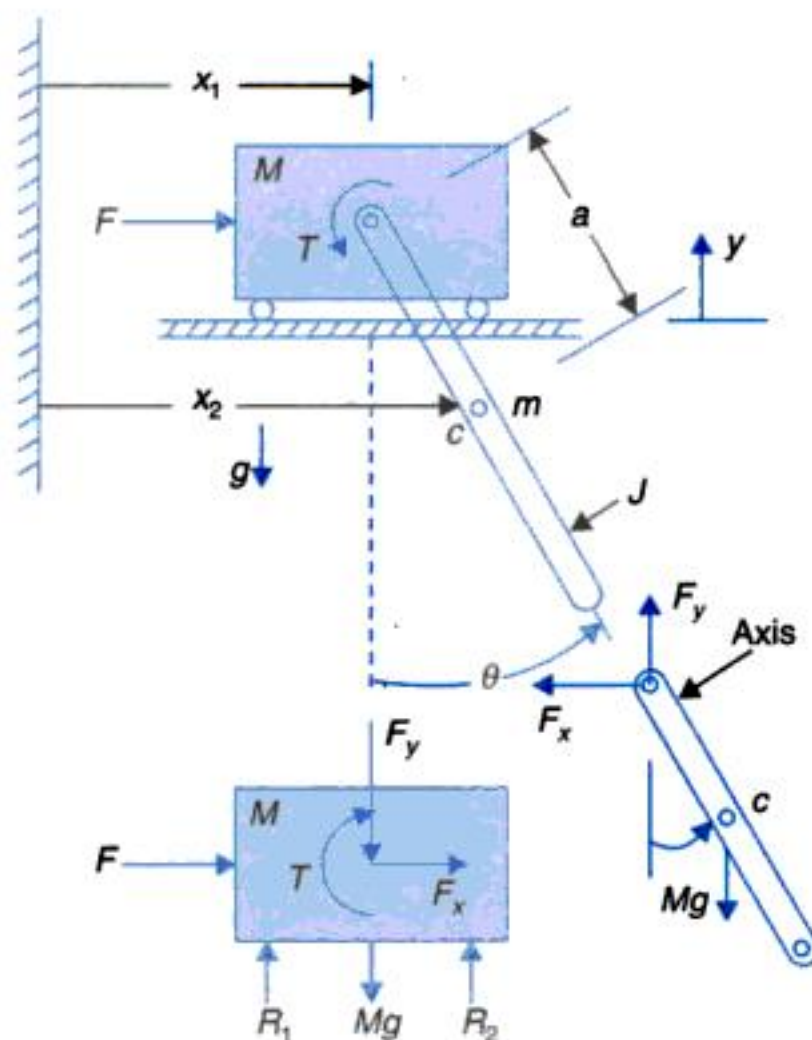


Fig. 2.17. Simplified model of a gantry robot.

Gantry Robot

A simple gantry robot mechanism is shown in Fig. 2.17(a) wherein the main body the crane is propelled by traction force, F . To the body is attached a rotating arm (mass m , and moment of

inertia J about the axis of rotation) driven by an actuator located on the crane body. At the end of the arm a hand (**end effector**) would be attached for picking up objects (not shown in figure).

The free-body diagrams of the masses M and m are drawn in Figs. 2.17(b) and (c).

For mass M

$$M\ddot{x}_1 = Fx + F \quad \dots(i)$$

$$M\ddot{y}_1 = R_1 + R_2 - F_y - Mg \quad \dots(ii)$$

Equation (ii) is needed to be used only if reaction R_1 and R_2 are to be calculated.

For mass m

$$m\ddot{x}_2 = -F_x \quad \dots(iii)$$

$$m\ddot{y}_2 = F_y - mg \quad \dots(iv)$$

$$J\ddot{\theta} = aF_x \cos \theta - F_y \sin \theta + T \quad \dots(v)$$

Eliminating F_x in eqns. (i) and (iii), we get

$$M\ddot{x}_1 + m\ddot{x}_2 = F \quad \dots(vi)$$

Eliminating F_y in eqns. (iv) and (v), we have

$$J\ddot{\theta} = m\ddot{x}_2 a \cos \theta + ma(\ddot{y}_2 + g) = T \quad \dots(vii)$$

The displacements x_2 and y_2 are related to θ as follows:

$$x_2 = x_1 + a \sin \theta$$

$$y_2 = -a \cos \theta$$

Differentiating twice

$$\ddot{x}_2 = \ddot{x}_1 - a \sin \theta \dot{\theta}^2 + \cos \theta \ddot{\theta} \quad \dots(viii)$$

$$\ddot{y}_2 = a \cos \theta \dot{\theta}^2 + a \sin \theta \ddot{\theta} \quad \dots(ix)$$

Substituting \ddot{x}_2 and \ddot{y}_2 into eqns. (vi) and (vii), we get

$$(J + ma^2)\ddot{\theta} + ma \cos \theta \ddot{x}_1 + mga \sin \theta = T \quad \dots(x)$$

$$(M + m)\ddot{x}_1 + ma \cos \theta \ddot{\theta} - ma \sin \theta \dot{\theta}^2 = F \quad \dots(xi)$$

It is observed that the dynamic equations are nonlinear and coupled. Serial link manipulator is too complex a mechanism to be modelled by the free-body technique. It is much simpler to use energy method which employs generalized coordinates.

Lagrangian Mechanics

The Lagrangian L is defined as the difference between the kinetic energy K and the potential energy P of the system

$$L = K - P \quad \dots(2.37)$$

The kinetic potential energy of the system may be expressed in any convenient coordinate system that will simplify the problem. It is not necessary to use Cartesian coordinates.

The dynamics equations, in terms of the coordinates used to express the kinetic and potential energy, are obtained as

$$F_i = \frac{d}{dt} \frac{\partial L}{\partial \dot{q}_i} - \frac{\partial L}{\partial q_i} \quad \dots(2.38)$$

where q_i are the coordinates in which the kinetic and potential energy are expressed \dot{q}_i is the corresponding velocity, and F_i the corresponding force or torque; F_i is either a force or a torque i , depending upon whether q_i is a linear or an angular coordinate. These factors, torques, and coordinates are referred to as generalized forces, torques, and coordinates.

Illustrative Example

We shall derive the dynamic equations for a two-link serial manipulator as shown in Fig. 2.18. Here the link masses are represented by point masses at the end of the link. The manipulator hangs down in a field of gravity g . As indicated in the figure θ_1 and θ_2 are chosen as the generalized coordinates.

The Kinetic and Potential Energy

The kinetic energy of a mass is $K = 1/2 m v^2$. So far the mass m_1 the kinetic energy is expressed as

$$K_1 = (1/2)m_1 d_1^2 \dot{\theta}_1^2 \quad \dots(i)$$

The potential energy with reference to the coordinate frame is expressed by the y -coordinate as

$$P_1 = -m_1 g d_1 \cos(\theta_1) \quad \dots(ii)$$

In the case of the second mass let us first write expressions for its Cartesian position coordinates. These are

$$x_2 = d_1 \sin(\theta_1) + d_2 \sin(\theta_1 + \theta_2) \quad \dots(iii)$$

$$y_2 = -d_1 \cos(\theta_1) - d_2 \cos(\theta_1 + \theta_2) \quad \dots(iv)$$

Differentiating these we get the velocity components of the mass m_2 as

$$\dot{x}_2 = d_1 \cos(\theta_1) \dot{\theta}_1 + d_2 \cos(\theta_1 + \theta_2) (\dot{\theta}_1 + \dot{\theta}_2)$$

$$\dot{y}_2 = d_1 \sin(\theta_1) \dot{\theta}_1 + d_2 \sin(\theta_1 + \theta_2) (\dot{\theta}_1 + \dot{\theta}_2)$$

The magnitude of the velocity squared is then

$$\begin{aligned} v_2^2 &= d_1^2 \dot{\theta}_1^2 + d_2^2 (\dot{\theta}_1^2 + 2\dot{\theta}_1 \dot{\theta}_2 + \dot{\theta}_2^2) \\ &\quad + 2d_1 d_2 \cos(\theta_1) \cos(\theta_1 + \theta_2) (\dot{\theta}_1^2 + \dot{\theta}_1 \dot{\theta}_2) \\ &\quad + 2d_1 d_2 \sin(\theta_1) \sin(\theta_1 + \theta_2) (\dot{\theta}_1^2 + \dot{\theta}_1 \dot{\theta}_2) \\ &= d_1^2 \dot{\theta}_1^2 + d_2^2 (\dot{\theta}_1^2 + 2\dot{\theta}_1 \dot{\theta}_2 + \dot{\theta}_2^2) + 2d_1 d_2 \cos(\theta_2) (\dot{\theta}_1^2 + \dot{\theta}_1 \dot{\theta}_2) \end{aligned}$$

and the kinetic energy of the mass m_2 is then

$$K_2 = 1/2 m_2 d_1^2 \dot{\theta}_1^2 + 1/2 m_2 d_2^2 (\dot{\theta}_1^2 + 2\dot{\theta}_1 \dot{\theta}_2 + \dot{\theta}_2^2) + m_2 d_1 d_2 \cos(\theta_2) (\dot{\theta}_1^2 + \dot{\theta}_1 \dot{\theta}_2)$$

From eqn. (iv) the potential energy of the mass m_2 is

$$P_2 = -m_2 g d_1 \cos(\theta_1) - m_2 g d_2 \cos(\theta_1 + \theta_2) \quad \dots(v)$$

The Lagrangian

The Lagrangian for the two-link system is

$$L = (K_1 + K_2) - (P_1 + P_2)$$

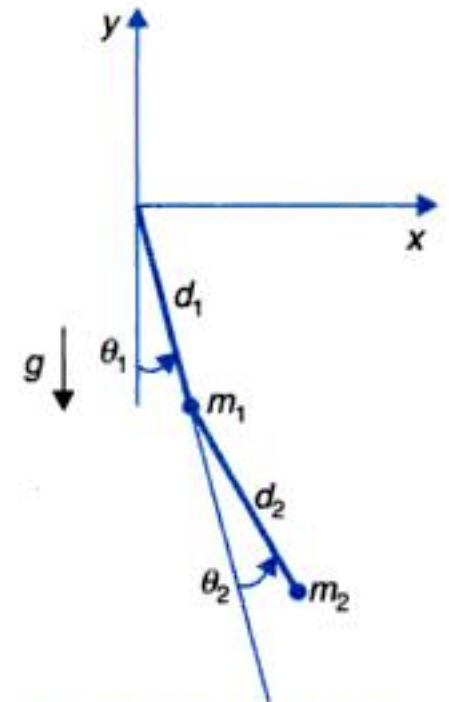


Fig. 2.18. A two link manipulator.

Substituting the values we get

$$\begin{aligned} L = & 1/2(m_1 + m_2)d_1^2\dot{\theta}_1^2 + 1/2m_2d_2^2(\dot{\theta}_1^2 + 2\dot{\theta}_1\dot{\theta}_2 + \dot{\theta}_2^2) \\ & + m_2d_1d_2 \cos(\theta_2)(\dot{\theta}_1^2 + \dot{\theta}_1\dot{\theta}_2) \\ & + (m_1 + m_2)gd_1 \cos(\theta_1) + m_2gd_2 \cos(\theta_1 + \theta_2) \quad \dots(vi) \end{aligned}$$

The Dynamic Equations

The dynamic equations are derived below using the Lagrangian of eqn. (vi)

$$\begin{aligned} \frac{\partial L}{\partial \dot{\theta}_1} &= (m_1 + m_2)d_1^2\dot{\theta}_1 + m_2d_2^2\dot{\theta}_1 + m_2d_1d_2 \cos(\theta_2)\dot{\theta}_1 \\ &+ 2m_2d_1d_2 \cos(\theta_2)\dot{\theta}_1 + m_2d_1d_2 \cos(\theta_2)\dot{\theta}_2 \\ \frac{d}{dt} \frac{\partial L}{\partial \dot{\theta}_1} &= [(m_1 + m_2)d_1^2 + m_2d_2^2 + 2m_2d_1d_2 \cos(\theta_2)]\ddot{\theta}_1 \\ &+ [m_2d_2^2 + m_2d_1d_2 \cos(\theta_2)]\ddot{\theta}_2 \\ &- 2m_2d_1d_2 \sin(\theta_2)\dot{\theta}_1\dot{\theta}_2 - m_2d_1d_2 \sin(\theta_2)\dot{\theta}_2^2 \\ \frac{\partial L}{\partial \theta_1} &= -(m_1 + m_2)gd_1 \sin(\theta_1) - m_2gd_2 \sin(\theta_1 + \theta_2) \end{aligned}$$

These equations yield the torque at joint 1 as

$$\begin{aligned} T_1 = & [(m_1 + m_2)d_1^2 + m_2d_2^2 + 2m_2d_1d_2 \cos(\theta_2)]\ddot{\theta}_1 \\ & + [m_2d_2^2 + m_2d_1d_2 \cos(\theta_2)]\ddot{\theta}_2 \\ & - 2m_2d_1d_2 \sin(\theta_2)\dot{\theta}_1\dot{\theta}_2 - m_2d_1d_2 \sin(\theta_2)\dot{\theta}_2^2 \\ & + (m_1 + m_2)gd_1 \sin(\theta_1) + m_2gd_2 \sin(\theta_1 + \theta_2) \quad \dots(vii) \end{aligned}$$

Performing similar operations at joint 2, we have

$$\begin{aligned} \frac{\partial L}{\partial \dot{\theta}_2} &= m_2d_1^2\dot{\theta}_1 + m_2d_2^2\dot{\theta}_2 + m_2d_1d_2 \cos(\theta_2)\dot{\theta}_1 \\ \frac{d}{dt} \frac{\partial L}{\partial \dot{\theta}_2} &= m_2d_2^2\ddot{\theta}_1 + m_2d_2^2\ddot{\theta}_2 + m_2d_1d_2 \cos(\theta_2)\ddot{\theta}_1 - m_2d_1d_2 \sin(\theta_2)\dot{\theta}_1\dot{\theta}_2 \\ \frac{\partial L}{\partial \theta_2} &= -m_2d_1d_2 \sin(\theta_2)\dot{\theta}_1\dot{\theta}_2 - m_2gd_2 \sin(\theta_1 + \theta_2) \end{aligned}$$

The torque at joint 2 is then given by

$$\begin{aligned} T_2 = & [m_1d_2^2 + m_2d_1d_2 \cos(\theta_2)]\ddot{\theta}_1 + m_2d_2^2\ddot{\theta}_2 - 2m_2d_1d_2 \sin(\theta_2)\dot{\theta}_1\dot{\theta}_2 \\ & - m_2d_1d_2 \sin(\theta_2)\dot{\theta}_1^2 + m_2gd_2 \sin(\theta_1 + \theta_2) \quad \dots(viii) \end{aligned}$$

The torques at joint 1 and 2 (eqns. (vii) and (viii)), can be rewritten in the general form

$$T_1 = D_{11}\ddot{\theta}_1 + D_{12}\ddot{\theta}_2 + D_{111}\dot{\theta}_1^2 + D_{122}\dot{\theta}_2^2 + D_{112}\dot{\theta}_1\dot{\theta}_2 + D_{121}\dot{\theta}_2\dot{\theta}_1 + D_1 \quad \dots(ix)$$

$$T_2 = D_{12}\ddot{\theta}_1 + D_{22}\ddot{\theta}_2 + D_{211}\dot{\theta}_1^2 + D_{222}\dot{\theta}_2^2 + D_{212}\dot{\theta}_1\dot{\theta}_2 + D_{221}\dot{\theta}_2\dot{\theta}_1 + D_2 \quad \dots(x)$$

Various coefficients in the torque expressions of eqns. (x) and (xi) are defined below:

$$\begin{aligned} D_{11} &= [(m_1 + m_2)d_1^2 + m_2d_2^2 + 2m_2d_1d_2 \cos(\theta_2)] \\ D_{22} &= m_2d_2^2 \end{aligned}$$

Coupling inertias

$$D_{12} = D_{21} = m_2 d_2^2 + m_2 d_1 d_2 \cos(\theta_2)$$

Centripetal acceleration coefficients

$$D_{111} = 0$$

$$D_{122} = D_{211} = -m_2 d_1 d_2 \sin(\theta_2)$$

$$D_{222} = 0$$

Coriolis acceleration coefficients

$$D_{112} = D_{121} = -m_2 d_1 d_2 \sin(\theta_2)$$

$$D_{212} = D_{221} = -m_2 d_1 d_2 \sin(\theta_2)$$

Gravity terms

$$D_1 = (m_1 + m_2)gd_1 \sin(\theta_1) + m_2gd_2 \sin(\theta_1 + \theta_2)$$

$$D_2 = m_2gd_2 \sin(\theta_1 + \theta_2).$$

2.4 TRANSFER FUNCTIONS

The transfer function of a linear time-invariant system is defined to be the ratio of the Laplace transform of the output variable to the Laplace transform of the input variable under the assumption that all initial conditions are zero.

Consider the mass-spring-dashpot system shown in Fig. 2.5 (a), whose dynamics is described by the second-order differential equation (2.1).

Taking the Laplace transform of each term of this equation (assuming zero initial conditions), we obtain

$$F(s) = Ms^2X(s) + fsX(s) + KX(s)$$

Then the transfer function is

$$G(s) = \frac{X(s)}{F(s)} = \frac{1}{Ms^2 + fs + K} \quad \dots(2.39)$$

The highest power of the complex variable s in the denominator of the transfer function determines the *order of the system*. The mass-spring-dashpot system under consideration is thus a second-order system, a fact which is already recognized from its differential equation.

The transfer function of the L - R - C circuits shown in Fig. 2.12 is similarly obtained by taking the Laplace transform of eqns. (2.22) and (2.23), with zero initial conditions. The resulting equations are

$$sLI(s) + RI(s) + \frac{1}{s} \frac{I(s)}{C} = E(s)$$

$$\frac{1}{s} \frac{I(s)}{C} = E_0(s)$$

If e is assumed to be the input variable and e_0 the output variable, the transfer function of the system is

$$\frac{E_0(s)}{E(s)} = \frac{1}{LCs^2 + RCs + 1} \quad \dots(2.40)$$

Equation (2.39) and (2.40) reveal that the transfer function is an expression in s -domain, relating the output and input of the linear time-invariant system in terms of the system parameters and is independent of the input. It describes the input output behaviour of the system and does not give any information concerning the internal structure of the system. Thus, when the transfer function of a physical system is determined, the system can be represented by a *block*, which is a shorthand pictorial representation of the cause and effect relationship between input and output of the system. The signal flowing into the block (called input) flows out of it (called output) after being processed by the transfer function characterizing the block, see Fig. 2.19 (a). Functional operation of a system can be more readily visualized by examination of a block diagram rather than by the examination of the equations describing the physical system. Therefore, when working with a linear time-invariant system, we can think of a system or its sub-systems simply as interconnected blocks with each block described by a transfer function.

Laplace transforming eqn. (2.29), the transfer function of the thermal system shown in Fig. 2.14 is

$$\frac{\Delta\theta(s)}{\Delta H(s)} = \frac{R}{RCs + 1} \quad \dots(2.41)$$

The block diagram representation of the system is shown in Fig. 2.19 (a). When this system is subjected to a disturbance, the dynamics is described by eqn. (2.30). Taking the Laplace transformation of this equation, we get

$$(RCs + 1) \Delta\theta(s) = \Delta\theta_i(s) + R\Delta H(s) \quad \dots(2.42)$$

The corresponding block diagram representation is given in Fig. 2.19 (b).

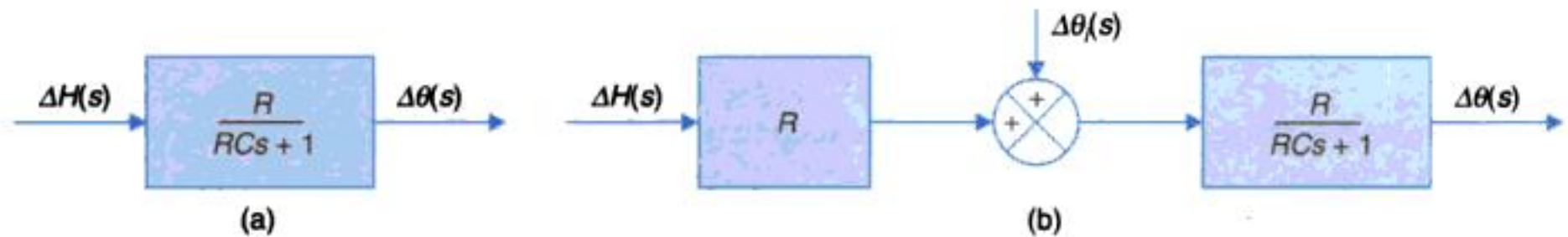


Fig. 2.19. Block diagram of the thermal system shown in Fig. 2.14.

Sinusoidal Transfer Functions

The steady-state response of a control system to a sinusoidal input is obtained by replacing s with $j\omega$ in the transfer function of the system.

Transfer function of the mechanical accelerometer shown in Fig. 2.6, obtained from eqn. (2.2), is

$$\frac{Y(s)}{X(s)} = \frac{Ms^2}{Ms^2 + fs + K} = \frac{s^2}{s^2 + \frac{f}{M}s + \frac{K}{M}}$$

Its sinusoidal transfer function becomes

$$\frac{Y(j\omega)}{X(j\omega)} = \frac{(j\omega)^2}{(j\omega)^2 + \frac{f}{M}(j\omega) + \frac{K}{M}} \quad \dots(2.43)$$

Equation (2.43) represents the behaviour of the accelerometer when used as a device to measure sinusoidally varying displacement. If the frequency of the sinusoidal input signal $X(j\omega)$ is very low, *i.e.*, $\omega \ll \omega_n = \sqrt{K/M}$, then the transfer function given by eqn. (2.43) may be approximated by

$$\frac{Y(j\omega)}{X(j\omega)} \approx \frac{-\omega^2}{K/M}$$

The output signal is very weak for values of frequency $\omega \ll \omega_n$. Weak output signal coupled with the fact that some inherent noise may always be present in the system, makes the displacement measurement by the accelerometer in the low frequency range as quite unreliable.

For $\omega \gg \omega_n$, the transfer function given by eqn. (2.43) may be approximated by

$$\frac{Y(j\omega)}{X(j\omega)} \approx 1$$

Thus, at very high frequencies the accelerometer output follows the sinusoidal displacement input. For this range of frequencies the basic accelerometer system can be used for displacement measurement particularly in seismographic studies.

For a sinusoidal input acceleration, the steady-state sinusoidal response of the accelerometer is given by

$$\frac{Y(j\omega)}{A(j\omega)} = \frac{1}{(j\omega)^2 + \frac{f}{M}(j\omega) + \frac{K}{M}}$$

As long as $\omega \ll \omega_n = \sqrt{K/M}$,

$$\frac{Y(j\omega)}{A(j\omega)} \approx \frac{M}{K}$$

The accelerometer is thus suitable for measurement of sinusoidally varying acceleration from zero frequency (constant acceleration) to a frequency which depends upon the choice of ω_n for the accelerometer. The sinusoidal behaviour of this type of transfer functions will be studied in greater details in Chapter 8.

Procedure for Deriving Transfer Functions

The following assumptions are made in deriving transfer functions of physical systems.

1. It is assumed that there is no loading, *i.e.*, no power is drawn at the output of the system. If the system has more than one nonloading elements in tandem, then the transfer function of each element can be determined independently and the overall transfer function of the physical system is determined by multiplying the individual transfer functions. In case of systems consisting of elements which load each other, the overall transfer function should be derived by basic analysis without regard to the individual transfer functions.
2. The system should be approximated by a linear lumped constant parameters model by making suitable assumptions.

To illustrate the point (1) above, let us consider two identical RC circuits connected in cascade so that the output from the first circuit is fed as input to the second as shown in Fig. 2.20.

The describing equations for this system are

$$\frac{1}{C} \int_{-\infty}^t (i_1 - i_2) dt + Ri_1 = e_i \quad \dots(2.44a)$$

$$\frac{1}{C} \int_{-\infty}^t (i_2 - i_1) dt + Ri_2 = -\frac{1}{C} \int_{-\infty}^t i_2 dt = -e_o \quad \dots(2.44b)$$

Taking the Laplace transforms of eqns. (2.44 (a)) and (2.44 (b)), assuming zero initial conditions, we obtain

$$\frac{1}{sC} [I_1(s) - I_2(s)] + RI_1(s) = E_i(s)$$

$$\frac{1}{sC} [I_2(s) - I_1(s)] + RI_2(s) = -\frac{1}{sC} [I_2(s)] = -E_o(s)$$

The transfer function obtained by eliminating $I_1(s)$ and $I_2(s)$ from the above equation is

$$\frac{E_o(s)}{E_i(s)} = \frac{1}{\tau^2 s^2 + 3\tau s + 1} \quad \dots(2.45)$$

where $\tau = RC$.

The transfer function of each of the individual RC circuits is $1/(1 + s\tau)$. From eqn. (2.45) it is seen that overall transfer function of the two RC circuits connected in cascades is not equal to $[1/(\tau s + 1)] [1/(\tau s + 1)]$ but instead it is $1/(\tau^2 s^2 + 3\tau s + 1)$.

This difference is explained by the fact that while deriving the transfer function of a single RC circuit, it is assumed that the output is unloaded. However, when the input of second circuit is obtained from the output of first, a certain amount of energy is drawn from the first circuit and hence its original transfer function is no longer valid. The degree to which the overall transfer function is modified from the product of individual transfer functions depends upon the amount of loading.

As an example to illustrate the point (2) above, let us derive the transfer function of a d.c. servomotor. In servo applications, a d.c. motor is required to produce rapid accelerations from standstill. Therefore the physical requirements of such a motor are low inertia and high starting torque. Low inertia is attained with reduced armature diameter with a consequent increase in armature length such that the desired power output is achieved. Thus, except for minor differences in constructional features, a d.c. servomotor is essentially an ordinary d.c. motor.

In control systems, the d.c. motors are used in two different control modes: armature-control mode with fixed field current, and field-control mode with fixed armature current.

Armature-control

Consider the armature-controlled d.c. motor shown in Fig. 2.21.

In this system,

R_a = resistance of armature (Ω).

L_a = inductance of armature winding (H).

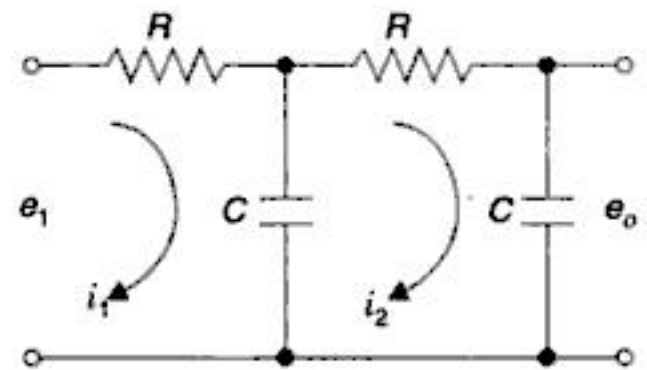


Fig. 2.20. RC circuits in cascade.

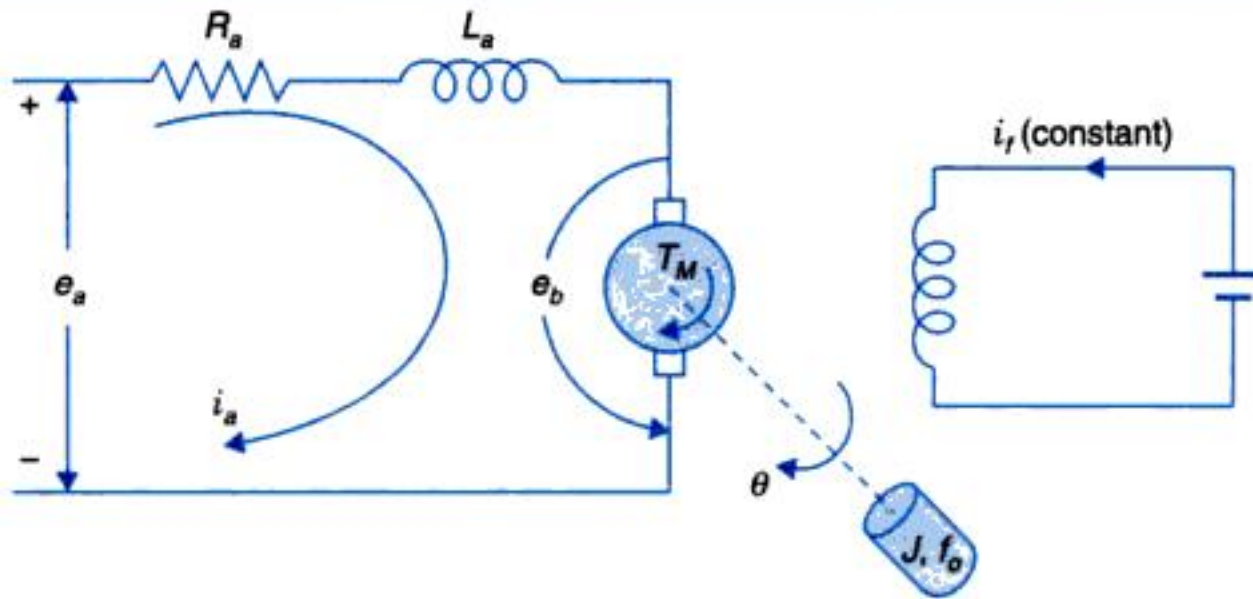


Fig. 2.21. Armature-controlled d.c. motor.

i_a = armature current (A).

i_f = field current (A).

e_a = applied armature voltage (V).

e_b = back emf (volts).

T_M = torque developed by motor (Nm).

θ = angular displacement of motor-shaft (rad).

J = equivalent moment of inertia of motor and load referred to motor shaft (kg-m^2).

f_0 = equivalent viscous friction coefficient of motor and load referred to motor shaft
 $\left(\frac{\text{Nm}}{\text{rad/s}} \right)$.

In servo applications, the d.c. motors are generally used in the linear range of the magnetization curve. Therefore, the air gap flux ϕ is proportional of the field current, i.e.,

$$\phi = K_f i_f \quad \dots(2.46)$$

where K_f is a constant.

The torque T_M developed by the motor is proportional to the product of the armature current and air gap flux, i.e.,

$$T_M = K_1 K_f i_f i_a \quad \dots(2.47)$$

where K_1 is a constant.

In the armature-controlled d.c. motor, the field current is kept constant, so that eqn. (2.46) can be written as

$$T_M = K_T i_a \quad \dots(2.48)$$

where K_T is known as the motor torque constant.

The motor back emf being proportional to speed is given as

$$e_b = K_b \frac{d\theta}{dt} \quad \dots(2.49)$$

where K_b is the back emf constant.

The differential equation of the armature circuit is

$$L_a \frac{di_a}{dt} + R_a i_a + e_b = e_a \quad \dots(2.50)$$

The torque equation is

$$J \frac{d^2\theta}{dt^2} + f_0 \frac{d\theta}{dt} = T_M = K_T i_a \quad \dots(2.51)$$

Taking the Laplace transforms of eqns. (2.48) to (2.50), assuming zero initial conditions, we get

$$E_b(s) = K_b s \theta(s) \quad \dots(2.52)$$

$$(L_a s + R_a) I_a(s) = E_a(s) - E_b(s) \quad \dots(2.53)$$

$$(Js^2 + f_0 s) \theta(s) = T_M(s) = K_T I_a(s) \quad \dots(2.54)$$

From eqns. (2.51) to (2.53), the transfer function of the system is obtained as

$$G(s) = \frac{\theta(s)}{E_a(s)} = \frac{K_T}{s[(R_a + sL_a)(Js + f_0) + K_T K_b]} \quad \dots(2.55)$$

The block diagram representation of eqn. (2.53) is shown in Fig. 2.22 (a) where the circular block representing the differencing action is known as the *summing point*. Equation (2.54) is represented by a block shown in Fig. 2.22 (b).

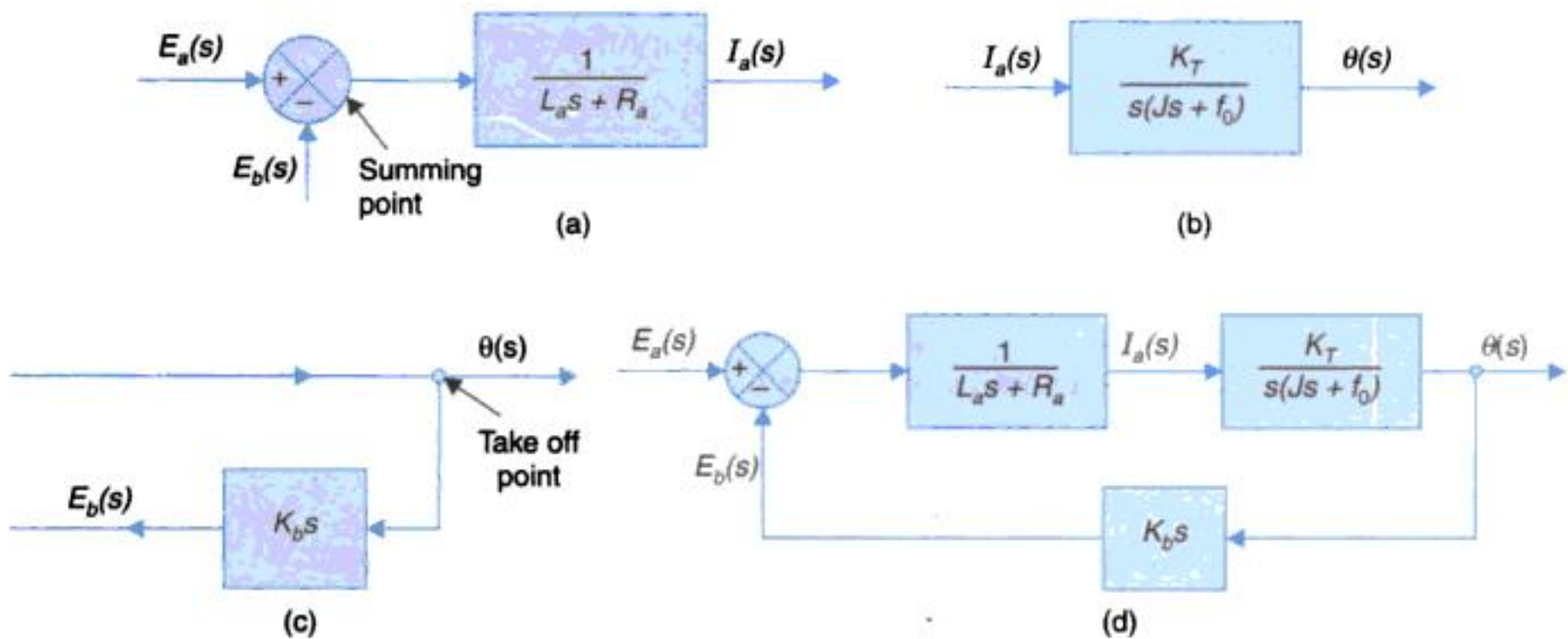


Fig. 2.22. Block diagram of armature-controlled d.c. motor.

Figure 2.22 (c) represents eqn. (2.52) where a signal is taken off from a *take-off point* and fed to the feedback block ($K_b s$). Fig. 2.22 (d) is the complete block diagram of the system under consideration, obtained by connecting the block diagram shown in Fig. 2.22 (a), (b) and (c). It may be pointed out here that when a signal is taken from the output of a block, this does not affect the output as per assumption 1 of the procedure for deriving transfer functions advanced earlier.

However, it should be noted that the block diagram of the system under consideration can be directly obtained from the physical system of Fig. 2.21 by using the transfer functions of simple electrical and mechanical networks derived already. The voltage applied to the armature circuit is $E_a(s)$ which is opposed by the back emf ($E_b(s)$). The net voltage ($E_a - E_b$) acts on a linear circuit comprised of resistance and inductance in series, having the transfer function $1/(sL_a + R_a)$. The result is an armature current $I_a(s)$. For fixed field, the torque developed by

the motor is $K_T I_a(s)$. This torque rotates the load at a speed $\dot{\theta}(s)$ against the moment of inertia J and viscous friction with coefficient f_0 [the transfer function is $1/(Js + f_0)$]. The back emf signal $E_b = K_b \dot{\theta}(s)$ is taken off from the shaft speed and fed back negatively to the summing point. The angle signal $\theta(s)$ is obtained by integrating (i.e., $1/s$) the speed $\dot{\theta}(s)$. This results in the block diagram of Fig. 2.23, which is equivalent to that of Fig. 2.22 as can be seen by shifting the take off point from $\dot{\theta}(s)$ to $\theta(s)$.

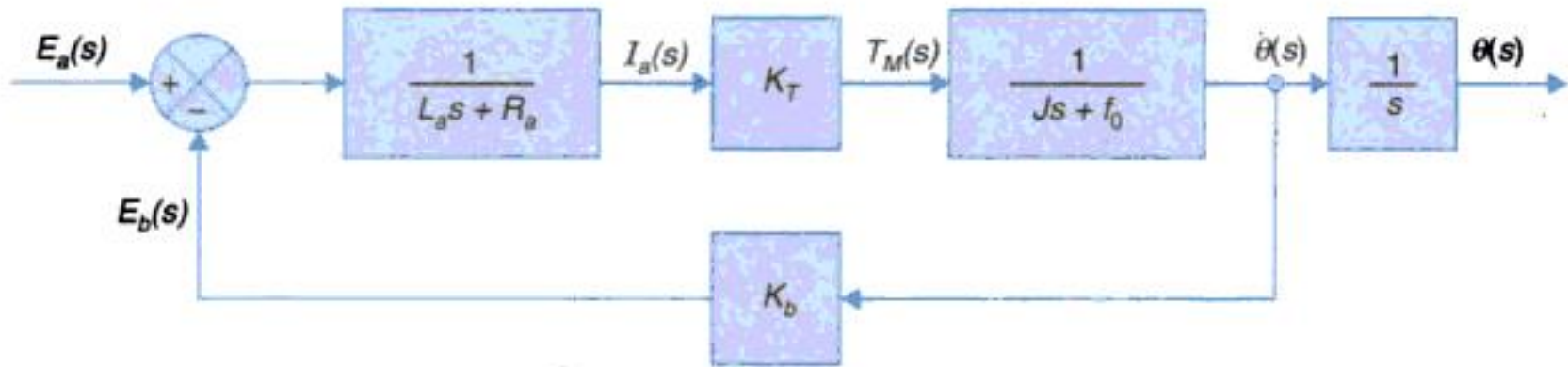


Fig. 2.23. Block diagram of armature-controlled d.c. motor.

The *armature circuit inductance* L_a is usually negligible. Therefore from eqn. (2.55), the transfer function of the armature controlled motor simplifies to

$$\frac{\theta(s)}{E_a(s)} = \frac{K_T/R_a}{Js^2 + s(f_0 + K_T K_b/R_a)} \quad \dots(2.56)$$

The term $(f_0 + K_T K_b/R_a)$ indicates that the back emf of the motor effectively increases the viscous friction of the system. Let

$$f = f_0 + K_T K_b/R_a$$

be the effective viscous friction coefficient. Then from eqn. (2.56)

$$\frac{\theta(s)}{E_a(s)} = \frac{K_T/R_a}{s(Js + f)} \quad \dots(2.57)$$

The transfer function given by eqn. (2.56) may be written in the form

$$\frac{\theta(s)}{E_a(s)} = \frac{K_m}{s(s\tau_m + 1)} \quad \dots(2.58)$$

where $K_m = K_T/R_a f$ = motor gain constant, and $\tau_m = J/f$ = motor time constant.

The motor torque and back emf constants K_T , K_b are interrelated. Their relationship is deduced below. In metric units, K_b is in V/rad/s and K_T is in Nm/A.

Electrical power converted to mechanical form = $e_b i_a = K_b \dot{\theta} i_a$ W

Power at shaft (in mechanical form) = $T \dot{\theta} = K_T i_a \dot{\theta}$ W

At steady speed these two powers balance. Hence

$$K_b \dot{\theta} i_a = K_T i_a \dot{\theta} \quad \text{or} \quad K_b = K_T \text{ (in MKS units)}$$

This result can be used to advantage in practice as K_b can be measured more easily and with greater accuracy than K_T .

Field-control

A field-controlled d.c. motor is shown in Fig. 2.24 (a).

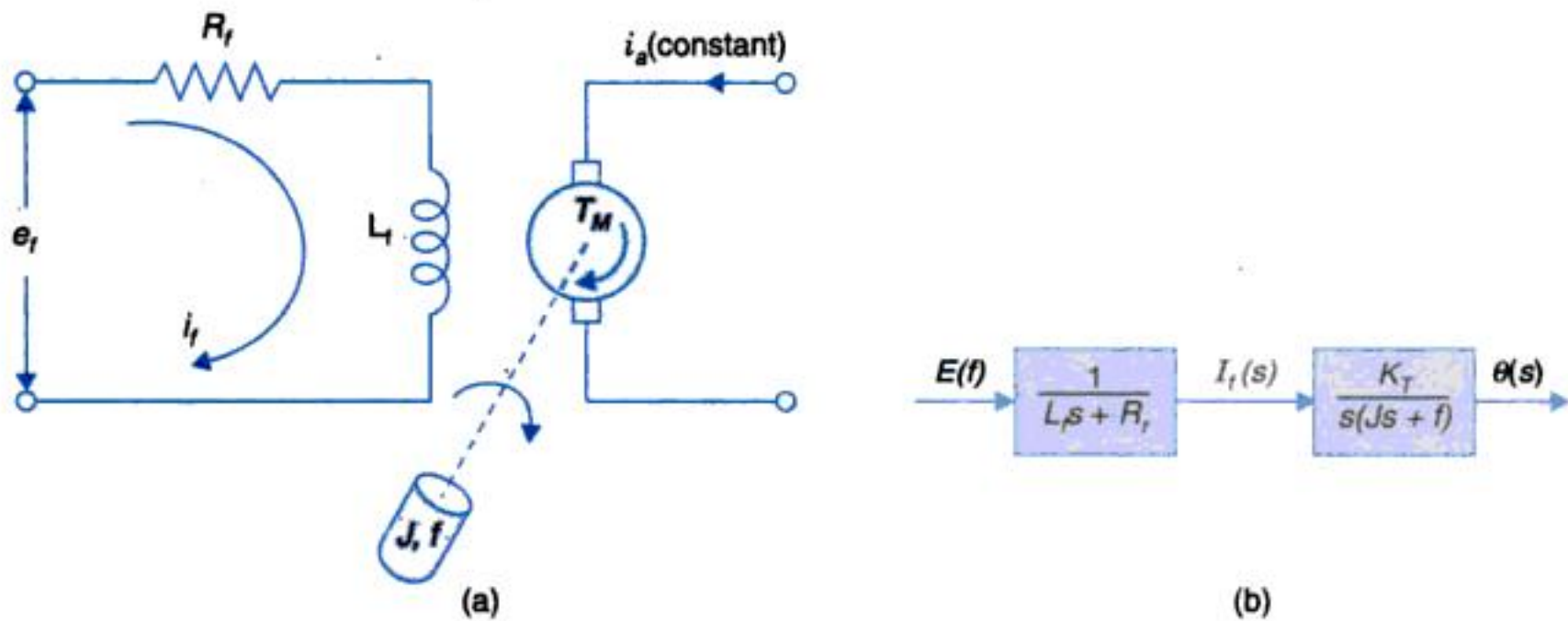


Fig. 2.24. (a) Field-controlled d.c. motor, (b) Block diagram of field-controlled motor.

In this system,

R_f = field winding resistance (Ω).

L_f = field winding inductance (H).

e = field control voltage (V).

i_f = field current (A).

T_M = torque developed by motor (Nm).

J = equivalent moment of inertia of motor and load referred to motor shaft (kg-m^2).

f = equivalent viscous friction coefficient of motor and load referred to motor shaft $\frac{\text{Nm}}{\text{rad/s}}$.

θ = angular displacement of motor shaft (rad).

In the field-controlled motor, the armature current is fed from a constant current source.

Therefore, from eqn. (2.36)

$$T_M = K_1 K_f i_f i_a = K_T' i_f$$

where K_T' is a constant.

The equation for the field circuit is

$$L_f \frac{di_f}{dt} + R_f i_f = e_f \quad \dots(2.59)$$

The torque equation is

$$J \frac{d^2\theta}{dt^2} = f \frac{d\theta}{dt} = T_M = K_T' i_f \quad \dots (2.60)$$

Taking the Laplace transform of eqns. (2.48) and (2.49), assuming zero initial conditions, we get

$$(L_f s + R_f) I_f(s) = E_f(s) \quad \dots(2.61)$$

$$(Js^2 + fs) \theta(s) = T_M(s) = K_T' I_f(s) \quad \dots(2.62)$$

From the above equations, the transfer function of the motor is obtained as

$$\frac{\theta(s)}{E_f(s)} = \frac{K_T'}{s(L_f s + R_f)(Js + f)} = \frac{K_m}{s(\tau_f s + 1)(\tau_{me} s + 1)} \quad \dots(2.63)$$

where $K_m = K_T'/R_f f$ = motor gain constant; $\tau_f = L_f/R_f$ = time constant of field circuit; and $\tau_{me} = J/f$; mechanical time constant.

The block diagram of the field-controlled d.c. motor obtained from eqns. (2.61) and (2.62) is given in Fig. 2.24 (b).

For small size motors field-control is advantageous because only a low power servo amplifier is required while the armature current which is not large can be supplied from an expensive constant current amplifier. For large size motors it is on the whole cheaper to use armature-control scheme. Further in armature-controlled motor, back emf contributes additional damping over and above that provided by load friction. With the advances made in permanent magnet materials, permanent magnet armature-controlled d.c. servomotor are now universally adopted (see Chapter 5).

2.5 BLOCK DIAGRAM ALGEBRA

As introduced earlier, the input-output behaviour of a linear system or element of a linear system is given by its transfer function

$$G(s) = C(s)/R(s)$$

where $R(s)$ = Laplace transformation of the input variable; and $C(s)$ = Laplace transform of the output variable.

A convenient graphical representation of this behaviour is the *block diagram* as shown in Fig. 2.25 (a) wherein the signal into the block represents the input $R(s)$ and the signal out of the block represents the output $C(s)$, while the block itself stands for the transfer function $G(s)$. The flow of information (signal) is unidirectional from the input to the output with the output being equal to the input multiplied by the transfer function of the block. A complex system comprising of several non-loading elements is represented by the interconnection of the blocks for individual elements. The blocks are connected by lines with arrows indicating the unidirectional flow of information from the output of one block to the input of the other. In addition to this, *summing* or *differencing* of signals is indicated by the symbols shown in Fig. 2.25 (b), while the *take-off* point of a signal is represented by Fig. 2.25 (c).

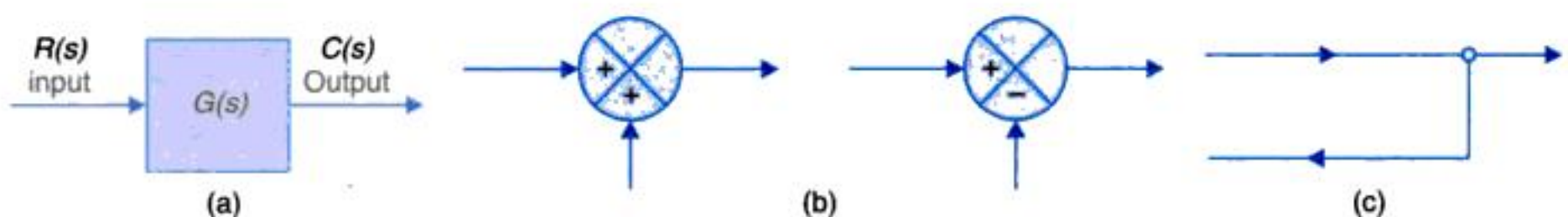


Fig. 2.25

Block diagrams of some of the control systems turn out to be very complex such that the evaluation of their performance requires simplification (or reduction) of block diagrams which

is carried out by block diagram rearrangements. Some of the important block diagram rearrangements are discussed in this section.

Block Diagram of a Closed-loop System

Fig. 2.26 (a) shows the block diagram of a negative feedback system. With reference to this figure, the terminology used in block diagrams of control systems is given below.

$R(s)$ = reference input.

$C(s)$ = output signal or controlled variable.

$B(s)$ = feedback signal.

$E(s)$ = actuating signal.

$G(s) = C(s)/E(s)$ = forward path transfer function.

$H(s)$ = transfer function of the feedback elements.

$G(s)H(s) = B(s)/E(s)$ = loop transfer function.

$T(s) = C(s)/R(s)$ = closed-loop transfer function.

From Fig. 2.26 (a) we have

$$C(s) = G(s)E(s) \quad \dots(2.64)$$

$$E(s) = R(s) - B(s) = R(s) - H(s)C(s) \quad \dots(2.65)$$

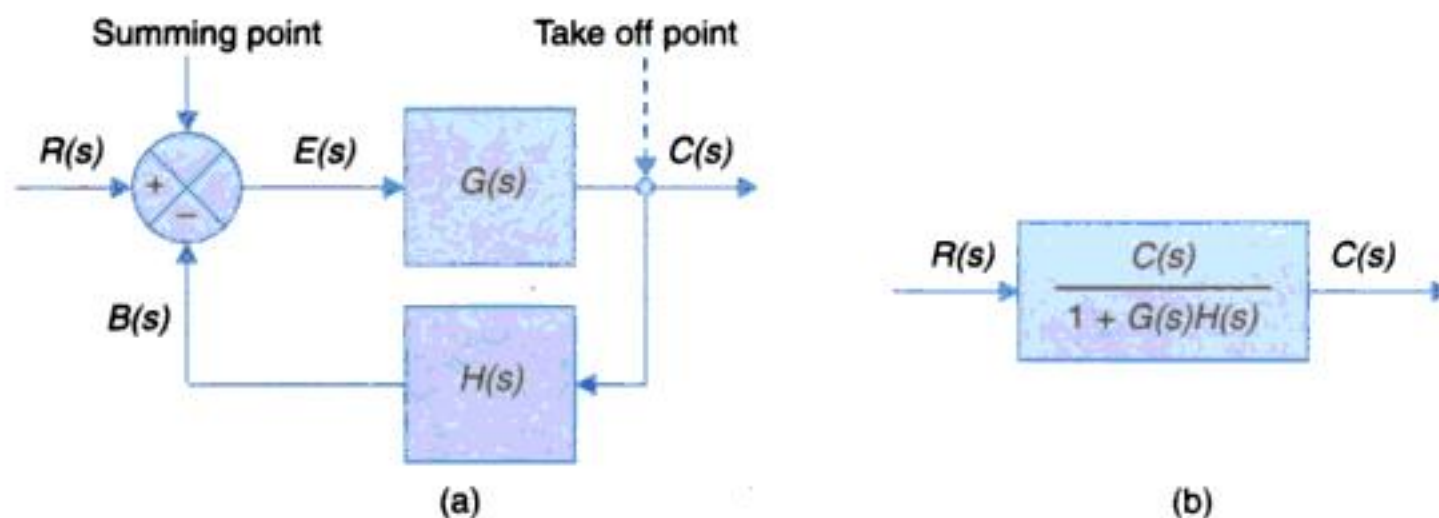


Fig. 2.26. (a) Block diagram of closed-loop system;
(b) Reduction of block diagram shown in Fig. 2.26 (a).

Eliminating $E(s)$ from eqns. (2.64) and (2.65) we have

$$C(s) = G(s)R(s) - G(s)H(s)C(s)$$

$$\text{or} \quad \frac{C(s)}{R(s)} = T(s) = \frac{G(s)}{1 + G(s)H(s)} \quad \dots(2.66)$$

Therefore the system shown in Fig. 2.26 (a) can be reduced to a single block shown in Fig. 2.26 (b).

Multiple-input-multiple-output Systems

When multiple inputs are present in a linear system, each input can be treated independently of the others. Complete output of the system can then be obtained by superposition, *i.e.*, outputs corresponding to each input along are added together.

Consider a two-input linear system shown in Fig. 2.27 (a). The response to the reference input can be obtained by assuming $U(s) = 0$. The corresponding block diagram shown in Fig. 2.27 (b) gives

$$\begin{aligned} C_R(s) &= \text{output due to } R(s) \text{ acting alone} \\ &= \frac{G_1(s)G_2(s)}{1 + G_1(s)G_2(s)H(s)} R(s) \end{aligned} \quad \dots(2.67)$$

Similarly the response to the input $U(s)$ is obtained by assuming $R(s) = 0$. The block diagram corresponding to this case is shown in Fig. 2.27 (c), which gives

$$\begin{aligned} C_U(s) &= \text{input due to } U(s) \text{ acting along} \\ &= \frac{G_2(s)}{1 + G_1(s)G_2(s)H(s)} U(s) \end{aligned} \quad \dots(2.68)$$

The response to the simultaneous application of $R(s)$ and $U(s)$ can be obtained by adding the two individual responses.

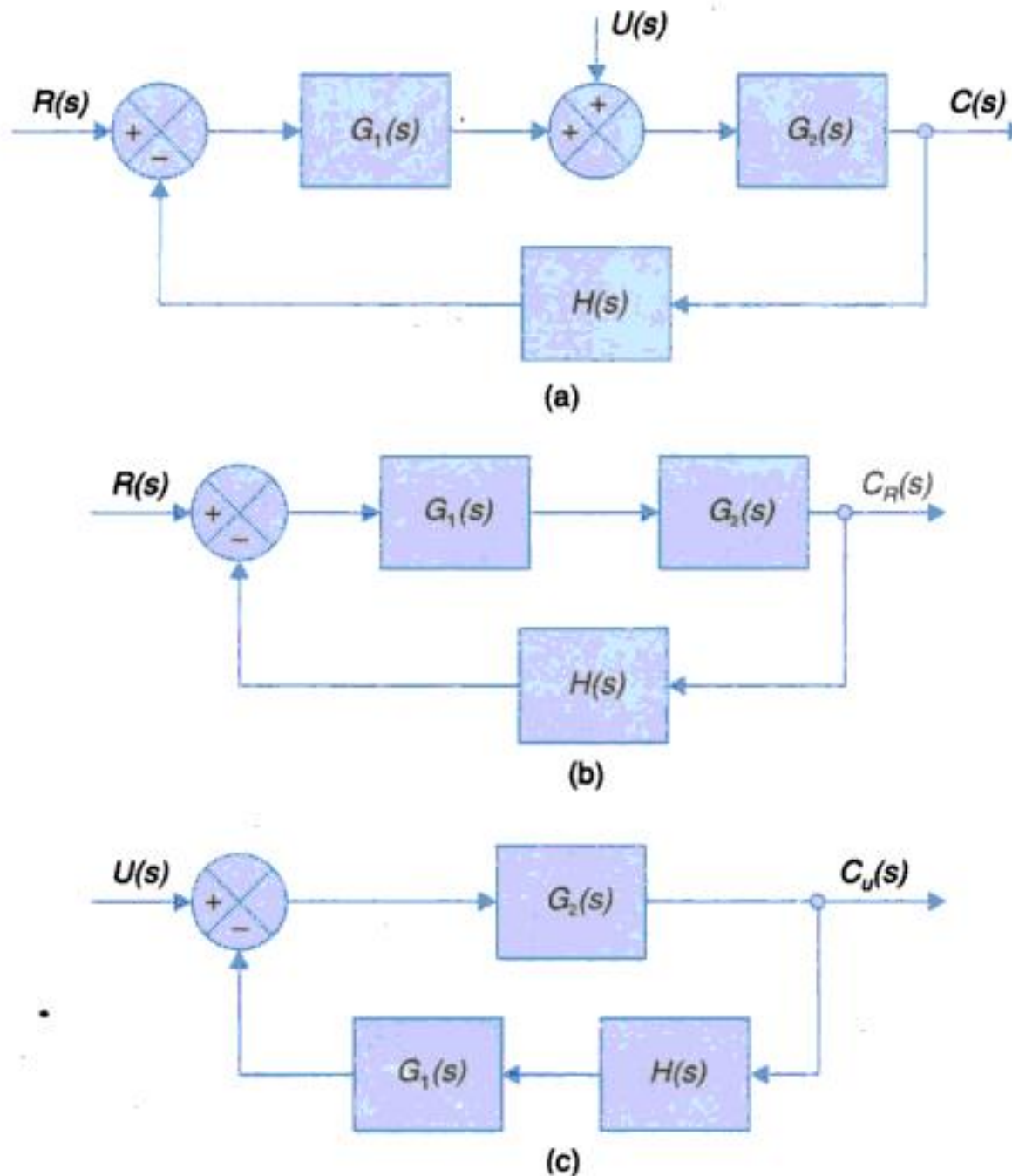


Fig. 2.27. Block diagram of two-input system.

Adding eqns. (2.67) and (2.68), we get

$$C(s) = C_R(s) + C_U(s) = \frac{G_2(s)}{1 + G_1(s)G_2(s)H(s)} [G_1(s)R(s) + U(s)] \quad \dots(2.69)$$

In case of multiple-input multiple-output system shown in Fig. 2.28 (r inputs and m outputs), the i -th output $C_i(s)$ is given by the principle of superposition as

$$C_i(s) = \sum_{j=1}^r G_{ij}(s)R_j(s); i = 1, 2, \dots, m \quad \dots(2.70)$$

where $R_j(s)$ is the j -th input and $G_{ij}(s)$ is the transfer function between the i -th output and j -th input with all other inputs reduced to zero.

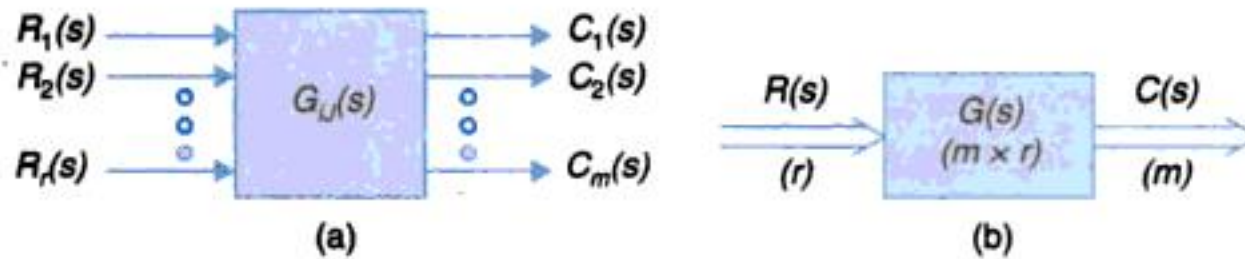


Fig. 2.28. Multiple-input-multiple-output systems.

Equation (2.69) can be expressed in matrix form as

$$\begin{bmatrix} C_1(s) \\ C_2(s) \\ \vdots \\ C_m(s) \end{bmatrix} = \begin{bmatrix} G_{11}(s) & G_{12}(s) & \dots & G_{1r}(s) \\ \vdots & \vdots & & \vdots \\ G_{m1}(s) & G_{m2}(s) & \dots & G_{mr}(s) \end{bmatrix} \begin{bmatrix} R_1(s) \\ R_2(s) \\ \vdots \\ R_r(s) \end{bmatrix} \quad \dots(2.71)$$

This can be expressed in compressed matrix notation as

$$\mathbf{C}(s) = \mathbf{G}(s)\mathbf{R}(s) \quad \dots(2.72)$$

where $\mathbf{R}(s)$ = vector of inputs (in Laplace transform), dimension r

$\mathbf{G}(s)$ = matrix transfer function ($m \times r$)

$\mathbf{C}(s)$ = vector of output (m)

The corresponding block diagram can be drawn as in Fig. 2.28(b) where thick arrows represent multi inputs and outputs.

When feedback loop is present each feedback signal is obtained by processing in general all the outputs. Thus for i th feedback signal we can write

$$B_i(s) = \sum_{j=1}^m H_{ij}(s)C_j(s) \quad \dots(2.73)$$

The i th error signal is then

$$E_i(s) = R_i(s) - B_i(s) \quad \dots(2.74)$$

Generalizing in matrix form we can write

$$\mathbf{C}(s) = \mathbf{G}(s) \mathbf{E}(s) \quad \dots(i)$$

$$\mathbf{E}(s) = \mathbf{R}(s) - \mathbf{B}(s) \quad \dots(ii)$$

$$\mathbf{B}(s) = \mathbf{H}(s) \mathbf{C}(s) \quad \dots(iii)$$

Substituting eqns. (ii) and (iii) in eqn. (i), we get

$$\mathbf{C}(s) = \mathbf{G}(s) [\mathbf{R}(s) - \mathbf{H}(s) \mathbf{C}(s)] = \mathbf{G}(s) \mathbf{R}(s) - \mathbf{G}(s) \mathbf{H}(s) \mathbf{C}(s) \quad \dots(iv)$$

This can be simplified as

$$\mathbf{C}(s) + \mathbf{G}(s) \mathbf{H}(s) \mathbf{C}(s) = \mathbf{G}(s) \mathbf{R}(s)$$

or $\mathbf{C}(s) [\mathbf{I} + \mathbf{G}(s) \mathbf{H}(s)] = \mathbf{G}(s) \mathbf{R}(s)$

or $\mathbf{C}(s) = [\mathbf{I} + \mathbf{G}(s) \mathbf{H}(s)]^{-1} \mathbf{G}(s) \mathbf{R}(s) \quad \dots(2.75)$

wherein closed loop matrix transfer function as

$$\mathbf{T}(s) = \mathbf{G}(s) [\mathbf{I} + \mathbf{G}(s) \mathbf{H}(s)]^{-1} \quad \dots(2.76)$$

The results are represented in thick arrow block diagram of Fig. 2.29. The reader may compare this block diagram and matrix equation (2.76) with the block diagram of Fig. 2.26 and eqn. (2.66) of the single-input-single-output case.

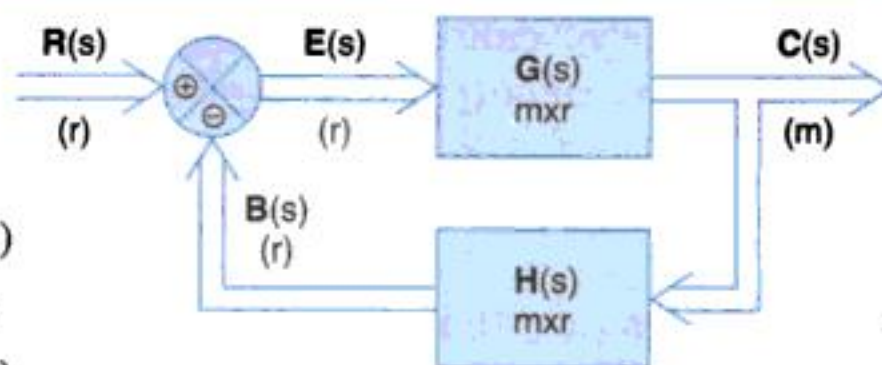


Fig. 2.29. Block diagram of multi-input multi-output closed-loop system.

Block Diagram Reduction

As indicated earlier, a complex block diagram configuration can be simplified by certain rearrangements of block diagram using the rules of block diagram algebra. Some of the important rules are given in Table 2.4. All these rules are derived by simple algebraic manipulations of the equations representing the blocks.

As an example, let us consider the liquid-level system shown in Fig. 2.30 (note that because of interaction of the tanks, the complete transfer function cannot be obtained by multiplying individual transfer functions of the tanks).

In this system, a tank having liquid capacitance C_1 is supplying liquid through a pipe of resistance R_1 to another tank of liquid capacitance C_2 , which delivers this liquid through a pipe of resistance R_2 . The steady-state outflow rates of tank 1 and that of tank 2 are Q_1 and Q_2 and heads are H_1 and H_2 respectively.

Let ΔQ be a small deviation in the inflow rate Q . This results in

ΔH_1 = small deviation of the head of tank 1 from its steady-state value.

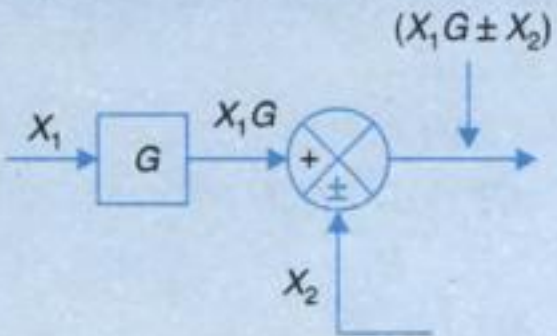
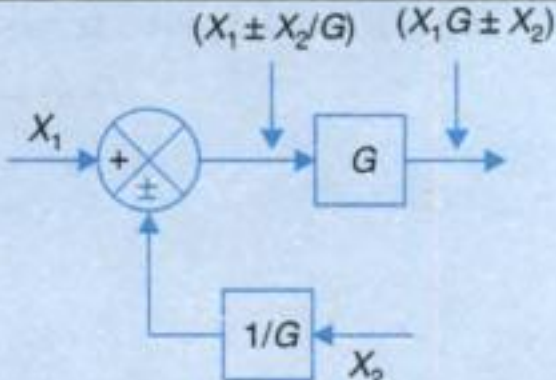
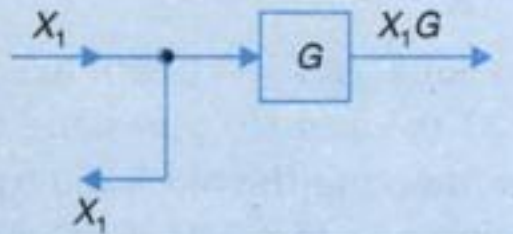
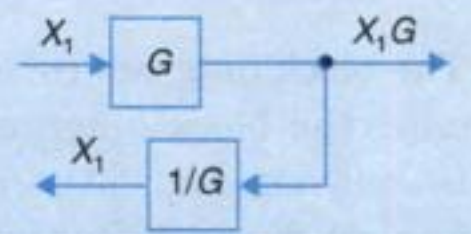
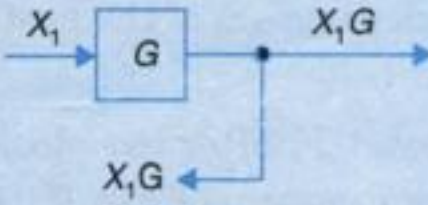
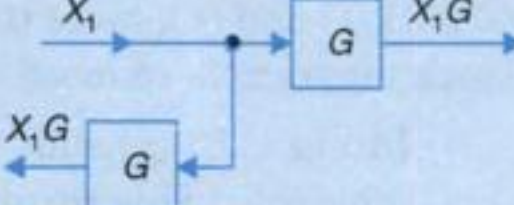
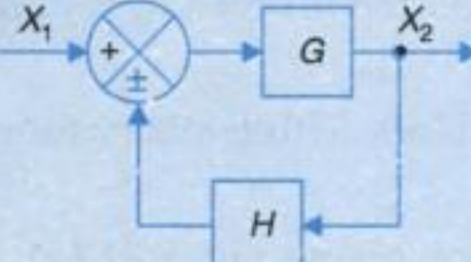
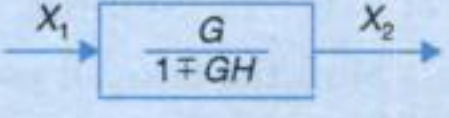
ΔH_2 = small deviation of the head of the tank 2 from its steady-state value.

ΔQ_1 = small deviation of the outflow rate of tank 1 from its steady-state value.

ΔQ_2 = small deviation of the outflow rate of tank 2 from its steady-state value.

Table 2.5. Rules of Block Diagram Algebra

Rule	Original diagram	Equivalent diagram
1. Combining blocks in cascade		
2. Moving a summing point after a block		

3. Moving a summing point ahead of a block		
4. Moving a take off point after a block		
5. Moving a take off point ahead of a block		
6. Eliminating a feedback loop		

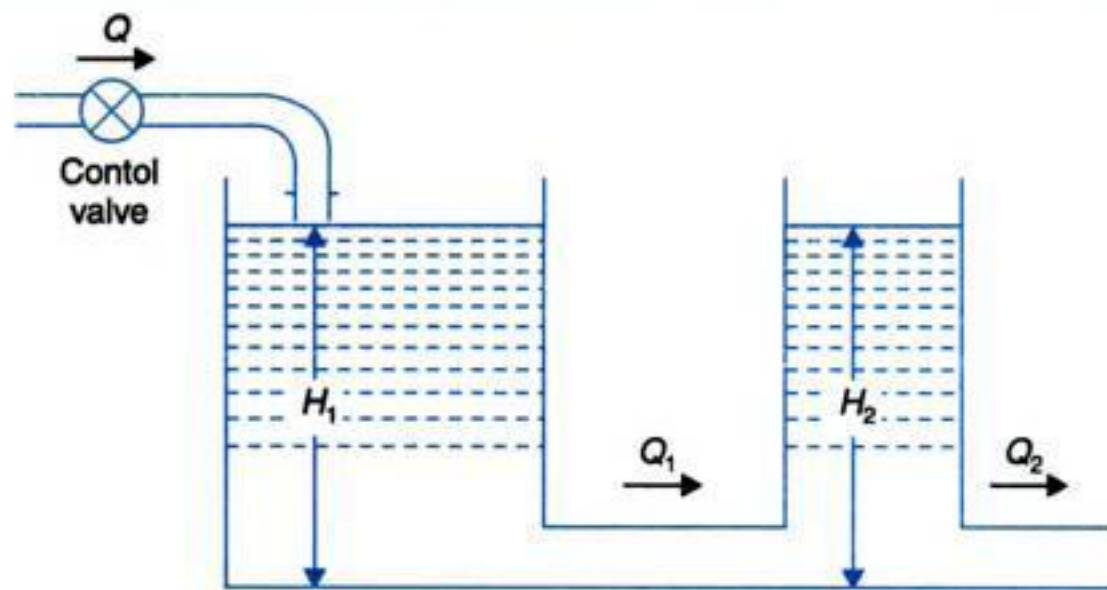


Fig. 2.30. Liquid-level system.

The flow balance equation for tank 1 is

$$\Delta Q = \Delta Q_1 + C_1 \frac{d}{dt}(\Delta H_1)$$

Similarly for tank 2

$$\Delta Q_1 = \Delta Q_2 + C_2 \frac{d}{dt}(\Delta H_2)$$

where

$$\Delta Q_1 = \frac{\Delta H_1 - \Delta H_2}{R_1} \quad \text{and} \quad \Delta Q_2 = \frac{\Delta H_2}{R_2}$$

Taking the Laplace transform of the above equations we get

$$\Delta Q(s) - \Delta Q_1(s) = sC_1\Delta H_1(s) \quad \dots(2.77)$$

$$\Delta Q_1(s) - \Delta Q_2(s) = sC_2\Delta H_2(s) \quad \dots(2.78)$$

$$\Delta Q_1(s) = \frac{\Delta H_1(s) - \Delta H_2(s)}{R_1} \quad \dots(2.79)$$

$$\Delta Q_2(s) = \frac{\Delta H_2(s)}{R_2} \quad \dots(2.80)$$

The block diagram corresponding to eqns. (2.77) – (2.80) are given in Figs. 2.31 (a)-(d). Connecting the block diagrams of Fig. 2.31 (a) and (b) gives the block diagram for tank 1, which is shown in Fig. 2.31 (e). Similarly connecting the block diagrams of Fig. 2.31 (c) and (d) gives the block diagram for tank 2 which is shown in Fig. 2.31 (f). Connecting the block diagrams of Figs. 2.31 (e) and (f), gives the overall block diagram of the system as shown in Fig. 2.31 (g). This block diagram is reduced in steps given below.

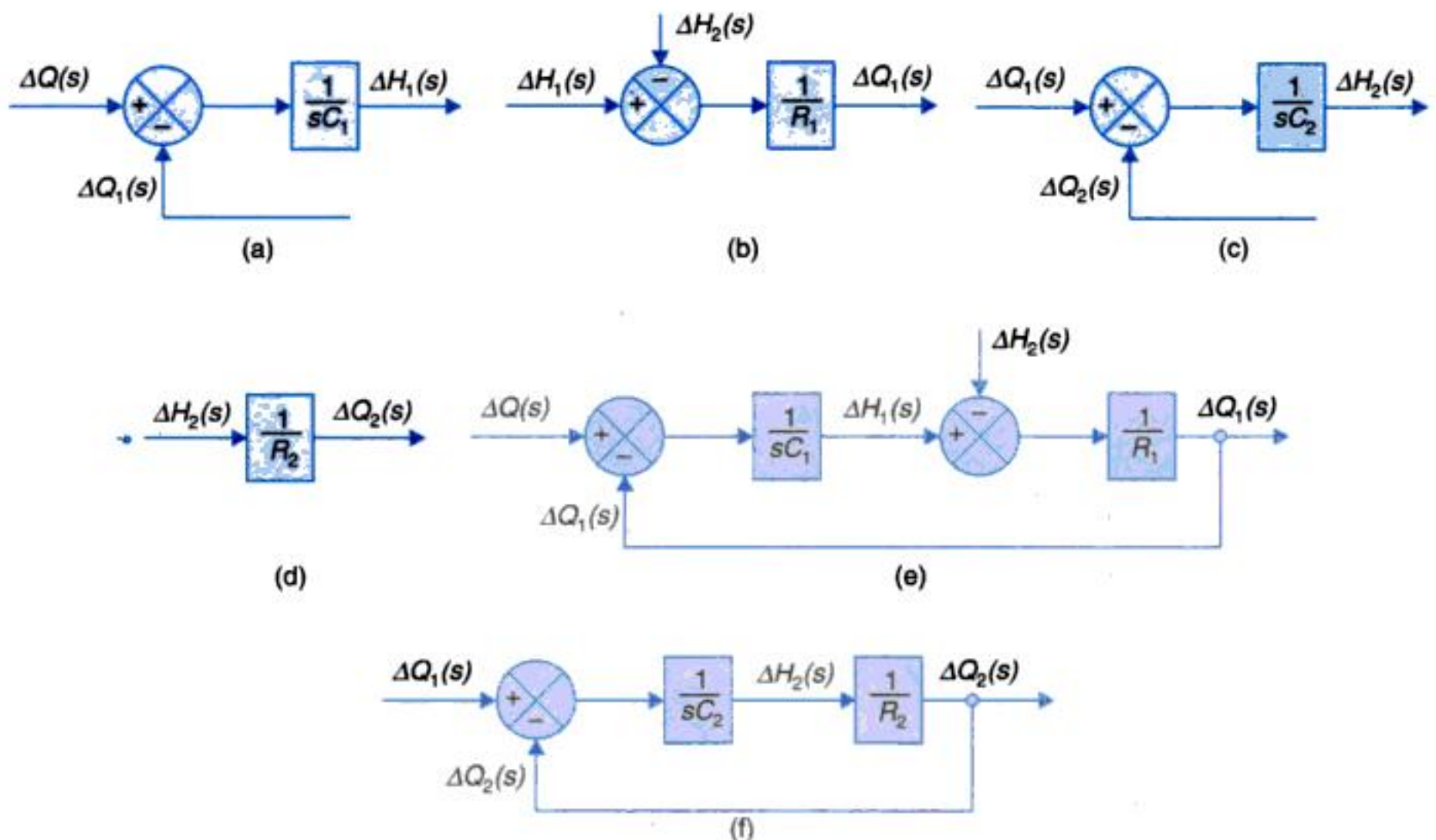
(i) In Fig. 2.31 (g) shift the take off point T_1 after the block with transfer function $1/R_2$ (rule 4 of Table 2.5). This results in the block diagram of Fig. 2.31.

(ii) Minor feedback loop enclosed in dotted line is now reduced to a single block by rules 1 and 6 of Table 2.5 resulting in Fig. 2.31.

(iii) Shift the take off point T_2 to the block with transfer function $1/(R_2C_2s + 1)$ resulting in Fig. 2.31.

(iv) Reduce the encircled feedback loop giving Fig. 2.31 (k).

(v) Reduce Fig. 2.31 (k) to the single block of Fig. 2.31, which gives the overall transfer function of the system.



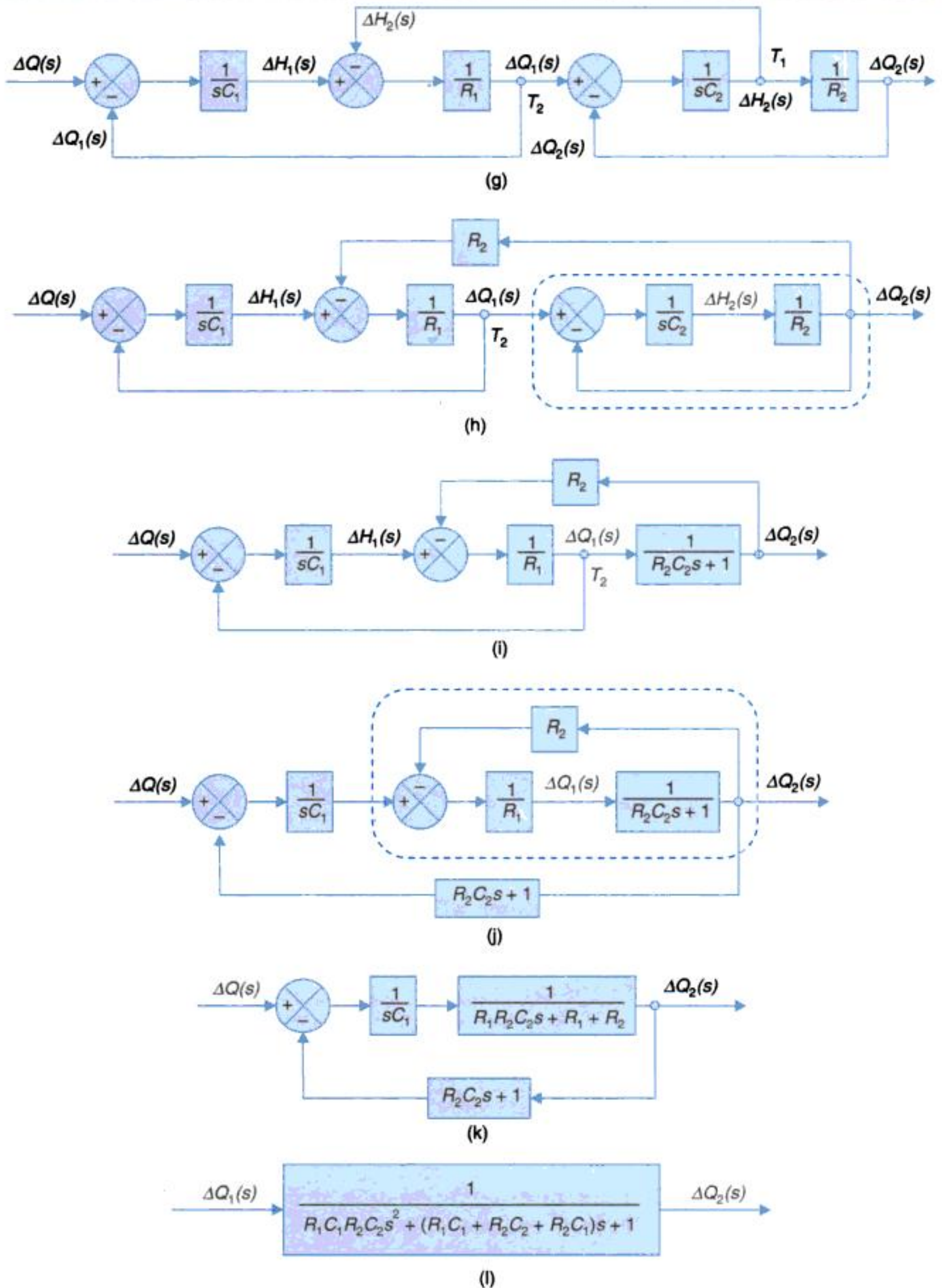


Fig. 2.31. Formation and reduction of block diagram of the system shown in Fig. 2.30.

Feedforward Compensation

Let us consider the example of Fig. 2.27 (a). The input $U(s)$ in this block diagram represents **Disturbance input** in control systems. Such an example will be considered later in this section 2.5 speed control system of Fig. 2.40. The effect of such an input is to introduce error into the system performance which needs to be kept low, within acceptable limits this is known as compensation. In several systems where the disturbance input can be predicted (or computed before hand), its effect can be eliminated by a feedforward compensation technique illustrated in the modified block diagram of Fig. 2.32.

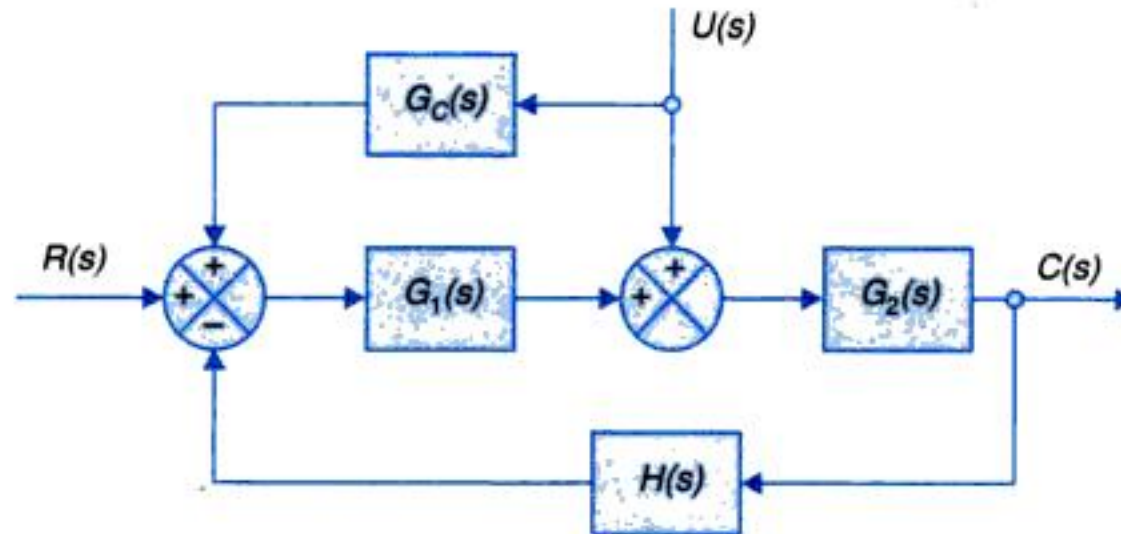


Fig. 2.32. Forward compensation.

The compensating block $G_c(s)$ causes additional input of $G_c(s)U(s)$ along with $U(s)$. It then follows from eqn. (2.67) that this would contribute to output a term

$$C_U(s) = \frac{G_2(s) + G_1(s)G_2(s)G_c(s)}{1 + G_1(s)G_2(s)H(s)} U(s) \quad \dots(2.81)$$

For this to cancel out the output component $C_U(s)$ due to disturbance input $U(s)$, the following condition has to be met.

$$G_2(s) + G_1(s)G_2(s)G_c(s) = 0 \quad \text{or} \quad G_c(s) = -\frac{1}{G_1(s)} \quad \dots(2.82)$$

The issues of this type of compensation will be considered further in chapter.

2.6 SIGNAL FLOW GRAPHS

Block diagrams are very successful for representing control systems, but for complicated systems, the block diagram reduction process is tedious and time consuming. An alternate approach is that of signal flow graphs developed by S.J. Mason, which does not require any reduction process because of availability of a flow graph gain formula which relates the input and output system variables.

A signal flow graph is a graphical representation of the relationships between the variables of a set of linear algebraic equations. It consists of a network in which nodes representing each of the system variables are connected by directed branches. The closed-loop system whose block diagram is shown in Fig. 2.26 (a) has the signal flow representation given

in Fig. 2.33 (a). The formulation of this signal flow graph is explained through the various signal flow terms defined below.

1. *Node*. It represents a system variable which is equal to the sum of all incoming signals at the node. Outgoing signals from the node do not affect the value of the node variable. For example, R , E , B and C are nodes in Fig. 2.33 (a). These symbols also represent the corresponding node variables.

2. *Branch*. A signal travels along a branch from one node to another in the direction indicated by the branch arrow and in the process gets multiplied by the gain or transmittance of the branch. For example, the signal reaching the node C from the node E is given by GE where G is the branch transmittance and the branch is directed from the node E to the node C in Fig. 2.33 (a). Thus the value of the node variable $C = GE$.

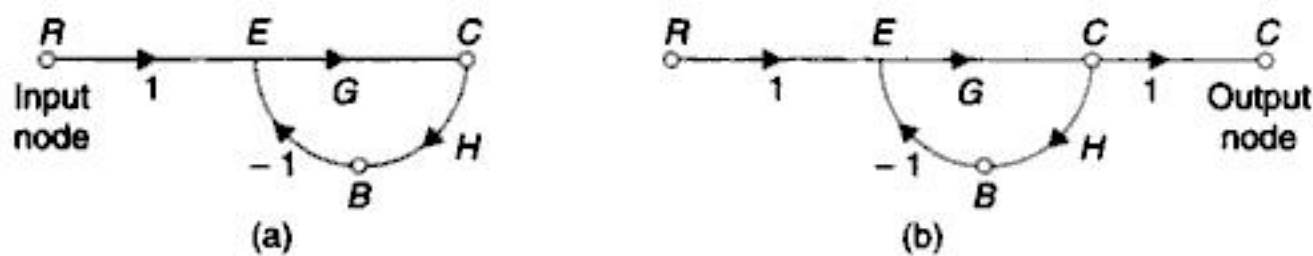


Fig. 2.33. Signal flow graph of a closed-loop system.

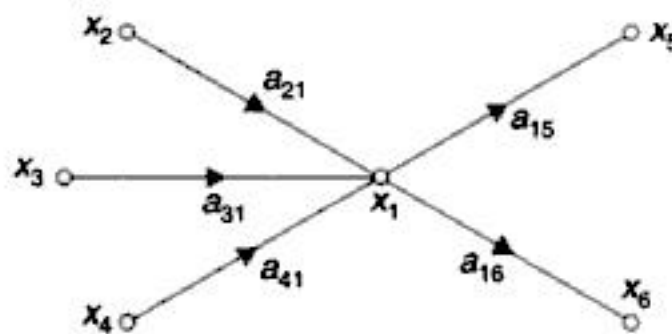


Fig. 2.34. Node as a summing point and as a transmitting point.

(a) *Node as a summing point*

With reference to the signal flow graph of Fig. 2.34, the node variable x_1 is expressed

$$x_1 = a_{21} x_2 + a_{31} x_3 + a_{41} x_4 = \text{sum of all incoming signals.}$$

(b) *Node as a transmitting point*

A node variable is transmitted through all branches outgoing from the node. Thus in the signal flow graph of Fig. 2.34.

$$x_5 = a_{15} x_1 \quad \dots(2.83)$$

$$x_6 = a_{16} x_1$$

As already stated in (1) above the value of the node variable is not affected by the outgoing branches.

3. *Notation*. a_{ij} is the transmittance of the branch directed from node x_i to node x_j .

4. *Input node or source*. It is a node with only outgoing branches. For example, R is an input node in Fig. 2.33 (a).

5. *Output node or sink.* It is a node with only incoming branches. However, this condition is not always met. An additional branch with unit gain may be introduced in order to meet this specified condition. For example, the node *C* in Fig. 2.33 (a) has one outgoing branch but after introducing an additional branch with unit transmittance as shown in Fig. 2.33 (b) the node becomes an output node.

6. *Path.* It is the traversal of connected branches in the direction of the branch arrows such that no node is traversed more than once.

7. *Forward path.* It is a path from the input node to the output node. For example, *R-E-C* is a forward path in Fig. 2.33 (a).

8. *Loop.* It is a path which originates and terminates at the same node. For example, *E-C-B-E* is a loop in Fig. 2.33 (a).

9. *Non-touching loops.* Loops are said to be non-touching if they do not possess any common node.

10. *Forward path gain.* It is the product of the branch gains encountered in traversing a forward path. For example, forward path gain of the path *R-E-C* in Fig. 2.33 (a) is *G*.

11. *Loop gain.* It is the product of branch gains encountered in traversing the loop. For example, loop gain of the loop *E-C-B-E* in Fig. 2.33 (a) is $-GH$.

Construction of Signal Flow Graphs

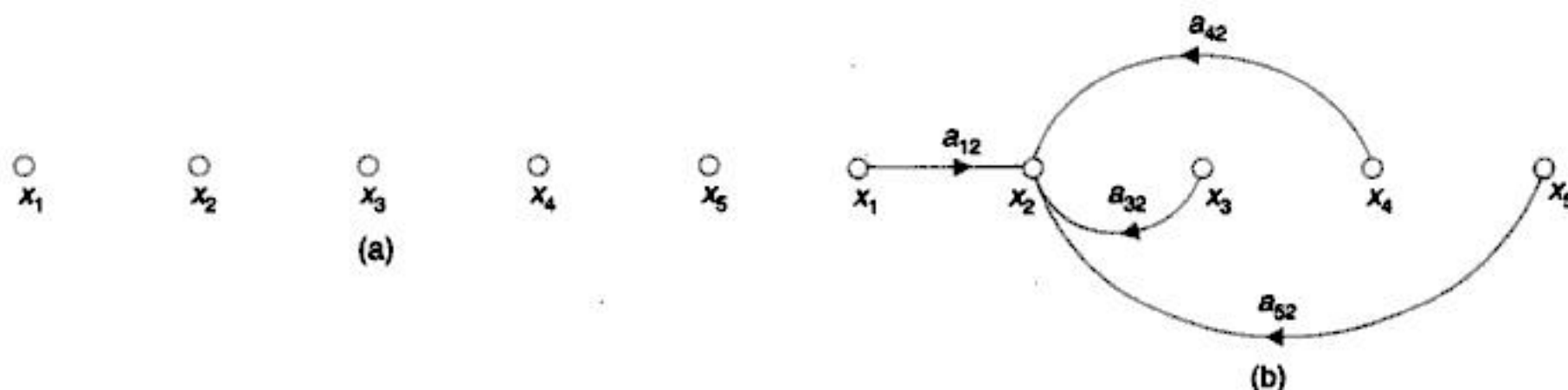
The signal flow graph of a system is constructed from its describing equations. To outline the procedure, let us consider a system described by the following set of equations:

$$\begin{aligned}x_2 &= a_{12}x_1 + a_{32}x_3 + a_{42}x_4 + a_{52}x_5 \\x_3 &= a_{23}x_2 \\x_4 &= a_{34}x_3 + a_{44}x_4 \\x_5 &= a_{35}x_3 + a_{45}x_4\end{aligned}\quad \dots(2.84)$$

where x_1 is the input variable and x_5 is the output variable.

The signal flow graph for this system is constructed as shown in Fig. 2.35. First the nodes are located as shown in Fig. 2.35 (a). The first equation in (2.84) states that x_2 is equal to sum of four signals and its signal flow graph is shown in Fig. 2.35 (b). Similarly, the signal flow graphs for the remaining three equations in (2.84) are constructed as shown in Figs. 2.35 (c), (d) and (e) respectively giving the complete signal flow graph of Figs. 2.35 (f).

The overall gain from input to output may be obtained by Mason's gain formula.



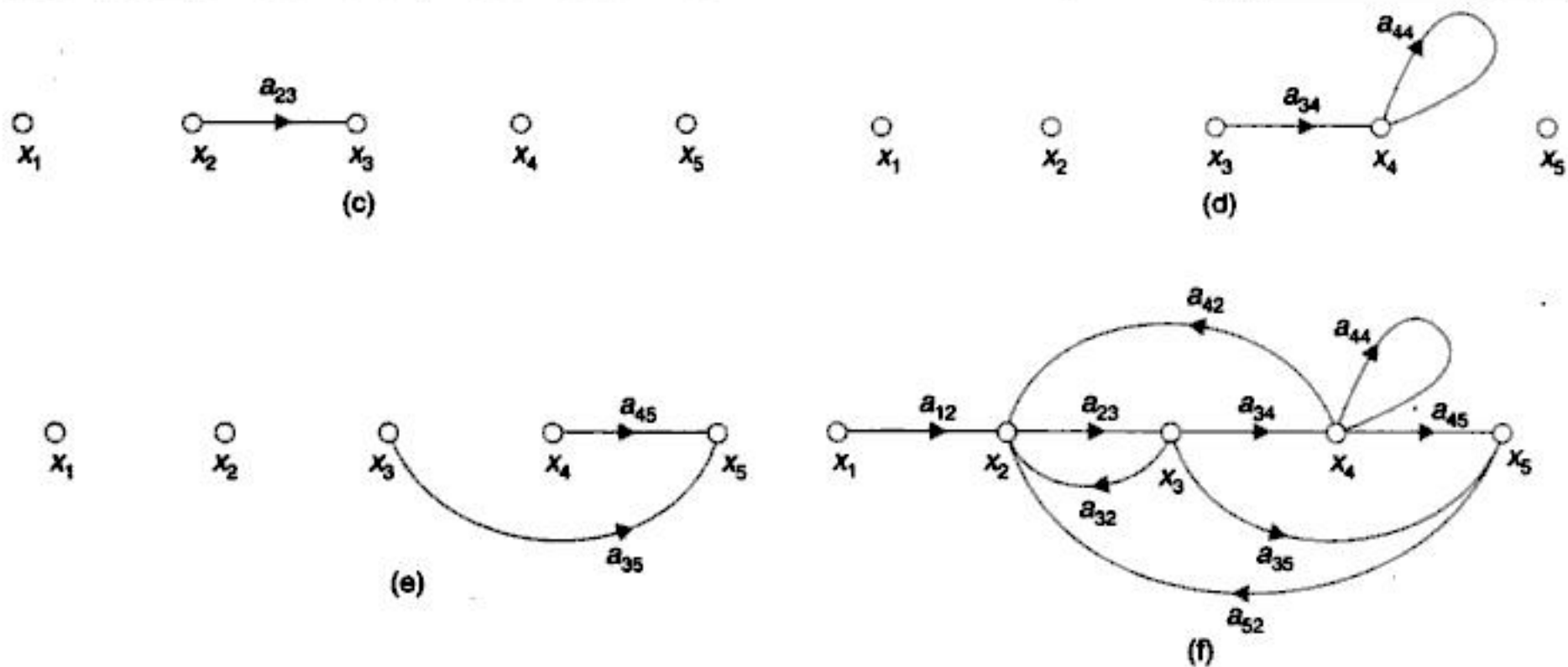


Fig. 2.35. Construction of signal flow graph for eqns. (2.84).

Mason's Gain Formula

The relationship between an input variable and an output variable of a signal flow graph is given by the net gain between the input and output nodes and is known as the overall gain of the system. Mason's gain formula for the determination of the overall system gain is given by:

$$T = \frac{1}{\Delta} \sum_K P_K \Delta_K \quad \dots(2.85)$$

where P_K = path gain of K -th forward path; Δ = determinant of the graph = $1 - (\text{sum of loop gains of all individual loops}) + (\text{sum of gain products of all possible combinations of two non-touching loops}) - (\text{sum of gain products of all possible combinations of three non-touching loops}) + \dots$, i.e.,

$$\Delta = 1 - \sum_m P_{m_1} + \sum_m P_{m_2} - \sum_m P_{m_3} + \dots \quad \dots(2.86)$$

where P_{mr} = gain product m -th possible combination of r non-touching* loops; Δ_K = the value of Δ for the part of the graph not touching the K -th forward path; and T = overall gain of the system.

Let us illustrate the use of Mason's formula by finding the overall gain of the signal flow graph shown in Fig. 2.35. The following conclusions are drawn by inspection of this signal flow graph.

1. There are two forward paths with path gains

$$P_1 = a_{12}a_{23}a_{34}a_{45} \quad \text{Fig. 2.36 (a)}$$

$$P_2 = a_{12}a_{23}a_{35} \quad \text{Fig. 2.36 (b)}$$

2. There are five individual loops with loop gains

$$P_{11} = a_{23}a_{32} \quad \text{Fig. 2.36 (c)}$$

*Non-touching implies that no node is common between the two.

$$P_{21} = a_{23}a_{34}a_{42} \quad \text{Fig. 2.36 (d)}$$

$$P_{31} = a_{44} \quad \text{Fig. 2.36 (e)}$$

$$P_{41} = a_{23}a_{34}a_{45}a_{52} \quad \text{Fig. 2.36 (f)}$$

$$P_{51} = a_{23}a_{35}a_{52} \quad \text{Fig. 2.36 (g)}$$

3. There are two possible combinations of two non-touching loops with loop gain products

$$P_{12} = a_{23}a_{32}a_{44} \quad \text{Fig. 2.36 (h)}$$

$$P_{22} = a_{23}a_{35}a_{52}a_{44} \quad \text{Fig. 2.36 (i)}$$

4. There are no combinations of three non-touching loops, four non-touching loops, etc.

Therefore

$$P_{m3} = P_{m4} = \dots = 0$$

Hence from eqn. (2.85)

$$\Delta = 1 - (a_{23}a_{32} + a_{23}a_{34}a_{42} + a_{44} + a_{23}a_{34}a_{45}a_{52} + a_{23}a_{35}a_{52}) + (a_{23}a_{32}a_{44} + a_{23}a_{35}a_{52}a_{44})$$

5. First forward path is in touch with all the loops. Therefore, $\Delta_1 = 1$. The second forward path is not in touch with one loop (Fig. 2.36 (j)). Therefore, $\Delta_2 = 1 - a_{44}$.

From eqn. (2.85), the

$$T = \frac{x_5}{x_1} = \frac{P_1\Delta_1 + P_2\Delta_2}{\Delta} = \frac{a_{12}a_{23}a_{34}a_{45} + a_{12}a_{23}a_{35}(1 - a_{44})}{1 - a_{23}a_{32} - a_{23}a_{34}a_{42} - a_{44} - a_{23}a_{34}a_{45}a_{52} + a_{23}a_{32}a_{44} + a_{23}a_{35}a_{52}a_{44}} \quad \dots(2.87)$$

State Variable Formulation

So far we have considered the transfer function approach (single/multi input, output) using both block diagram algebra and signal flow graph. Before we consider further examples of signal flow graphs in control systems, we will consider an alternate organization of a system's differential equations as a set of first-order differential equations. This is known as the state variable formulation and will be studied in detail in Chapter 12. Here we shall introduce the technique through a simple example by using the insight acquired into the physical systems considered so far.

Consider a simple system described by the first-order differential equation

$$\dot{x} = ax; x(t=0) = x(0) \quad \dots(2.88)$$

As x defines the system *state* for $t \geq 0$, it is called a *state variable* and eqn. (2.88) is the *state equation*.

Observe that the system has no input but has an initial condition (at $t = 0$). Integrating \dot{x} we have

$$x = \int \dot{x} dt + x(0) \quad \dots(2.89)$$

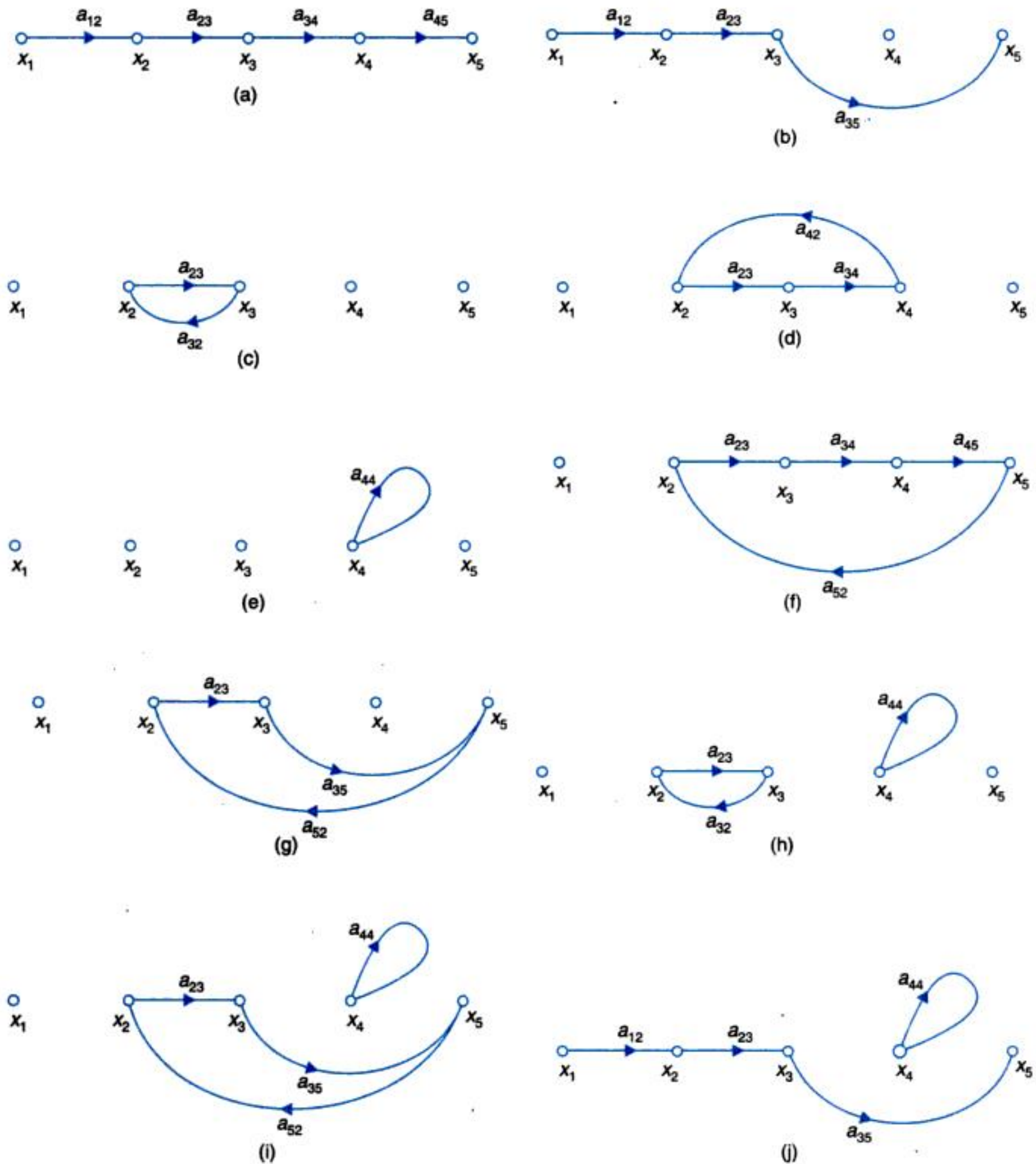


Fig. 2.36. Application of Mason's formula to the signal flow graph shown in Fig. 2.35.

The signal flow diagram for eqns. (2.88) and (2.89) can be drawn as in Fig. 2.37 (a) with integration symbol introduced as a transmittance of the branch from node \dot{x} to x . This is the time-domain representation.

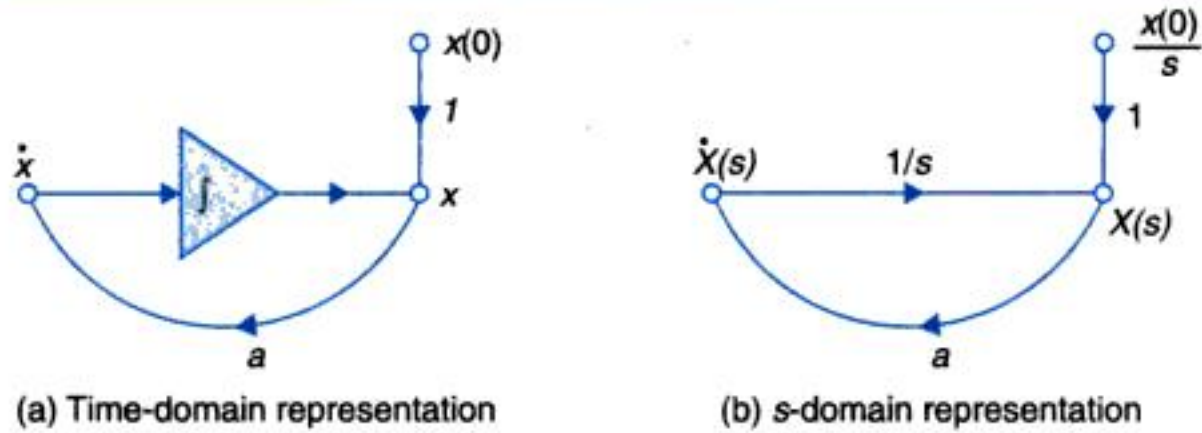


Fig. 2.37. Signal flow graph of first-order system.

Take now the Laplace transform of eqn. (2.88)

$$\dot{X}(s) = aX(s) \quad \dots(2.90a)$$

But

$$\dot{X}(s) = sX(s) - x(0) \quad \dots(2.90b)$$

or

$$X(s) = \frac{1}{s} \dot{X}(s) + \frac{1}{s} x(0) \quad \dots(2.91)$$

Equations (2.90a) and (2.91) would give the signal flow graph in s-domain, as in Fig. 2.37 (b).

Consider now a first-order system with input u

$$\dot{x} = ax + bu; x(t=0) = x(0) \quad \dots(2.92)$$

whose s-domain signal flow diagram is drawn in Fig. 2.38 (a).

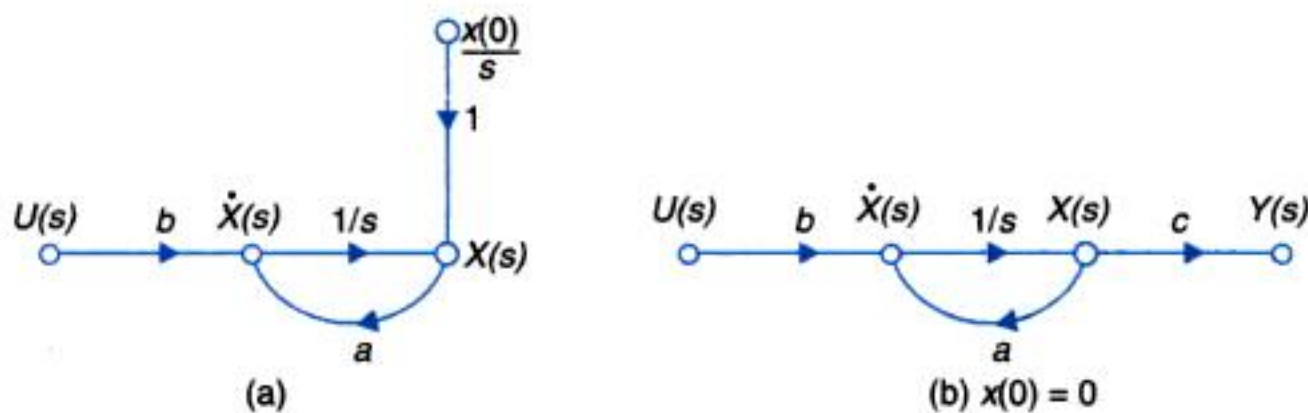


Fig. 2.38

Assume that the system output is given as

$$y = cx \quad \dots(2.93)$$

The modified signal flow graph is drawn in Fig. 2.38 (b) wherein it is assumed that $x(0) = 0$. Observing that there is one forward path and one loop and applying the Mason's gain formula, we have

$$\begin{aligned} P_1 &= bc/s \\ \Delta_1 &= 1 \\ \Delta &= 1 - \Delta_{11} = 1 - (a/s) = (s - a)/s \\ T(s) &= \frac{Y(s)}{U(s)} = \frac{P_1 \Delta_1}{\Delta} = \frac{(bc/s)}{(s - a)/s} = \frac{bc}{s - a} \quad \dots(2.94) \end{aligned}$$

In case of second-order system two first-order state variable equations would be needed and in general n equations for n -th-order system. Let us consider the example of armature-

controlled *dc* motor of Fig. 2.21 wherein we shall now regard the output of interest as motor speed $\omega = \dot{\theta}$. The block diagram of Fig. 2.22 is then redrawn as in Fig. 2.38 from which we can write

$$\begin{aligned} K_T I_a(s) &= Js\omega(s) + f_0 \omega(s) \\ E(s) - K_b \omega(s) &= L_a s I_a(s) + R_a I_a(s) \end{aligned}$$

Taking the inverse Laplace transform (initial condition being zero)

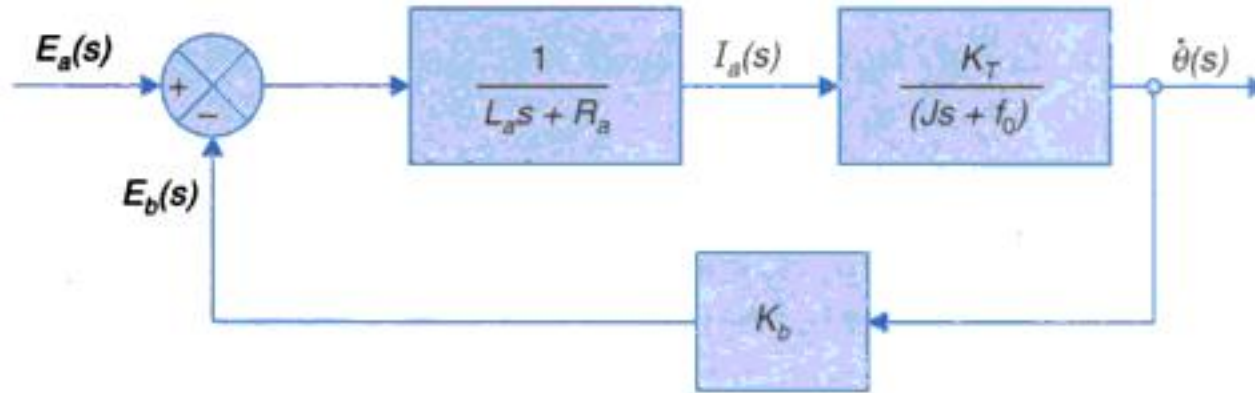


Fig. 2.38. Armature-controlled d.c. motor.

$$\begin{aligned} K_T i_a(t) &= J \frac{d\omega(t)}{dt} + f_0 \omega(t) \\ e_a(t) - K_b \omega(t) &= L_a \frac{di_a(t)}{dt} + R_a i_a(t) \end{aligned}$$

We can recognize these equations as first-order equations in ω and i_a which are then recognized as state variables, while $e(t)$ is the system input. We thus have

$$\frac{d\omega(t)}{dt} = (f_0/J)\omega(t) + (K_T/J)i_a(t) \quad \dots(2.95a)$$

$$\frac{di_a(t)}{dt} = -(K_b/L_a)\omega(t) - (R_a/L_a)i_a(t) + (1/L_a)e_a(t) \quad \dots(2.95b)$$

Dropping the bracketed variable t for convenience of writing we can then rewrite these state equations in vector-matrix form as

$$\begin{bmatrix} \frac{d\omega}{dt} \\ \frac{di_a}{dt} \end{bmatrix} = \begin{bmatrix} -(f_0/J) & (K_T/J) \\ -(K_b/L_a) & -(R_a/L_a) \end{bmatrix} \begin{bmatrix} \omega \\ i_a \end{bmatrix} + \begin{bmatrix} 0 \\ 1/L_a \end{bmatrix} e_a \quad \dots(2.96a)$$

We will reidentify the state variables as

$$x_1 = \omega, x_2 = i_a$$

and input as $u = e$ and output as

$$y = \omega = [1 \ 0] \begin{bmatrix} \omega \\ i_a \end{bmatrix} \quad \dots(2.96b)$$

We can now write eqns. (2.96a) and (b) in standard form as

$$\begin{bmatrix} \dot{x}_1 \\ \dot{x}_2 \end{bmatrix} = \begin{bmatrix} a_{11} & a_{12} \\ a_{21} & a_{22} \end{bmatrix} \begin{bmatrix} x_1 \\ x_2 \end{bmatrix} + \begin{bmatrix} b_1 \\ b_2 \end{bmatrix} u; u = e_a \quad \dots(2.97a)$$

$$y = [c_1 \ c_2] \begin{bmatrix} x_1 \\ x_2 \end{bmatrix} \quad \dots(2.97b)$$

In compact vector-matrix notation

$$\dot{\mathbf{x}} = \mathbf{Ax} + \mathbf{bu} \quad \dots(2.98a)$$

$$\mathbf{y} = \mathbf{Cx} \quad \dots(2.98b)$$

This is the state variable representation of a single-input-single-output (SISO) system. In multi-input multi-output (MIMO) system u and y will acquire the vector form.

The state variables identified in the above example are physical variables and are directly available for measurement. Indeed the state variables for a given system are not unique and these can be defined in a number of other ways. These and associated topics will be discussed at length in Chapter 12.

Speed Control System

As an example let us consider a feedback speed control system whose objective is move the load at desired speed. This is easily achieved using the armature controlled *dc* motor of Fig. 2.21 by providing a feedback control loop as in Fig. 2.39 wherein the voltage signal e_t proportional to input speed (ω) generated by a *dc* tachometer coupled the motor armature is fed back negatively and is subtracted from the reference voltage e_r , creating the difference (error) signal e . This error signal e is then amplified to control the armature current i_a such that the motor acquires the desired speed, while driving the load (J, f and torque T_D).

A *dc* tachometer is just a conventional *dc* generator usually of permanent magnet kind, whose output voltage is a measure of speed. Thus

$$e_t = K_t \omega, \text{ excitation being constant} \quad \dots(2.99)$$

where K_t (V/rad/s) is the tachometer constant.

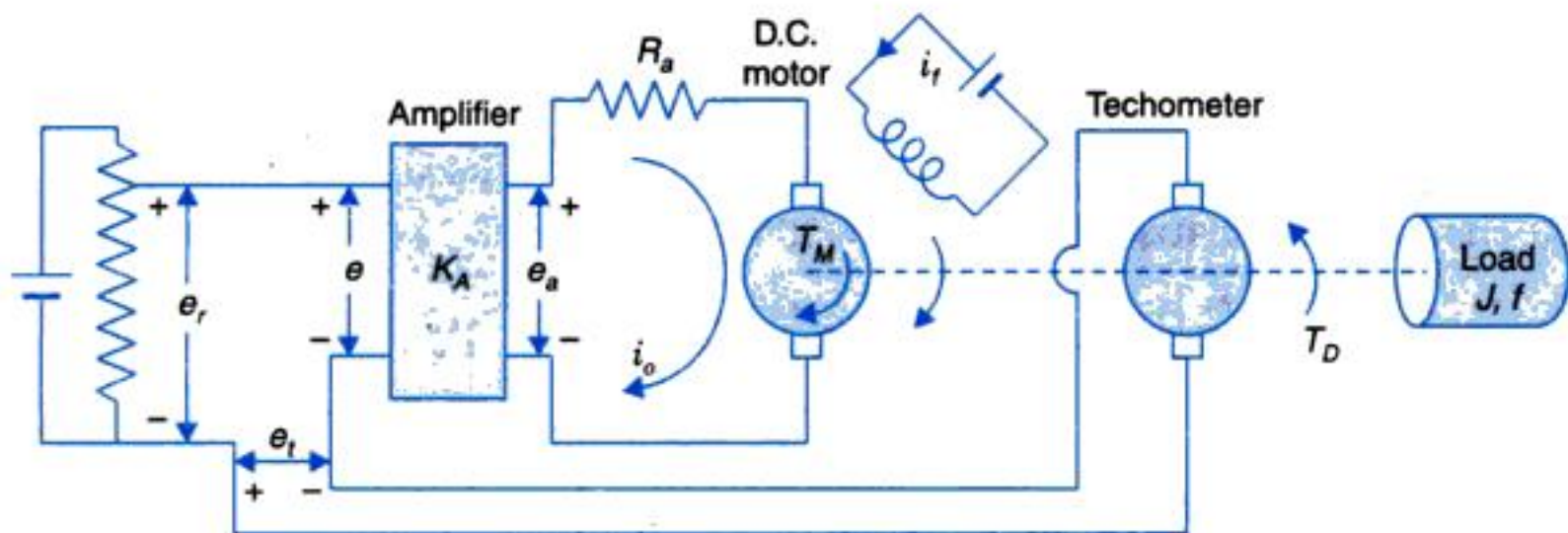
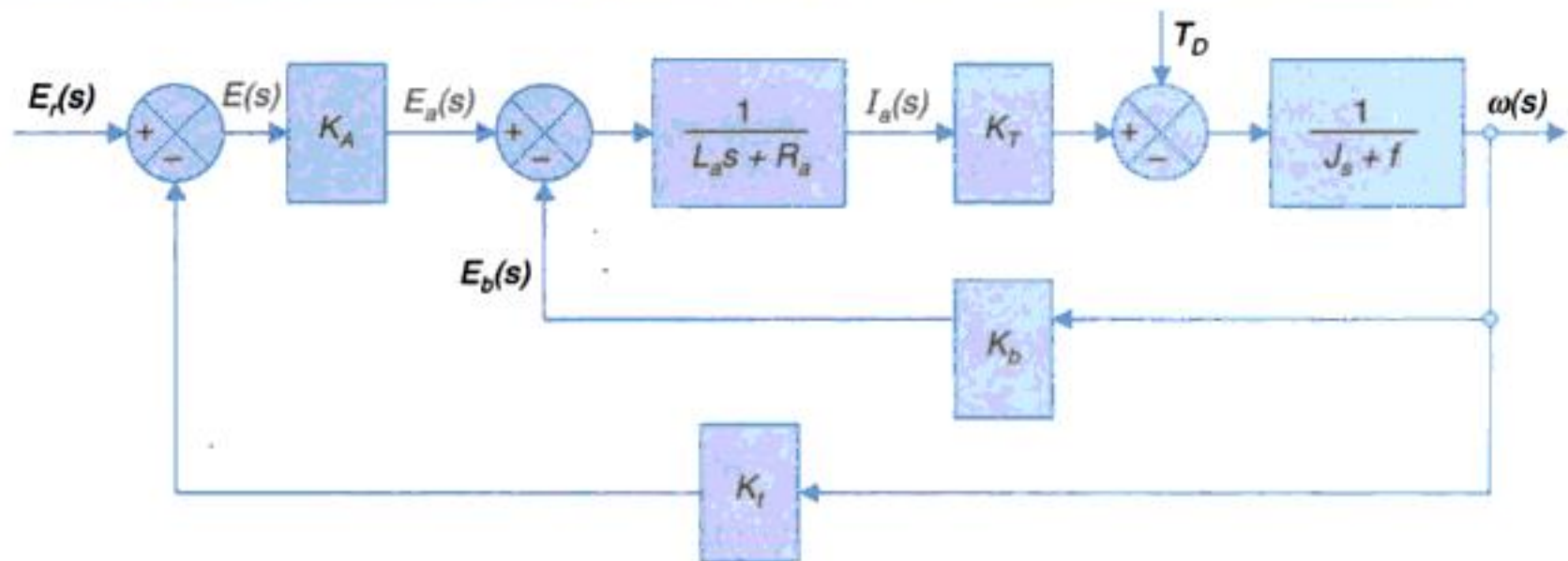


Fig. 2.39. A speed control system.

The block diagram of the speed control system of Fig. 2.39 can be easily drawn as in Fig. 2.40 (a) by modifying the block diagram of Fig. 2.23 of the armature-controlled *dc* motor. The outer feedback loop accounts for the speed feedback which is basic to the speed regulation action. The load torque T_D which opposes the motor torque enters negatively in the block diagram so that the torque applied to load (and motor) inertia and friction is $(T_M - T_D)$.

Let us convert this block diagram into a signal flow graph while making the simplifying assumption that $L_a \approx 0$. The signal flow graph is drawn in Fig 2.40 (b). Various system transfer functions are derived below using the Mason's gain formula.



(a) Block diagram

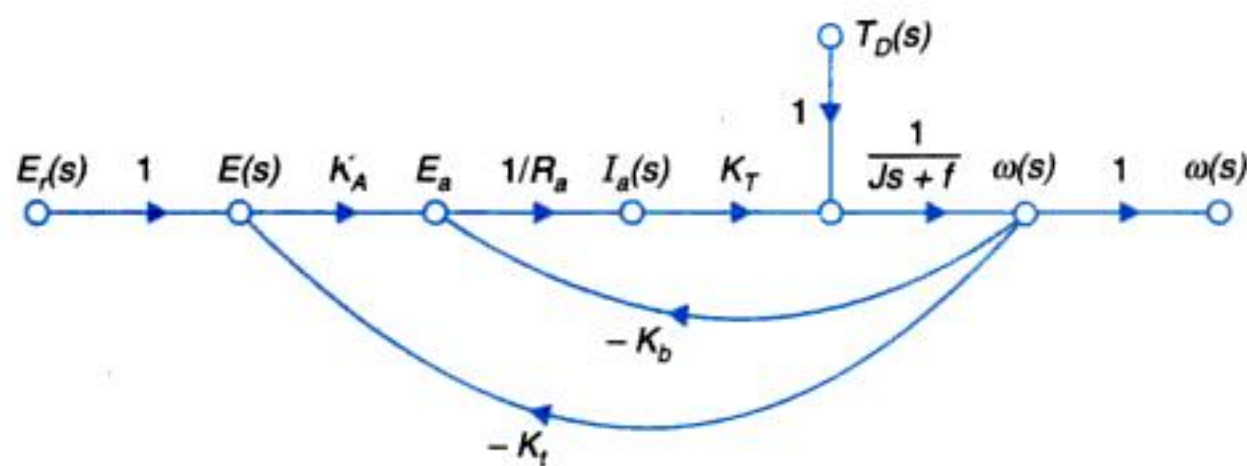

 (b) Signal flow graph ($L_a \approx 0$)

Fig. 2.40. Speed control system.

Consider first the case with zero disturbance torque. By inspection of the signal flow graph, with $T_D(s) = 0$, it is found that:

1. There is only one forward path with path gain

$$P_1 = \frac{K_A K_T}{R_a (J s + f)}$$

2. There are two individual loops with loop gains

$$P_{11} = \frac{-K_T K_b}{R_a (J s + f)}$$

$$P_{21} = \frac{K_A K_T K_t}{R_a (J s + f)}$$

3. There are no combinations of two non-touching loops, three non-touching loops, etc. Therefore

$$P_{m2} = P_{m3} = \dots = 0$$

Hence from eqn. (2.86)

$$\Delta = 1 - \left[\frac{K_T K_b}{R_a (J s + f)} + \frac{K_A K_T K_t}{R_a (J s + f)} \right] = 1 + \frac{K_T K_b + K_A K_T K_t}{R_a (J s + f)}$$

4. The forward path is in touch with both the loops. Therefore

$$\Delta_1 = 1$$

From the Mason's gain formula of eqn. (2.84), the overall gain is

$$T(s) = \frac{\omega(s)}{E_r(s)} = \frac{P_1 \Delta_1}{\Delta} = \frac{K_A K_T}{R_a (Js + f) + K_T K_b + K_A K_T K_t} \quad \dots(2.100)$$

With $K_t = 0$, the system is reduced to open-loop with the transfer function

$$G(s) = \frac{K_A K_T}{R_a (Js + f) + K_b K_T} = \frac{K}{(\tau s + 1)} \quad \dots(2.101)$$

where

$$K = \frac{K_A K_T}{R_a f + K_T K_b}; \tau = \frac{R_a J}{R_a f + K_T K_b}$$

From eqn. (2.100), the closed-loop transfer function of the system is given by

$$T(s) = \frac{K/\tau}{s + \left(\frac{1 + KK_t}{\tau} \right)} \quad \dots(2.102)$$

When the load (*disturbance*) torque $T_D(s)$ is present, the only change in the graph is the additional input $T_D(s)$.

Applying Mason's gain formula to the graph, the following transfer function is obtained between output speed and disturbance torque with zero reference voltage, i.e., $E_r(s) = 0$

$$\left. \frac{\omega(s)}{T_D(s)} \right|_{E_r(s)=0} = \frac{\omega_D(s)}{T_D(s)} = \frac{-1}{Js + f + \frac{K_T}{R_a} (K_A K_t + K_b)} \quad \dots(2.103)$$

When there is no feedback ($K_t = 0$), eqn. (2.102) modifies to

$$\left. \frac{\omega(s)}{T_D(s)} \right|_{E_r(s)=0} = \frac{\omega_D(s)}{T_D(s)} = \frac{-1}{Js + f + \frac{K_T K_b}{R_a}} \quad \dots(2.104)$$

The additional term $\left(\frac{K_T K_A}{R_a} \right) K_t$ in the denominator of eqn. (2.102) (compared to eqn.

(2.103)) arises on account of output (speed) feedback. As we shall see in Chapter 5 that this term reduces the effect of load (disturbance) torque on motor speed.

2.7 ILLUSTRATIVE EXAMPLES

Example 2.1 : Consider the mechanical system shown in Fig. 2.41 (a). A force $F(t)$ is applied to mass M_2 . The free-body diagrams for the two masses are shown in Fig. 2.41 (b). From this figure, we have the following differential equations describing the dynamics of the system.

Solution.

$$F(t) - f_2(\dot{y}_2 - \dot{y}_1) - K_2(y_2 - y_1) = M_2 \ddot{y}_2$$

$$f_2(\dot{y}_2 - \dot{y}_1) + K_2(y_2 - y_1) - f_1 \dot{y}_1 - K_1 y_1 = M_1 \ddot{y}_1$$

Rearranging we get

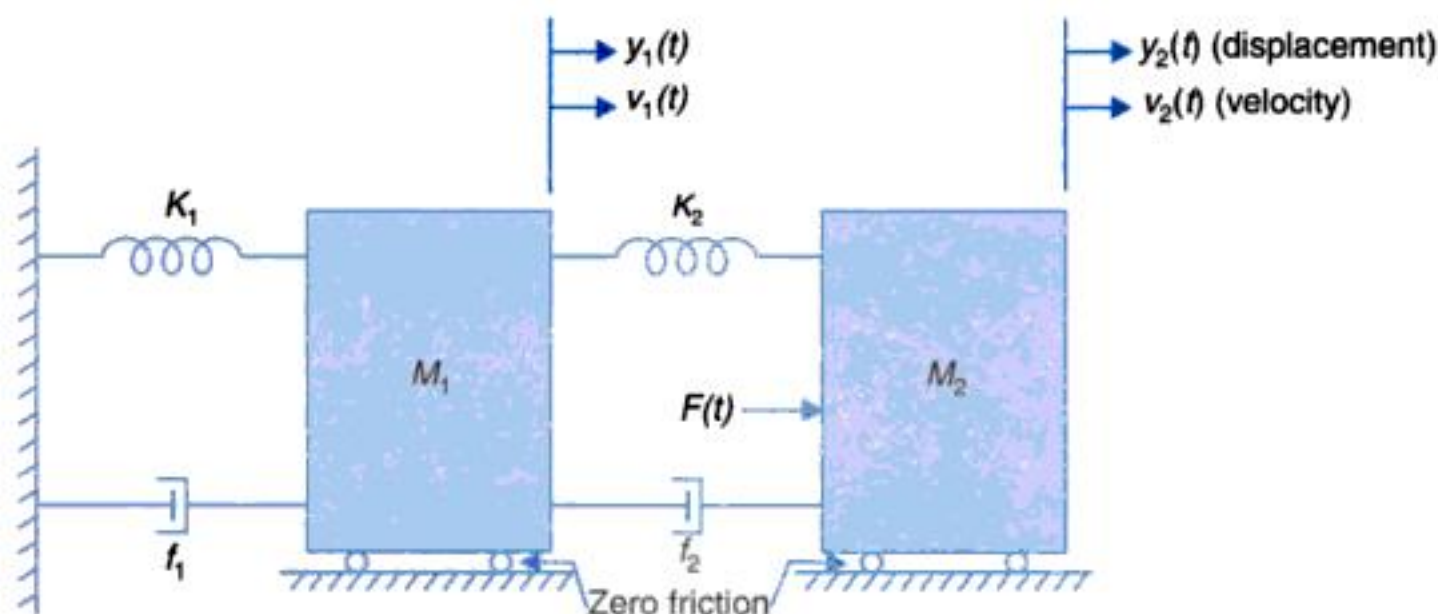
$$M_2 \ddot{y}_2 + f_2(\dot{y}_2 - \dot{y}_1) + K_2(y_2 - y_1) = F(t) \quad \dots(2.105)$$

$$M_1 \ddot{y}_1 + f_1 \dot{y}_1 - f_2(\dot{y}_2 - \dot{y}_1) + K_1 y_1 - K_2(y_2 - y_1) = 0 \quad \dots(2.106)$$

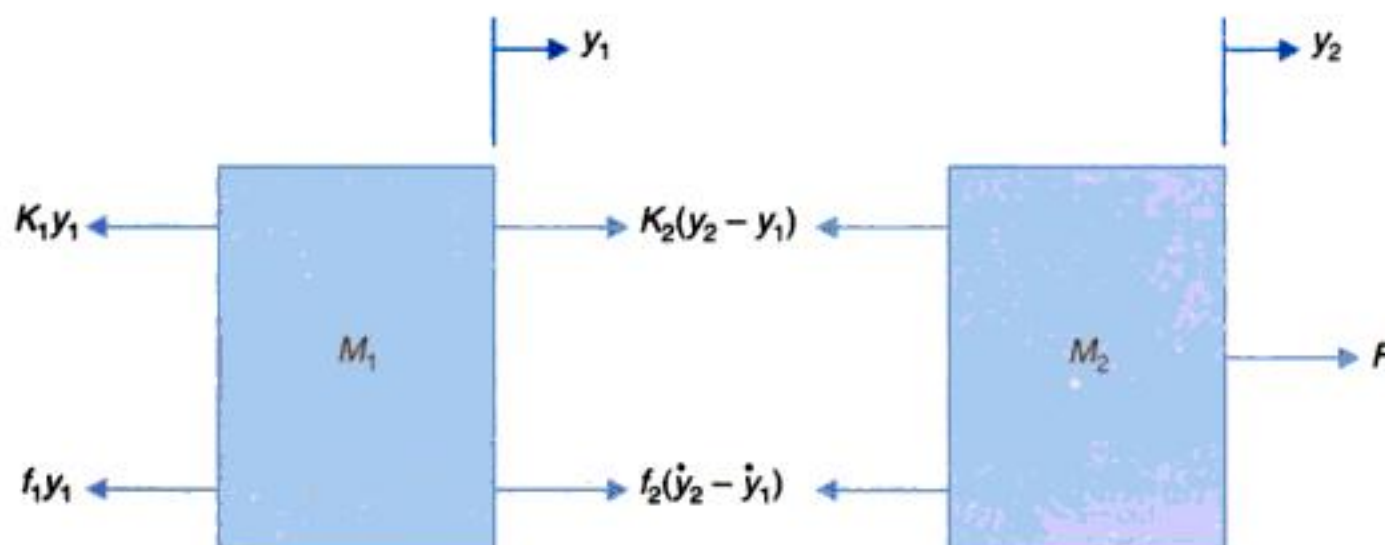
These are two simultaneous second-order linear differential equations. Manipulation of these equations will result in a single differential equation (fourth-order) relating the response y_2 (or y_1) to input $F(t)$.

A spring-mass-damper system may be schematically represented as a network by showing the inertial reference frame as the second terminal of every mass (or inertia) element. As an example, the mechanical system of Fig. 2.41 (a) is redrawn in Fig. 2.42 which may be referred to as the *mechanical network*. Analogous electrical circuit based on force-current analogy (Table 2.2) is shown in Fig. 2.43. A look at Fig. 2.43 (electrical analog of Fig. 2.41 (a)) and Fig. 2.42 reveals that they are alike topologically.

The dynamical equations of the system [eqns. (2.105)-(2.106)] could also be obtained by writing nodal equations for the electrical network of Fig. 2.43 or for the mechanical network of Fig. 2.42 (with force and velocity analogous to current and voltage respectively) since the two are alike topologically. The result is:



(a) A mechanical system



(b) Free-body diagram

Fig. 2.41. (a) A mechanical system; (b) Free-body diagram.

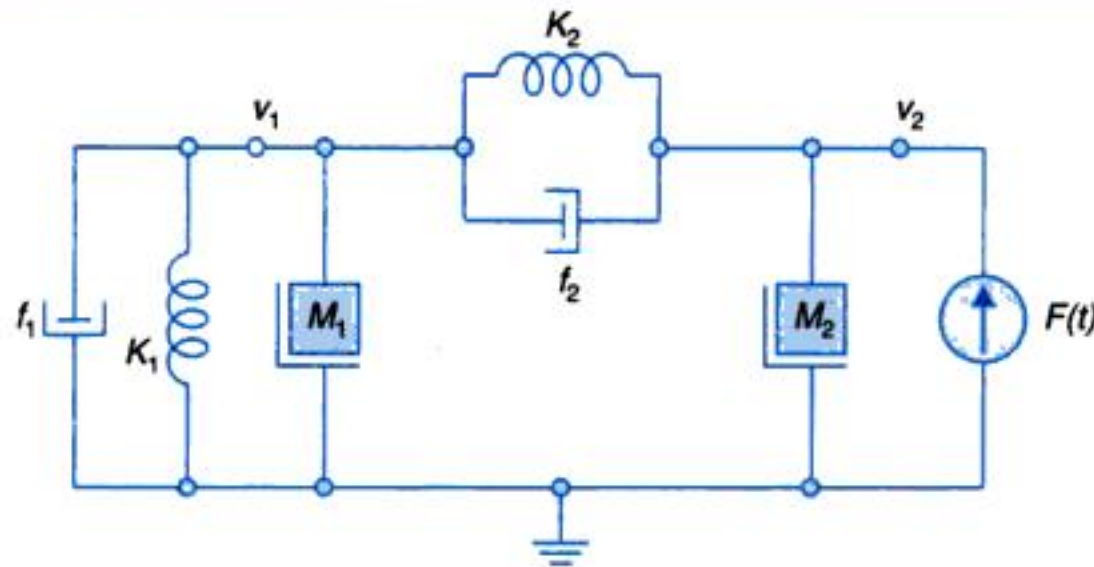


Fig. 2.42. Mechanical network for the system of Fig. 2.41.

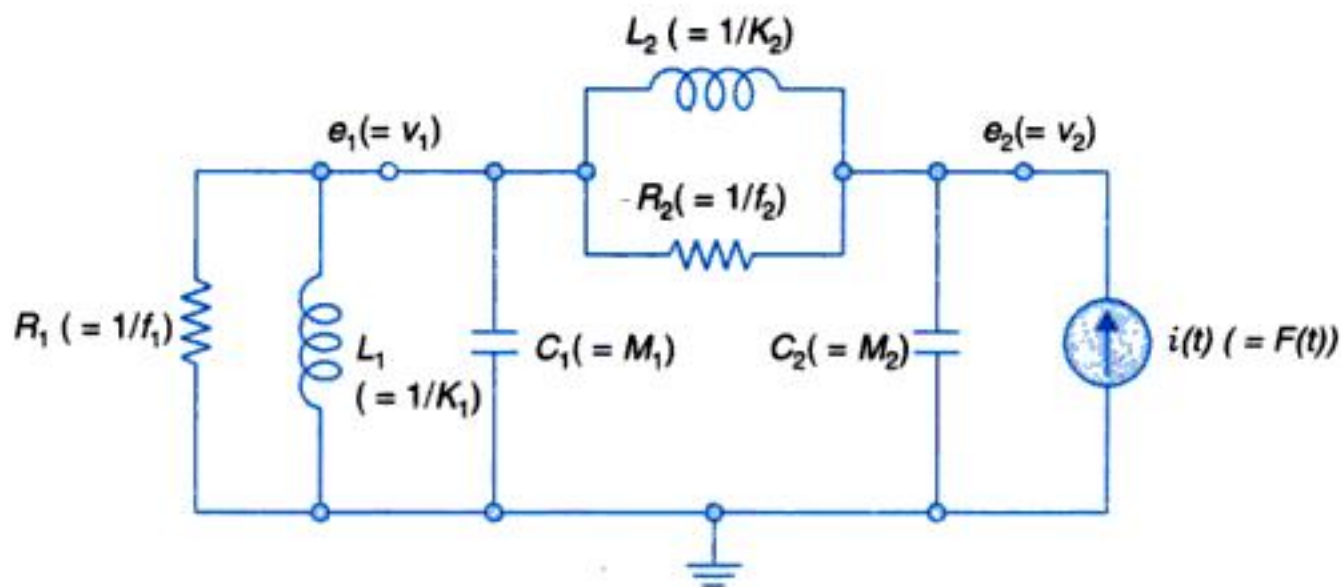


Fig. 2.43. Electrical analog for the system of Fig. 2.30 (a).

$$f_1 v_1 = K_1 \int_{-\infty}^t v_1 dt + M_1 \dot{v}_1 + K_2 \int_{-\infty}^t (v_1 + v_2) dt + f_2 (v_1 - v_2) = 0$$

$$M_2 \dot{v}_2 + K_2 \int_{-\infty}^t (v_2 - v_1) dt + f_2 (v_2 - v_1) = F(t)$$

The result is same as obtained earlier (with $y = \int_{-\infty}^t v dt$, $\dot{y} = v$ and $\ddot{y} = \dot{v}$) in eqns. (2.105) and (2.106) using the free-body diagram approach.

Signal Flow Graph

The mechanical system of Fig. 2.41(a) has four storage elements so it is a fourth order system and would be identified by four state variables. These can be defined as $x_1 = y_1$, $x_2 = \dot{y}_1$, $x_3 = y_2$, $x_4 = \dot{y}_2$. With reference to the free-body diagram of Fig. 2.41(b), the signal flow graph of Fig. 2.44 can be immediately drawn. The state variable equations can be written directly from the signal flow graph. The reader should write out these equations and organize them in matrix form. Here again the state variables are defined as physical variables, but this is not a unique choice.

Using Mason's gain formula the transfer function between any output and input $F(s)$ can be derived. It is identified here that there are seven loops but no combinations of two or more loops. Further there are two forward paths but there are no loops non-touching these paths. The reader should find the transfer function $y_1(s)/F(s)$.

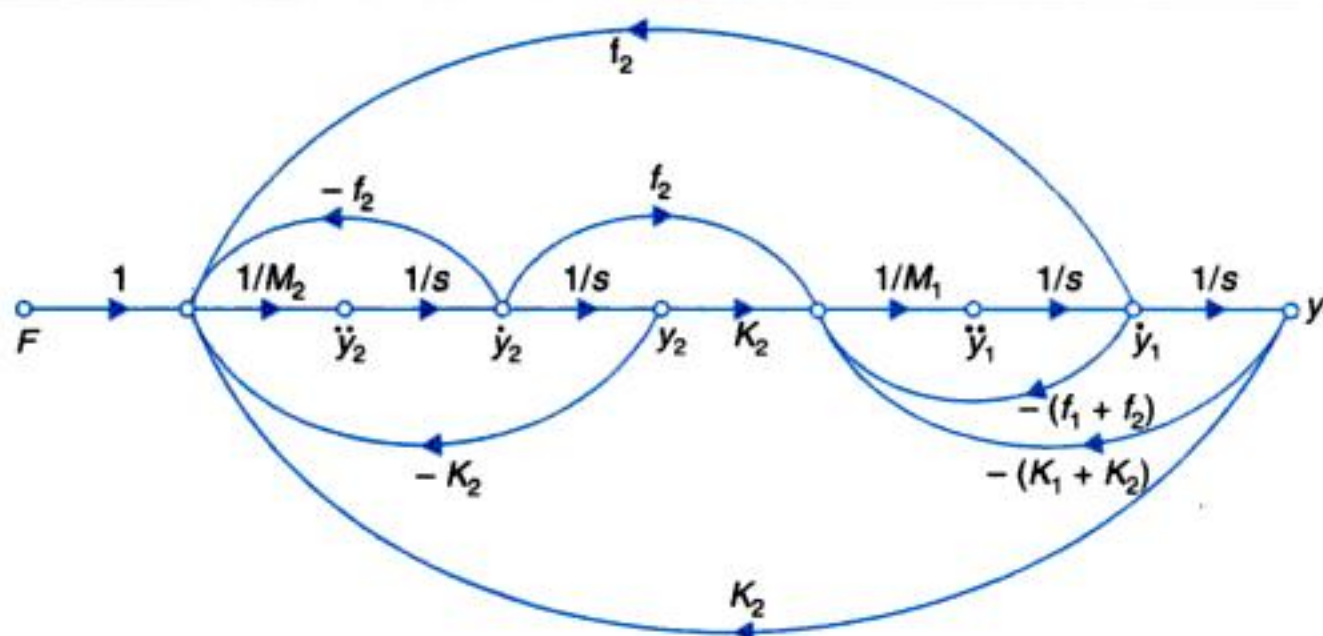


Fig. 2.44. Signal flow graph of the mechanical system of Fig. 2.41 (a).

Example 2.2 : Consider the circuit (electrical) of Fig. 2.45.

- Identify a set of state variables (physical variables).
- Draw the signal flow graph of the circuit in terms of the state variables identified in part (a).
- From the signal flow graph, write the state variable equations of the circuit.
- From the signal flow graph, determine the transfer function $E_C(s)/E(s)$.

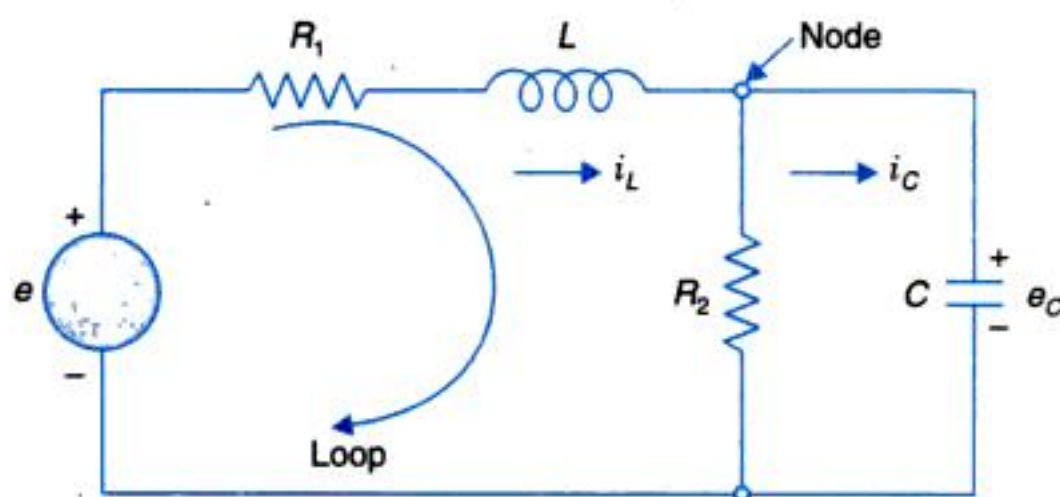


Fig. 2.45

Solution.

(a) This circuit has two storage elements, so these shall be two state variables. We shall identify these as the inductor current i_L and capacitor voltage e_C ; both these are associated with energy storage. Remember that the state variables do not form a unique set.

From the elemental laws of inductor and capacitor we can draw the signal flow graph as in Fig. 2.46(a). The complete signal flow graph is then constructed by the KCL equation at the node and the KVL equation round the loop. These equations are:

$$i_L = \frac{e_C}{R_2} + i_C \quad \text{or} \quad i_C = i_L - \frac{e_C}{R_2} \quad \dots(i)$$

$$\text{and} \quad e = R_1 i_L + e_L + e_C \quad \text{or} \quad e_L = e - R_1 i_L - e_C \quad \dots(ii)$$

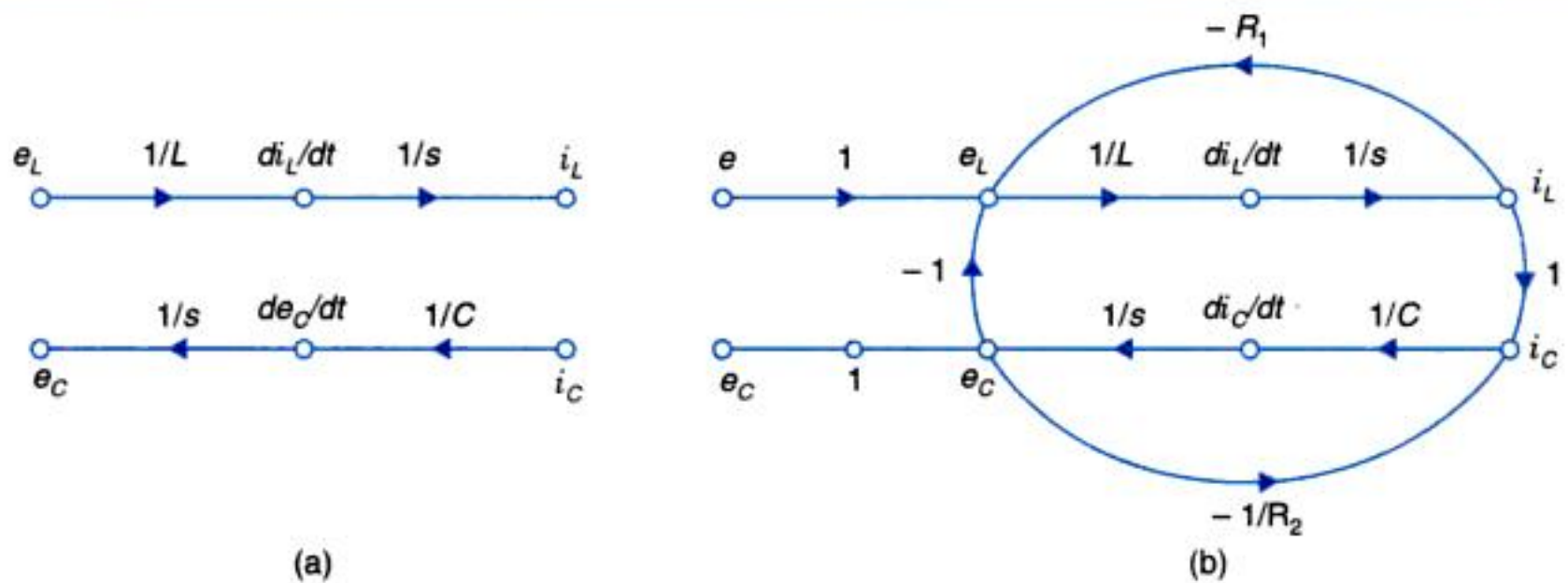


Fig. 2.46

The complete signal flow graph is drawn in Fig. 2.47(b).

(c) From the signal flow graph the two state variable equations can be written as below.

$$\frac{di_L}{dt} = \frac{1}{L}e_L = \frac{1}{L}(-e_C - R_1 i_L + e) = -\frac{R_1}{L}i_L - \frac{1}{L}e_C + \frac{1}{L}e \quad \dots(iii)$$

and

$$\frac{de_C}{dt} = \frac{1}{C}i_C = \frac{1}{C}\left(i_L + \frac{e_C}{R_2}\right) = \frac{1}{C}i_L - \frac{1}{R_2 C}e_C \quad \dots(iv)$$

Equations (iii) and (iv) can be written in matrix form

$$\begin{bmatrix} di_L/dt \\ di_C/dt \end{bmatrix} = \begin{bmatrix} -R_1/L & -1/L \\ 1/C & 1/R_2 C \end{bmatrix} \begin{bmatrix} i_L \\ e_C \end{bmatrix} + \begin{bmatrix} 1/L \\ 0 \end{bmatrix} e$$

These are also known as **state space** equations.

(d) Input $E(s)$, output $E_C(s)$. From the signal flow graph we have,

Forward path $P_1 = \frac{1}{sL} \times \frac{1}{sC} = \frac{1}{s^2 LC}; \Delta_1 = 1$

Single loops $P_{11} = -\frac{R_1}{sL}, P_{21} = -\frac{1}{sR_2 C}, P_{31} = -\frac{1}{s^2 LC}$

$$\Delta = 1 + \frac{R_1}{sL} + \frac{1}{sR_2 C} + \frac{1}{s^2 LC}$$

Hence
$$\frac{E_C(s)}{E(s)} = \frac{P_1 \Delta_1}{\Delta} = \frac{\frac{1}{s^2 LC}}{1 + \frac{R_1}{sL} + \frac{1}{sR_2 C} + \frac{1}{s^2 LC}} = \frac{1}{1 + s\left(R_1 C + \frac{L}{R_2}\right) + s^2 LC}$$

Example 2.3 : Consider a salt mixing tank shown in Fig. 2.48. A solution of salt in water at a concentration C_f (moles* of salt/m³ of solution) is mixed with pure water to obtain an outflow

*A mole of a substance is defined as the amount of substance whose mass numerically equals its molecular weight. For example, a gram-mole of helium would have a mass of 4.003 g (molecular weight of helium = 4.003).

stream with salt concentration C_o . The water flow rate is assumed fixed at Q_w and the solution flow rate may be varied to achieve the desired concentration C_o (also see Problem 2.6). Volumetric hold-up of the tank is V , which is held constant. Let us assume that stirring causes perfect mixing so that composition of the liquid in the tank is uniform throughout.

Solution. For this system,

$$Q_f = K_v x_v; K_v \text{ is valve coefficient}$$

$$Q_o = Q_w + Q_f$$

The rate of salt inflow in the tank

$$m_i = Q_f C_f; \left(\frac{\text{m}^3}{\text{s}} \cdot \frac{\text{moles}}{\text{m}^3} = \text{moles / s} \right)$$

The rate of salt outflow from the tank

$$m_o = Q_o C_o; (\text{moles/s})$$

The rate of salt accumulation in the tank

$$\dot{m}_a = \frac{d}{dt} [VC_o(t)] = V \frac{dC_o}{dt}$$

where $VC_o(t)$ the salt hold-up of the tank at time t .

From the law of conversation of mass, we have

$$m_i = m_a + m_o \quad \text{or} \quad Q_f C_f = V \frac{dC_o}{dt} + Q_o C_o$$

or
$$\tau \frac{dC_o}{dt} + C_o = K x_v$$

where $K = (C_f K_v)/Q_o$ and $\tau = V/Q_o$ is the tank hold-up time.

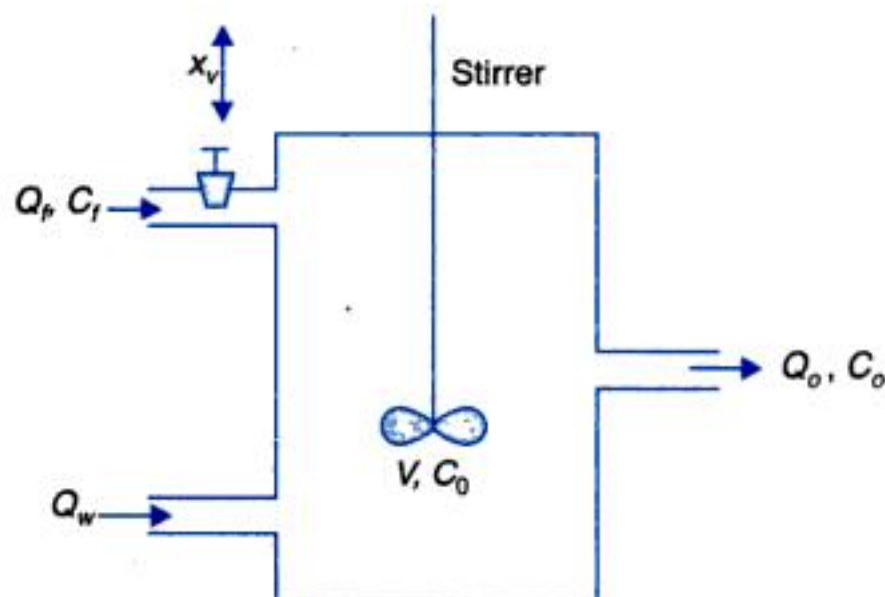


Fig. 2.48. A salt mixing tank.

The transfer function of the system is

$$\frac{C_o(s)}{X_v(s)} = \frac{K}{s\tau + 1}$$

Example 2.4 : The manipulator shown in Fig. 2.49 has a rotating joint followed by a linear (prismatic) joint. The whole mass of links is concentrated at the centre of mass. Derive the dynamic equations for the manipulator.

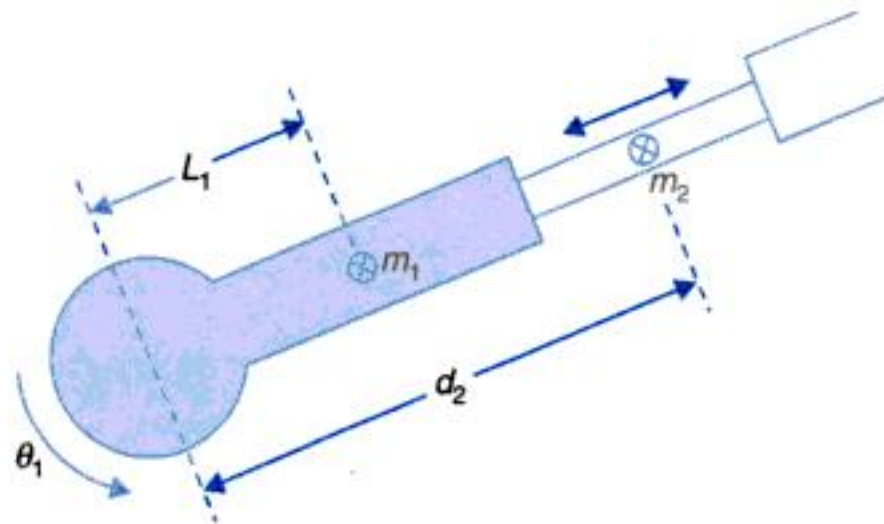


Fig. 2.49

Solution. Linear velocity of first centre of mass, $v_{c1} = l_1 \dot{\theta}_1$... (i)

Kinetic energy of link 1 is

$$K_1 = (1/2)m_1 l_1^2 \dot{\theta}_1^2 \quad \dots (ii)$$

Linear velocity of second centre of mass is

$$v_{c2} = \sqrt{(d_2^2 \dot{\theta}_1^2 + \dot{d}_2^2)} \quad \dots (iii)$$

Kinetic energy of link 2 is

$$K_2 = \frac{1}{2} m_2 (d_2^2 \dot{\theta}_1^2 + \dot{d}_2^2) \quad \dots (iv)$$

Hence the total kinetic energy of manipulator is

$$K = K_1 + K_2 \quad \dots (v)$$

or
$$K(\theta_1, \dot{\theta}_1, d_2, \dot{d}_2) = (1/2)(m_1 l_1^2 + m_2 d_2^2) \dot{\theta}_1^2 + \frac{1}{2} m_2 \dot{d}_2^2 \quad \dots (vi)$$

Potential energy of link 1 is

$$u_1 = m_1 l_1 g \sin \theta_1 \quad \dots (vii)$$

Potential energy of link 2 is

$$u_2 = m_2 d_2 g \sin \theta_1 \quad \dots (viii)$$

Hence total potential energy of manipulator is

$$U(\theta_1, d_2) = u_1 + u_2 = g(m_1 l_1 + m_2 d_2) \sin \theta_1 \quad \dots (ix)$$

Taking partial derivatives, we have

$$\begin{bmatrix} \frac{\partial K}{\partial \dot{\theta}_1} \\ \frac{\partial K}{\partial \dot{d}_2} \end{bmatrix} = \begin{bmatrix} (m_1 l_1^2 + m_2 d_2^2) \dot{\theta}_1 \\ m_2 d_2 \end{bmatrix} \quad \dots (x)$$

$$\begin{bmatrix} \frac{\partial K}{\partial \theta_1} \\ \frac{\partial K}{\partial d_2} \end{bmatrix} = \begin{bmatrix} 0 \\ m_2 d_2 \dot{\theta}_1^2 \end{bmatrix} \quad \dots(x_i)$$

$$\begin{bmatrix} \frac{\partial U}{\partial \theta_1} \\ \frac{\partial U}{\partial d_2} \end{bmatrix} = \begin{bmatrix} g(m_1 l_1 + m_2 d_2) \cos \theta_1 \\ g m_2 \sin \theta_1 \end{bmatrix} \quad \dots(x_{ii})$$

From Lagrangian mechanics we know that

$$\begin{bmatrix} \tau_1 \\ \tau_2 \end{bmatrix} = \begin{bmatrix} \frac{d}{dt} \left(\frac{\partial K}{\partial \dot{\theta}_1} \right) \\ \frac{d}{dt} \left(\frac{\partial K}{\partial \dot{d}_2} \right) \end{bmatrix} - \begin{bmatrix} \frac{\partial K}{\partial \theta_1} \\ \frac{\partial K}{\partial d_2} \end{bmatrix} + \begin{bmatrix} \frac{\partial U}{\partial \theta_1} \\ \frac{\partial U}{\partial d_2} \end{bmatrix} \quad \dots(x_{iii})$$

Thus from (x), (xi), (xii), and (xiii) we have

$$\tau_1 = (m_1 l_1^2 + m_2 d_2^2) \ddot{\theta}_1 + 2m_2 d_2 \dot{\theta}_1 \dot{d}_2 + (m_1 l_1 + m_2 d_2) g \cos \theta_1 \quad \dots(x_{iv})$$

$$\tau_2 = m_2 \dot{d}_2 - m_2 d_2 \dot{\theta}_1^2 + m_2 g \sin \theta_1 \quad \dots(x_v)$$

Equations (xiv) and (xv) are the dynamic equations of the manipulator.

Example 2.5 : The schematic diagram of a position control system is drawn in Fig. 2.50.

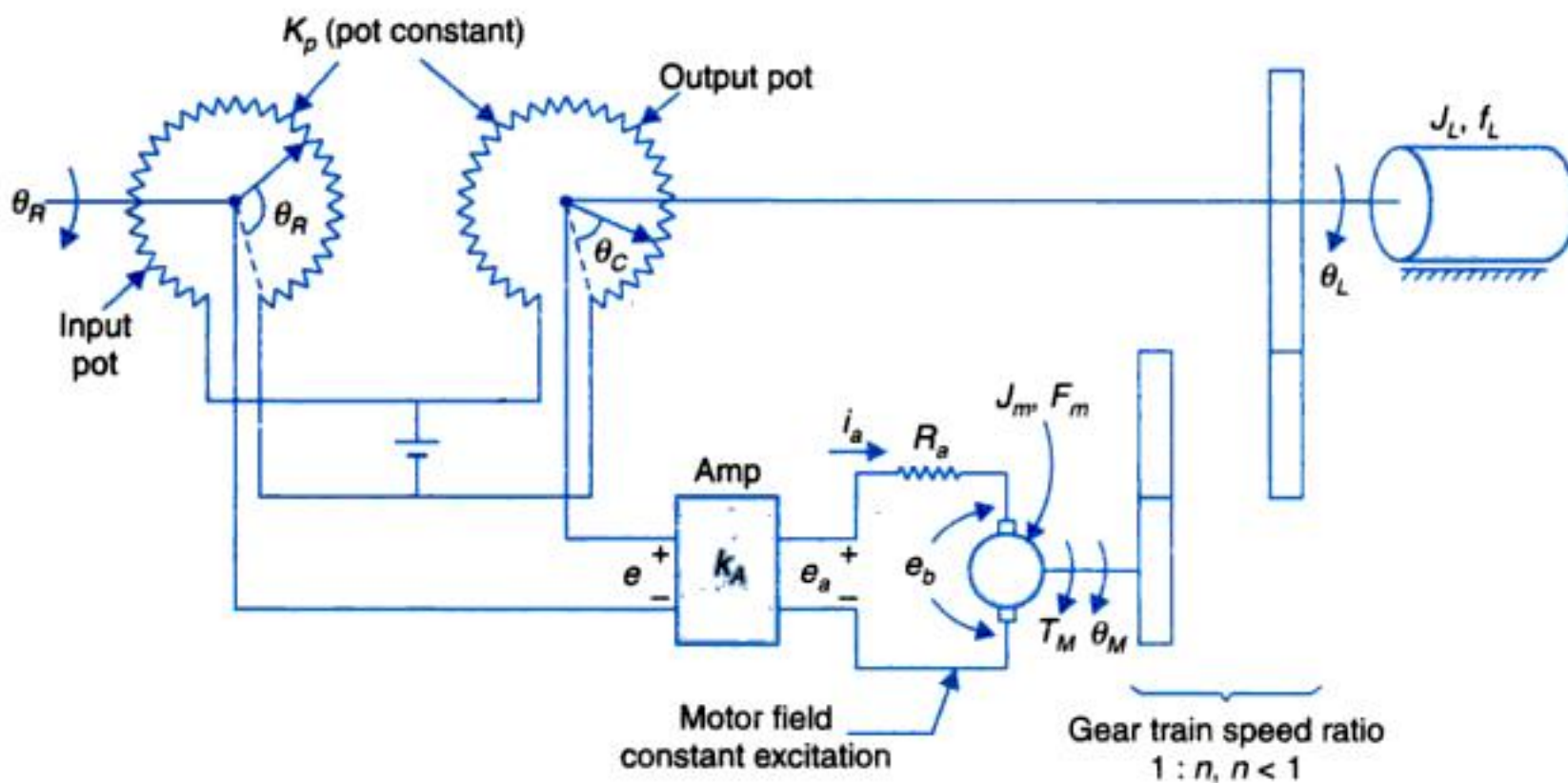


Fig. 2.50

— Various constituents of the system are:

- Drive motor-dc armature controlled.
- Load is driven through a reduction gearing, to amplify torque for moving the load.

- Load angular position is sensed by a circular potentiometer.
- Angle reference input is sensed by an identical potentiometer.
- Position error (in form of voltage e) is fed to amplifier with a power stage to feed the motor armature at voltage e_a .

From physical reasoning it is easily seen that at steady position of load, voltage e should be zero so the motor armature is stationary. It means $\theta_C = \theta_R$ i.e. steady-state error is zero. Any change in command θ_R introduces error e and the motor drives the load till $\theta_C = \theta_R$ once again. The nature of this moment is an important performance measure.

Various parameters and variables are indicated in Fig. 2.50. Motor parameters are:

Torque constant $= K_T$ kg-m/Amp. (armature)

Back emf $= K_b$ V/rad/sec

It is reminded here that numerically $K_T = K_b$.

Motor armature inductance L_a is negligible.

(a) Draw the block diagram of the motor and reduce it to the form $\omega_M(s)/E_a(s)$; ω_M = motor speed.

(b) Draw the complete system block diagram.

(c) Determine the overall transfer function $T(s) = \theta_C(s)/\theta_R(s)$.

(d) Briefly discuss the nature of $T(s)$.

(e) For numerical data given within the solution determine $T(s)$; K_A is variable gain.

Solution. From the control system knowledge acquired so far the block of the position control system (Fig. 2.50) can be drawn directly. For this purpose the load is reflected to the motor shaft giving the effective inertia and friction at motor shaft as

$$J = J_M + n^2 J_L \quad \dots(i)$$

$$f = f_M + n^2 f_L \quad \dots(ii)$$

(a) To begin with let us first draw the motor block diagram linking ω_M , motor speed, to armature voltage e_a . It is given in Fig. 2.51 (a) (this has been presented earlier and is repeated here for the reader to become fully conversant with it).

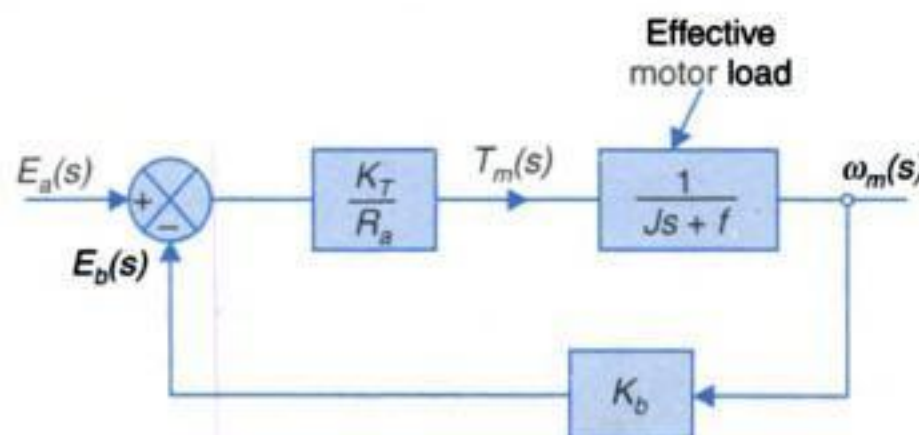


Fig. 2.51

Reducing the block diagram of Fig. 2.51, we get

$$\frac{\omega_M(s)}{E_a(s)} = \frac{K_m}{\tau' s + 1} \quad \dots(iii)$$

$$\text{where } K_m = \frac{K_T}{R_a f + K_T K_b} \quad \dots(iv)$$

$$\tau' = \frac{J}{f + (K_T K_b)/R_a} \quad \dots(v)$$

This is represented in Fig. 2.52

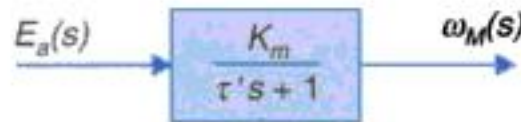


Fig. 2.52. Motor and load.

Note. τ' is the effective motor time constant including friction f and equivalent frictional effect caused by motor back emf $(K_b K_T)/R_a$. Symbol τ is reserved for motor's mechanical time constant i.e. $\tau = J/f$.

(b) The complete block diagram of the speed control system is now drawn in Fig. 2.53.

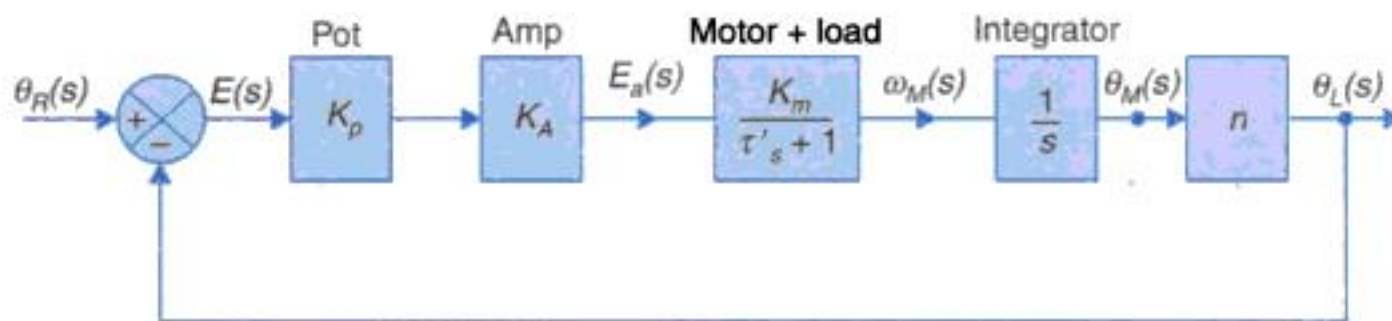


Fig. 2.53

(c) Forward path transfer function

$$G(s) = \frac{K_p K_A K_m n}{s(\tau' s + 1)} \quad \dots(vi)$$

Overall transfer function

$$T(s) = \frac{\theta_L(s)}{\theta_R(s)} = \frac{G(s)}{1 + G(s)}$$

Substituting $G(s)$, we get

$$\frac{\theta_L(s)}{\theta_R(s)} = \frac{K_p K_A K_m n}{\tau' s^2 + s + K_p K_A K_m n} \quad \dots(vii)$$

It is to be noticed that it is a second-order system compared to the first-order speed control system of Fig. 2.39. Increase in order has been caused by the integrator to get angle θ_M from speed $\dot{\theta}_M$.

(d) Data of system components

DC Motor

$$K_T = 60 \times 10^{-3} \text{ kg-m/A}$$

$$J_M = 1 \times 10^{-3} \text{ kg-m}^2$$

$$f_M = 10 \times 10^{-3} \text{ kg-m/rad/sec}$$

$$R_a = 1 \Omega$$

Potentiometer

$$K_p = 1 \text{ V/rad}$$

Gear Train

$$n = 1/10 = 0.1$$

Load

$$J_L = 900 \times 10^{-3} = \text{kg-m}^2$$

$$f_L = 9,000 \times 10^{-3} \text{ kg-m/rad/sec.}$$

Effective load at motor shaft

$$J = 1 \times 10^{-3} + 900 \times 10^{-3} \times (0.1)^2$$

$$= 10 \times 10^{-3} \text{ kg-m}^2$$

$$f = 10 \times 10^{-3} + 9,000 \times 10^{-3} \times (0.1)^2$$

$$= 100 \times 10^{-3} \text{ kg-m/rad/sec.}$$

From Eqs. (iv) and (v)

$$K_m = \frac{60 \times 10^{-3}}{1 \times 100 \times 10^{-3} + (60 \times 10^{-3})^2} ; K_b = K_T$$

$$= \frac{60}{10 + 3.6} = 4.41$$

$$\tau' = \frac{10 \times 10^{-3}}{100 \times 10^{-3} + (60 \times 10^{-3})^2/1} = \frac{10}{100 + 3.6} = 0.097 \text{ sec.}$$

Substituting (values in Eq. (vii))

$$\frac{\theta_L(s)}{\theta_R(s)} = \frac{1 \times K_A \times 4.41 \times 0.1}{0.097s^2 + s + 1 \times K_A \times 4.41 \times 0.1}$$

or

$$\frac{\theta_L(s)}{\theta_R(s)} = \frac{4.55 K_A}{s^2 + 10.31s + 4.55 K_A} \quad \dots(viii)$$

Choice of gain K_A in this transfer function depends on the system dynamics desired. The issues involved will be discussed in Chapter 5.

Example 2.6 : The block diagram of a speed control system is drawn in Fig. 2.54. Define the state variables and write the state and output equations of the system in vector-matrix form.

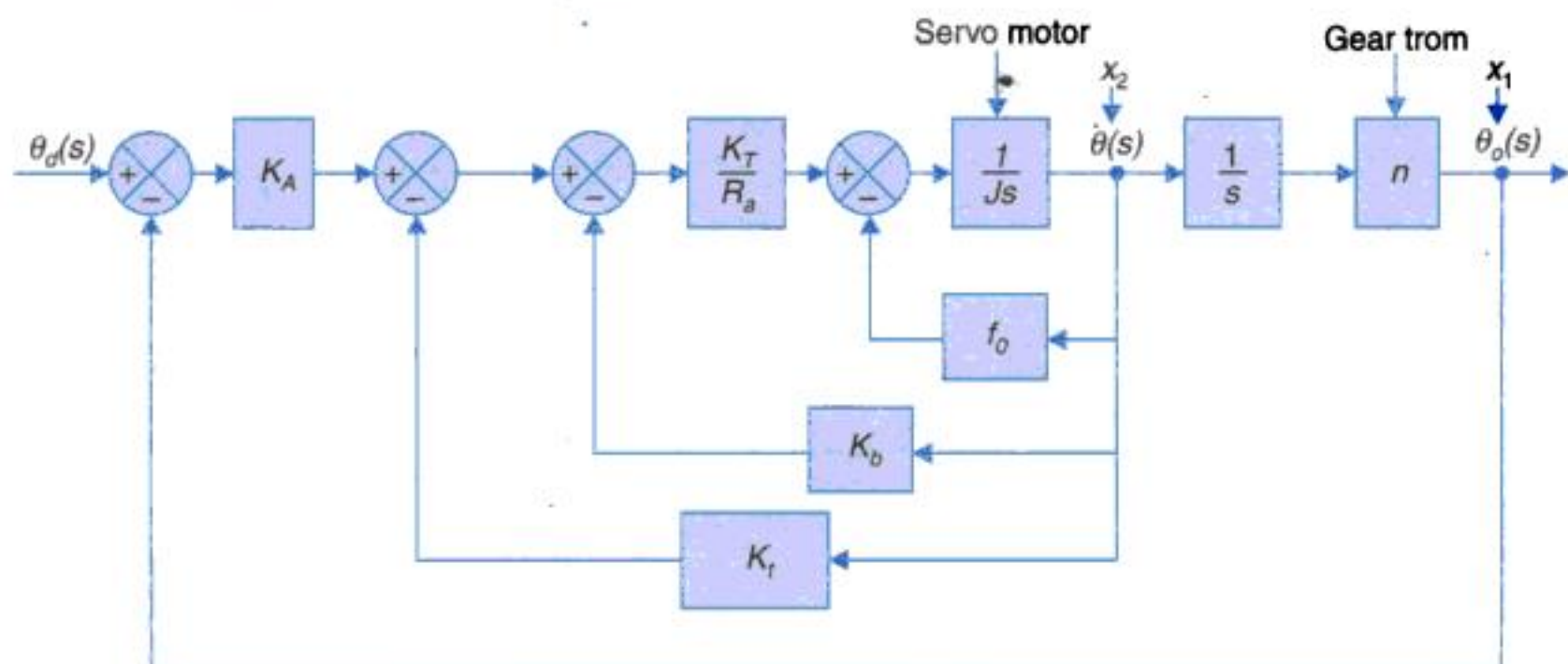


Fig. 2.54

Solution. There will be two state variables as this is a second-order system. We define the state variables as:

$$x_1 = \theta_o, \quad x_2 = \dot{\theta}$$

State equations written from the block diagram. For each block with one denominator s , input-output relations are written. In this block diagram there are two such blocks (2nd order system)

- Block $\left(\frac{n}{s}\right)$

$$x_1 = \left(\frac{n}{s}\right) x_2$$

In time domain $\dot{x}_1 = nx_2$

- Block $\left(\frac{1}{Js}\right)$

$$\left\{ (x_d - x_1)K_A - \left[(K_t + K_b) \frac{K_T}{R_a} + f_0 \right] x_2 \right\} \frac{1}{Js} = x_2$$

In time domain it can be expressed as

$$\dot{x}_2 = -\left(\frac{K_A}{J}\right)x_1 - \frac{f_0 + (K_t + K_b)\left(\frac{K_T}{R_a}\right)}{J}x_2 + \left(\frac{K_A}{J}\right)\theta_d$$

These two equations are written below as state equation

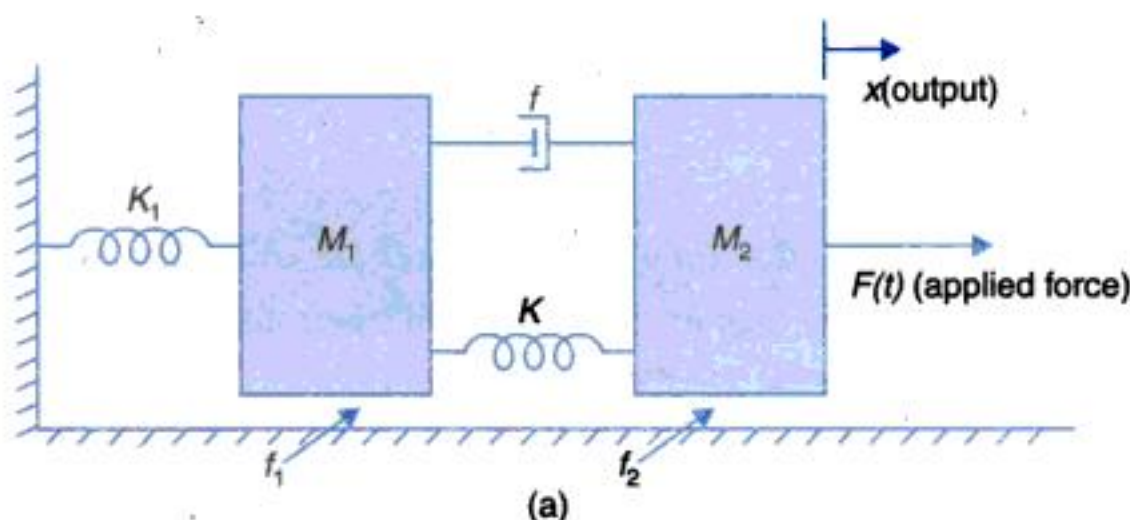
$$\begin{bmatrix} \dot{x}_1 \\ \dot{x}_2 \end{bmatrix} = \begin{bmatrix} 0 & n \\ -\left(\frac{K_A}{J}\right) & -\frac{f_0 + (K_t + K_b)\left(\frac{K_T}{R_a}\right)}{J} \end{bmatrix} \begin{bmatrix} x_1 \\ x_2 \end{bmatrix} + \begin{bmatrix} 0 \\ \frac{K_A}{J} \end{bmatrix} \theta_d \quad \dots(iii)$$

Output equation

$$y = \theta_o = x_1 \quad \text{or} \quad y = [1 \quad 0] \begin{bmatrix} x_1 \\ x_2 \end{bmatrix}. \quad \dots(iv)$$

PROBLEMS

2.1. Obtain the transfer functions of the mechanical systems shown in Figs. P-2.1(a) and (b).



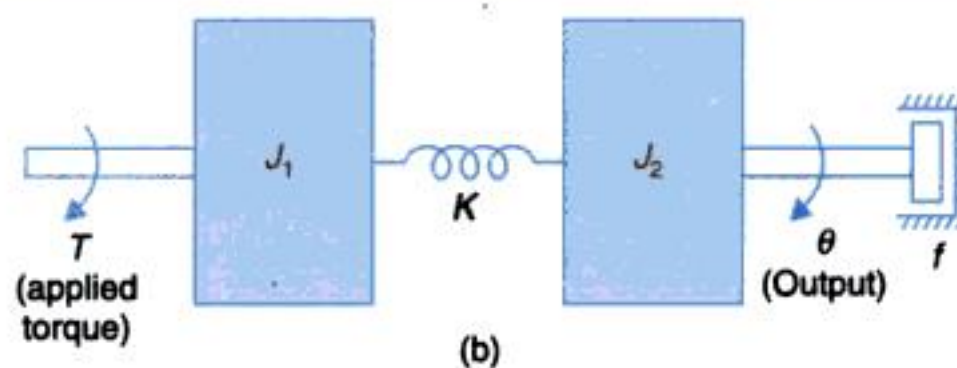


Fig. P-2.1.

- 2.2. Write the differential equations governing the behaviour of the mechanical system shown in Fig. P-2.2. Also obtain an analogous electrical circuit based on force-current analogy.

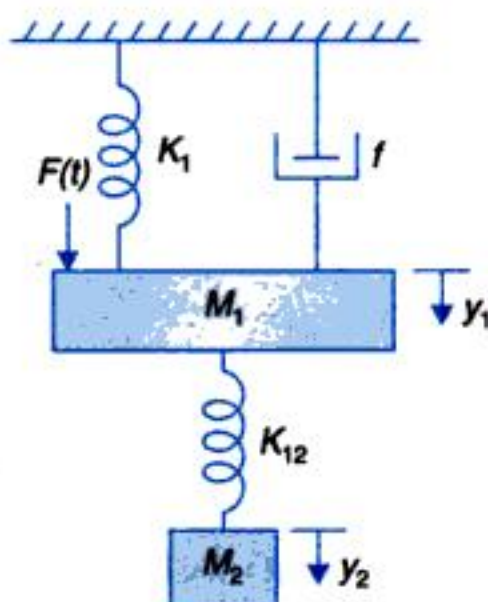


Fig. P-2.2.

- 2.3. Write the differential equations for the mechanical system shown in Fig. P-2.3. Also obtain an analogous electrical circuit based on force-current analogy.

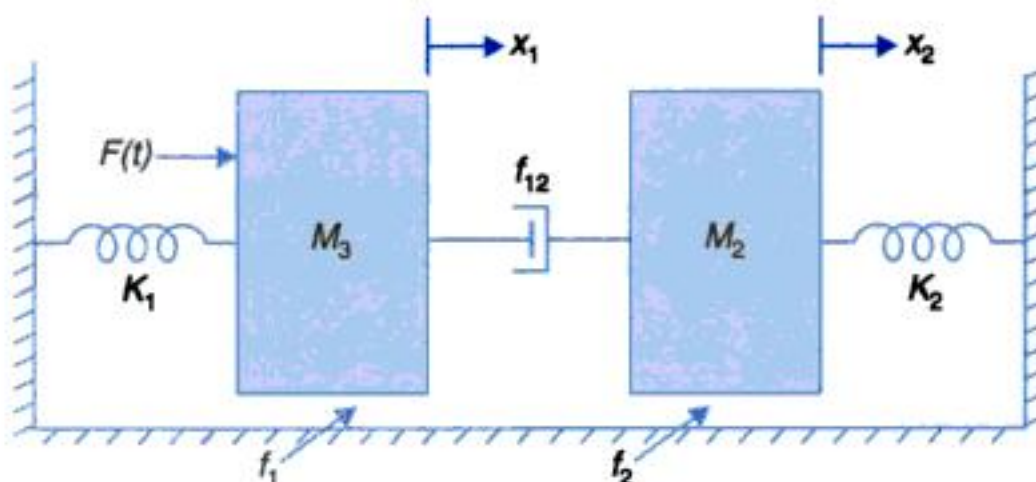


Fig. P-2.3.

- 2.4. Find the transfer function $X(s)/E(s)$ for the electromechanical system shown in Fig. P-2.4. [Hint: for a simplified analysis, assume that the coil has a back emf $e_b = k_1 dx/dt$ and the coil current i produces a force $F_c = k_2 i$ on the mass M]

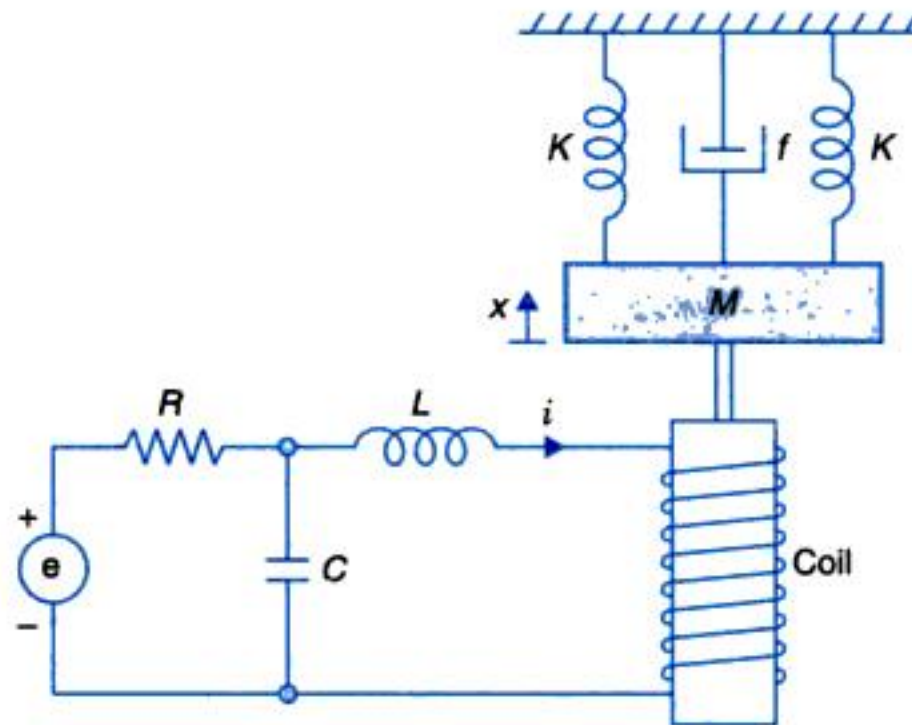


Fig. P-2.4.

- 2.5. Fig. P-2.5 shows a thermometer plugged into a bath of temperature θ_i . Obtain the transfer function $\theta(s)/\theta_i(s)$ of the thermometer and its electrical analogue. (The thermometer may be considered to have a thermal capacitance C which stores heat and a thermal resistance R which limits the heat flow). How the temperature indication of the thermometer will vary with time after the thermometer is suddenly plugged in ?

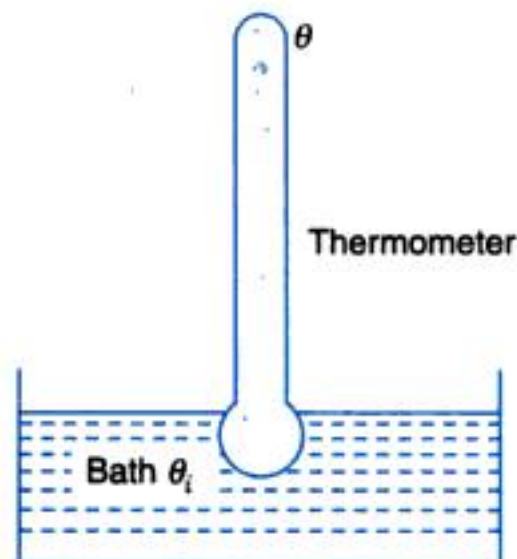


Fig. P-2.5.

- 2.6. The scheme of Fig. P-2.6 produces a steady stream flow of dilute salt solution with controlled concentration C_0 . A concentrated solution of salt with concentration C_i is continuously mixed with pure water in a mixing valve. The valve characteristic is such that the total flow rate Q_0 through it is maintained constant but the inflow Q_i of concentrated salt solution may be linearly varied by controlling valve stem position x . The outflow rate from the salt mixing tank is the same as the flow rate into it from the mixing valve, such that the level of the dilute salt solution in the tank is maintained constant. Obtain the transfer function $C_0(s)/X(s)$. If from fully closed position, the valve stem is suddenly opened by x_0 , determine the outstream salt concentration C_0 as a function of time.

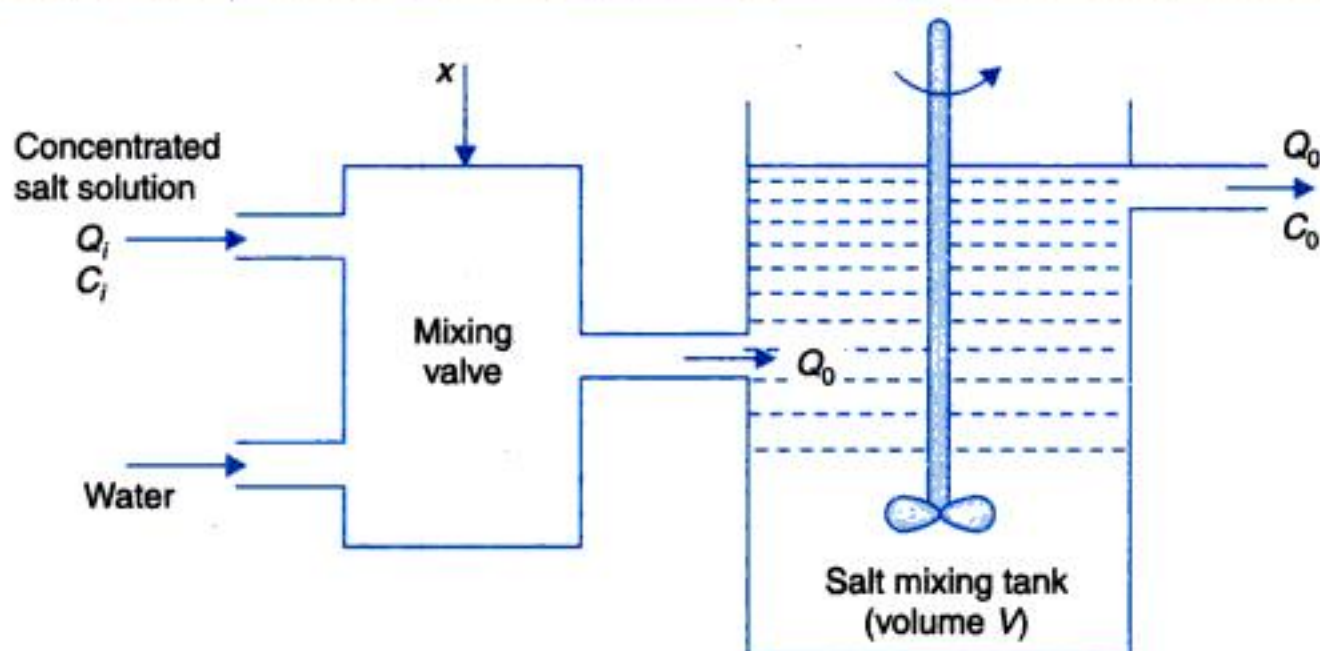


Fig. P-2.6.

- 2.7. In the speed control system shown in Fig. P-2.7, the generator field time constant is negligible. It is driven at constant speed giving a generated voltage of K_g volts/field amp. The motor is separately excited so as to have a counter emf of K_b volts per rad/sec. It produces a torque of K_T newton-m/amp. The motor and its load have a combined moment of inertia J kg-m² and negligible friction. The tachometer has K_t volts per rad/sec and the amplifier gain is K_A amps/volt. Draw the block diagram of this system and determine therefrom the transfer function $\omega(s)/E_i(s)$, where ω is the load speed.

With the system originally at rest, a control voltage $e_i = 100$ volts is suddenly applied. Determine how the load speed will change with time.

Given:

$$J = 6 \text{ kg-m}^2$$

$$K_A = 4 \text{ amp/volt}$$

$$K_T = 1.5 \text{ newton-m/amp}$$

$$K_g = 50 \text{ volts/amp}$$

$$R_a = 1 \text{ ohm}$$

$$K_t = 0.2 \text{ volts per rad/sec}$$

[Hint: $K_b = K_T$ in MKS units]

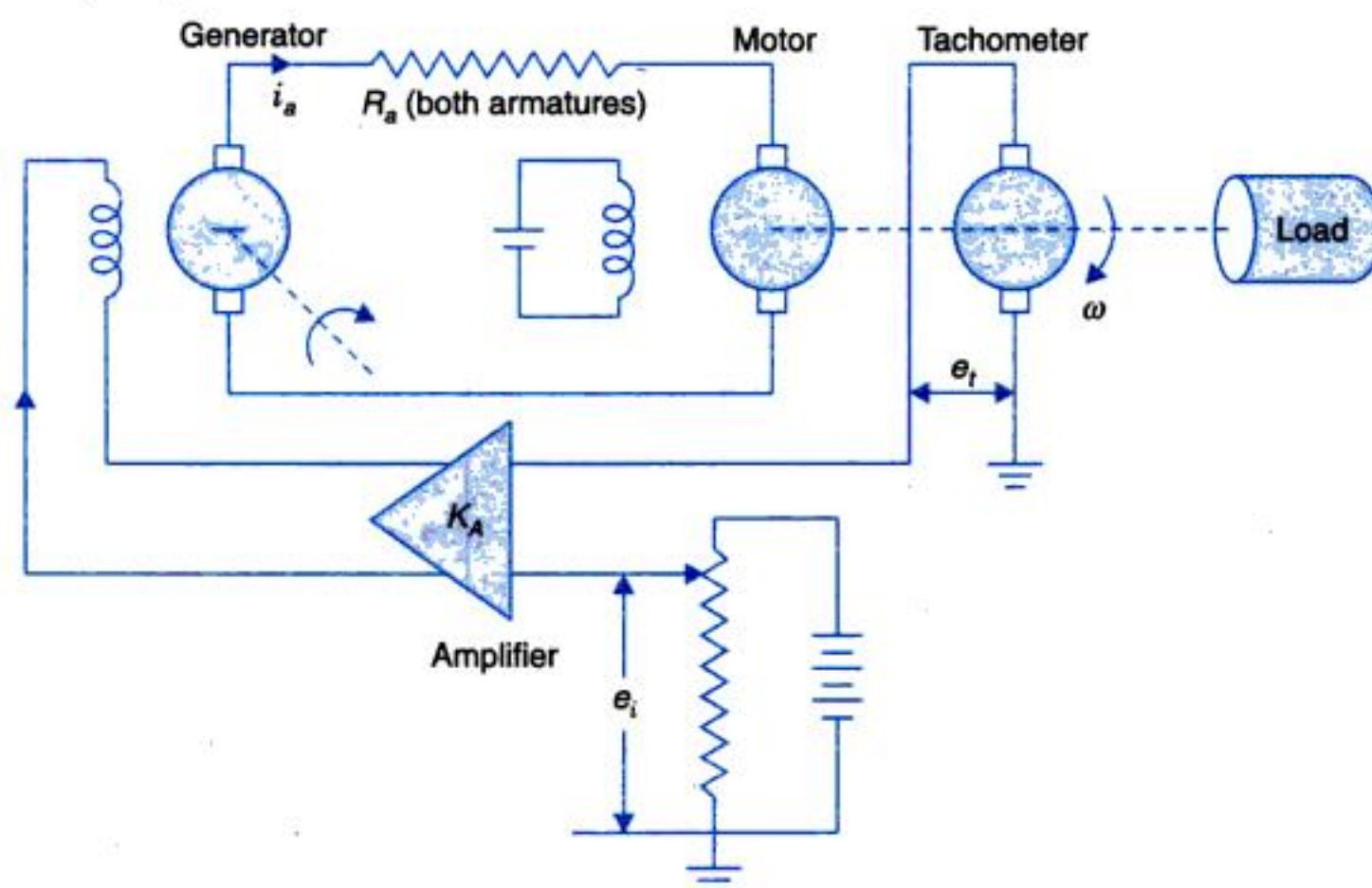


Fig. P-2.7.

- 2.8. Consider the positional servomechanism shown in Fig. P-2.8. Assume that the input to the system is the reference shaft position θ_R and the system output is the load shaft position θ_L . Draw the block diagram of the system indicating the transfer function of each block. Simplify the block diagram to obtain $\theta_L(s)/\theta_R(s)$ for the closed-loop system and also when the loop is open (in opening the loop, the lead from the output potentiometer driven by θ_C is disconnected and grounded). The parameters of the system are given below:

Sensitivity of error detector,	$K_p = 10$ volt/rad
Gain of d.c. amplifier,	$K_A = 50$ volts/volt
Motor field resistance,	$R_f = 100$ ohms
Motor field inductance,	$L_f = 20$ henrys
Motor torque constant,	$K_T = 10$ newton-m/amp
Moment of inertia of load,	$J_L = 250$ kg-m ²
Coefficient of viscous friction of load,	$f_L = 2,500$ newton-m per rad/sec
Motor to load gear ratio,	$(\dot{\theta}_L/\dot{\theta}_M) = 1/50$
Load to potentiometer gear ratio,	$(\dot{\theta}_C/\dot{\theta}_L) = 1$
Motor inertia and friction are negligible.	

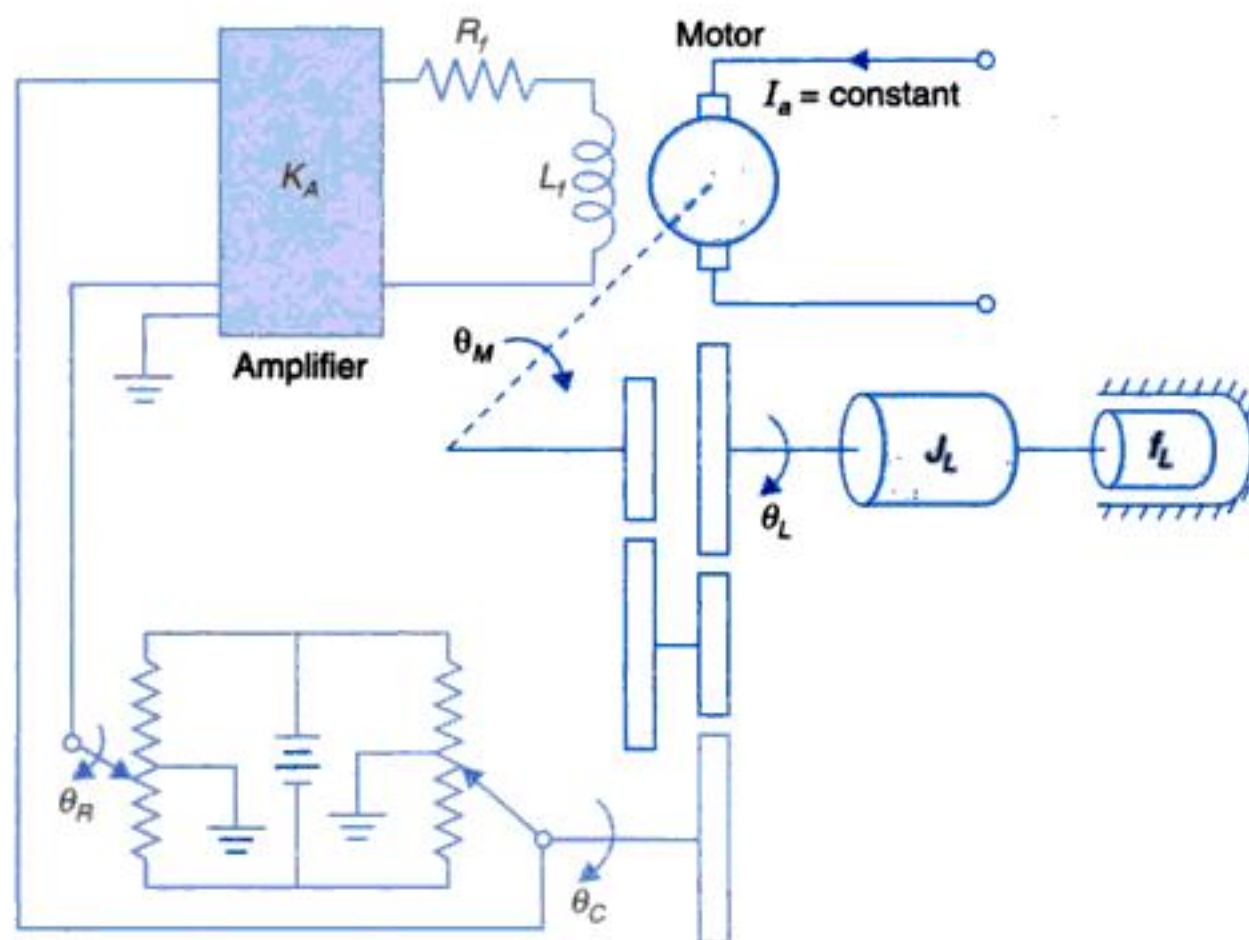


Fig. P-2.8.

- 2.9. Using block diagram reduction techniques, find the closed-loop transfer functions of the systems whose block diagrams are given in Figs. P-2.9(a) and (b).
- 2.10. For the system represented by the block diagram shown in Fig. P-2.10, evaluate the closed-loop transfer function, when the input R is (i) at station I, (ii) at station II.
- 2.11. From the block diagrams shown in Fig. P-2.11, determine C_1/R_1 and C_2/R_1 (assuming $R_2 = 0$).
- 2.12. Fig. P-2.12 shows a schematic diagram of liquid-level system. The flow of liquid Q_i into the tank is controlled by the pressure P of the incoming liquid and valve opening V_x (note that this is a more realistic model than the one shown in Fig. 2.15) through a nonlinear relationship.

$$Q_i = f(P, V_x)$$

Linearized liquid-level model and about the operating point ($P_0, Q_i = Q_0 H_0$) is given as $\Delta Q_i = K_1 \Delta P + K_2 \Delta V_x$. Draw the signal flow graph and obtain therefrom the transfer function $\left. \frac{\Delta Q_0(s)}{\Delta V_x(s)} \right|_{\Delta Q_D = 0}$

with pressure remaining constant.

(The tank and output pipe may be considered to have liquid capacitance C and flow resistance R respectively).

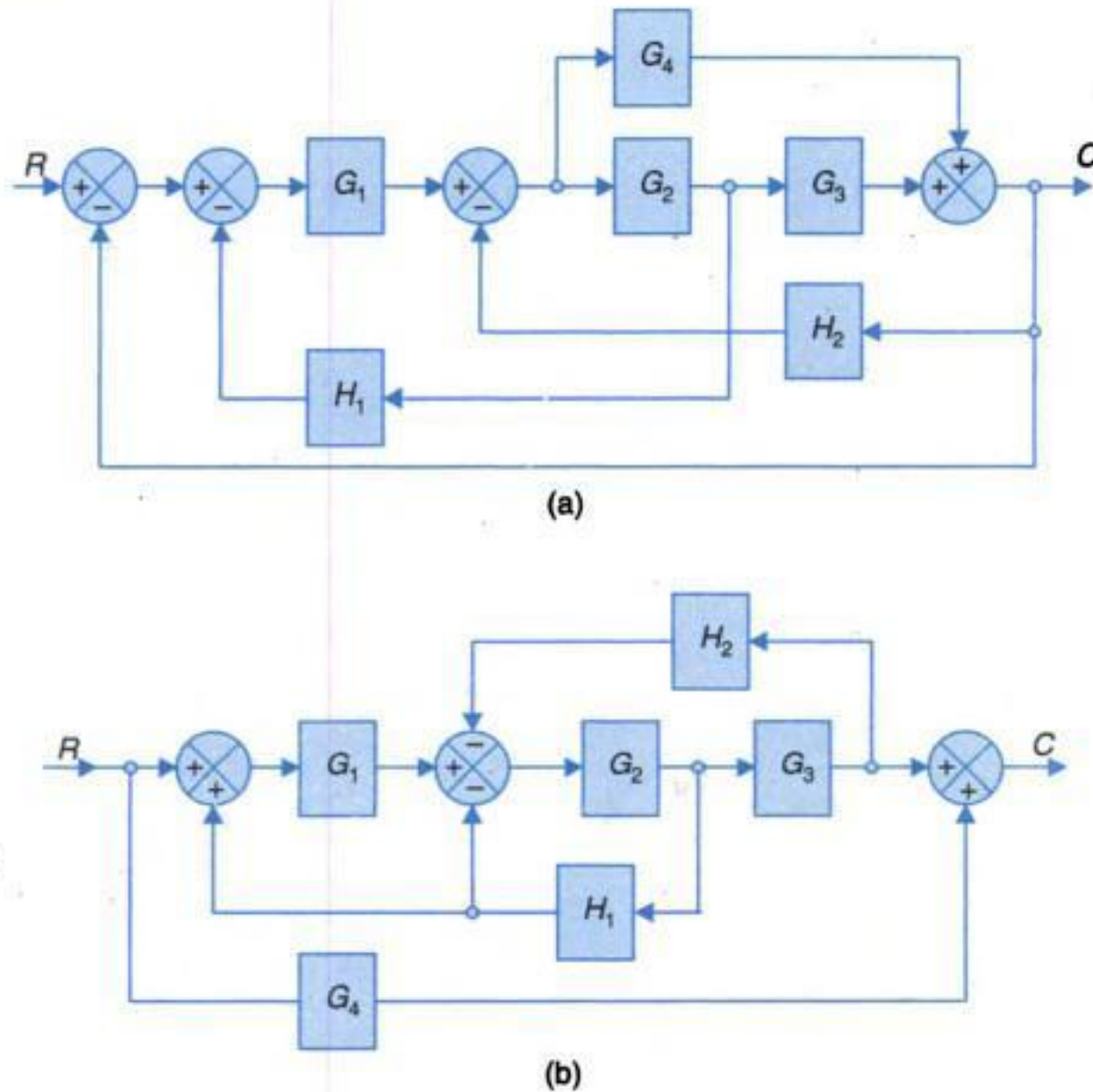


Fig. P-2.9.

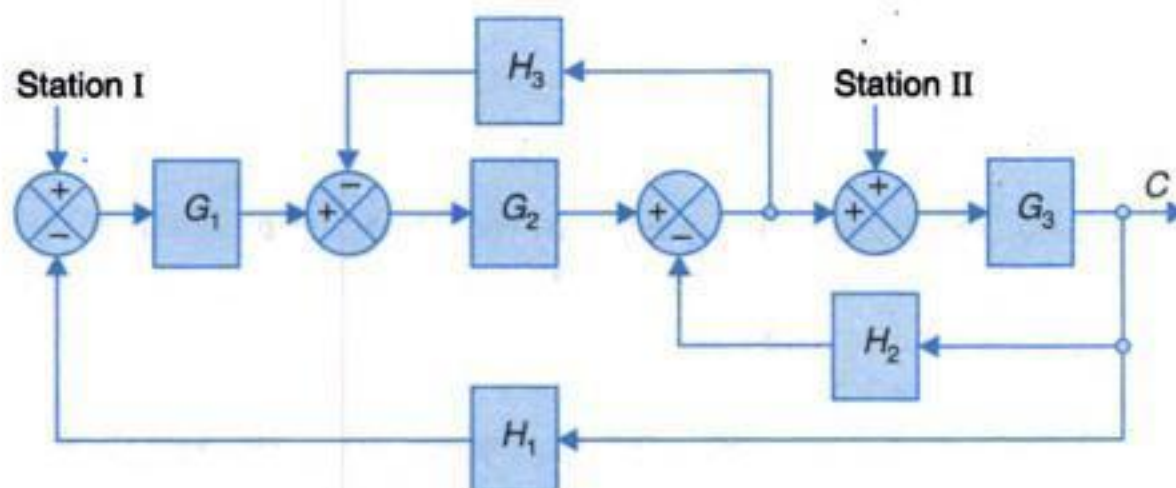


Fig. P-2.10.

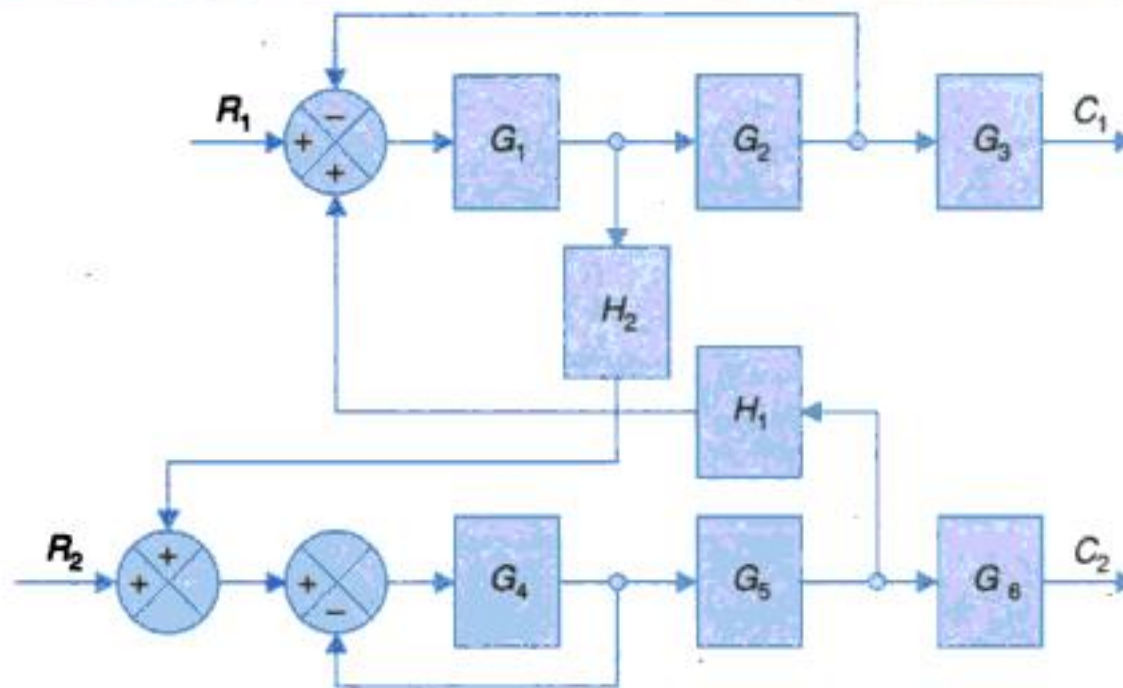


Fig. P-2.11.

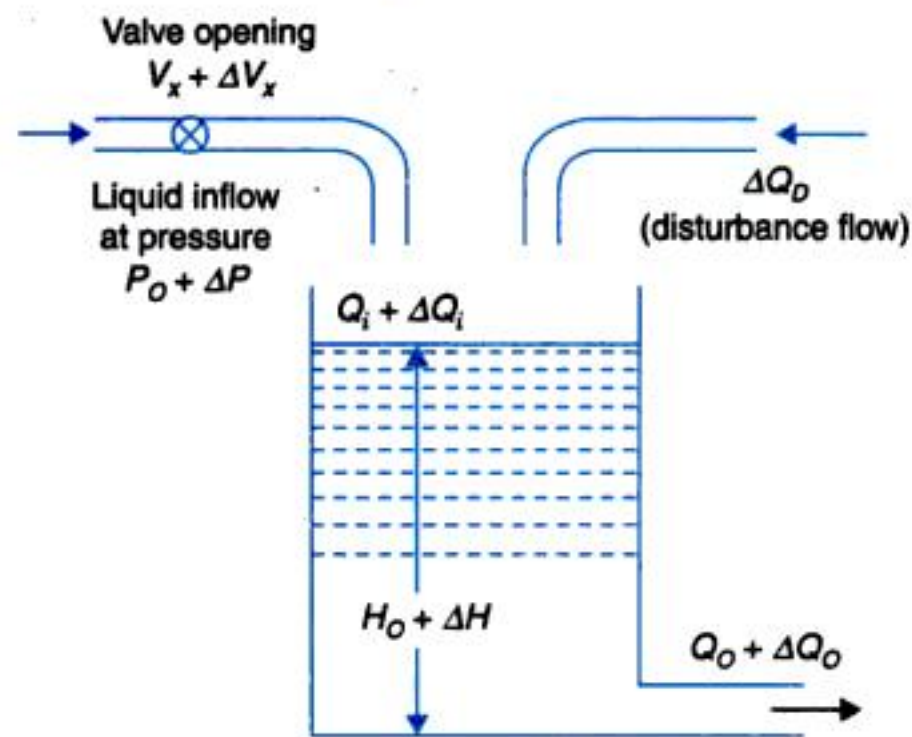


Fig. P-2.12.

2.13. Draw a signal flow graph and evaluate the closed-loop transfer function of a system whose block diagram is given in Fig. P-2.13.

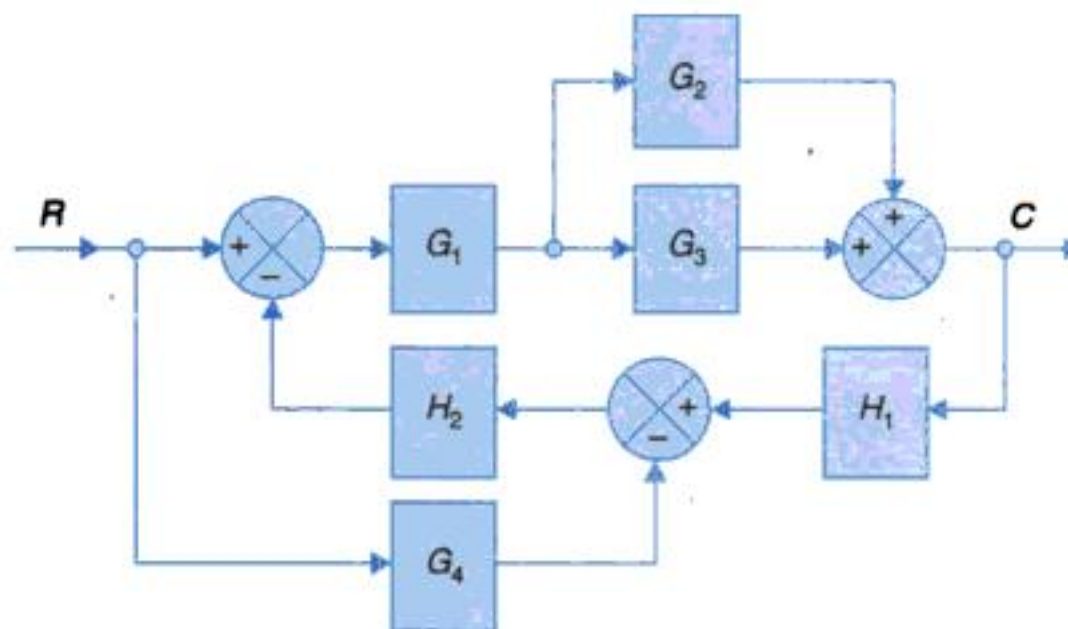


Fig. P-2.13.

2.14. Obtain the overall transfer function C/R from the signal flow graph shown in Fig. P-2.14.

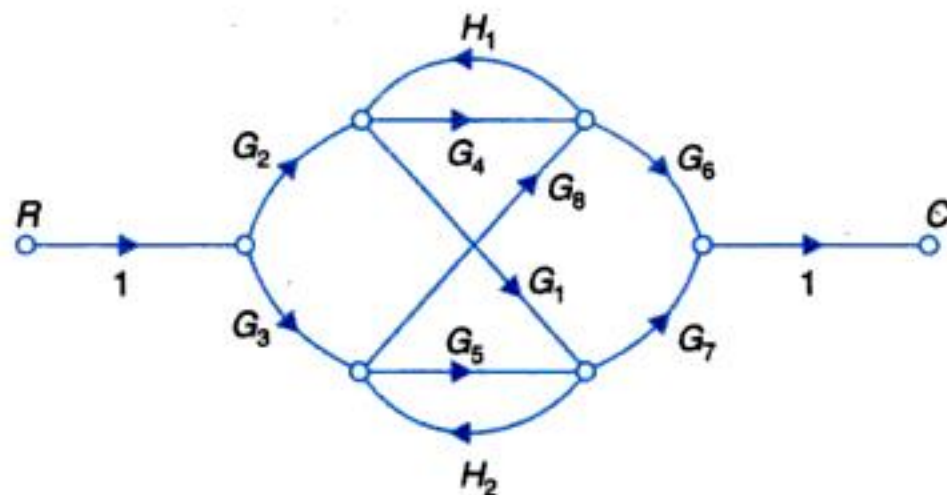


Fig. P-2.14.

2.15. Fig. P-2.15 gives the signal flow graph of a system with two inputs and two outputs. Find expressions for the outputs C_1 and C_2 . Also determine the condition that makes C_1 independent of R_2 and C_2 independent of R_1 .

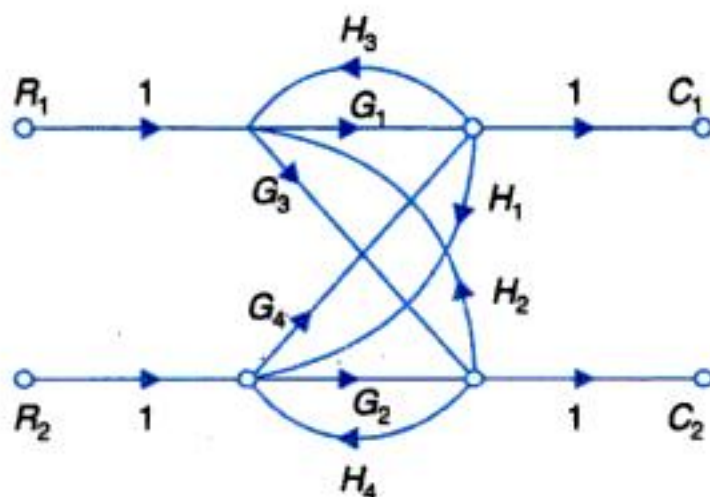


Fig. P-2.15.

2.16. For the system represented by the following equations, find the transfer function $X(s)U(s)$ by signal flow graph technique.

$$x = x_1 + \beta_3 u$$

$$\dot{x}_1 = -a_1 x_1 + x_2 + \beta_2 u$$

$$\dot{x}_2 = -a_2 x_1 + \beta_1 u.$$

3

FEEDBACK CHARACTERISTICS OF CONTROL SYSTEMS

3

FEEDBACK CHARACTERISTICS OF CONTROL SYSTEMS

3.1 FEEDBACK AND NON-FEEDBACK SYSTEMS

Feedback systems play an important role in modern engineering practice because they have the possibility for being adopted to perform their assigned tasks automatically. A *non-feedback (open-loop) system* represented by the block diagram and signal flow graph in Fig. 3.1 (a), is activated by a single signal at the input (for single-input systems). There is no provision within this system for supervision of the output and no mechanism is provided correct (or compensate) the system behaviour for any lack of proper performance of system components, changing environment, loading or ignorance of the exact value of process parameters. On the other hand, a *feedback (closed-loop) system* represented by the block diagram and signal flow graph in Fig. 3.1 (b) is driven by two signals (more signals could be employed), one the input signal and the other, a signal called the feedback signal derived from the output of the system. The feedback signal gives this system the capability to act as self-correcting mechanism as explained below.

The output signal c is measured by a sensor $H(s)$, which produces a feedback signal b . The comparator compares the feedback signal b with the input (command) signal r generating the actuating signal e , which is as measure of discrepancy between r and b . The actuating signal is applied to the process $G(s)$ so as to influence the output c in a manner which tends to reduce the errors.

Feedback as a means of automatic regulation and control is, in fact, inherent in nature and can be noticed in many physical, biological and soft systems. For example, the body temperature of any living being is automatically regulated through a process which is essentially a feedback process, only it is far more complex than the diagram of Fig. 3.1 (b).

The beneficial effects of feedback in feedback systems with high loop gain, which will be elaborated in this Chapter, are enumerated below (discussion will not follow this order).

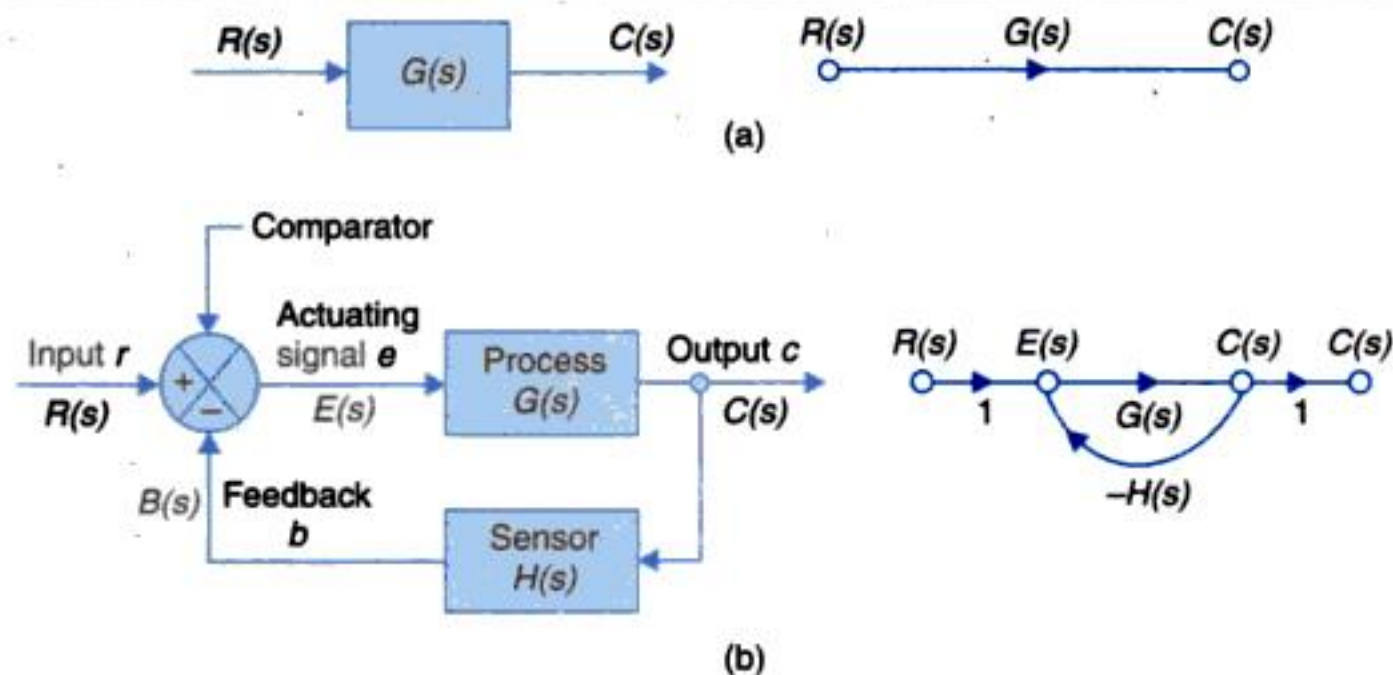


Fig. 3.1. (a) A non-feedback (open-loop) system
(b) A feedback (closed-loop) system

1. The controlled variable accurately follows the desired value.
2. Effect on the controlled variable of external disturbances other than those associated with the feedback sensor are greatly reduced.
3. Effect of variation in controller and process parameters (the forward path) on system performance is reduced to acceptable levels. These variations occur due to wear, aging, environmental changes etc.

Feedback in the control loop allows accurate control of the output (by means of the input signal) even when process or controlled plant parameters are not known accurately.

4. Feedback in a control system greatly improves the speed of its response compared to the response speed capability of the plant/components composing the system (forward path).

The cost of achieving these improvements in system's performance through feedback will be discussed alongwith. These are: greater system complexity, need for much larger forward path gain and possibility of system instability (it means undesired/persistent oscillations of the output variable).

3.2 REDUCTION OF PARAMETER VARIATIONS BY USE OF FEEDBACK

One of the primary purpose of using feedback in control systems is to reduce the sensitivity of the system to parameter variations. The parameters of a system may vary with age, with changing environment (e.g., ambient temperature), etc. Conceptually, *sensitivity* is a measure of the effectiveness of feedback in reducing the influence of these variations on system performance.

Let us define sensitivity on a quantitative basis. In the open-loop case

$$C(s) = G(s) R(s)$$

Suppose due to parameter variations $G(s)$ changes to $[G(s) + \Delta G(s)]$ where $|G(s)| \gg |\Delta G(s)|$. The output of the open-loop system then changes to

$$C(s) + \Delta C(s) = [G(s) + \Delta G(s)] R(s)$$

or

$$\Delta C(s) = \Delta G(s) R(s) \quad \dots(3.1)$$

Similarly, in the closed-loop case, the output

$$C(s) = \frac{G(s)}{1 + G(s)H(s)} R(s)$$

changes to

$$C(s) + \Delta C(s) = \frac{G(s) + \Delta G(s)}{1 + G(s)H(s) + \Delta G(s)H(s)} R(s)$$

due to the variation $\Delta G(s)$ in $G(s)$, the forward path transfer function. Since $|G(s)| \gg |\Delta G(s)|$ we have from the above, the variation in the output as

$$\Delta C(s) \approx \frac{\Delta(s)}{1 + G(s)H(s)} R(s) \quad \dots(3.2)$$

From eqns. (3.1) and (3.2) it is seen that in comparison to the open-loop system, the change in the output of the closed-loop system due to variation $G(s)$ is reduced by a factor of $[1 + G(s)H(s)]$ which is much greater than unity in most practical cases over the frequency ($s = j\omega$) of interest.

The term *system sensitivity* is used to describe the relative variation in the overall transfer function $T(s) = C(s)/R(s)$ due to variation in $G(s)$ and is defined below:

$$\text{Sensitivity} = \frac{\text{percentage change in } T(s)}{\text{percentage change in } G(s)}$$

For small incremental variation in $G(s)$, the sensitivity is written in the quantitative form as

$$S_G^T = \frac{\partial T / T}{\partial G / G} = \frac{\partial \ln T}{\partial \ln G} \quad \dots(3.3)$$

where S_G^T denotes the sensitivity of T with respect to G .

In accordance with the above definition, the sensitivity of the closed-loop system is

$$S_G^T = \frac{\partial T}{\partial G} \times \frac{G}{T} = \frac{(1 + GH) - GH}{(1 + GH)^2} \times \frac{G}{G / (1 + GH)} = \frac{1}{1 + GH} \quad \dots(3.4)$$

Similarly, the sensitivity of the open-loop system is

$$S_G^T = \frac{\partial T}{\partial G} \times \frac{G}{T} = 1 \text{ (in this case } T = G) \quad \dots(3.5)$$

Thus, the sensitivity of a closed-loop system with respect to variation in G is reduced by a factor $(1 + GH)$ as compared to that of an open-loop system.

The sensitivity of T with respect to H , the feedback sensor, is given as

$$S_H^T = \frac{\partial T}{\partial H} \times \frac{H}{T} = G \left[\frac{-G}{(1 + GH)^2} \right] \frac{H}{G / (1 + GH)} = \frac{-GH}{1 + GH} \quad \dots(3.6)$$

The above equation shows that for large values of GH , sensitivity of the feedback system with respect to H approaches unity. Thus, we see that the changes in H directly affect the system output. Therefore, it is important to use feedback elements which do not vary with environmental changes or can be maintained constant.

Very often the system's sensitivity is to be determined with a particular parameter (or parameters), with the transfer function expressed in ratio of polynomial form *i.e.*,

$$T(s) = \frac{N(s, \alpha)}{D(s, \alpha)}; \alpha = \text{parameter under consideration}$$

From eqn.(3.3)

$$S_{\alpha}^T = \frac{\partial \ln N}{\partial \ln \alpha} \Big|_{\alpha_0} - \frac{\partial \ln D}{\partial \ln \alpha} \Big|_{\alpha_0} \quad \dots(3.7a)$$

$$= S_{\alpha}^N - S_{\alpha}^D \quad \dots(3.7b)$$

where α_0 is the nominal value of the parameter around which the variation occurs.

The use of feedback in reducing sensitivity to parameter variations is an important advantage of feedback control systems. To have a highly accurate open-loop system, the components of $G(s)$ must be selected to meet the specifications rigidly in order to fulfil the overall goals of the system. On the other hand, in a closed-loop system $G(s)$ may be less rigidly specified, since the effects of parameter variations are mitigated by the use of feedback. However, a closed-loop system requires careful selection of the components of the feedback sensor $H(s)$. Since $G(s)$ is made up of power elements and $H(s)$ is made up of measuring elements which operate at low power levels, the selection of accurate $H(s)$ is far less costly than that of $G(s)$ to meet the exact specifications.

The price for improvement in sensitivity by use of feedback is paid in terms of *loss of system gain*. The open-loop system has a gain $G(s)$, while the gain of the closed-loop system is $G(s)/[1 + G(s)H(s)]$. Hence by use of feedback, the system gain is reduced by the same factor as by which the sensitivity of the system to parameter variations is reduced. Sufficient open-loop gain can, however, be easily built into a system so that we can afford to lose some gain to achieve improvement in sensitivity.

As a first example of feedback in reducing the system's sensitivity to parameter variations consider the feedback amplifier of Fig. 3.2(a) with negative feedback provided through a potential divider (feedback gain less than unity). Assuming the input impedance of the amplifier

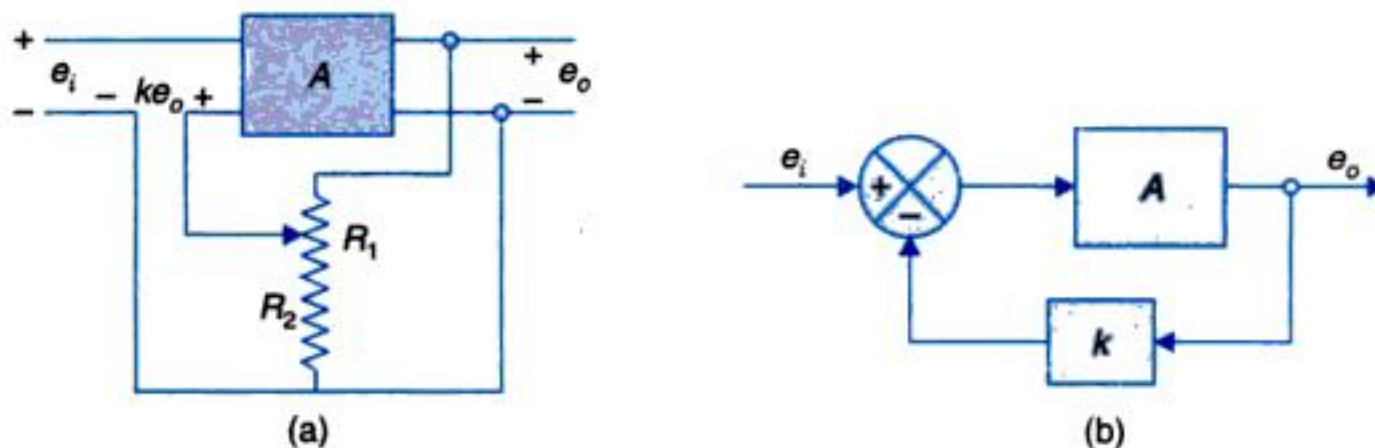


Fig. 3.2. Feedback amplifier.

to be infinite and its output impedance as zero, the equivalent block diagram of the system is drawn in Fig. 3.2 (b). Observe that both the forward gain A and feedback gain $k(< 1)$ are independent of frequency (in the range of frequencies of interest here).

It easily follows from the block diagram of Fig. 3.2 (b) that the overall gain of the amplifier circuit is

$$\frac{e_0}{e_i} = T = \frac{A}{1 + kA}; \quad k = \frac{R_2}{R_1} \leq 1 \quad \dots(3.8a)$$

$$S_A^T = \frac{dT}{dA} \cdot \frac{A}{T} = \frac{1}{1 + kA}; \text{ see eqn. (3.4)} \quad \dots(3.8b)$$

For $A = 10^4$, $k = 0.1$

$$S_A^T = \frac{1}{1 + 10^3} = 0.001$$

While the feedback reduces the sensitivity to variation in forward gain to a very low figure (0.001), it also reduces the overall gain to

$$T = \frac{10^4}{1 + 10^3} = 10; \text{ compare with forward gain of } 10^4$$

Now sensitivity to feedback gain is given by

$$\begin{aligned} S_k^T &= \frac{dT}{dk} \cdot \frac{k}{T} = \frac{-kA}{1 + kA}; \text{ eqn. (3.6)} \quad \dots(3.8c) \\ &= \frac{-10^3}{1 + 10^3} = -1 \end{aligned}$$

S_k^T being equal to unity, the feedback constant $k = R_2/R_1$ must not vary *i.e.*, the resistor ratio R_2/R_1 must be accurate and stable.

In fact for such large A ($= 10^4$), $kA \gg 1$ and so from eqn. (3.8a)

$$T = \frac{1}{k} = \frac{R_1}{R_2} = 10; \text{ independent of } A$$

As an example of control of system sensitivity, let us consider the speed control system of Fig. 2.39 which may be operated in open-or-closed-loop mode. The signal flow graph of this system is given in Fig. 2.40(b). The reduced signal flow graph of this system with $T_D = 0$, is drawn in Fig. 3.3

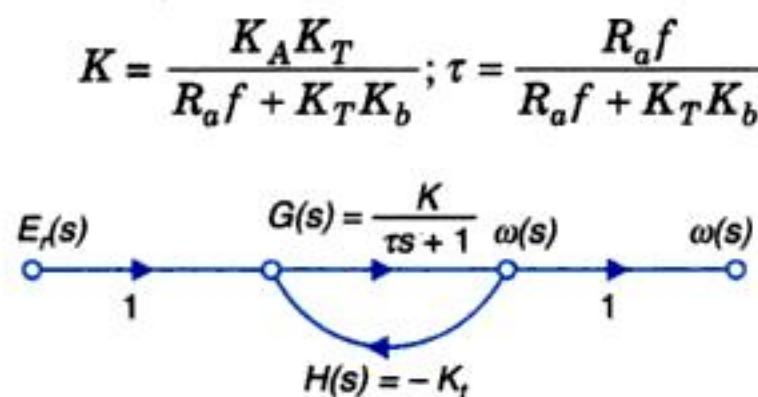


Fig. 3.3. Reduced signal flow graph ($T_D = 0$) obtained from Fig. 2.29.

The sensitivity of the open-loop mode of operation to variation-in the constant K is unity, while the corresponding sensitivity of the closed-loop mode is evaluated below.

From the signal flow graph of Fig. 3.3

$$T(s) = \frac{K}{\tau s + (1 + KK_t)} \quad (3.9a)$$

$$S_K^T = \frac{\partial T}{\partial K} \times \frac{K}{T} = \frac{s + \frac{1}{\tau}}{s + \left(\frac{1 + KK_t}{\tau} \right)} \quad (3.9b)$$

The expression (3.9b) can also be obtained by substituting $G(s) = K/(\tau s + 1)$ and $H(s) = K_t$ in eqn. (3.4).

For a typical application of this system, we might have $1/\tau = 0.1$ and $(1 + KK_t)\tau = 10$. Therefore from eqn. (3.4) we obtain

$$S_K^T = \frac{s + 0.1}{s + 10}$$

It follows from above that the sensitivity is a function of s and must be evaluated over the complete frequency band within which input has significant components. Our interest is to determine the upper limit for the sensitivity function $|S_K^T|$ over the frequency band and the frequency at which the maximum value occurs.

At a particular frequency, *e.g.*, $s = j\omega = j1$, the magnitude of the sensitivity is approximately:

$$|S_K^T| = 0.1$$

Thus the sensitivity of the closed-loop speed control system at this frequency is reduced by a factor of ten compared to that of the open-loop case.

Sensitivity studies in the frequency domain will be taken up in Chapter 9.

3.3 CONTROL OVER SYSTEM DYNAMICS BY USE OF FEEDBACK

Let us consider the elementary single-loop feedback system of Fig. 3.4. The open-loop transfer function of this system is

$$\frac{C(s)}{R(s)} = G(s) = \frac{K'}{s + \alpha} \quad \dots(3.10 (a))$$

$$= \frac{K}{\tau s + 1}; K = K'/\alpha, \tau = 1/\alpha \quad \dots(3.10 (b))$$

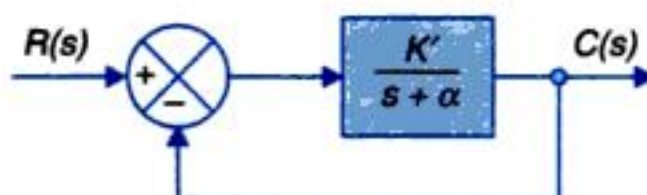


Fig. 3.4. A simple feedback system.

These are two alternative forms of expressing a transfer function. At $s = -\alpha$, $G(s)$ tends to infinity so is known as the **pole** of the system, while $\tau = 1/\alpha$ is known as its **time constant**. The *dc* gain of the system is

$$G(0) = K = K'/\alpha$$

With the feedback loop closed the closed-loop transfer function is

$$\frac{C(s)}{R(s)} = \frac{K}{s + (1+K)} = \frac{K'}{s + (\alpha + K')} \quad \dots(3.11 (a))$$

$$= \frac{K/(1+K)}{\tau_c s + 1} ; \tau_c = \tau/(1+K) \quad \dots(3.11 (b))$$

We find from eqns (3.11 (a)) and (3.11 (b)) that the effect of closing the loop (that is introduction of negative feedback) is to shift the system's pole from $-\alpha$ to $-(\alpha + K')$ or $-\alpha(1 + K)$; alternatively to reduce the system time constant from τ to $\tau/(1 + K)$. Of course in the mean time the *dc* gain has reduced to $K/(1 + K)$.

We shall now examine the effect of these changes in system transfer function on its dynamic response.

For this purpose we shall assume that the system is excited (disturbed) by an impulse input $r(t) = \delta(t)$ (infinitely large input lasting for infinity short time). The Laplace transform of an impulse excitation is $R(s) = 1$ (this will be further discussed in Chapter 5). Taking the inverse Laplace transform of eqn. (3.10 (a)) and (3.11 (a)) with $R(s) = 1$, we have

$$\begin{aligned} c(t) &= \mathcal{L}^{-1} \frac{K'}{s + \alpha} = K' e^{-\alpha t} \\ &= K' e^{-t/\tau} \text{ (for non-feedback (open-loop) system)} \end{aligned} \quad \dots(3.12)$$

and

$$\begin{aligned} c(t) &= \mathcal{L}^{-1} \frac{K'}{s + \alpha(1+K)} = K' e^{-\alpha(1+K)t} \\ &= K' e^{-t/\tau_c} \text{ (for feedback (closed-loop) system)} \end{aligned} \quad \dots(3.13)$$

The location of pole and the dynamic response of non-feedback (open-loop) and feedback (closed-loop) system are shown in Fig. 3.5. These responses decay in accordance with respective

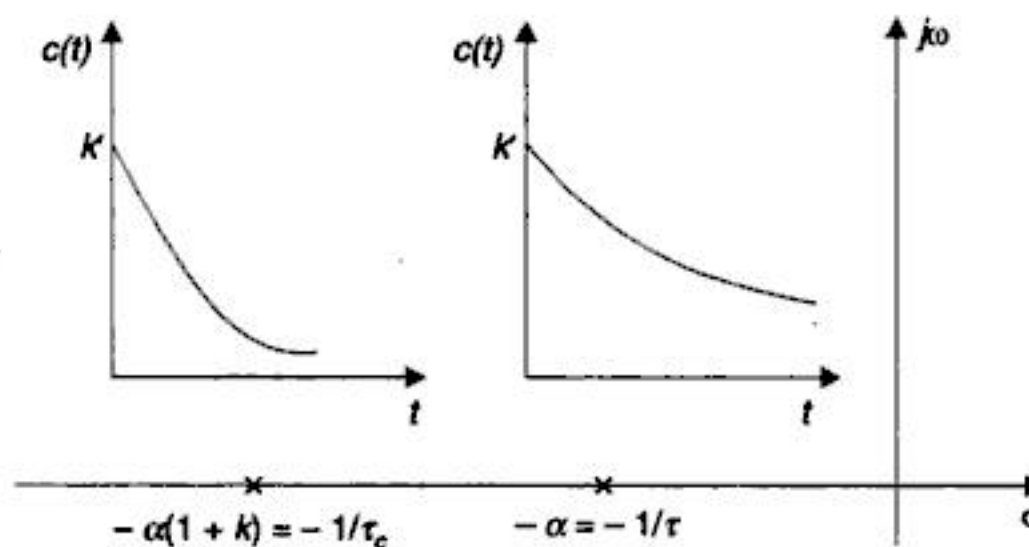


Fig. 3.5. Impulse response of open and closed-loop system (Fig. 3.4).

time constants. As the closed-loop time constant $\tau_c = \tau/(1 + K)$, its response decays much faster* which means that the speed of system's response with loop closed is faster by a factor of $(1 + K)$ compared to the open-loop system.

From this example, it is concluded that feedback controls the dynamics of the system by adjusting the location of its poles. It is, however, important to note here that feedback introduces the possibility of instability, that is, a closed-loop system may be unstable even though the open-loop is stable. The question of stability of control systems is treated in details in Chapter 6.

Consider once again the speed control system of Fig. 2.40 (a). Let the system be subjected to a suddenly applied constant input called step** input for which $E_r(s) = A/s$, where A is a constant. The output response of the system obtained by reference to the signal flow graph of Fig. 3.3 or directly from eqn. (2.101) is given by

$$\begin{aligned} \omega(s) &= \frac{K/\tau}{s\left(s + \frac{1}{\tau}\right)} && \text{(for open-loop operation, i.e., } K_t = 0) \\ &= \frac{K/\tau}{s\left(s + \frac{1 + KK_t}{\tau}\right)} && \text{(for closed-loop operation)} \end{aligned}$$

Taking the inverse Laplace transform of the above equations, we get

$$\omega(t) = K(1 - e^{-t/\tau}) \quad \text{(for open-loop operation)} \quad \dots(3.14)$$

$$= \frac{K}{1 + KK_t}(1 - e^{-t/\tau_c}) \quad \text{(for closed-loop operation)} \quad \dots(3.15)$$

where τ_c (closed-loop time constant) $= \tau/(1 + KK_t)$.

It is seen from above that if the open-loop time constant τ is large, the transient response is poor and one choice is to replace the motor by another one with a lower time constant. Such a motor will obviously be more expensive and further due to physical limitations it is not possible to design and manufacture motor of a given size with time constant lower than a certain minimum value. Under such circumstances the closed-loop mode provides a lower time constant τ_c which can be conveniently adjusted by a suitable choice of KK_t . Unlimited reduction in τ_c is of course not practicable.

It is seen from eqn (2.102) and also eqn. (3.15) that the dc gain $T(0)$ of the closed-loop system is reduced by a factor of $(1 + KK_t)$ on account of the feedback loop. However, this only needs a scaling of $r(t)$ to obtain the desired $c(t)$.

From the above illustration we conclude that feedback is a powerful technique for control of system dynamics.

Effect of feedback on bandwidth

A control system is a low-pass filter—it responds to frequencies from dc up to a certain value ω_b at which the gain drops to $1/\sqrt{2}$ of its dc value. This frequency ω_b is the bandwidth of the

*In time 5τ the response decay to $e^{-5} = 0.0067$ or 0.67% of the value immediately after application of impulse.

**Discussed in detail in Chapter 5.



You have either reached a page that is unavailable for viewing or reached your viewing limit for this book.



You have either reached a page that is unavailable for viewing or reached your viewing limit for this book.

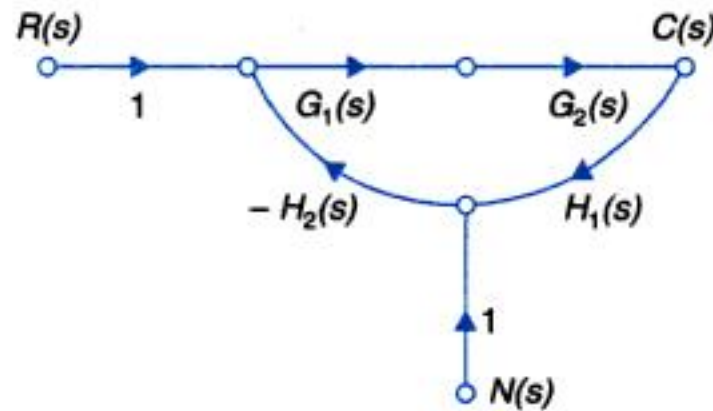


Fig. 3.7. Closed-loop system with measurement noise.

For large values of loop gain ($|G_1 G_2 H_1 H_2(s)| \gg 1$), the above equation reduces to

$$\frac{C_n(s)}{N(s)} \approx -\frac{1}{H_1(s)}$$

Therefore, the effect of noise on output is

$$C_n(s) = -\frac{N(s)}{H_1(s)} \quad \dots(3.24)$$

Thus, for optimum performance of the system, the measurement sensor should be designed such that $H_1(s)$ is maximum, which is equivalent to maximizing the signal-to-noise ratio of the sensor.

The design specifications of the feedback sensor are far more stringent than those of the forward path transfer function. The feedback sensor must have low parameter variations as these are directly reflected in system response (the sensitivity $S_H^T \approx -1$). Further the signal-to-noise ratio for the sensor must be high as explained above. Usually it is possible to design and construct the sensor with such stringent specifications and at reasonable cost because the feedback elements operate at low power level.

To conclude, the use of feedback has the advantages of reducing sensitivity, improving transient response and minimizing the effects of disturbance signals in control systems. On the other hand, the use of feedback increases the number of components of the system, thereby increasing its complexity. Further it reduces the gain of the system and also introduces the possibility of instability. However, in most cases the advantages outweigh the disadvantages and therefore the feedback systems are commonly employed in practice.

3.5 LINEARIZING EFFECT OF FEEDBACK

Yet another property of feedback is its linearizing effect which is illustrated by means of the simple single-loop static system of Fig. 3.8 (a). In a static system various gains (transmittances) are independent of time. We shall assume that the forward block function is nonlinear expresses as

$$e = f(e) = e^2; \text{ square law function}$$

When the feedback loop is open

$$e = r \Rightarrow c = r^2$$



You have either reached a page that is unavailable for viewing or reached your viewing limit for this book.



You have either reached a page that is unavailable for viewing or reached your viewing limit for this book.



You have either reached a page that is unavailable for viewing or reached your viewing limit for this book.

Subtracting eqn. (3.28) from eqn. (3.27), we have the describing equation in terms of the incremental values about the operating point as

$$2K_s^2 e_o R \Delta e = C(d\Delta\theta/dt) + (\Delta\theta - \Delta\theta_i)/R_t \quad \dots(3.29)$$

The incremental error is given by

$$\Delta e = \Delta e_r - \Delta e \quad \dots(3.30)$$

Now

$$\Delta e = K_t \Delta\theta \quad \dots(3.31)$$

K_t being the constant of the temperature sensor.

Taking the Laplace transform of eqns. (3.29), (3.30) and (3.31) and reorganizing we get

$$\Delta\theta(s) = \frac{K\Delta E(s)}{\tau s + 1} + \frac{\Delta\theta_i(s)}{\tau s + 1} \quad \dots(3.32)$$

$$\Delta E(s) = \Delta E_r(s) - \Delta E_i(s) \quad \dots(3.33)$$

$$\Delta E_i(s) = K_t \Delta\theta(s) \quad \dots(3.34)$$

where

$$K = 2K_s^2 e_o R R_t ; \tau = R_t C$$

From eqns. (3.32), (3.33) and (3.34) we can draw the block diagram of the system as shown in Fig. 3.12 where the open-loop transfer function is

$$G(s) = \frac{K}{\tau s + 1}$$

and $\Delta\theta_i(s)$ is the change in the temperature of the inflowing liquid which can be regarded as a disturbance input entering the system through $1/(\tau s + 1)$.

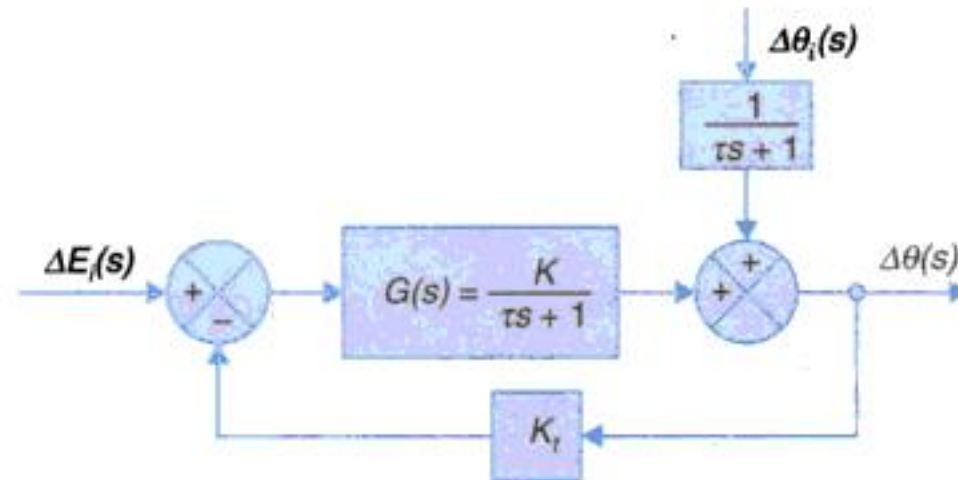


Fig. 3.12. Block diagram of the system shown in Fig. 3.9.

Assuming the disturbance signal $\Delta\theta_i$ to be zero, the steady change in the temperature of the outflowing liquid caused by an unwanted step change ΔE_r in the reference voltage is given by

$$\Delta\theta(t) = \lim_{t \rightarrow \infty} s \left(\frac{\Delta E_r}{s} \right) \frac{K}{\tau s + 1 + KK_t} = \frac{\Delta E_r K}{1 + KK_t} \quad (\text{for closed-loop}) \quad \dots(3.35)$$

$$= \Delta E_r K \quad (\text{for open-loop ; } K_t = 0) \quad \dots(3.36)$$

It is easily observed from above that the steady change in the temperature of the outflowing liquid caused by an unwanted change in reference voltage is reduced by the factor $1/(1 + KK_t)$ in the closed-loop compared to the open-loop case.



You have either reached a page that is unavailable for viewing or reached your viewing limit for this book.



You have either reached a page that is unavailable for viewing or reached your viewing limit for this book.



You have either reached a page that is unavailable for viewing or reached your viewing limit for this book.

(c) Under vehicle stalled conditions:

Vehicle speed, tachometer output (feedback signal), input to engine-vehicle block are all = 0

$$\text{Hence} \quad AK_1 = K_g D \quad \text{or} \quad D = \frac{AK_1}{K_g} = \frac{60.8 \times 50}{100} = 30.4\%$$

(d) Steady vehicle speed on level road = 10 km/h

$$\text{Then} \quad A = 60.8 \times \frac{10}{60} = 10.133 \text{ km/h}$$

$$[(10.133 - 10) K_1 - (-D) K_g] K = 100$$

$$(6.65 + 100 D) \times 1.5 = 100 \quad \text{or} \quad D = 0.6\% \text{ (down)}$$

$$(e) \text{ As in part (c)} \quad AK_1 = K_g D \quad \text{or} \quad K_g/K_1 = A/D = \frac{60.4}{50} = 1.21$$

$$(f) \text{ Open-loop system} \quad R \times K_1 \times K = 60 \quad \text{or} \quad R = \frac{60}{50 \times 15} = 0.8 \text{ km/h}$$

$$\text{Closed-loop system} \quad R \times \frac{K_1 K}{1 + K_1 K} = 60 \quad \text{or} \quad R = 60.8 \text{ km/h}$$

$$(g) \text{ Open-loop system} \quad V(s) = \frac{K_1 K}{\tau s + 1} \cdot \frac{0.8}{s}$$

Taking inverse Laplace transform

$$v(f) = 0.8 K_1 K (1 - e^{-t/\tau}) ; \tau = 20s \quad (\text{given}) \\ = 60 (11 - e^{-t/20})$$

If 90% speed, $t = t_1$

$$0.9 = 1 - e^{-t_1/20} \quad \text{or} \quad t_1 = 46 \text{ s}$$

Closed-loop system

$$V(s) = \frac{K_1 K}{\tau s + 1 + K_1 K} \cdot \frac{60.8}{s} = \frac{60.8 K'}{s(\tau' s + 1)}$$

Taking the inverse Laplace transform

$$v(t) = 0.8 k' (1 - e^{-t/\tau'})$$

$$K' = \frac{K_1 K}{1 + K_1 K} = \frac{50 \times 15}{1 + 50 \times 15} = \frac{75}{76}$$

$$\tau' = \frac{\tau}{1 + K_1 K} = \frac{20}{76} = 0.263 \text{ s}$$

$$\text{Substituting value} \quad v(t) = 60 (1 - e^{-t/0.263})$$

From which we get time at 90% speed as

$$t_1 = 0.6 \text{ s}$$

Remarks : Observe that the closed-loop system reaches 90% of steady state speed in 0.6s compared to the corresponding time 46s for the open-loop system i.e., speeding up of dynamic response by a faster of $46/0.6 \approx 77$ times.



You have either reached a page that is unavailable for viewing or reached your viewing limit for this book.



You have either reached a page that is unavailable for viewing or reached your viewing limit for this book.



You have either reached a page that is unavailable for viewing or reached your viewing limit for this book.

Example 3.5 : Consider the speed control system of Fig. 3.17 wherein the inner loop corresponds to motor back emf. The controller is an integrator with gain k observe that the load is inertia only.

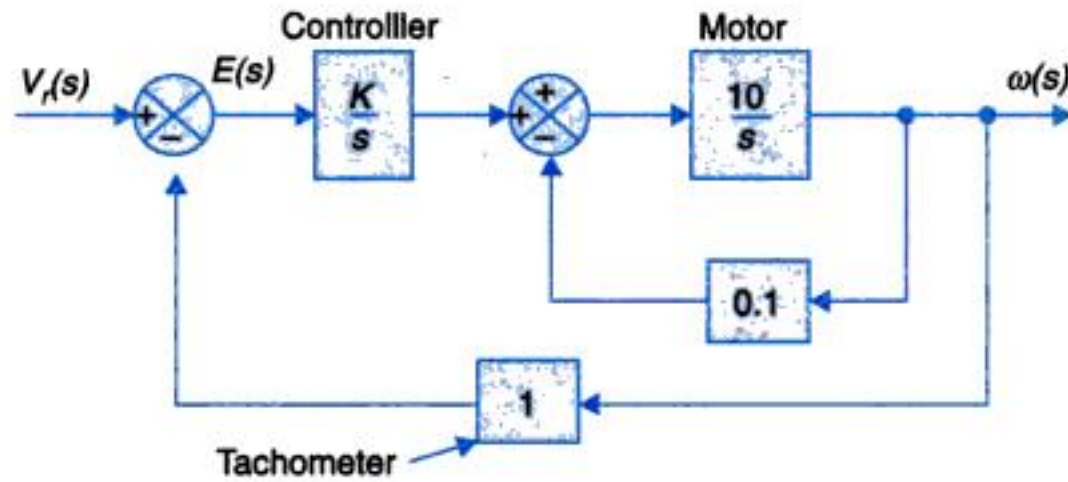


Fig. 3.17

- (a) Determine the value of K for which steady-state error to unit ramp input ($V_r(s) = 1/s^2$) is less than 0.01 rad/sec.
- (b) For the value of K found in part (a) determine, the sensitivity S_K^T , $T(s) = \omega(s)/V_r(s)$. What will be the limiting value of S_K^T at low frequencies ?

Solution. (a) Reducing the inner loop

$$G_{\text{mot}}(s) = \frac{10/s}{1 + 0.1 \times 10/s} = \frac{10}{s+1} \quad \dots(i)$$

From the forward path

$$\omega(s) = \left[\frac{10K}{s(s+1)} \right] E(s) \quad \dots(ii)$$

$$E(s) = V_r(s) - \omega(s) \quad \dots(iii)$$

$$E(s) = V_r(s) - \left[\frac{10K}{s(s+1)} \right] E(s)$$

$$\text{or} \quad E(s) = \left[\frac{s(s+1)}{s(s+1) + 10K} \right] V_r(s) \quad \dots(iv)$$

Input unit ramp, $V_r(s) = 1/s^2$. Then

$$E(s) = \frac{s(s+1)}{s(s+1) + 10K} \cdot \frac{1}{s^2} \quad \dots(v)$$

$$\text{Steady-state error} \quad e(ss) = \lim_{s \rightarrow 0} sE(s) = \lim_{s \rightarrow 0} \frac{(s+1)}{s(s+1) + 10K}$$

$$\text{or} \quad e(ss) = \frac{1}{10K} = 0.01$$

which gives $K = 10$

$$(b) \quad T(s) = \frac{\omega(s)}{V_r(s)} = \frac{\frac{10K}{s(s+1)}}{1 + \frac{10K}{s(s+1)}}$$



You have either reached a page that is unavailable for viewing or reached your viewing limit for this book.



You have either reached a page that is unavailable for viewing or reached your viewing limit for this book.



You have either reached a page that is unavailable for viewing or reached your viewing limit for this book.

Laplace transforming yields

$$Q_i(s) + Q_d(s) = \frac{(RCs + 1)}{R} H(s) \quad \dots(iv)$$

or
$$H(s) = \frac{R}{(RCs + 1)} [Q_i(s) + Q_d(s)] \quad \dots(v)$$

According to level sensing feedback controller

$$Q_i(s) = -G_c(s) H(s) ; \text{negative feedback} \quad \dots(vi)$$

From Eqs. (v) and (vi) the block diagram of Fig. 3.20 can be drawn.

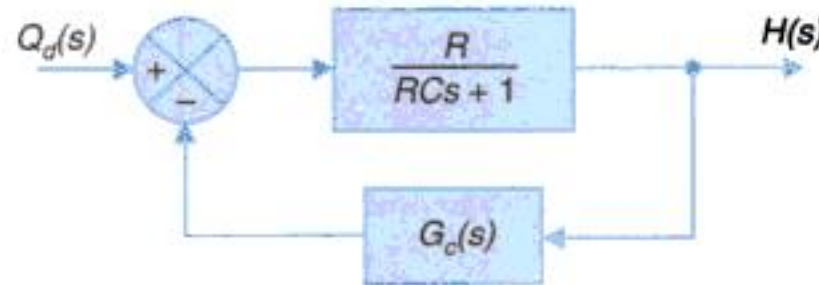


Fig. 3.21

(i) $G_c(s) = K$

From Fig. 3.20

$$\frac{H(s)}{Q_d(s)} = \frac{\frac{R}{RCs + 1}}{1 + \frac{KR}{RCs + 1}}$$

or
$$\frac{H(s)}{Q_d(s)} = \frac{R}{RCs + (1 + KR)} \quad \dots(vii)$$

For unit step $Q_d(s) = \frac{1}{s}$. Then

$$h_{ss} = \lim_{s \rightarrow 0} sH(s) = \lim_{s \rightarrow 0} \frac{sR}{s[RCs + (1 + KR)]}$$

or
$$h_{ss} = \frac{R}{1 + KR} \quad \dots(viii)$$

(ii) $G_c(s) = \frac{K}{s}$

From Fig. 3.20

$$\frac{H(s)}{Q_d(s)} = \frac{Rs}{RCs + (1 + KR)}$$

For unit step disturbance $\theta_d(s) = \frac{1}{s}$ (ix)

$$h_{ss} = \lim_{s \rightarrow 0} sH(s) = \lim_{s \rightarrow 0} \frac{s \times sR}{s[RCs + (1 + KR)]}$$

or
$$h_{ss} = 0 \quad \dots(x)$$



You have either reached a page that is unavailable for viewing or reached your viewing limit for this book.



You have either reached a page that is unavailable for viewing or reached your viewing limit for this book.



You have either reached a page that is unavailable for viewing or reached your viewing limit for this book.

- 3.7. The field of a d.c. servomotor is separately excited by means of a d.c. amplifier of gain $K_A = 90$ (see Fig. P-3.7). The field has an inductance of 2 henrys and a resistance of 50 ohms. Calculate the effective field time constant.

A voltage proportional to the field current is now fed back negatively to the amplifier input. Determine the value of the feedback constant K to reduce the field time constant to 4 milliseconds.

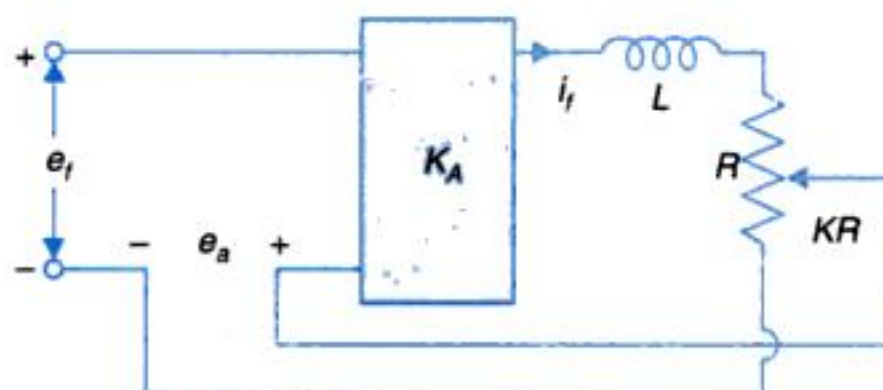


Fig. P-3.7

- 3.8. For the speed control system shown in Fig. P-3.8 assume that
- the reference and feedback tachometer are identical;
 - generator field time constant is negligible and its generated voltage is K_g volts/amp;
 - friction of motor and mechanical load is negligible.
- Find the time variation of output speed (ω_o) for a sudden reference input of 10 rad/sec. Find also the steady-state output speed.
 - If the feedback loop is opened and gain K_A adjusted to give the same steady-state speed as in the case of the closed-loop, determine how the output speed varies with time and compare the speed of response in the two cases (closed- and open-loop).
 - Compare the sensitivity of ω_o to changes in amplifier gain K_A and generator speed ω_g , with and without feedback.

[Hint : The generator gain constant K_g changes in direct proportion to generator speed i.e., $K_g = K'_g \omega_g$ where K'_g is constant.]

The system constants are given below:

Moment of inertia of motor and load

$$J = 5 \text{ kg-m}^2$$

Motor back emf constant

$$K_t = 5 \text{ volts per rad/sec}$$

Total armature resistance of motor and generator

$$R_a = 1 \text{ ohm}$$

Generator gain constant

$$K_g = 50 \text{ volts/amp}$$

Amplifier gain

$$K_A = 5 \text{ amps/volt}$$

Tachometer constant

$$K_t = 0.5 \text{ volts per rad/sec}$$

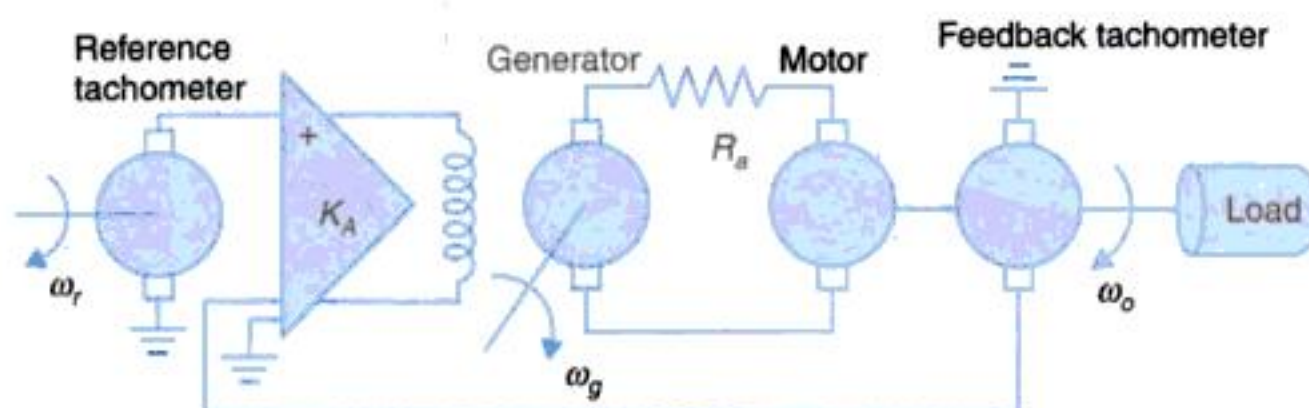


Fig. P-3.8



You have either reached a page that is unavailable for viewing or reached your viewing limit for this book.



You have either reached a page that is unavailable for viewing or reached your viewing limit for this book.



You have either reached a page that is unavailable for viewing or reached your viewing limit for this book.

3.13. For the system whose signal flow graph is drawn in Fig. P-3.13

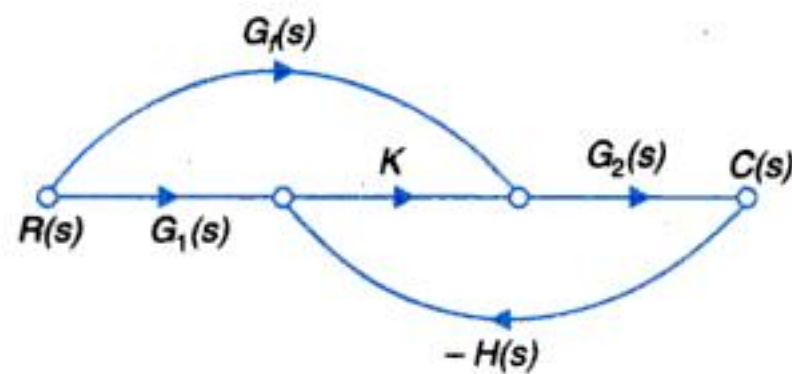


Fig. P-3.13

Find the transfer function $T(s) = C(s)/R(s)$

Find the system sensitivity S_K^T using eqn. (3.7a)

3.14 Fig. P-3.14 shows the block diagram of a speed control system with an integrator (K/s) in the forward path for a desired speed of 100 rad/s, show that steady output speed will be 100 rad/s (indicative of zero steady state error).

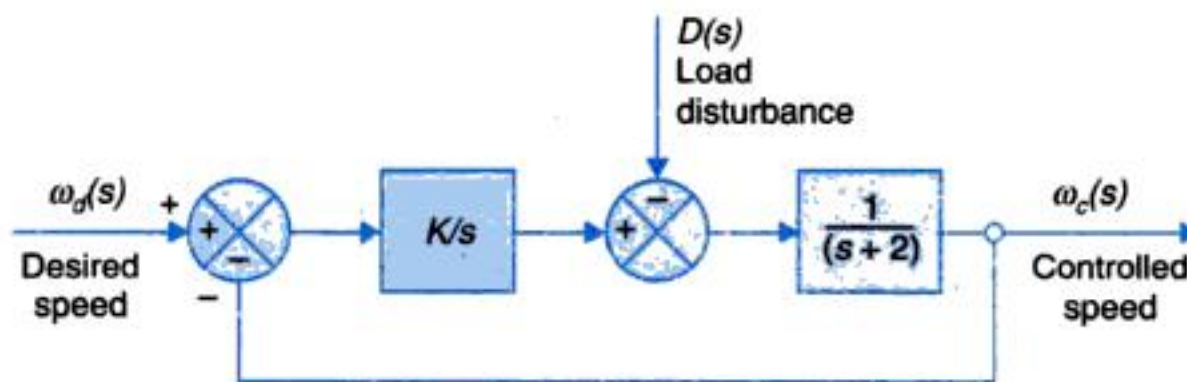


Fig. P-3.14

For a unit load disturbance $D(s) = 1/s$ find the s -domain expression for change in controlled speed, $\omega_c^D(s)$. Find the change in speed, caused by the disturbance at $t = 0$ and $t = \infty$ (steady state change).

Find the expression for $\omega_c^D(t)$ for $K = 0.5, 1, 2$ and 4 . Sketch the nature of response. Which value of K should be preferred and why? You may use Table 1.3 (Appendix 1) for finding Laplace inverse.

3.15 In a radar system, an electromagnetic pulse is radiated from an antenna into space. An echo pulse is received back if a conducting surface such as an airplane appears in the path of the signal. When the radar is in search of target, the antenna is continuously rotated. When target is located, the antenna is stopped and pointed towards the target by varying its angular direction until a maximum echo is heard. If energy is radiated in a narrow directional beam, accurate information about target location can be obtained. Narrow beam can be realised if the antenna size is large (e.g., 20 m diameter). To drive this size of antenna, hydraulic or electric motors are used. One of the schemes utilizing electric motor is depicted in Fig. P-3.15. Determine:

- Sensitivity to changes in SCR gain, K_s for $\omega = 0.1$.
- The steady-state error of motor shaft, i.e., $(\theta_R - \theta_M)$ when antenna is subjected to a constant wind gust torque of 100 newton-m.



You have either reached a page that is unavailable for viewing or reached your viewing limit for this book.



You have either reached a page that is unavailable for viewing or reached your viewing limit for this book.



You have either reached a page that is unavailable for viewing or reached your viewing limit for this book.

4

CONTROL SYSTEMS AND COMPONENTS



You have either reached a page that is unavailable for viewing or reached your viewing limit for this book.



You have either reached a page that is unavailable for viewing or reached your viewing limit for this book.



You have either reached a page that is unavailable for viewing or reached your viewing limit for this book.

process (plant), turn a robot link w.r.t. to its neighbouring link, move a transformer tap (up or down), move up/down the control rods of a nuclear reactor etc.

Because of the flexibility inherent in transmitting electrical power (through cables) and desirable speed-torque characteristics which are linear, electric actuators (motors) are now widely adopted in control systems except in low speed but high torque applications where hydraulic actuators are still in use. Pneumatic actuators are not as messy as hydraulic ones but suffer from leakages and inherent inaccuracies.

4. *Electric system.* DC and ac motors are the two kinds of electric actuators; in low power ratings these are known as servomotors. DC motors are costlier than ac motors because of the additional cost of commutation gear. These have, however, the important advantages of linearity of characteristics and higher **stalled torque/inertia** ratio; this being an important figure of merit for a servomotor. Stalled torque is the torque developed by motor when stationary with full applied voltage (and full field in case of a DC motor). It may be pointed out here that high torque/inertia ratio means lower motor time constant and so faster dynamic response.

With advanced manufacturing techniques, low brush commutator friction and still higher torque/inertia ratios have been achieved in dc servomotors, such that these have practically taken over from ac servomotors in most control applications.

Electric actuators for stepped motion are known as stepper motors which will be dealt in details in section 4.

DC Servomotors

Modelling of dc motors, armature controlled and field controlled, has been considered at length in Chapter 2. Here we shall consider some of the constructional features of dc servomotors. With recent development in rare earth permanent magnets (PM) which have high residual flux density and a very high coercivity, dc servomotors are now constructed with PMs resulting in much higher torque/inertia ratio and also higher operating efficiency as these motor have no field losses. The speed of a permanent magnet dc (PMDC) motor is nearly directly proportional to armature voltage at a given load torque. Also the speed-torque characteristic at a given voltage is more flat than in a wound field motor as the effect of armature reaction is less pronounced in a PM motor.

Three types of constructions employed in PMDC servomotors are illustrated in Fig. 4.3 (a), (b) and (c). In Fig. 4.3 (a) the armature is slotted with dc winding placed inside these slots (as in a normal dc motor). Though quite reliable and rugged this type of construction has high inertia to reduce which the construction of Fig. 4.3 (b) is adopted where the winding is placed on the armature surface. Because of the larger air gap, stronger PMs are needed in this construction. A much lower inertia is achieved by placing the winding on a nonmagnetic cylinder which rotates in annular space between the PM stator and stationary rotor as illustrated in Fig. 4.3 (c). The air gap has to be still larger with consequent need of much stronger PMs. The constructional details of this low inertia motor are further brought out in Fig. 4.3 (d).



You have either reached a page that is unavailable for viewing or reached your viewing limit for this book.



You have either reached a page that is unavailable for viewing or reached your viewing limit for this book.



You have either reached a page that is unavailable for viewing or reached your viewing limit for this book.

1. The rotor of the servomotor is built with high resistance so that its X/R ratio is small and the torque-speed characteristic, as shown by the curve b of Fig. 4.7, is nearly linear in contrast to the highly nonlinear characteristic when large X/R ratio is used for servo applications, then because of the positive slope for part of the characteristic, the system using such a motor becomes unstable.

The rotor construction is usually squirrel cage or drag-cup type. The diameter of the rotor is kept small in order to reduce inertia and thus to obtain good accelerating characteristics. Drag-cup construction is used for very low inertia applications.

2. In servo applications, the voltages applied to the two stator windings are seldom balanced. As shown in Fig. 4.8, one of the phases known as the *reference phase* is excited by a constant voltage and the other phase, known as the *control phase* is energized by a voltage which is 90° out of phase with respect to the voltage of the reference phase. The control phase voltage is supplied from a servo amplifier and it has a variable magnitude and polarity ($\pm 90^\circ$ phase angle with respect to the reference phase). The direction of rotation of the motor reverses as the polarity of the control phase signal changes sign.

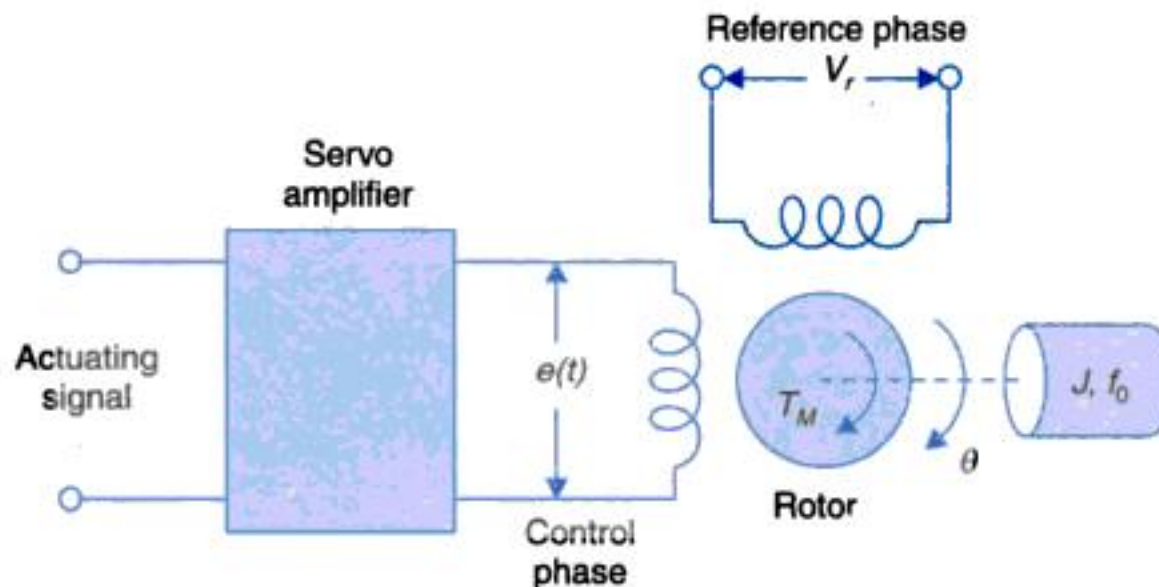


Fig. 4.8. Schematic diagram of a two-phase servomotor.

It can be proved using symmetrical components that starting torque of servomotor under unbalanced operation, is proportional to E , the rms value of the sinusoidal control voltage $e(t)$. A family of torque-speed curves with variable rms control voltage is shown in Fig. 4.9 (a). All these curves have negative slope. Note that the curve for zero control voltage goes through the origin and the motor develops a decelerating torque.

As seen from Fig. 4.9 (a), the torque-speed curves are still somewhat nonlinear. However, in the low-speed region, the curves are nearly linear and equidistant, i.e., the torque varies linearly with speed as well as with control voltage. Since a servomotor seldom operates at high speeds, these curves can be linearized about the operating point.

The torque generated by the motor is a function of both the speed $\dot{\theta}$ and rms control, voltage E , i.e., $T_M = f(\dot{\theta}, E)$. Expanding this equation into Taylor's series about the normal operating point $(T_{M0}, E_0, \dot{\theta}_0)$ and dropping off the terms of second- and higher-order derivatives, we get



You have either reached a page that is unavailable for viewing or reached your viewing limit for this book.



You have either reached a page that is unavailable for viewing or reached your viewing limit for this book.



You have either reached a page that is unavailable for viewing or reached your viewing limit for this book.



You have either reached a page that is unavailable for viewing or reached your viewing limit for this book.



You have either reached a page that is unavailable for viewing or reached your viewing limit for this book.



You have either reached a page that is unavailable for viewing or reached your viewing limit for this book.

$$\text{Resolution (Pot)} = \frac{V_{REF}(\text{Pot})}{x_t} \text{ V/degree, } x_t = \text{total pot turns (in degrees)}$$

Hence,

Mechanical resolution of the system

$$= \frac{V_{REF}(\text{ADC})}{2^N} \frac{V_{REF}(\text{Pot})}{x_t} = \frac{V_{REF}(\text{ADC}) x_t}{2^N V_{REF}(\text{Pot})}$$

For a single turn pot (340°), $N = 8$ bit, $V_{REF}(\text{ADC}) = V_{REF}(\text{Pot}) = 5 \text{ V}$

$$\text{Resolution (ADC)} = \frac{5}{2^8} = 20 \text{ mV}$$

$$\text{Mechanical resolution (system)} = \frac{340^\circ}{2^8} = 1.36^\circ/\text{bit}$$

It may also be noted that $V_{REF}(\text{Pot})$ should not be more than $V_{REF}(\text{ADC})$, otherwise ADC would get damaged.

Optical Encoders

Optical encoders are frequently used in control systems (robots in particular) to convert linear or rotary displacement into digital code or pulse signals. Encoders are of two types:

Absolute encoders: Their output is a digitally coded signal with distinct digital code indicative of each particular least significant increment of resolution.

Incremental encoders: Their output is a pulse for each increment of resolution but these make no distinction between increments.

Because of their simple construction, low cost, ease of application and versatility incremental encoders are by far one of the most popular encoders.

Incremental Encoder

An incremental encoder typically has four parts: a light source (LED), a rotary (or translatory) disc, a stationary mask and a sensor (photodiode) as shown in Fig. 4.14. The disc has alternate opaque and transparent sectors (of equal width) which are etched by means of a photographic process on to a plastic disc (slots are cut out in case a metal disc is used). As the disc rotates during half of the increment cycle the transparent sectors of rotating and stationary discs come in alignment permitting the light from LED to reach the sensor thereby generating an electrical pulse (see Fig. 4.15). For fine resolution encoders (upto thousands of increments/revolution), multi-slit mask is often used to maximize the reception of shutter light.

The wave form of the sensor output of an encoder is generally triangular or sinusoidal depending upon the resolution required. Square wave signal compatible with digital logic are obtained from it by means of linear OPAM and comparator. Alternate transparent/opaque sectors of the disc (in developed form) and the square wave pulse train (obtained after signal processing) in synchronous with the disc are shown in Fig 4.15. The resolution of such an incremental encoder is give as:

$$\text{Basic resolution} = (360^\circ/N)$$

where N = no. of sectors of disc; each sector is half transparent and half opaque.



You have either reached a page that is unavailable for viewing or reached your viewing limit for this book.



You have either reached a page that is unavailable for viewing or reached your viewing limit for this book.



You have either reached a page that is unavailable for viewing or reached your viewing limit for this book.

$$v_{s_2 s_3} = v_{s_2 n} - v_{s_3 n} = \sqrt{3} K V_r \sin (\theta + 120^\circ) \sin \omega_c t \quad \dots(4.16)$$

$$v_{s_3 s_1} = v_{s_3 n} - v_{s_1 n} = \sqrt{3} K V_r \sin \theta \sin \omega_c t \quad \dots(4.17)$$

when $\theta = 0$, from eqns. (4.12)—(4.14) it is seen that maximum voltage is induced in the stator coil S_2 , while it follows from eqn. (4.17) that the terminal voltage $v_{s_3 s_1}$ is zero. This position of the rotor is defined as the *electrical zero* of the transmitter and is used as reference for specifying the angular position of the rotor (see Fig. 4.20).

Thus it is seen that the input to the synchro transmitter is the angular position of its rotor shaft and the output is a set of three single-phase voltages given by eqns. (4.15)—(4.17); the magnitudes of these voltages are functions of the shaft position.

The output of the synchro transmitter is applied to the stator windings of a *synchro control transformer*. The control transformer is similar in construction to a synchro transmitter except for the fact that the rotor of the control transformer is made cylindrical in shape so that the air gap is practically uniform. The system (transmitter-control transformer pair) acts as an error detector. Circulating currents of the same phase but of different magnitudes flow through the two sets of stator coils. The result is the establishment of an identical flux pattern in the air gap of the control transformer as the voltage drops in resistances and leakage reactances of the two sets of stator coils are usually small. The control transformer flux axis thus being in the same position as that of the synchro transmitter rotor, the voltage induced in the control transformer rotor is proportional to the cosine of the angle between the two rotors and is given by

$$e(t) = K V_r \cos \phi \sin \omega_c t \quad \dots(4.18)$$

where ϕ is the angular displacement between the two rotors. When $\phi = 90^\circ$, i.e., the two rotors are at right angles, then the voltage induced in the control transformer rotor is zero. This position is known as the *electrical zero* position of the control transformer. In Fig. 4.19, the transmitter and control transformer rotors are shown in their respective electrical zero positions.

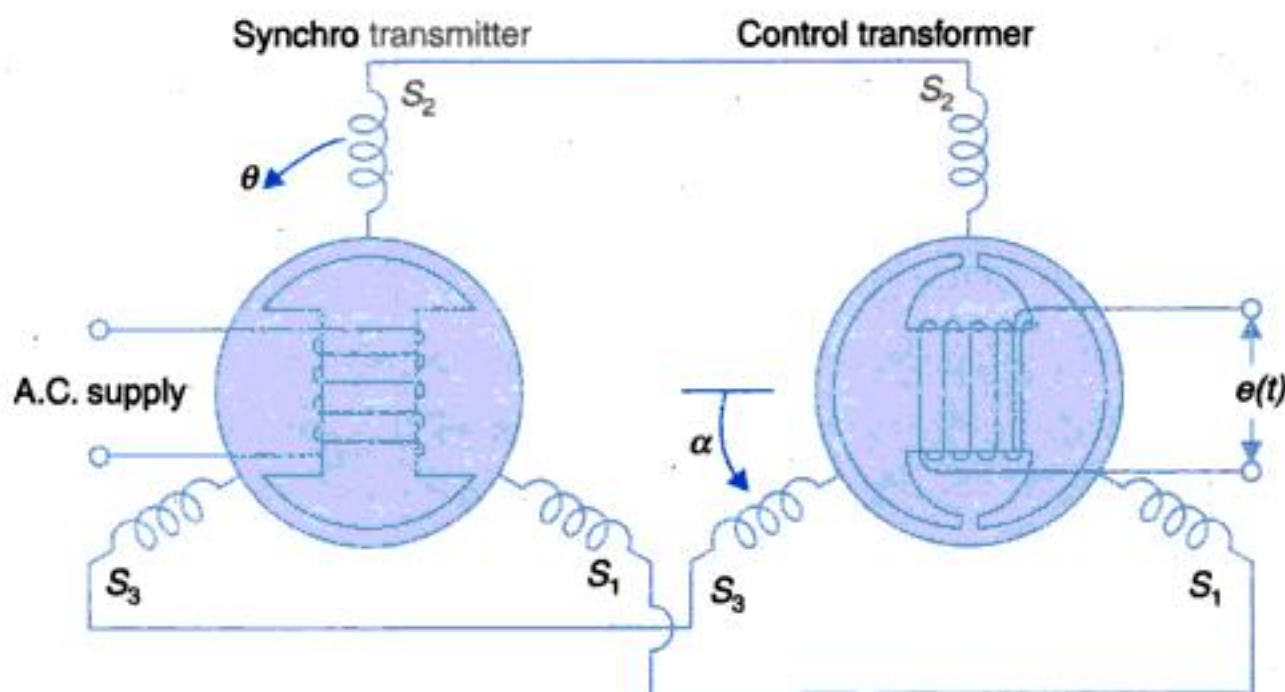


Fig. 4.19. Synchro error detector.

Let the rotor of the transmitter rotate through an angle θ in the direction indicated and let the control transformer rotor rotate in the same direction through an angle α resulting in a net



You have either reached a page that is unavailable for viewing or reached your viewing limit for this book.



You have either reached a page that is unavailable for viewing or reached your viewing limit for this book.



You have either reached a page that is unavailable for viewing or reached your viewing limit for this book.



You have either reached a page that is unavailable for viewing or reached your viewing limit for this book.



You have either reached a page that is unavailable for viewing or reached your viewing limit for this book.

presents infinite reluctance to the phase 'a' axis and so the torque has also a zero there. Thus the rotor torque is a function of the $\sin 2\theta$ as drawn in Fig. 4.24 (b). Seen from stator there are thus two possible excitation for a given rotor position. For example, for rotor $\theta = 0^\circ$ locking takes place when either 'a' or 'b' phase is excited. This fact is in contrast to the PM stepper motor and has to be kept in mind in using this type of motor.

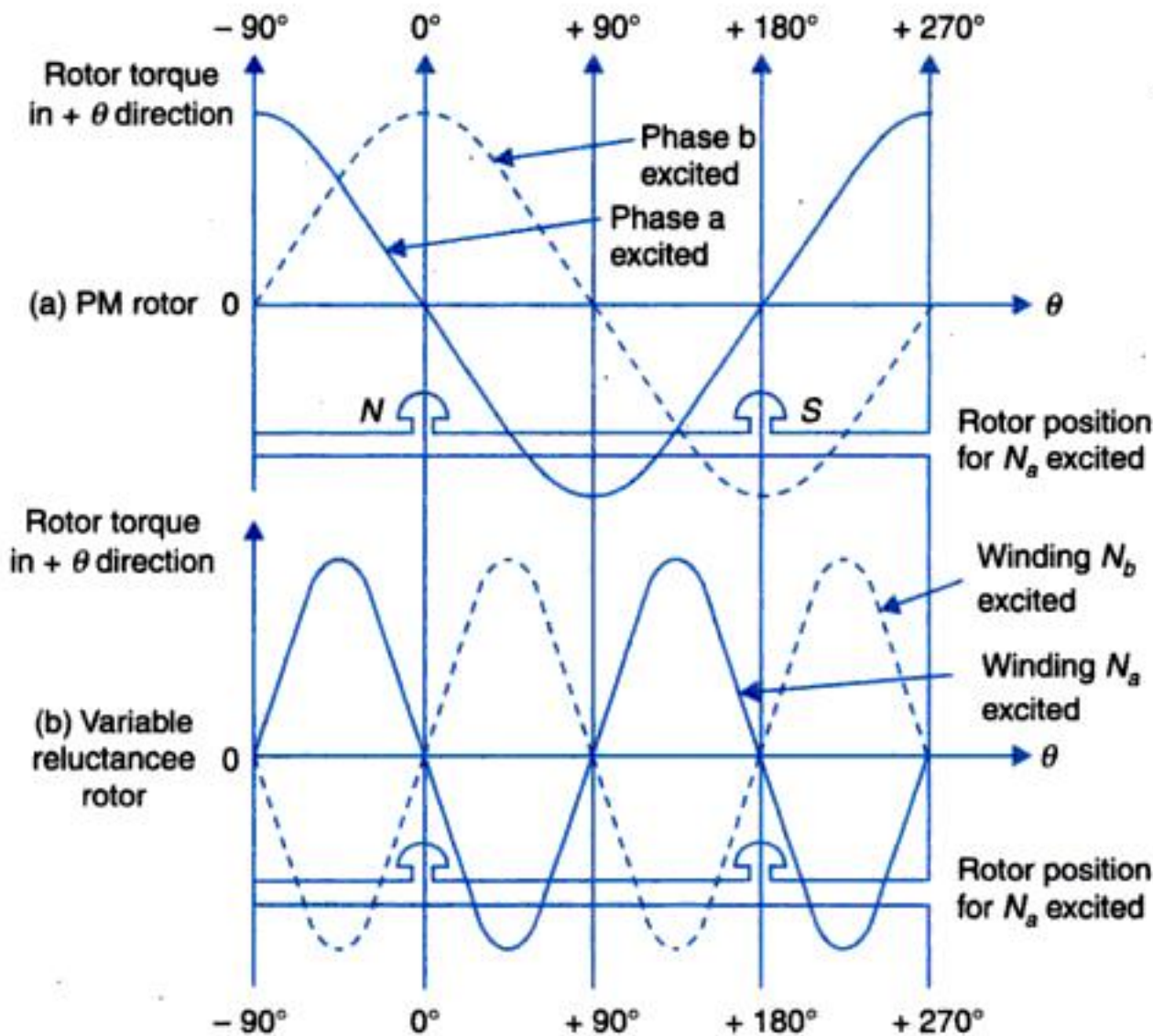


Fig. 4.24. Torque-angle characteristics of stepper motor
(a) PM motor (b) variable-reluctance motor.

Having illustrated the operation of an elementary stepper motor and its two types, we shall now consider some further details.

Variable-reluctance Stepper Motor

A variable-reluctance stepper motor consists of a single or several stacks of stators and rotors—stators have a common frame and rotors have a common shaft as shown in the longitudinal cross-sectional view of Fig. 4.25 for a 3-stack motor. Both stators and rotors have toothed structure as shown in the end view of Fig. 4.26. The stator and rotor teeth are of same size and therefore can be aligned as shown in this figure. The stators are pulse excited, while the rotors are unexcited.

Consider a particular stator and rotor set shown in the developed diagram of Fig. 4.27. As the stator is excited, the rotor is pulled into the nearest minimum reluctance position—the position where stator and rotor teeth are aligned. The stator torque acting on the rotor is a function of the angular misalignment θ . There are two positions of zero torque: $\theta = 0$, rotor and stator teeth aligned and $\theta = 360^\circ/(2 \times T) = 180^\circ/T$ (T = number of rotor teeth), rotor teeth



You have either reached a page that is unavailable for viewing or reached your viewing limit for this book.



You have either reached a page that is unavailable for viewing or reached your viewing limit for this book.



You have either reached a page that is unavailable for viewing or reached your viewing limit for this book.

another step of $22\frac{1}{2}^\circ$. The reversal of phase a winding current will produce a farther forward movement of $22\frac{1}{2}^\circ$, and so on. It is easy to visualize as to how the direction of movement can be reversed.

To simplify the switching arrangement, which is accomplished electronically double coils are provided for each phase. The schematic diagram of the switching circuit is shown in Fig. 4.31.

Compared to variable-reluctance motors, typical permanent-magnet stepper motors operate at larger steps up to 90° , and at maximum response rates of 300 pps.

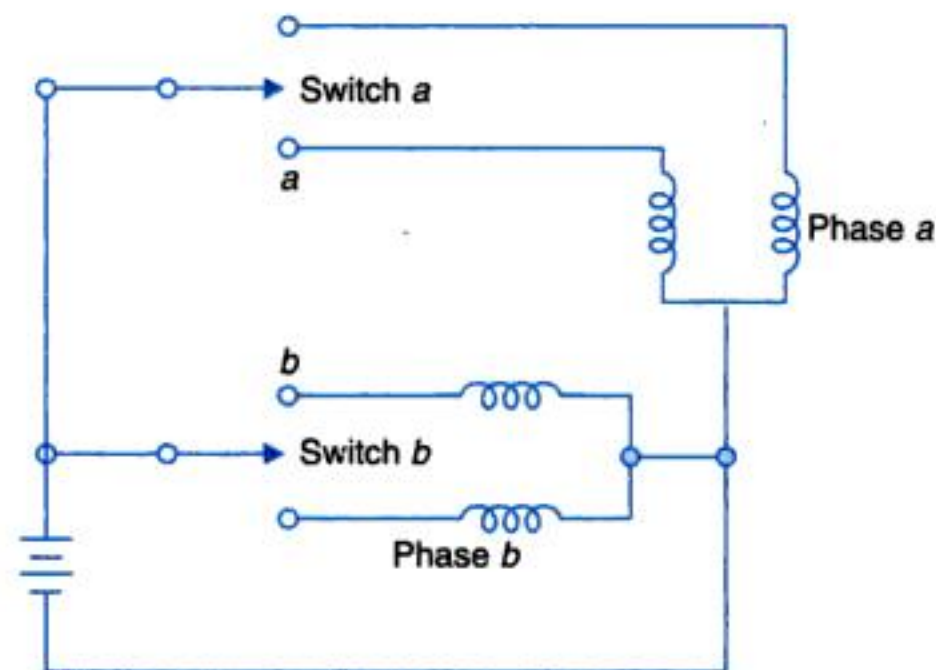


Fig. 4.31. Switching arrangement 2-phases permanent-magnet stepper motor.

Hybrid Stepper Motor

This is in fact a PM stepper motor with constructional features of toothed and stacked rotor adopted from the variable reluctance motor. The stator has only one set of winding-excited poles which interact with two rotor stacks. The permanent magnet is placed axially along the rotor in form of an annular cylinder over the motor shaft. The stacks at each end of the rotor are toothed. So all the teeth on the stack at one of the rotor acquire the same polarity while all the teeth of the stack at the other end of the rotor require the opposite polarity. The two sets of teeth are displaced from each other by one half of the tooth pitch (also called pole pitch). These constructional details are brought out by Figs. 4.32 (a) and (b) for the case of three teeth on each stack so that tooth pitch $\gamma_t = 360^\circ/3 = 120^\circ$. This motor has a 2-phase, 4-pole stator.

Consider now that the stator phase 'a' is excited such that the top stator pole acquires north polarity while the bottom stator pole acquires south polarity. As a result the nearest tooth of the front stack (assumed to be of north polarity) is pulled into locking position with the stator south pole (top) and the diametrically opposite tooth of the rear stack (south polarity) is simultaneously locked into the stator north pole (bottom). The repulsive forces on the remaining two front stack teeth balance out as these are symmetrically located w.r.t. the bottom stator pole and so do the repulsive forces due to the top stator pole on the remaining two rear stack teeth. This rotor position is thus a stable position with net torque on rotor being zero.



You have either reached a page that is unavailable for viewing or reached your viewing limit for this book.



You have either reached a page that is unavailable for viewing or reached your viewing limit for this book.



You have either reached a page that is unavailable for viewing or reached your viewing limit for this book.

pump and a fixed stroke hydraulic motor. Control of the motor is exercised by varying the amount of oil delivered by the pump. This is carried out by mechanically changing the pump stroke. Like in a dc generator and motor, there is no essential difference between hydraulic pump and motor. In a pump, the input is mechanical power (torque at a certain speed) and output, hydraulic power (flow at a certain pressure) and in a motor, the input is hydraulic and output mechanical.

Figure 4.37 shows the constructional features of hydraulic pump and motor. The pistons in hydraulic pump bear against the stationary wobble plate and are carried round by the cylinder

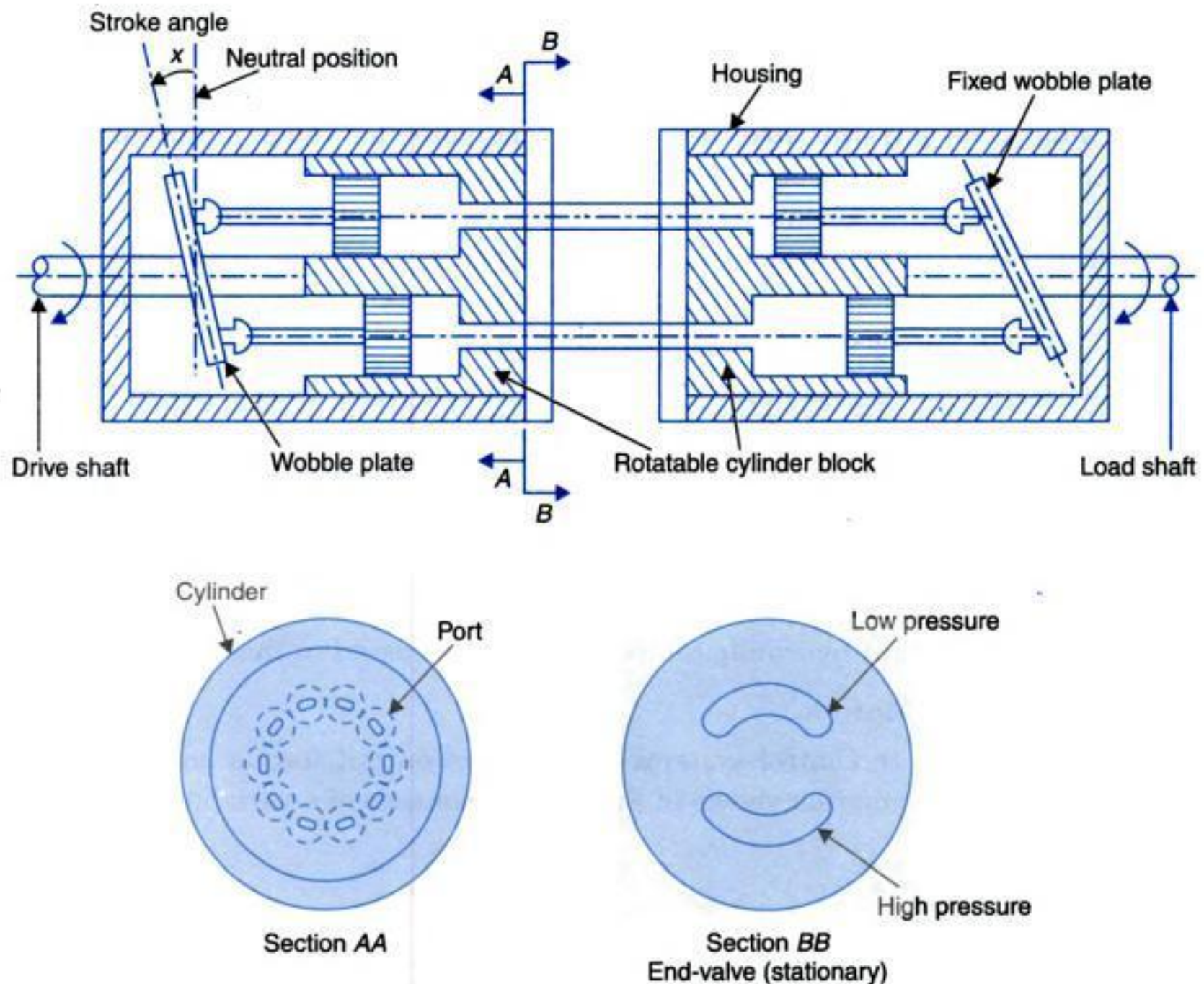


Fig. 4.37. Constructional details of hydraulic transmission system.

block which is made to rotate by the prime mover. (In some designs, the cylinder block is kept stationary and the wobble plate rotated). First consider that the wobble plate of the pump is in the neutral position. Now as the shaft is driven, the cylinder block with pistons rotates, but there is no displacement of the pistons into the cylinders and hence no pumping action takes place. Let the wobble plate be now tilted (Fig. 4.37). As the cylinder block is now rotated, the pistons rotate along with and are guided along the ridge of the wobble plate. Each piston therefore moves outwards in its cylinder as it comes in the top position and moves inwards in its cylinder as it comes in the bottom position. The result is a reciprocating pumping action with the high pressure oil being collected by the end-valve plate (fixed member) from cylinders



You have either reached a page that is unavailable for viewing or reached your viewing limit for this book.



You have either reached a page that is unavailable for viewing or reached your viewing limit for this book.



You have either reached a page that is unavailable for viewing or reached your viewing limit for this book.

Since $q_1 = q_2 = q$, we have from above equations

$$q = \frac{Kx}{\sqrt{2}} \sqrt{P_0 - p}; x > 0$$

where $p = P_1 - P_2$.

For $x < 0$, the relationship between p , q and x may be obtained in a similar manner.

The valve characteristics are shown in Fig. 4.39 which relate the volumetric oil flow rate q to the motor and the differential pressure p across the motor for different values of spool displacement x . Although the valve characteristics are nonlinear, for small values of x , these can be linearized. The relationship between q , x and p may be written as

$$q = f(x, p) \quad \dots(4.37)$$

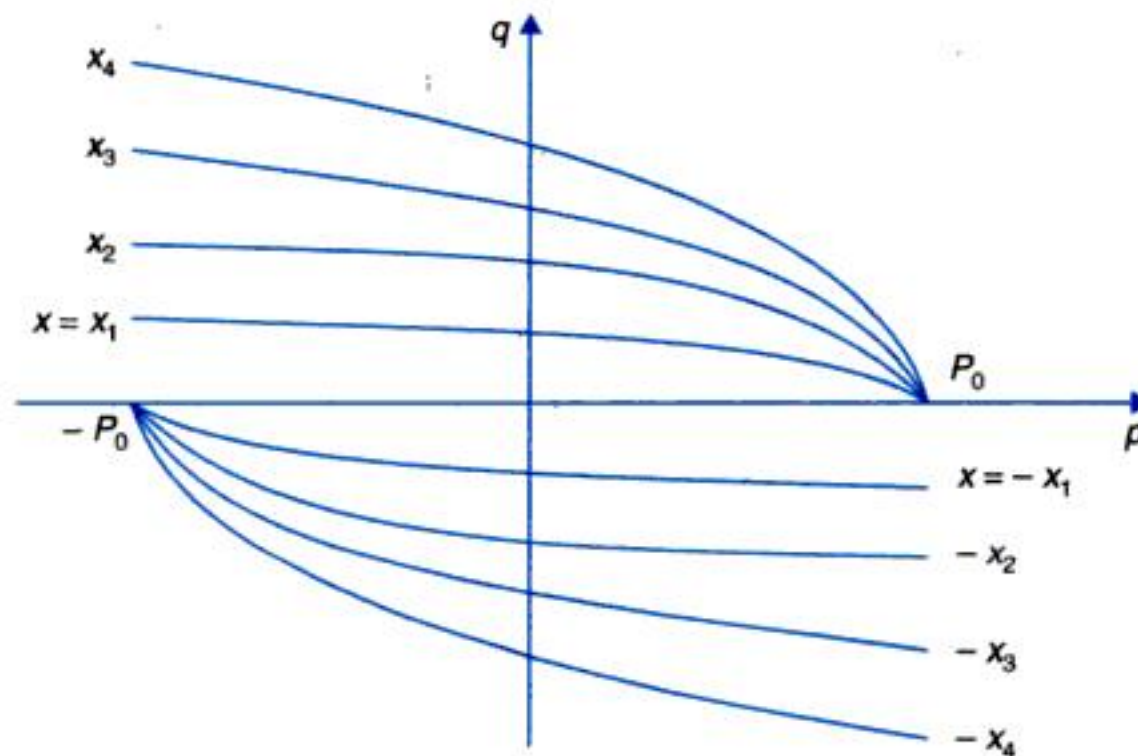


Fig. 4.39. Typical valve characteristics.

Expanding eqn. (4.37) into Taylor's series about the normal operating point (q_0, x_0, p_0) and neglecting all the terms of second and higher derivatives, we get

$$q = q_0 + \left. \frac{\partial q}{\partial x} \right|_{\substack{x=x_0 \\ p=p_0}} (x - x_0) + \left. \frac{\partial q}{\partial p} \right|_{\substack{x=x_0 \\ p=p_0}} (p - p_0) \quad \dots(4.38)$$

For this system, the normal operation point corresponds to $q_0 = 0, p_0 = 0, x_0 = 0$, therefore, from eqn. (4.38)

$$q = K_1 x - K_2 p \quad \dots(4.39)$$

where

$$K_1 = \left. \frac{\partial q}{\partial x} \right|_{\substack{x=0 \\ p=0}}; K_2 = - \left. \frac{\partial q}{\partial p} \right|_{\substack{x=0 \\ p=0}}$$

Equation (4.39) gives a linearized relationship among q , x and p .

The response equation of the valve-motor combination can now be written down from eqn. (4.29) of the pump-motor system by replacing its left-hand side by $q = K_1 x - K_2 p$, the inflow rate to the pipe-line-motor combination. Furthermore the compressibility is neglected right at this stage. Thus



You have either reached a page that is unavailable for viewing or reached your viewing limit for this book.



You have either reached a page that is unavailable for viewing or reached your viewing limit for this book.



You have either reached a page that is unavailable for viewing or reached your viewing limit for this book.

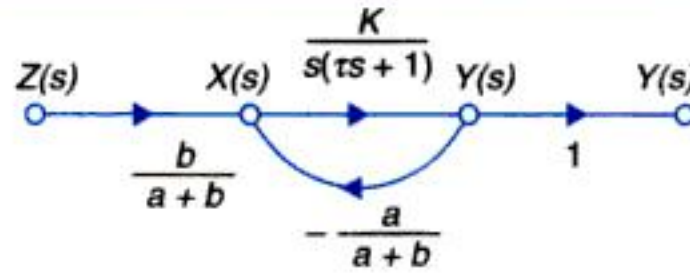


Fig. 4.43. Signal flow graph of system shown in Fig. 4.42.

Hydraulic linear actuator can also be modified to act as hydraulic amplifier (proportional controller) by providing a negative feedback through a link mechanism as shown in Fig. 4.42 (a). For small movements x , y and z can be regarded as linear. From the link geometry in Fig. 4.42 (b),

$$\frac{C'E}{A'E} = \frac{B'D}{A'D} \quad \text{or} \quad \frac{y+z}{a+b} = \frac{z-x}{a} \quad \text{or} \quad x = \frac{b}{a+b}z - \frac{a}{a+b}y \quad \dots(4.51)$$

The transfer function $Y(s)/X(s)$ of the actuator already derived, is give in eqn, (4.44). Combining eqns. (4.44) and (4.51) we draw the signal flow graph of Fig. 4.42. The overall transfer function is obtained therefrom as

$$\frac{Y(s)}{Z(s)} = \frac{bK}{(a+b)s(\tau s + 1) + Ka} \quad \dots(4.52)$$

In the normal frequency range of hydraulic control systems

$$|(a+b)s(\tau s + 1)| \ll Ka$$

$$\text{Therefore,} \quad \frac{Y(s)}{Z(s)} \approx \frac{b}{a} \quad \dots(4.53)$$

Thus the hydraulic actuator can be made to function as a linear amplifier over the frequency range of interest. The amplifier gain can be adjusted by a suitable choice of the link mechanism lever ratio b/a .

Hydraulic Feedback System

Let us discuss a hydraulic power steering mechanisms whose simplified schematic diagram is shown in Fig. 4.44. The input to the system is the rotation of the steering wheel by the driver and the output is positioning of the car wheels in accordance with the input signal.

When the steering wheel is in the zero position, i.e., the cross bar is horizontal, the wheels are directed parallel to the longitudinal axis of the car. For this condition, the spool is in the neutral position and the oil supply to the power cylinder is cut-off. When the steering wheel is turned anticlock-wise through an angle θ_p , the spool is made to move towards right by an amount x with the help of the gear mechanism. The high pressure oil enters on the left hand side of the power cylinder causing the power piston and hence the power ram to move towards right by an amount y . Through a proper drive linkage, a torque is applied to the wheels causing the desired displacement θ_o of the wheels.

A rigid linkage bar connects the power ram and the moveable valve housing. When the power ram moves towards right, the linkage moves as shown in Fig. 4.45. It is seen from this figure that movement of the power ram towards right causes a movement of the movable valve housing in such a direction as to seal off the high pressure side. The system then operates with a fixed θ_o for a given input x under steady conditions.



You have either reached a page that is unavailable for viewing or reached your viewing limit for this book.



You have either reached a page that is unavailable for viewing or reached your viewing limit for this book.



You have either reached a page that is unavailable for viewing or reached your viewing limit for this book.

Solution. The fly-ball governor is coupled to engine shaft via speed reduction gearing, thereby sensing engine speed. As engine speed increases the fly balls move outwards under centrifugal force. So that the governor sleeve moves upwards (e) corresponding to the speed error with reference to the speed setting of the governor. This movement via the lever and hydraulic actuator causes the power piston to move downward which in turn reduces the fuel valve opening therefore reducing engine speed. The reverse happens when engine speed decreases. The system thus has inherent negative feedback regulating action.

Using the lever eqn. (4.51) with appropriate symbols, we have

$$X(s) = \left(\frac{a_2}{a_1 + a_2} \right) E(s) - \left(\frac{a_1}{a_1 + a_2} \right) Z(s) \quad \dots(i)$$

If the hydraulic actuator's time constant is assumed negligible (refer eqn (4.41)), it acts as an integrator *i.e.*,

$$\frac{Y(s)}{X(s)} = \frac{K_A}{s} ; K_A = \text{actuator gain} \quad \dots(ii)$$

Assuming the force input at z to be negligible

$$K\dot{z} + B(\dot{z} - \dot{y}) = 0 \quad \text{or} \quad \frac{Z(s)}{Y(s)} = \frac{sB}{sB + K} \quad \dots(iii)$$

Using component transfer functions of eqns. (i)-(iii), the system block diagram is drawn in Fig. 4.50. The overall transfer can be written down as

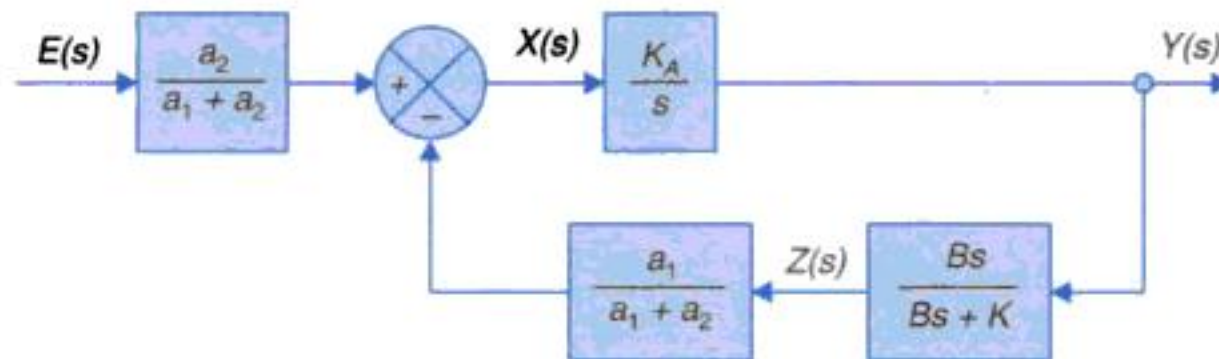


Fig. 4.50. Block diagram of the system of Fig. 4.48 transfer function can be written down as

$$\frac{Y(s)}{X(s)} = \left(\frac{a_2}{a_1 + a_2} \right) \frac{K_A/s}{1 + \left(\frac{a_1}{a_1 + a_2} \right) \left(\frac{BK_A}{Bs + K} \right)} \quad \dots(iv)$$

Let the gain be so adjusted that for the frequency range of interest (in hydraulic systems bandwidth is very low)

$$\left| \left(\frac{a_1}{a_1 + a_2} \right) \left(\frac{BK_A}{Bs + K} \right) \right| \gg 1$$

The transfer function of eqn. (iv) then simplifies to

$$\frac{Y(s)}{X(s)} = \frac{a_2}{a_1} \left[1 + \frac{K}{Bs} \right] = \text{proportional plus integral terms} \quad \dots(v)$$



You have either reached a page that is unavailable for viewing or reached your viewing limit for this book.



You have either reached a page that is unavailable for viewing or reached your viewing limit for this book.



You have either reached a page that is unavailable for viewing or reached your viewing limit for this book.

f and mass M . For a small variation ΔP in the input pressure, the force acting on the diaphragm is $A(\Delta P)$ where A is the area of the diaphragm. If Δy is the displacement of the actuator stem because of this force, then the force balance equation is

$$A(\Delta P) = M\Delta\ddot{y} + f\Delta\dot{y} + K\Delta y$$

Therefore the transfer function of the actuator is

$$\frac{\Delta Y(s)}{\Delta P(s)} = \frac{A}{Ms^2 + fs + K} \quad \dots(4.64)$$

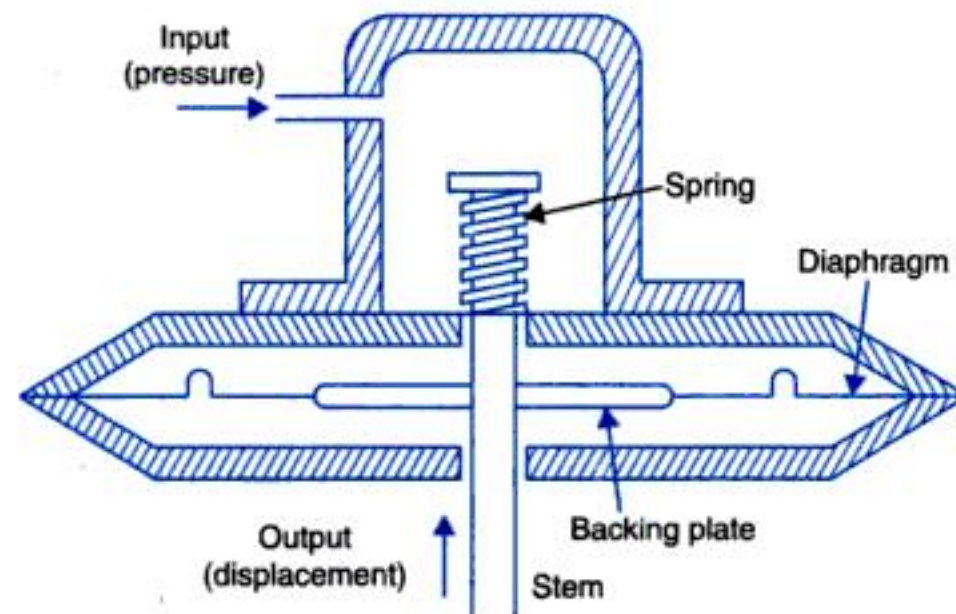


Fig. 4.55. Pneumatic actuator.

It may be noted that the stiffness and mass of the diaphragm and backing plate, are considered to be negligible.

Pneumatic Position Control System

The pneumatic position control system shown in Fig. 4.56 is used to position a fluid flow valve. The principle of operation of this system is that an input signal is applied to the flapper corresponding to the required opening of the plug valve. The nozzle back pressure operates the actuator and the actuator stem moves to give the required opening of the plug valve.

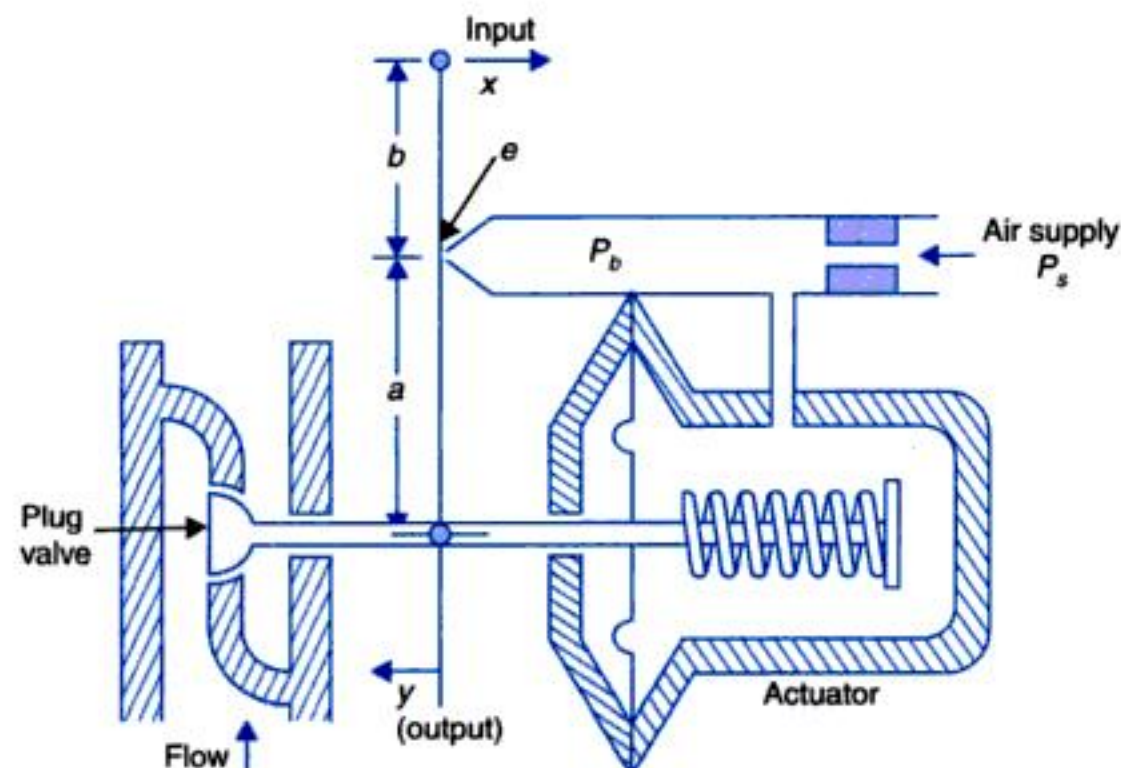


Fig. 4.56. Pneumatic position control system.



You have either reached a page that is unavailable for viewing or reached your viewing limit for this book.



You have either reached a page that is unavailable for viewing or reached your viewing limit for this book.



You have either reached a page that is unavailable for viewing or reached your viewing limit for this book.

For the lever (positive x is in positive direction of e)

$$x = \frac{b}{a+b}e - \frac{a}{a+b}y \quad \dots(iv)$$

For the pneumatic relay

$$p_c = Kx \quad (K > 0) \quad \dots(v)$$

The block diagram of Fig. 4.62 can now be drawn.

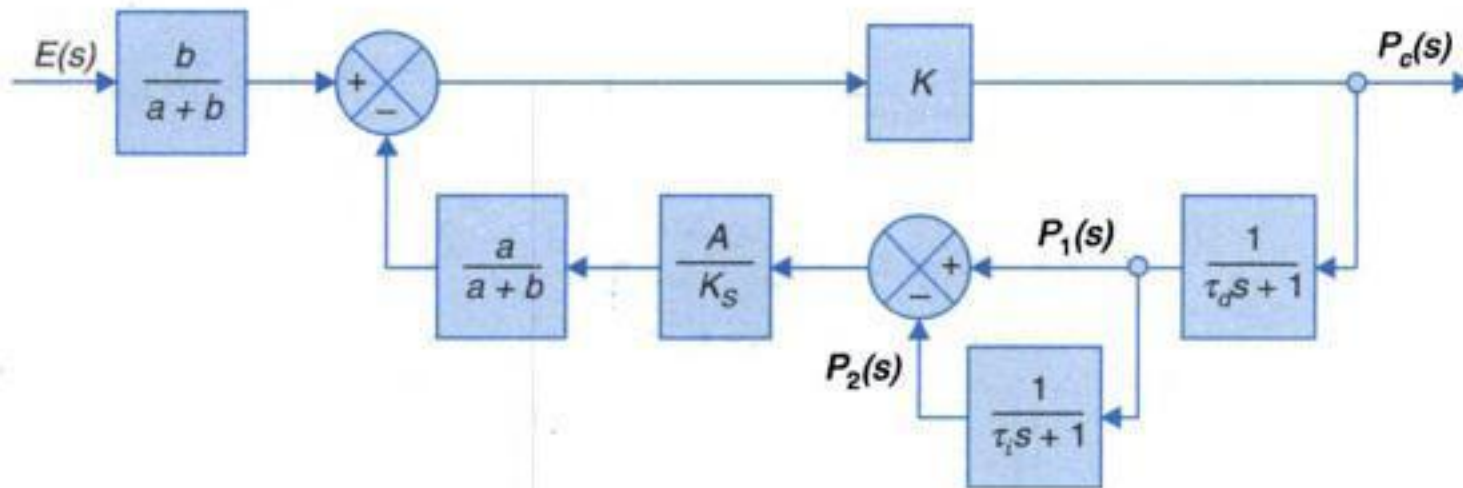


Fig. 4.62

It is easily established from the block diagram that

$$\frac{P_c(s)}{E(s)} = \frac{b/(a+b)E(s)}{1 + K \left(\frac{a}{a+b} \right) \left(\frac{A}{K_s} \right) \left(\frac{\tau_i s}{\tau_i s + 1} \right) \left(\frac{1}{\tau_d s + 1} \right)} \quad \dots(vi)$$

Magnitude of second term in denominator $\gg 1$ (for practical controller)

The transfer function of eqn. (vi) for frequencies of interest then approximates to

$$\frac{P_c(s)}{E(s)} = \frac{bK_s(\tau_i s + 1)(\tau_d s + 1)}{aA\tau_i s} = \frac{bK_s}{aA} \left(\frac{\tau_i + \tau_d}{\tau_i} + \frac{1}{\tau_i s} + \tau_d s \right) \quad \dots(vii)$$

As $\tau_i \gg \tau_d$, we can write

$$\frac{P_c(s)}{E(s)} = K_p \left(1 + \frac{1}{\tau_i s} + \tau_d s \right); \quad K_p = \frac{bK_s}{aA} \quad \dots(viii)$$

The controller is thus a proportional-plus-integral-plus-derivative controller (to be discussed in Section 5.7).

(i) If $R_i = 0$

$$\frac{P_c(s)}{E(s)} = K_p(1 + \tau_d s); \text{ proportional-plus-derivative controller} \quad \dots(ix)$$

(ii) If $R_d = 0$

$$\frac{P_c(s)}{E(s)} = K_p \left(1 + \frac{1}{\tau_i s} \right); \text{ proportional-plus-integral controller} \quad \dots(x)$$



You have either reached a page that is unavailable for viewing or reached your viewing limit for this book.



You have either reached a page that is unavailable for viewing or reached your viewing limit for this book.



You have either reached a page that is unavailable for viewing or reached your viewing limit for this book.

its amplitude. Find the transfer function $X(s)/Y(s)$ assuming rate of oil-flow to piston to be proportional to valve opening and neglecting oil compressibility, leakage effects and mass of the piston.

- 4.6. A hydraulic servo system used to control the transverse feed of a machine tool is shown in Fig. P-4.6. Each angular piston of the cam corresponds to a desired reference position x_r such that $y_r = K_r x_r$. The load on the piston is that due to tool reactive force and may be assumed to consist of mass M , friction f and spring with constant K .

Draw the block diagram and obtain the transfer function $Y_c(s)/X_r(s)$, assuming that:

Rate of oil flow to the piston = $K_1 \times$ valve opening

Leakage flow across the piston = $K_2 \times$ pressure across the piston

The compressibility effect is negligible.

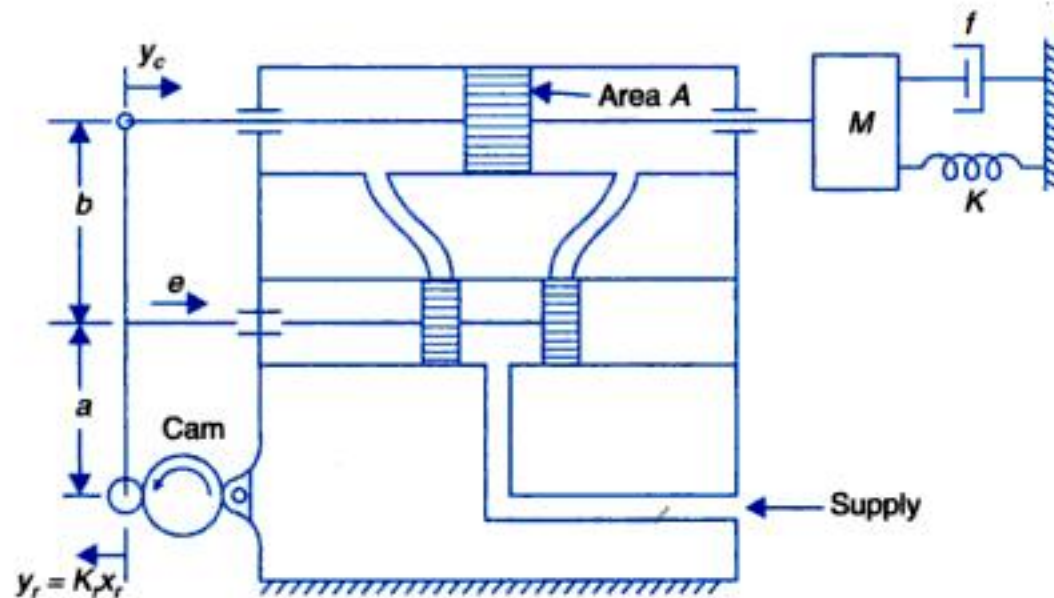


Fig. P-4.6. [From F. Raven, *Automatic Control Engineering*, 2nd ed, 1968, McGraw-Hill, New York. Reproduced with permission.]

- 4.7 The electrohydraulic position control system shown in Fig. P-4.6 positions a mass M with negligible friction. Assume that the rate of oil flow to the piston is $q = K_x x - K_p p$, where x is the control valve opening and p is the differential pressure. The mass of piston, oil compressibility and leakage are assumed negligible. Draw the signal flow graph of the system and obtain therefrom the transfer function $Y(s)/X_i(s)$. How the transfer function will modify if the mass M is also negligible such that the differential pressure p needed to move the piston is nearly zero?

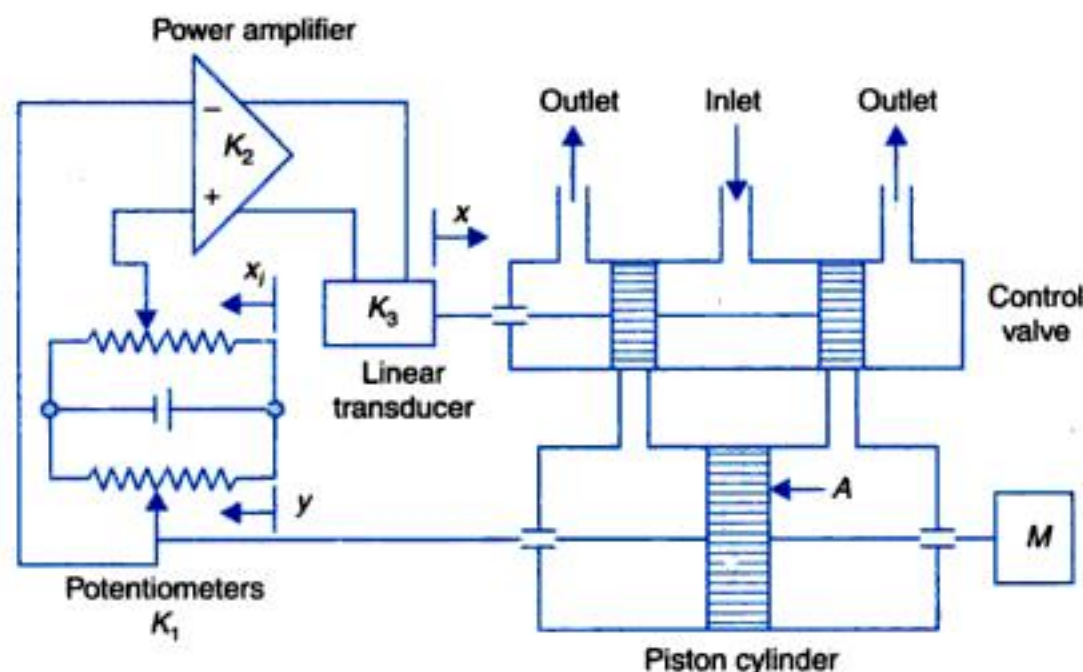


Fig. 4.7



You have either reached a page that is unavailable for viewing or reached your viewing limit for this book.



You have either reached a page that is unavailable for viewing or reached your viewing limit for this book.



You have either reached a page that is unavailable for viewing or reached your viewing limit for this book.



You have either reached a page that is unavailable for viewing or reached your viewing limit for this book.



You have either reached a page that is unavailable for viewing or reached your viewing limit for this book.

The nature of the transient response is revealed by any one of these test signals as this nature is dependent upon system poles and not upon the type of input.

It is therefore sufficient to analyze the transient response to one of the standard test signals—a step is generally used for this purpose as this signal can be easily generated. Steady state response is then examined to this particular test signal (the step) as well other test signals; the ramp and the parabolic signal. So except for the step test signal the time consuming transient analysis need not be carried out for the ramp and parabolic signals, while their steady state can be quickly determined by the final value theorem as illustrated in Section 5.5 and will also elaborated in other sections of this chapter.

As explained above control systems are inherently time-domain systems subject to time-varying inputs and are to be tested, analyzed and designed by the time-domain test signals like step, ramp and parabolic. The time-domain command signals in a control can also be visualized as (through Fourier Transform) a band of sinusoidal signals of frequencies from dc upwards (control systems are low-pass filters). So another important test signal for control systems is the sinusoidal signal which can be easily generated and its frequency varied. Steady-state sinusoidal response of a control system over a range of frequencies yields a great deal of information about the system; both about its time-domain response and its stability, as there is normally a good correlation between the frequency-domain response and time-domain response of a system. Chapters 8 and 9 will be wholly devoted to steady-state sinusoidal response of control systems.

The time response performance of a control system is measured by computing several time response performance indices as well as steady-state accuracy for the standard input signals described above. These indices give a quantitative method to compare the performance of alternative system configurations or to adjust the parameters of a given system. As a given parameter is varied, various performance indices may change in a conflicting manner. The best parameter choice would thus be the best compromise solution. Certain of the performance indices may be specified as upper or lower bounds in a design.

5.2 STANDARD TEST SIGNALS

Step Signal

The *step* is a signal whose value changes from one level (usually zero) to another level A in zero time. The mathematical representation of the step function is

$$r(t) = Au(t)$$

where

$$\begin{aligned} u(t) &= 1 ; t > 0 \\ &= 0 ; t < 0 \end{aligned} \quad \dots(5.1)$$

In the Laplace transform form, $R(s) = A/s$

The graphical representation of a step signal is shown in Fig. 5.1(a).

Ramp Signal

The *ramp* is a signal which starts at a value of zero and increases linearly with time. Mathematically,

$$\begin{aligned} r(t) &= At ; t > 0 \\ &= 0 ; t < 0 \end{aligned} \quad \dots(5.2)$$



You have either reached a page that is unavailable for viewing or reached your viewing limit for this book.



You have either reached a page that is unavailable for viewing or reached your viewing limit for this book.



You have either reached a page that is unavailable for viewing or reached your viewing limit for this book.

Reducing the system time constant therefore not only improves its speed of response but also reduces its steady-state error to a ramp input.

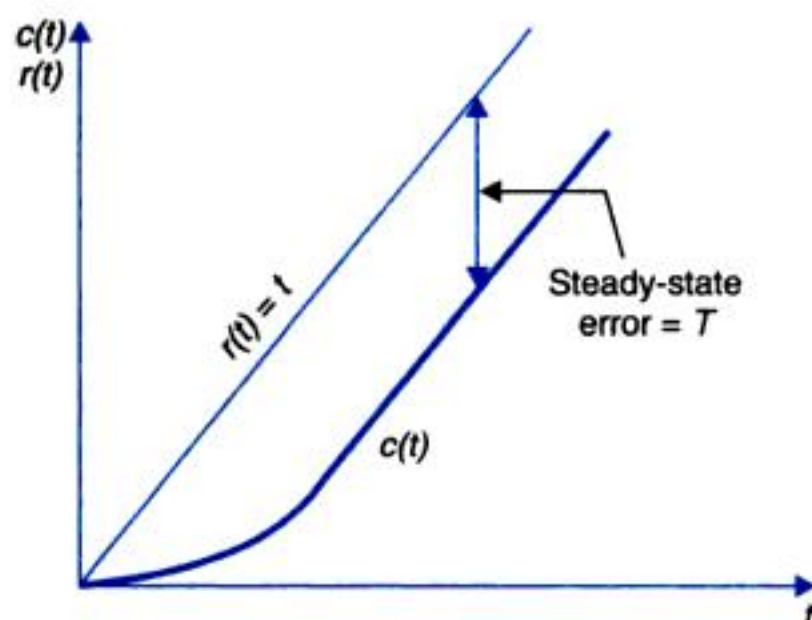


Fig. 5.5. Unit-ramp response of a first-order system.

If we examine the derivative of $c(t)$, i.e.,

$$\dot{c}(t) = 1 - e^{-t/T}$$

we find that it is identical to the system response to the unit-step input. The transient response to the ramp input signal thus yields no additional information about the speed of response of the system. We therefore need examine only the steady-state error to the ramp input which can be obtained directly by the final value theorem as given below:

$$\begin{aligned} e_{ss} &= \lim_{t \rightarrow \infty} e(t) = \lim_{s \rightarrow 0} s E(s) = \lim_{s \rightarrow 0} s [R(s) - C(s)] \\ &= \lim_{s \rightarrow 0} s \left[\frac{1}{s^2} - \frac{1}{s^2(Ts + 1)} \right] = T \end{aligned}$$

This avoids the need to obtain the inverse Laplace transform resulting in a considerable labour saving in higher-order systems.

5.4 TIME RESPONSE OF SECOND-ORDER SYSTEMS

Consider the servomechanism shown in Fig. 5.6, which controls the position of a mechanical load in accordance with the position of the reference shaft. The two potentiometers convert the input and output positions into proportional electrical signals, which are in turn compared and an error signal equal to the difference of the two appears at the leads coming from potentiometer wiper arms.

The error signal (voltage) is

$$v_e = K_p(r - c)$$

where r = reference shaft position in rad; c = output shaft position in rad; and K_p = potentiometer sensitivity in volts/rad.

The error signal is amplified by a factor K_A by the amplifier and is applied to the armature circuit of the d.c. motor whose field winding is excited with a constant voltage or it could also



You have either reached a page that is unavailable for viewing or reached your viewing limit for this book.



You have either reached a page that is unavailable for viewing or reached your viewing limit for this book.



You have either reached a page that is unavailable for viewing or reached your viewing limit for this book.

As ζ is increased, the response becomes progressively less oscillatory till it becomes critically damped (just non-oscillatory) for $\zeta = 1$ and becomes overdamped for $\zeta > 1$. Robotic control systems cannot be allowed to have oscillatory response otherwise the end effector would strike against the object that the robot is meant to manipulate. Highest possible speed of response and yet non-oscillating response dictates that a robotic control system shall be designed to have a damping factor of $\zeta = 1$ (or close to it but less than unity). For $\zeta = 1$, it easily follows by inverse Laplace transferring eqn (5.12) that

$$c(t) = 1 - e^{-\omega_n t} - \omega_n t e^{-\omega_n t} \quad \dots(5.13)$$

where from the characteristic equation (5.10), the roots are

$$s_1 = s_2 = -\omega_n$$

i.e., repeated real negative roots, also see Fig. 5.10.

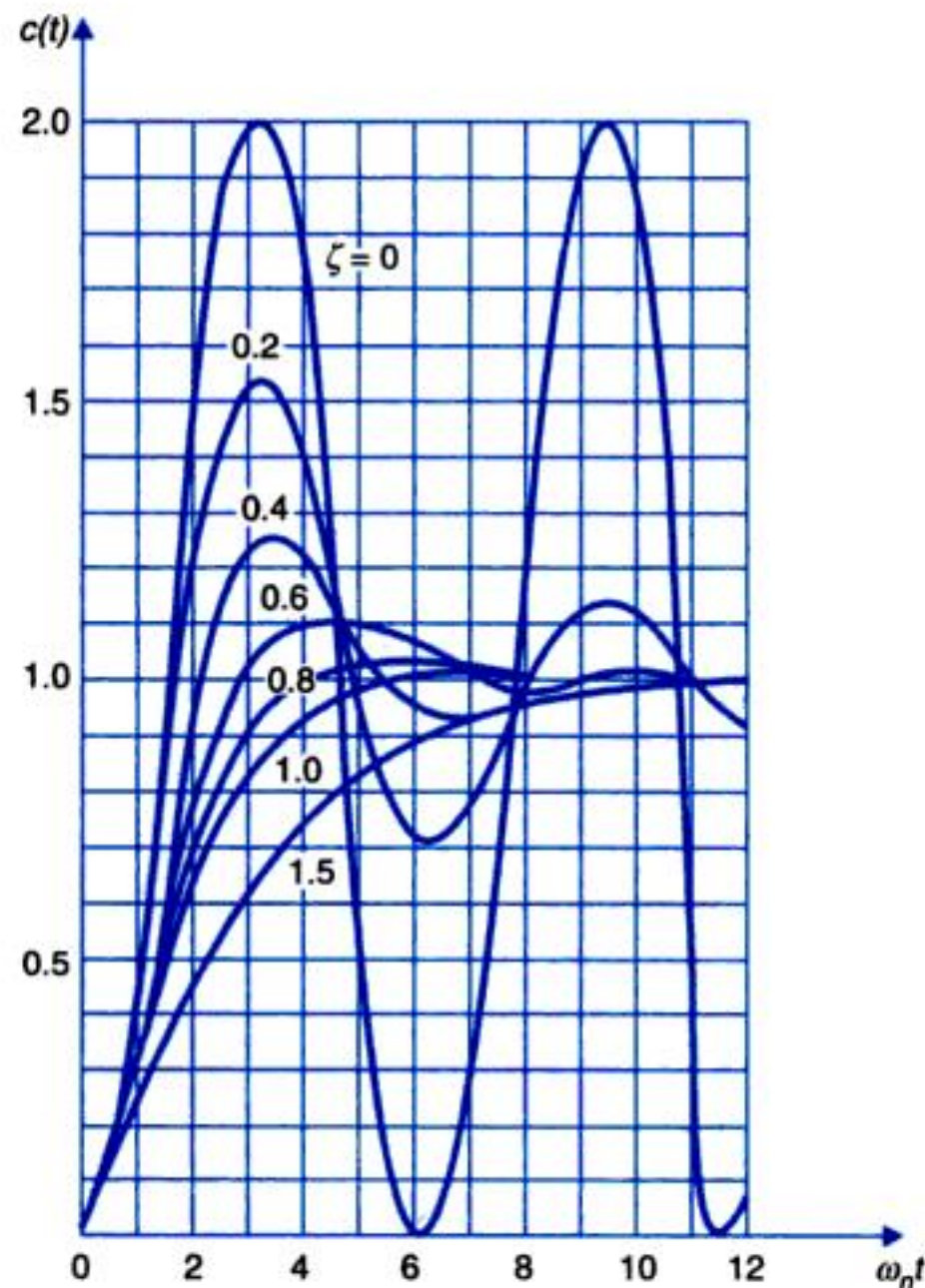


Fig. 5.9. Unit-step response curves of second-order system.

Fig. 5.10 shows the locus of the poles of the second-order system discussed above with ω_n held constant and ζ varying from 0 to ∞ . As ζ increases the poles move away from the imaginary axis along a circular path of radius ω_n meeting at the point $\sigma = -\omega_n$ and then separating and travelling along the real axis, one towards zero and the other towards infinity. For $0 < \zeta < 1$, the poles are complex conjugate pair making an angle of $\theta = \cos^{-1} \zeta$ with the negative real axis.



You have either reached a page that is unavailable for viewing or reached your viewing limit for this book.



You have either reached a page that is unavailable for viewing or reached your viewing limit for this book.



You have either reached a page that is unavailable for viewing or reached your viewing limit for this book.

The first undershoot will occur at $t = 2\pi/\omega_n \sqrt{1-\zeta^2}$, the second overshoot at $t = 3\pi/\omega_n \sqrt{1-\zeta^2}$ and so on. A plot of normalized peak time $\omega_n t_p$ versus ζ is given in Fig. 5.13.

3. Peak overshoot M_p : From eqn. (5.11) and Fig. 5.11,

$$\begin{aligned} M_p &= c(t_p) - 1 \\ &= -\frac{e^{-\zeta\omega_n t_p}}{\sqrt{1-\zeta^2}} \sin\left[\omega_n \sqrt{1-\zeta^2} t_p + \tan^{-1} \frac{\sqrt{1-\zeta^2}}{\zeta}\right] \\ &= e^{-\pi\zeta/\sqrt{1-\zeta^2}} \end{aligned}$$

Therefore the peak percent overshoot

$$= 100 e^{-\pi\zeta/\sqrt{1-\zeta^2}} \% \quad \dots(5.20)$$

As seen from Fig. 5.13, the peak overshoot is a monotonically decreasing function of damping ζ and is independent of ω_n . It is, therefore an excellent measure of system damping.

4. Settling time t_s : From Fig. 5.8, it is observed that the time response $c(t)$ given by eqn. (5.12) for $\zeta < 1$, oscillates between a pair of envelopes before reaching steady-state. The transient is comprised of a product of an exponentially decaying term $[\exp(-\zeta\omega_n t)]/\sqrt{1-\zeta^2}$ and a sinusoidally oscillating term $\sin[\omega_n \sqrt{1-\zeta^2} t + \phi]$. The time constant of the exponential envelopes is $T = 1/\zeta\omega_n$. It may be noted that this time constant is equal to 2τ where τ is the motor time constant in Fig. 5.7(b).

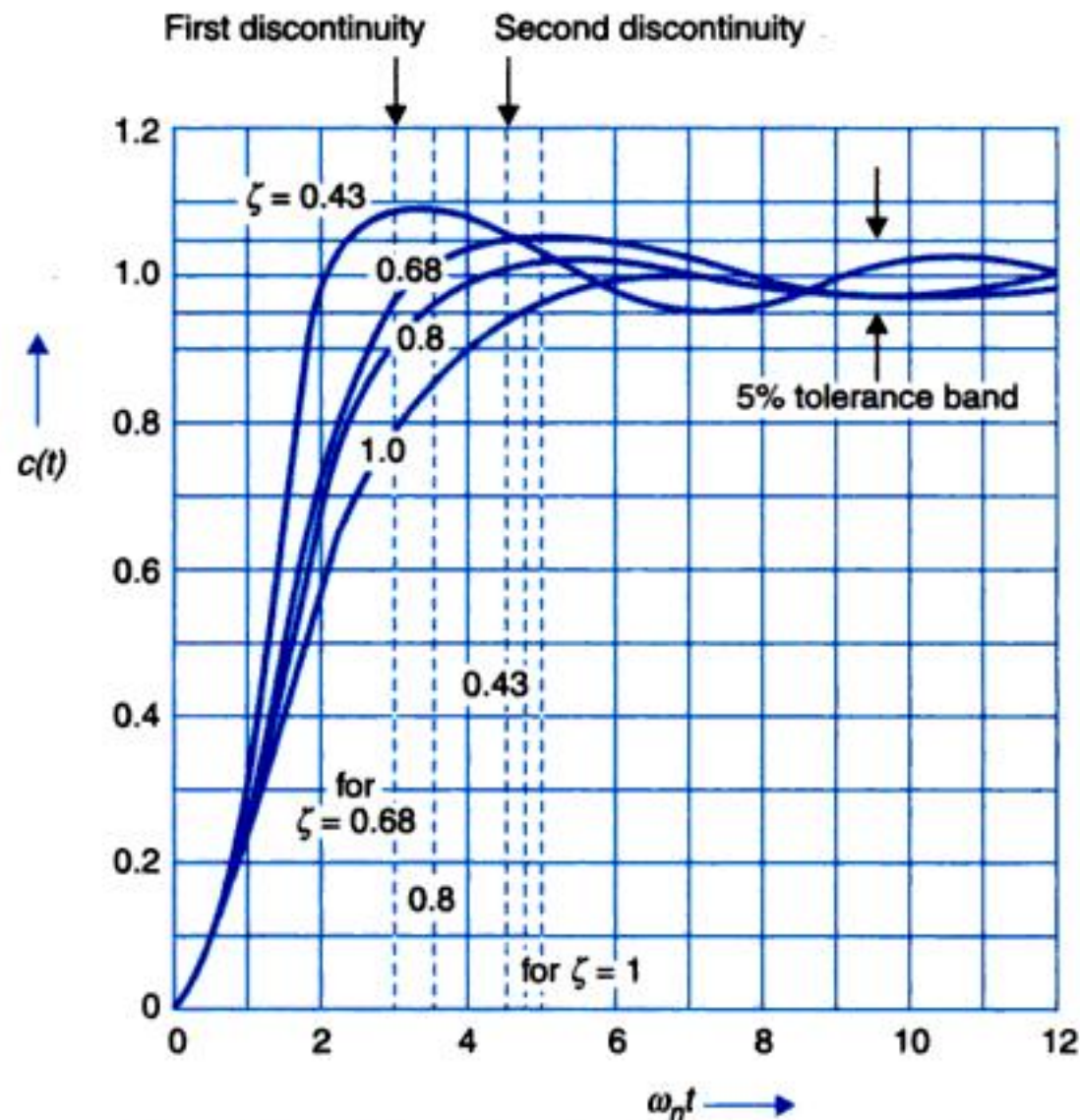


Fig. 5.14. Settling time for various values of ζ .



You have either reached a page that is unavailable for viewing or reached your viewing limit for this book.



You have either reached a page that is unavailable for viewing or reached your viewing limit for this book.



You have either reached a page that is unavailable for viewing or reached your viewing limit for this book.

From Fig. 5.17, we see that

$$\frac{C(s)}{R(s)} = \frac{G(s)}{1 + G(s)}$$

$$C(s) = E(s)G(s)$$

Therefore

$$E(s) = \frac{1}{1 + G(s)} R(s) \quad \dots(5.23)$$

The steady-state error e_{ss} may now be found by use of the final value theorem as follows.

$$e_{ss} = \lim_{t \rightarrow \infty} e(t) = \lim_{s \rightarrow 0} sE(s) = \lim_{s \rightarrow 0} \frac{sR(s)}{1 + G(s)} \quad \dots(5.24)$$

Equation (5.24) shows that the steady-state error depends upon the input $R(s)$ and the forward transfer function $G(s)$. The expression for steady-state errors for various types of standard test signals are derived below:

1. Unit-step Input

$$\text{Input } r(t) = u(t)$$

$$R(s) = 1/s$$

From eqn. (5.24)

$$e_{ss} = \lim_{s \rightarrow 0} \frac{1}{1 + G(s)} = \frac{1}{1 + G(0)} = \frac{1}{1 + K_p} \quad \dots(5.25)$$

where $K_p = G(0)$ is defined as the *position error constant*.

2. Unit-ramp (Velocity) Input

$$\text{Input } r(t) = t \text{ or } \dot{r}(t) = 1$$

$$R(s) = 1/s^2$$

From eqn. (5.24)

$$e_{ss} = \lim_{s \rightarrow 0} \frac{1}{s + sG(s)} = \lim_{s \rightarrow 0} \frac{1}{sG(s)} = \frac{1}{K_v} \quad \dots(5.26)$$

where $K_v = \lim_{s \rightarrow 0} sG(s)$ is defined as the *velocity error constant*.

3. Unit-parabolic (Acceleration) Input

$$\text{Input } r(t) = t^2/2 \text{ or } \ddot{r}(t) = 1$$

$$R(s) = 1/s^3$$

From eqn. (5.24)

$$e_{ss} = \lim_{s \rightarrow 0} \frac{1}{s^2 + s^2G(s)} = \lim_{s \rightarrow 0} \frac{1}{s^2G(s)} = \frac{1}{K_a} \quad \dots(5.27)$$

where $K_a = \lim_{s \rightarrow 0} s^2G(s)$ is defined as the *acceleration error constant*.

Types of Feedback Control System

The open-loop transfer function of a unity feedback system can be written in two standard forms—the *time-constant form* and the *pole-zero form*. In these two forms, $G(s)$ is as given below.



You have either reached a page that is unavailable for viewing or reached your viewing limit for this book.



You have either reached a page that is unavailable for viewing or reached your viewing limit for this book.



You have either reached a page that is unavailable for viewing or reached your viewing limit for this book.

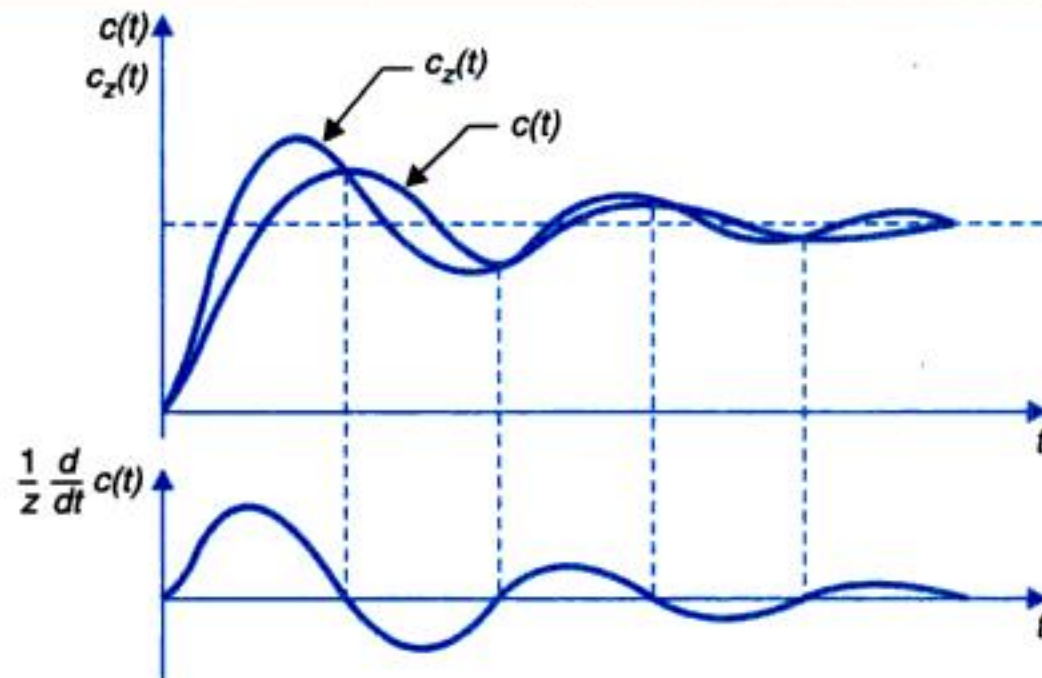


Fig. 5.19(a). Effect of closed-loop zero on unit-step response of a second-order system.

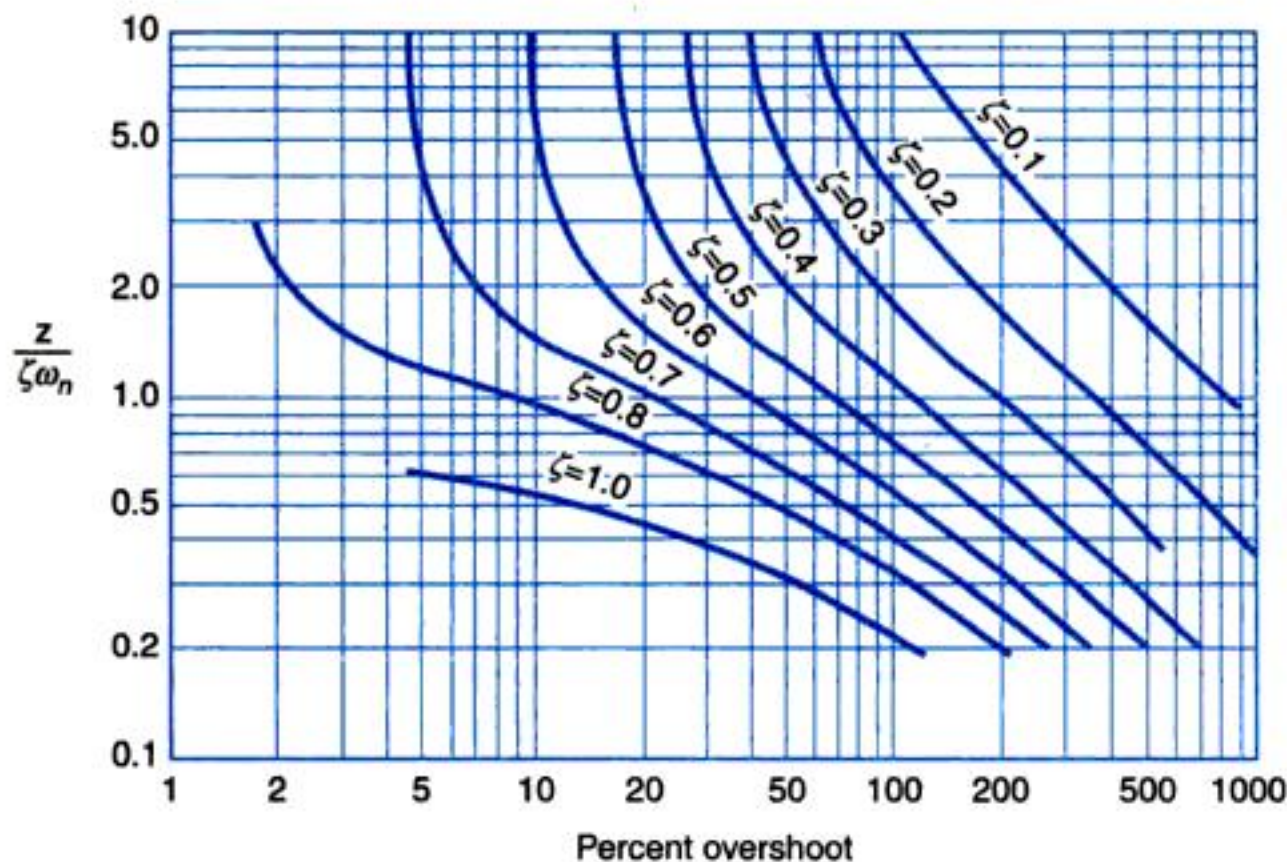


Fig. 5.19(b). Peak overshoot to unit step input of a second-order system with closed-loop zero.

5.7 DESIGN SPECIFICATIONS OF SECOND-ORDER SYSTEMS

A control system is generally required to meet three time response specifications: steady-state accuracy (specified in terms of permissible error e_{ss}), damping factor ζ (or peak overshoot to step input, M_p) and settling time t_s . If the rise time t_r is also specified, it should be consistent with the specification of t_s as both these depend upon ζ and ω_n . Steady-state accuracy requirement is met by a suitable choice of K_p , K_v or K_a depending upon the type of the system. As explained earlier, the damping factor ζ sufficiently less than one is preferred in most control



You have either reached a page that is unavailable for viewing or reached your viewing limit for this book.



You have either reached a page that is unavailable for viewing or reached your viewing limit for this book.



You have either reached a page that is unavailable for viewing or reached your viewing limit for this book.

$$\tau' = \frac{JR_a}{R_a f + K_A K_T K_t} \quad \dots(5.42)$$

The natural frequency and damping of the closed-loop can then be expressed as

$$\omega_n' = \sqrt{(K_v' / \tau')} = \sqrt{(K_P K_A K_T n / JR_a)} \quad \dots(5.43)$$

$$\zeta' = (1/2) / \sqrt{(K_v' \tau')} = (R_a f + K_A K_T K_t) / 2 \sqrt{(K_P K_A K_T n JR_a)} \quad \dots(5.44)$$

For a specified K_v' , and ζ' , we can write from eqns. (5.41) and (5.44)

$$\zeta K_v' = \frac{1}{2} \sqrt{(K_P K_A K_T n / JR_a)}$$

from which K_A is determined as

$$K_A = 4(\zeta K_v')^2 (JR_a / K_P K_T n)$$

Using this value of K_A , K_t the tachometer constant is obtained from eqn. (5.41) as

$$K_t = \left(\frac{K_P n}{K_v'} - \frac{R_a f}{K_A K_T} \right)$$

Thus, we notice that by a suitable choice of K_A , K_P we can simultaneously meet the specification of K_v' and ζ' . On account of the negative derivative feedback, K_A required may sometimes be excessively large. Under such circumstances additional gain outside the derivative loop is very helpful.

Further, it is to be noticed that for the same value of velocity error constant, the system with compensation requires a higher value of K_A and hence it will have a higher natural frequency (eqn. 5.43). Compensation thus increases both the system damping and natural frequency resulting in reduced settling time.

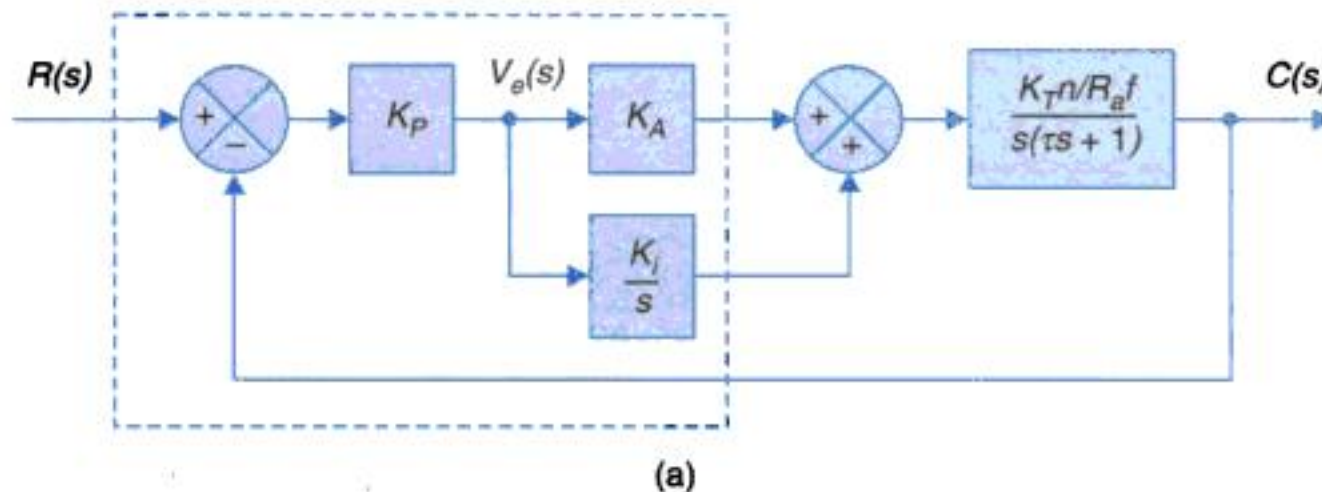
Integral Error Compensation

In an integral error compensation scheme, the output response depends in some manner upon the integral of the actuating signal. This type of compensation is introduced by using a controller which produces an output signal consisting of two terms, one proportional to the actuating signal and the other proportional to its integral. Such a controller is called *proportional plus integral controller* or *PI controller*.

The block diagram of the system of Fig. 5.6 with proportional plus integral compensation is shown in Fig. 5.23(a), while its simplified block diagram is given in Fig. 5.23(b) where

$$K_v' = K_P K_t K_T n / R_a f$$

$$K_A' = K_A / K_i$$





You have either reached a page that is unavailable for viewing or reached your viewing limit for this book.



You have either reached a page that is unavailable for viewing or reached your viewing limit for this book.



You have either reached a page that is unavailable for viewing or reached your viewing limit for this book.

5.9 PERFORMANCE INDICES

As discussed already, the design of a control system is an attempt to meet a set of specifications which define the overall performance of the system in terms of certain measurable quantities. A number of performance measures have been introduced so far in respect of dynamic response to step input (ζ , M_p , t_r , t_p , t_s etc.) and the steady-state error, e_{ss} , to both step and higher-order inputs. These measures have to be satisfied simultaneously in design and hence the design necessarily becomes a trial and error procedure. If, however, a single performance index could be established on the basis of which one may describe the goodness of the system response, then the design procedure will become logical and straightforward.

Furthermore, in many of the modern control schemes, the system parameters are automatically adjusted to keep the system at an optimum level of performance under varying inputs and varying conditions of operation. Such class of systems is called *adaptive control systems*. These systems require a performance index which is a function of the variable system parameters. Extremum (minimum or maximum) value of this index then corresponds to the optimum set of parameter values. Other desirable features of a performance index are its selectivity, i.e., its power to clearly distinguish between an optimum and non-optimum system, its sensitivity to parameter variations and the ease of its analytical computation or its online analogic or digital determination.

A number of such performance indices are used in practice, the most common being the *integral square error* (ISE), given by

$$\text{ISE} = \int_0^{\infty} e^2(t) dt \quad \dots(5.51)$$

Apart from the ease of implementation, this index has the advantage that it is mathematically convenient both for analysis and computation. Fig. 5.27(a) and (b) show the system response $c(t)$ and error $e(t)$ respectively to unit-step input. The square error is shown in Fig. 5.27(c) and its integral in Fig. 5.27(d). It is obvious that ISE converges to a limit as $t \rightarrow \infty$. Minimization of ISE by adjusting system parameters is a good compromise between reduction of rise time to limit the effect of large initial error, reduction of peak overshoot and reduction of settling time to limit the effect of small error lasting for a long time.

Consider now the second-order system discussed previously in this chapter from eqn. (5.12), the error response to unit-step is given by

$$e(t) = \frac{e^{-\zeta\omega_n t}}{\sqrt{1-\zeta^2}} \sin \left[\omega_n \sqrt{1-\zeta^2} t + \tan^{-1} \frac{\sqrt{1-\zeta^2}}{\zeta} \right]$$

Therefore

$$\text{ISE} = \int_0^{\infty} e^2(t) dt = \frac{1}{\omega_n} \int_0^{\infty} e^2(t_n) dt_n$$

where $t_n = \omega_n t$, i.e., the normalized time.



You have either reached a page that is unavailable for viewing or reached your viewing limit for this book.



You have either reached a page that is unavailable for viewing or reached your viewing limit for this book.



You have either reached a page that is unavailable for viewing or reached your viewing limit for this book.

Table 5.2. Optimum Forms of the Closed-Loop Transfer Functions Based on the ITAE Criterion (Zero Steady-State Step Error Systems)

$\frac{C(s)}{R(s)} = \frac{a_n}{s^n + a_1 s^{n-1} + \dots + a_{n-1} s + a_n}$
$s + \omega_n$
$s^2 + 1.4\omega_n s + \omega_n^2$
$s^3 + 1.75\omega_n s^2 + 2.15\omega_n^2 s + \omega_n^3$
$s^4 + 2.1\omega_n s^3 + 3.4\omega_n^2 s^2 + 2.7\omega_n^3 s + \omega_n^4$
$s^5 + 2.8\omega_n s^4 + 5.0\omega_n^2 s^3 + 5.5\omega_n^3 s^2 + 3.4\omega_n^4 s + \omega_n^5$
$s^6 + 3.25\omega_n s^5 + 6.60\omega_n^2 s^4 + 8.60\omega_n^3 s^3 + 7.45\omega_n^4 s^2 + 3.95\omega_n^5 s + \omega_n^6$

In the case of zero steady-state ramp error systems, the general closed-loop transfer function is

$$T(s) = \frac{C(s)}{R(s)} = \frac{a_{n-1}s + a_n}{s^n + a_1 s^{n-1} + \dots + a_{n-1} s + a_n} \quad \dots(5.54)$$

Table 5.3 gives the optimum forms of the closed loop transfer functions based on the ITAE criterion (refer Problem 5.18)

Table 5.3. Optimum Forms of the Closed-Loop Transfer Functions Based on the ITAE Criterion (Zero Steady-State Ramp Error Systems)

$\frac{C(s)}{R(s)} = \frac{a_{n-1}s + a_n}{s^n + a_1 s^{n-1} + \dots + a_{n-1} s + a_n}$
$s^2 + 3.2\omega_n s + \omega_n^2$
$s^3 + 1.75\omega_n s^2 + 3.25\omega_n^2 s + \omega_n^3$
$s^4 + 2.41\omega_n s^3 + 4.93\omega_n^2 s^2 + 5.14\omega_n^3 s + \omega_n^4$
$s^5 + 2.19\omega_n s^4 + 6.50\omega_n^2 s^3 + 6.30\omega_n^3 s^2 + 5.24\omega_n^4 s + \omega_n^5$
$s^6 + 6.12\omega_n s^5 + 13.42\omega_n^2 s^4 + 17.16\omega_n^3 s^3 + 14.14\omega_n^4 s^2 + 6.76\omega_n^5 s + \omega_n^6$

5.10 ILLUSTRATIVE EXAMPLES

The design concepts introduced in this chapter are further illustrated with the help of following examples.



You have either reached a page that is unavailable for viewing or reached your viewing limit for this book.



You have either reached a page that is unavailable for viewing or reached your viewing limit for this book.



You have either reached a page that is unavailable for viewing or reached your viewing limit for this book.

$$\left(K + \frac{K_i}{s}\right) = \frac{Ks + K_i}{s}$$

Since this introduces one more integration in the forward path, the system becomes type-2 and hence the steady-state error to ramp input is reduced to zero.

Example 5.3 : In a d.c. position control servomechanism the load is driven by a motor supplied with constant armature current. The motor field current is supplied from a d.c. amplifier, the input to which is the difference between the voltages obtained from input and output potentiometers.

The load and motor together have a moment of inertia of $J = 0.4 \text{ kg-m}^2$ and the viscous friction is $f = 2 \text{ newton-m/rad/sec}$. Each potentiometer constant is $K_p = 0.6 \text{ V/rad}$. The motor develops a torque of $K_T = 2 \text{ newton-m per amp of field current}$. The field time constant is negligible.

(a) Make a sketch of the system showing how the hardware is connected.

(b) Derive the equation of motion of the system and find the value of the amplifier gain K_A (in amperes output per volt input) to give a natural frequency of 10 rad/sec .

(c) A tachogenerator of negligible inertia and friction is connected in the system to improve the damping. Determine the tachogenerator constant (in V/rad/sec) to give critical damping for $K_A = 5$.

Solution.

(a) Figure 5.30 gives the sketch of the position control servomechanism. The switch 'S' can be closed to provide the tachogenerator feedback.

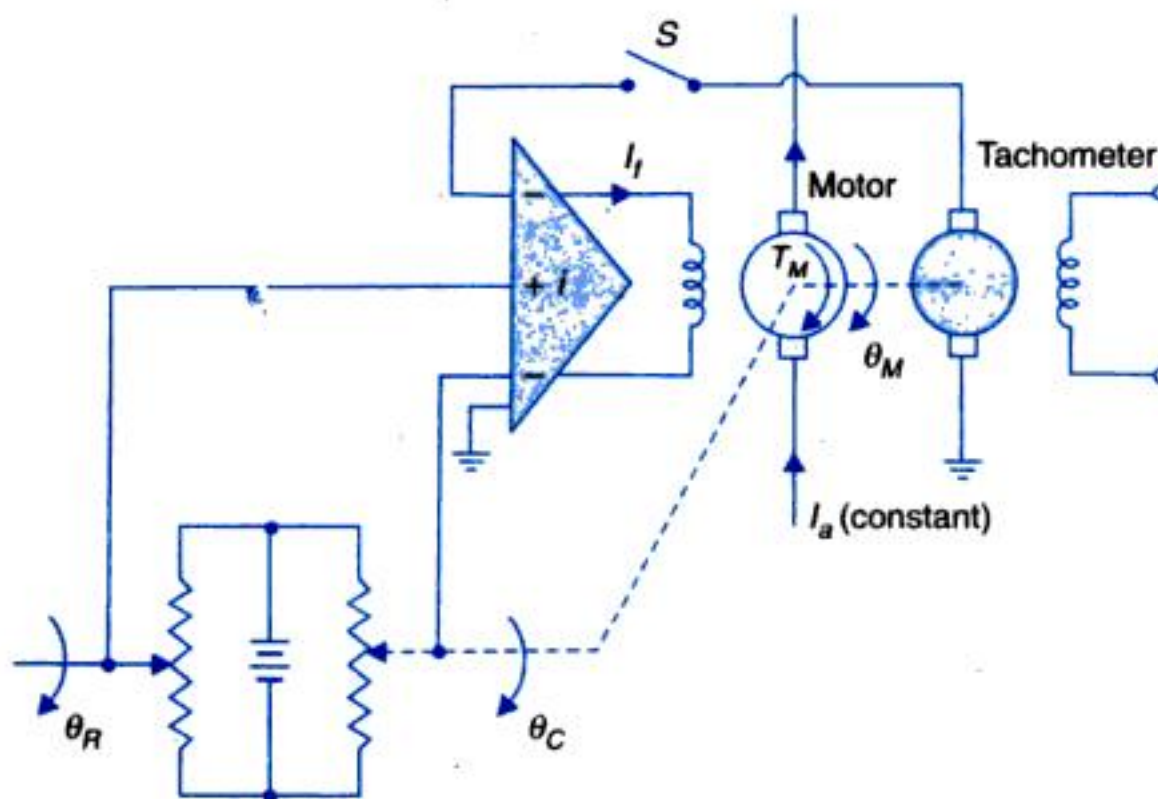


Fig. 5.30

(b) Figure 5.31 gives the signal flow graph of the system with switch 'S' open, i.e., tachogenerator not in the loop.

$$\frac{\theta_C(s)}{\theta_R(s)} = \frac{\theta_M(s)}{\theta_R(s)} = \frac{K_p K_A K_T}{s(Js + f) + K_p K_A K_T}$$



You have either reached a page that is unavailable for viewing or reached your viewing limit for this book.



You have either reached a page that is unavailable for viewing or reached your viewing limit for this book.



You have either reached a page that is unavailable for viewing or reached your viewing limit for this book.

For unit-step input

$$E(s) = \frac{1}{s + K}$$

Therefore

$$e(t) = e^{-Kt} \quad \dots(5.63)$$

$$\text{ISE} = J_e = \int_0^{\infty} e^2(t) dt = 1/(2K) \quad \dots(5.64)$$

Obviously, the minimum value of J_e is obtained as $K \rightarrow \infty$. This is an impractical solution resulting in excessive strain on physical components of the system. Increasing the gain means in effect increasing the pump size.

Sound engineering judgement tells us that we must include in our performance index the 'cost' of the control effort. We can do this in many ways. One of the ways is to modify the performance index J_e so as to include the cost of control effort as a performance measure. For the system under consideration, this cost is proportional to power rating of pump which depends upon kinetic energy required to accelerate the fluid.

Mass of fluid/sec = $Q\rho$; ρ = fluid density

Velocity of fluid = $\frac{Q}{A} = Q$; A = area of cross-section of tank
 $= 1 \text{ m}^2$

Kinetic energy/sec required to accelerate the fluid

$$= \frac{Q^3 \rho}{2} = \text{pump power}$$

Therefore, total control effort required = $\int_0^{\infty} \frac{Q^3 \rho}{2} dt$

We may limit this control effort, i.e.,

$$\int_0^{\infty} \frac{Q^3 \rho}{2} dt \leq M$$

where M is a constant.

The above inequality may be expressed in the form

$$J_u = \int_0^{\infty} u^3 dt \leq N \quad \dots(5.65)$$

where $u = Q$ (Fig. 5.34) and N is the constant determined by M and ρ . J_u is the index based on the cost of control effort.

As per eqn. (5.63)

$$u = Q = K e^{-Kt}$$

$$J_u = \int_0^{\infty} K^3 e^{-3Kt} dt = \frac{K^2}{3} \leq N$$

Now J_e given by (5.64) is minimized when K has the largest permissible value, i.e.,

$$\frac{K^2}{3} = N \quad \text{or} \quad K = \sqrt{3N} \quad \dots(5.66)$$



You have either reached a page that is unavailable for viewing or reached your viewing limit for this book.



You have either reached a page that is unavailable for viewing or reached your viewing limit for this book.



You have either reached a page that is unavailable for viewing or reached your viewing limit for this book.

It can be easily seen from eqn. (5.72) that the actuator inertia which is a constant tends to reduce any variation in D , the structural component of inertia.

A dc servomotor is characterized by an actuator gain and effective viscous friction (which also accounts for motor back emf) *expressed in terms of link variables*. These are:

Actuator gain K_m = motor torque in Nm per unit desired speed in rad/s (which is scaled value of motor armature current *i.e.*, the unit are Nm/rad/s)

F = Effective viscous friction in Nm/rad/s
Coulomb friction is ignored in our modelling of the link-actuator mechanism whose block diagram

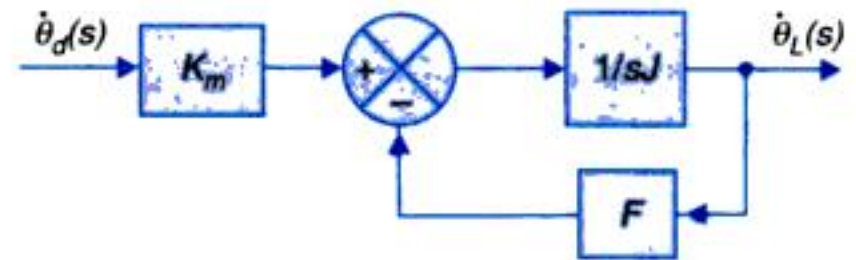


Fig. 5.36

is drawn as in Fig. 5.36 where $\dot{\theta}_d$ = desired speed and $\dot{\theta}_L$ = link speed in rad/s.

The transfer function corresponding to the block diagram of Fig. 5.36 is

$$\frac{\dot{\theta}_L(s)}{\dot{\theta}_d(s)} = \frac{K_m}{sJ + F} \quad \dots(5.73)$$

The damping factor of the closed-loop actuators can be increased by providing rate feedback from a tachogenerator (refer Section 5.6.) resulting in the block diagram of Fig. 5.37. The transfer function of eqn (5.73) now modifies to

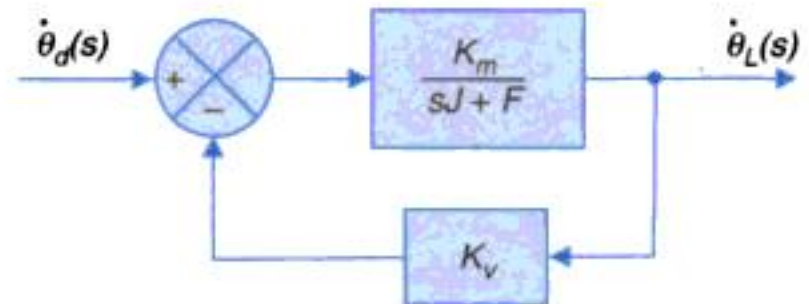


Fig. 5.37

$$\frac{\dot{\theta}_L(s)}{\dot{\theta}_d(s)} = \frac{K_m}{sJ + (F + K_v K_m)} \quad \dots(5.74)$$

For controlling the position (link angle) feedback is provided from the output angle θ_L as in the block diagram of Fig. 5.38 where in an adjustable gain K_e is included in the forward path. The units of K_e are s^{-1} . The closed-loop transfer function of this position control system is

$$\frac{\theta_L(s)}{\theta_d(s)} = \frac{K_e K_m}{s^2 J + s(F + K_v K_m) + K_e K_m} \quad \dots(5.75)$$

$$= \frac{(K_e K_m / J)}{s^2 + s(F + K_v K_m) / J + K_e K_m / J} \quad \dots(5.76)$$

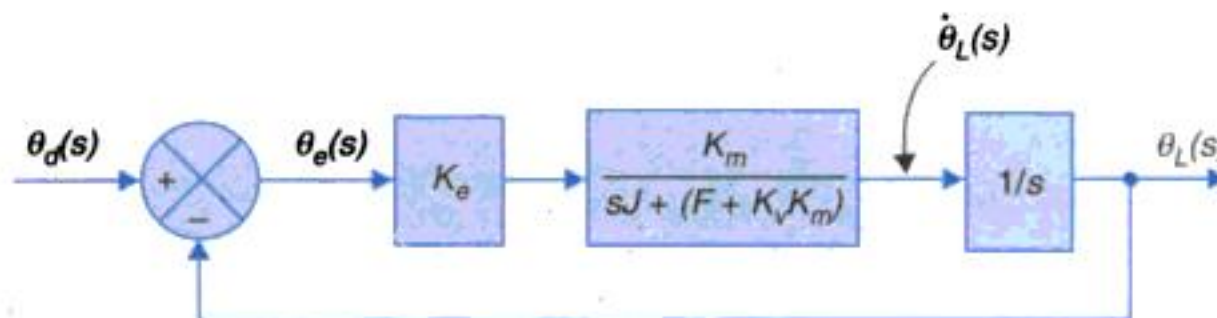


Fig. 5.38



You have either reached a page that is unavailable for viewing or reached your viewing limit for this book.



You have either reached a page that is unavailable for viewing or reached your viewing limit for this book.



You have either reached a page that is unavailable for viewing or reached your viewing limit for this book.

Find the steady-state error for ramp input. Suggest ways of eliminating this error and draw the block diagram of the modified system.

Solution.

$$G(s) = \frac{100/s^2}{1 + 100K/s} = \frac{100}{s(s + 100K)}$$

Characteristic equation is

$$\text{or} \quad 1 + \frac{100}{s(s + 100K)} = 0 \quad \text{or} \quad s^2 + 100Ks + 100 = 0$$

which gives

$$\omega_n = 10, 2\zeta\omega_n = 100K$$

For lowest possible settling time with nonoscillatory response

$$\zeta = 1 \Rightarrow K = 20/100 = 0.2$$

For ramp input

$$R(s) = V/s^2$$

$$\begin{aligned} E(s) &= \frac{1}{1 + G(s)} R(s) = \frac{V/s^2}{1 + 100/s(s + 100K)} \\ &= \frac{V(s + 100K)}{s(s^2 + 100Ks + 100)} \end{aligned}$$

$$e(ss) = \lim_{s \rightarrow 0} s E(s) = KV = 0.2V$$

For reducing this steady-state error to zero, system is provided with feedforward as in Fig. 5.42.

Check

With $R(s) = V/s^2$ consider the steady-state contributed by additional input $sR(s) = V/s$.

$$\left[\frac{KV}{100s} + E(s) \right] G(s) = C(s)$$

$$\text{But } C(s) = -E(s)$$

$$\frac{KV}{100s} G(s) = -[1 + G(s)]E(s)$$

$$\text{or} \quad E(s) = \frac{(KV/100s)G(s)}{1 + G(s)}$$

Substituting value of $G(s)$

$$E(s) = - \frac{KV}{s(s^2 + 100Ks + 100)}$$

$$e(ss) = -KV = -0.2V, \text{ due to additional input}$$

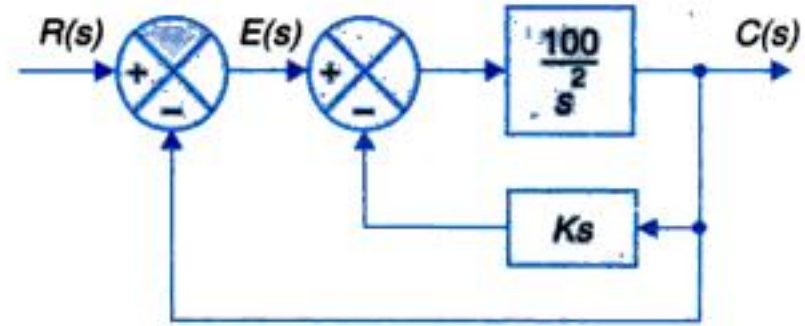


Fig. 5.41

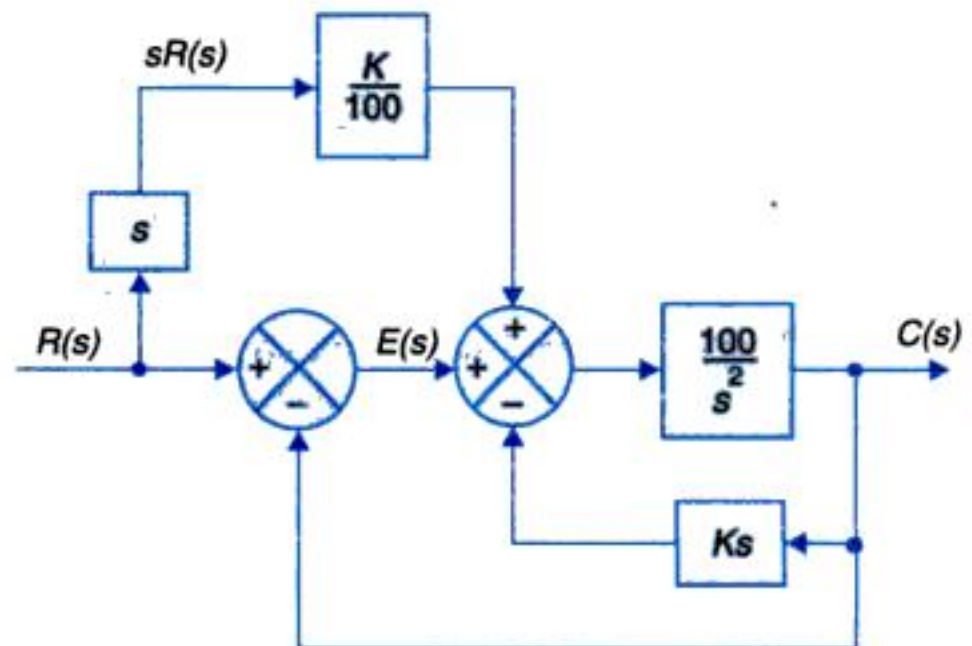


Fig. 5.42



You have either reached a page that is unavailable for viewing or reached your viewing limit for this book.



You have either reached a page that is unavailable for viewing or reached your viewing limit for this book.



You have either reached a page that is unavailable for viewing or reached your viewing limit for this book.

Let us take the inverse transform of the resolvent matrix

$$\begin{aligned}\text{adj}(s\mathbf{I} - \mathbf{A}) &= \begin{bmatrix} s+20 & 1 \\ -100 & s \end{bmatrix} \\ \det(s\mathbf{I} - \mathbf{A}) &= \begin{bmatrix} s & -1 \\ 100 & s+20 \end{bmatrix} = D(s) \\ D(s) &= s(s+20) + 100 = 0\end{aligned}$$

or $s^2 + 20s + 100 = 0$

Its eigenvalues are given as

$s_1, s_2 = -10$; the two eigen values are repeated. This is a critically damped case.

$\Phi(s) = (s\mathbf{I} - \mathbf{A})^{-1} = \text{resolvent matrix}$

$$= \frac{\text{adj}(s\mathbf{I} - \mathbf{A})}{\det(s\mathbf{I} - \mathbf{A})} = \begin{bmatrix} s+20 & 1 \\ -100 & s \end{bmatrix} \frac{1}{D(s)} \quad \dots(iv)$$

Taking the inverse Laplace transform term by term

$$\begin{aligned}\mathcal{L}^{-1}\left[\frac{s+20}{D(s)}\right] &= \mathcal{L}^{-1}\left[\frac{s+20}{(s+10)^2}\right] = 10t e^{-10t} + e^{-10t}; t > 0 \\ \mathcal{L}^{-1}\frac{1}{D(s)} &= \mathcal{L}^{-1}\frac{1}{(s+10)^2} = e^{-10t}; t > 0 \\ \mathcal{L}^{-1}\frac{-100}{D(s)} &= -100t e^{-10t}; t > 0 \\ \mathcal{L}^{-1}\frac{s}{D(s)} &= \mathcal{L}^{-1}\frac{s}{(s+10)^2} = -10t e^{-10t} + e^{-10t}; t > 0\end{aligned}$$

Thus the state transition matrix is given as

$$\phi(t) = \begin{bmatrix} 10te^{-10t} + e^{-10t} & te^{-10t} \\ -100te^{-10t} & -10te^{-10t} + e^{-10t} \end{bmatrix}; t > 0 \quad \dots(v)$$

For $\mathbf{X}(s) = [(s\mathbf{I} - \mathbf{A})^{-1} \mathbf{B} (1/s)]; U(s) = 1/s$

$$= \frac{1}{sD(s)} \begin{bmatrix} s+20 & 1 \\ -100 & s \end{bmatrix} \begin{bmatrix} 0 \\ 100 \end{bmatrix} = 100 \begin{bmatrix} 1/s \\ 1 \end{bmatrix} \frac{1}{D(s)} \quad \dots(vi)$$

Taking the inverse Laplace transform term by term

$$\begin{aligned}\mathcal{L}^{-1}\frac{1}{D(s)} &= \mathcal{L}^{-1}\frac{1}{(s+10)^2} = te^{-10t}; t > 0 \\ \mathcal{L}^{-1}\frac{1}{sD(s)} &= \mathcal{L}^{-1}\frac{1}{s(s+10)^2} \\ &= \frac{1}{100} (1 - 10te^{-10t} - e^{-10t})\end{aligned}$$

Thus

$$\mathbf{x}(t) = 100 \begin{bmatrix} 1 - 10te^{-10t} - e^{-10t} \\ 10te^{-10t} \end{bmatrix}; t > 0 \quad \dots(vii)$$

The output is given as

$$y(t) = x_1(t) = 1 - 10e^{-10t} - e^{-10t}; t > 0 \quad \dots(viii)$$



You have either reached a page that is unavailable for viewing or reached your viewing limit for this book.



You have either reached a page that is unavailable for viewing or reached your viewing limit for this book.



You have either reached a page that is unavailable for viewing or reached your viewing limit for this book.

The area on s plane where the complex dominant roots should be in Fig. 5.45

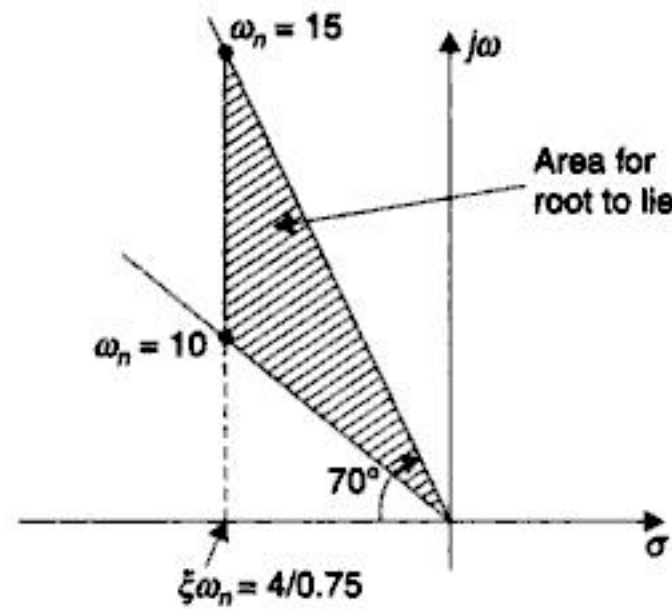


Fig. 5.45

(b) From Eq. (i) $\xi\omega_n = \frac{4}{0.75}$

We choose the third root to be at least 6-time further on negative real axis than the real part of the complex conjugate roots. Thus

$$s = -6 \times (\xi\omega_n) = \frac{6 \times 4}{0.75}$$

$$s = -32$$

or

(c) $t_s = 0.75$, $M_p = 30\% \Rightarrow \xi = 0.35$, $\xi\omega_n = \frac{4}{0.75} = 5.33$, $\omega_n = 15$

Complex conjugate roots term is

$$(s^2 + 2\xi\omega_n s + \omega_n^2) = (s^2 + 10.66s + 225)$$

Third root $s = -32$

The closed-loop transfer function can then be written as

$$T(s) = \frac{C(s)}{R(s)} = \frac{32 \times 225}{(s + 32)(s^2 + 10.66s + 225)}$$

The numerator (32×225) assures that $T(s = 0) = 1$, which mean $C(0) = R(0)$ or steady state error is zero, system type-1.

Now
$$T(s) = \frac{G(s)}{1 + G(s)} = \frac{32 \times 225}{(s + 32)(s^2 + 10.66s + 225)}$$

From which we can write

$$G(s) = \frac{T(s)}{1 - T(s)}$$

Solving yield
$$G(s) = \frac{32 \times 225}{s(s^2 + 43s + 566)}$$

Example 5.11. The open-loop transfer function of a unity feedback system is

$$G(s) = \frac{K}{s(s + 2)}$$



You have either reached a page that is unavailable for viewing or reached your viewing limit for this book.



You have either reached a page that is unavailable for viewing or reached your viewing limit for this book.



You have either reached a page that is unavailable for viewing or reached your viewing limit for this book.



You have either reached a page that is unavailable for viewing or reached your viewing limit for this book.



You have either reached a page that is unavailable for viewing or reached your viewing limit for this book.



You have either reached a page that is unavailable for viewing or reached your viewing limit for this book.



You have either reached a page that is unavailable for viewing or reached your viewing limit for this book.



You have either reached a page that is unavailable for viewing or reached your viewing limit for this book.



You have either reached a page that is unavailable for viewing or reached your viewing limit for this book.

$$\frac{\omega_n^2}{s^2 + 2\xi\omega_n s + \omega_n^2} \rightarrow 1 - \frac{1}{\sqrt{1-\xi^2}} e^{-\xi\omega_n t} \sin[\omega_n \sqrt{1-\xi^2} t + \phi];$$

From eqn. (iv), we find ;

$$\phi = \tan^{-1} \frac{\sqrt{1-\xi^2}}{\xi}, \quad \xi < 1$$

$$\omega_n \sqrt{1-\xi^2} = 10.85; \quad \frac{1}{\sqrt{1-\xi^2}} = 1.262$$

$$\phi = \tan^{-1} \frac{0.792}{0.61} = 52.4^\circ$$

By use of Laplace transform pair of eqn. (iv), we have

$$\theta_o(t) = 1 - 1.262e^{-8.375t} \sin(10.85t + 52.4^\circ) \quad \dots(iv)$$

This is the well-known response to unit step input of a second-order undamped system. The reader may plot of this response and check its nature. The result of Eq. (iv) may be checked that $\theta_o(t=0) = 0$, $\theta_o(t=\infty) = 1$.

PROBLEMS

- 5.1** A servomechanism is used to control the angular position θ_o of a mass through a command signal θ_i . The moment of inertia of moving parts referred to the load shaft is 200 kg-m^2 and the motor torque at the load is 6.88×10^4 newton-m per rad of error. The damping torque coefficient referred to the load shaft is 5×10^3 newton-m per rad/sec.
- (a) Find the time response of the servomechanism to a step input of 1 rad and determine the frequency of transient oscillation, the time to rise to the peak overshoot and the value of the peak overshoot.
- (b) Determine the steady-state error when the command signal is a constant angular velocity of 1 revolution/min.
- (c) Determine the steady-state error which exists when a steady torque of 1,200 newton-m is applied at load shaft.
- 5.2** In the position control system shown in Fig. P-5.2, the transfer function of the motor is found to be

$$\theta_M(s)/V_C(s) = K_M/s(\tau_m s + 1)$$

where $K_M = 15 \text{ rad/s/V}$; $\tau_m = 0.15 \text{ s}$. The gear ratios are given as

$$\dot{\theta}_C / \dot{\theta}_L = 1; \quad \dot{\theta}_L / \dot{\theta}_M = 1/50$$

The input is given through a pot of sensitivity $K_p = 0.1 \text{ V/deg}$. The input and output are given to a d.c. difference amplifier of gain $K_A \text{ V/V}$. The output of this amplifier is then modulated by a carrier of 50 Hz. The gain of this modulator is $K_D = s/5 \text{ V}_{\text{rms}}/\text{V}_{\text{d.c.}}$. This signal is then amplified by an a.c. amplifier of gain $K_C = 25 \text{ V/V}$ and given to the control phase winding of the a.c. servomotor.

- (a) If the input shaft is driven at a constant speed of $\pi \text{ rad/sec}$, determine the value of the amplifier gain K_A , such that the steady-state error in the position is less than 5 degree. For this value of K_A , determine the damping ratio and the 2% settling time of the system.
- (b) To improve the system dynamics, the amplifier is modified by introducing an additional derivative term such that its output is given by

$$e_A = K_A e(t) + K_X \dot{e}(t)$$



You have either reached a page that is unavailable for viewing or reached your viewing limit for this book.



You have either reached a page that is unavailable for viewing or reached your viewing limit for this book.



You have either reached a page that is unavailable for viewing or reached your viewing limit for this book.

- (c) Illustrate how the steady-state error of the system with derivative feedback to unit-ramp input can be reduced to same value as in part (a), while the damping factor is maintained at 0.6.

5.11 A unity feedback system is characterized by the open-loop transfer function

$$G(s) = 1/s(0.5s + 1)(0.2s + 1)$$

Determine the steady-state errors for unit-step, unit-ramp and unit-acceleration inputs. Also determine the damping ratio and natural frequency of the dominant roots.

5.12 The open-loop transfer function of a servo system with unity feedback is

$$G(s) = 10/s(0.1s + 1)$$

Evaluate the static error constants (K_p , K_v , K_a) for the system. Obtain the steady-state error of the system when subjected to an input given by the polynomial

$$r(t) = a_0 + a_1 t + \frac{a_2}{2} t^2$$

5.13 For Problem 5.12, evaluate the dynamic error using the dynamic error coefficients.

Hint : For a unity feedback system

$$\frac{E(s)}{R(s)} = \frac{1}{1+G(s)} = \frac{1}{K_1} + \frac{1}{K_2} s + \frac{1}{K_3} s^2 + \dots$$

Coefficients K_1 , K_2 , K_3 , ... are defined to be dynamic-error coefficients.

$$E(s) = \frac{1}{K_1} R(s) + \frac{1}{K_2} sR(s) + \frac{1}{K_3} s^2 R(s) + \dots$$

$$e(t) = \frac{1}{K_1} r(t) + \frac{1}{K_2} \dot{r}(t) + \frac{1}{K_3} \ddot{r}(t) + \dots$$

5.14 A machine tool is required to cut a 30° circular arc of 1 cm radius. The tool moves at a constant feed velocity of 0.1 cm/sec parallel to the x -axis, as shown in Fig. P-5.14. A unity feedback servomechanism with open-loop transfer function $G(s) = 10/s(s + 1)$ drives the tool in y -direction. Estimate the error when $x = 0.3$.

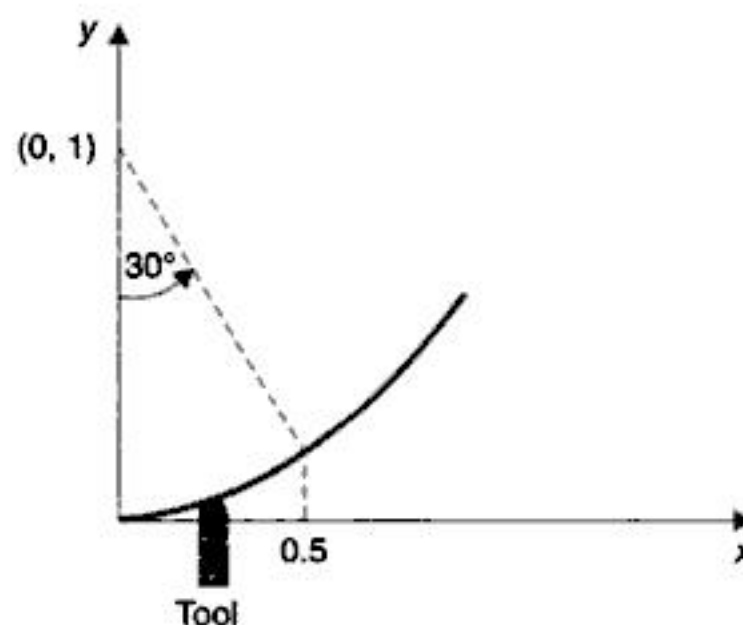


Fig. P-5.14

Hint : The equation of the circular arc is

$$x^2 + (y - 1)^2 = 1$$

which gives

$$y = 1 - \sqrt{1 - x^2}, \text{ for } 0 < x < 0.5$$



You have either reached a page that is unavailable for viewing or reached your viewing limit for this book.



You have either reached a page that is unavailable for viewing or reached your viewing limit for this book.



You have either reached a page that is unavailable for viewing or reached your viewing limit for this book.



You have either reached a page that is unavailable for viewing or reached your viewing limit for this book.

that there is no clearcut correspondence between the two notions of stability defined above. For a free stable nonlinear system, there is no guarantee that output will be bounded whenever input is bounded. Also if the output is bounded for a particular bounded input, it may not be bounded for other bounded inputs. Many of the important results obtained thus far concern the stability of the nonlinear systems in the sense of the second notion above, *i.e.*, when the system has no input. Here in this chapter, we are concerned with the stability determination of linear time-invariant systems.

Let us observe the physical implication of the two notions of stability defined earlier, by considering a single-input, single-output system with transfer function

$$\frac{C(s)}{R(s)} = G(s) = \frac{b_0 s^m + b_1 s^{m-1} + \dots + b_m}{a_0 s^n + a_1 s^{n-1} + \dots + a_n}; m < n \quad \dots(6.1)$$

With initial conditions assumed zero, the output of the system is given by

$$c(t) = \mathcal{L}^{-1}[G(s)R(s)]$$

Therefore (see Appendix 1)

$$c(t) = \int_0^\infty g(\tau)r(t-\tau)d\tau$$

where $g(t) = \mathcal{L}^{-1}(G(s))$ is the *impulse response* of the system (eqn. (5.4)).

Taking the absolute value on both sides we get

$$|c(t)| = \left| \int_0^\infty g(\tau)r(t-\tau)d\tau \right|$$

Since the absolute value of integral is not greater than the integral of the absolute value of the integrand,

$$\begin{aligned} |c(t)| &\leq \int_0^\infty |g(\tau)r(t-\tau)|d\tau \\ &\leq \int_0^\infty |g(\tau)||r(t-\tau)|d\tau \end{aligned} \quad \dots(6.2)$$

The first notion of stability is satisfied if for every bounded input ($|r(t)| \leq M_1 < \infty$), the output is bounded ($|c(t)| \leq M_2 < \infty$). From (6.2), we have for bounded input, the bounded output condition as

$$|c(t)| \leq M_1 \int_0^\infty |g(\tau)|d\tau \leq M_2$$

Thus the first notion of stability is satisfied if the impulse response $g(t)$ is absolutely integrable, *i.e.*, $\int_0^\infty |g(\tau)|d\tau$ is finite (area under the absolute-value curve of the impulse response $g(t)$ evaluated from $t = 0$ to $t = \infty$ must be finite).

The nature of $g(t)$ is dependent on the poles of the transfer function $G(s)$ which are the roots of the characteristic equation. These roots may be both real and complex conjugate and may have multiplicity of various orders. The nature of response terms contributed by all possible types of roots are given in Table 6.1 and have been illustrated in Fig. 6.1.



You have either reached a page that is unavailable for viewing or reached your viewing limit for this book.



You have either reached a page that is unavailable for viewing or reached your viewing limit for this book.



You have either reached a page that is unavailable for viewing or reached your viewing limit for this book.

- (i) If all the roots of the characteristic equation have negative real parts, the system is *stable*.
- (ii) If any root of the characteristic equation has a positive real part or if there is a repeated root on the $j\omega$ -axis, the system is *unstable*.
- (iii) If the condition (i) is satisfied except for the presence of one or more nonrepeated roots on the $j\omega$ -axis, the system is *limitedly stable*.

In further subdivision of the concept of stability, a linear system is characterized as:

- (i) *Absolutely stable* with respect to a parameter of the system if it is stable for all values of this parameter.
- (ii) *Conditionally stable* with respect to a parameter, if the system is stable for only certain bounded ranges of values of this parameter.

It follows from the above discussion that stability can be established by determining the roots of the characteristic equation. Unfortunately, no general formula in algebraic form is available to determine the roots of the characteristic equations of higher than second-order. Though various numerical methods exist for root determination of a characteristic equation, these are quite cumbersome even for third-and fourth-order systems.

However, simple graphical and algebraic criteria have been developed which permit the study of stability of a system without the need of actually determining the roots of its characteristic equation. These criteria answer the question, whether a system be stable or not, in 'yes' or 'no' form.

Relative Stability

In practical systems, it is not sufficient to know that the system is stable but a stable system must meet the specifications on *relative stability* which is a quantitative measure of how fast the transients die out in the system.

Relative stability may be measured by relative settling times of each root or pair of roots. It has been shown in the preceding chapter that the settling time of a pair of complex conjugate poles is inversely proportional to the real part (negative) of the roots. This result is equally valid for real roots. As a root (or a pair of roots) moves farther away from the imaginary axis as shown in Fig. 6.3, the relative stability of the system improves.

6.2 NECESSARY CONDITIONS FOR STABILITY

Certain conclusions regarding the stability of a system can be drawn by merely inspecting the coefficients of its characteristic equation in polynomial form. In the following sections, we shall show that a necessary (but not sufficient) condition for stability of a linear system is that all the coefficients of its characteristic equation $q(s) = 0$, be real and have the same sign. Furthermore, none of the coefficients should be zero.

Consider the characteristic equation

$$q(s) + a_0 s^n + a_1 s^{n-1} + \dots + a_{n-1} s + a_n = 0; a_0 > 0 \quad \dots(6.3)$$

It is to be noted that there is no loss of generality in assuming $a_0 > 0$. In case $a_0 < 0$, it can be made positive by multiplying the characteristic equation by -1 throughout.



You have either reached a page that is unavailable for viewing or reached your viewing limit for this book.



You have either reached a page that is unavailable for viewing or reached your viewing limit for this book.



You have either reached a page that is unavailable for viewing or reached your viewing limit for this book.

Routh Array

$$\begin{array}{c|cccccc}
 s^n & a_0 & a_2 & a_4 & a_6 & \cdot & \cdot \\
 s^{n-1} & a_1 & a_3 & a_5 & \cdot & \cdot & \cdot \\
 s^{n-2} & b_1 & b_2 & b_3 & \cdot & \cdot & \cdot \\
 s^{n-3} & c_1 & c_2 & & & & \\
 s^{n-4} & d_1 & d_2 & & & & \\
 \cdot & \cdot & \cdot & & & & \\
 \cdot & \cdot & \cdot & & & & \\
 s^2 & e_1 & a_n & & & & \\
 s^1 & f_1 & & & & & \\
 s^0 & a_n & & & & &
 \end{array}
 \quad \dots(6.9)$$

The coefficients $b_1, b_2 \dots$, are evaluated as follows:

$$\begin{aligned}
 b_1 &= (a_1 a_2 - a_0 a_3) / a_1; \\
 b_2 &= (a_1 a_4 - a_0 a_5) / b_1; \dots
 \end{aligned}$$

This process is continued till we get a zero as the last coefficient in the third row. In a similar way, the coefficients of 4th, 5th, ..., n th and $(n + 1)$ th rows are evaluated, e.g.,

$$\begin{aligned}
 c_1 &= (b_1 a_3 - a_1 b_2) / b_1; \\
 c_2 &= (b_1 a_5 - a_1 b_3) / b_1; \dots \\
 d_1 &= (c_1 b_2 - b_1 c_2) / c_1; \\
 d_2 &= (c_1 b_3 - b_1 c_3) / c_1; \dots
 \end{aligned}$$

and

It is to be noted here that in the process of generating the Routh array, the missing terms are regarded as zero. Also all the elements of any row can be divided by a positive constant during the process to simplify the computational work.

The Routh stability criterion is stated as below.

For a system to be stable, it is necessary and sufficient that each term of first column of Routh array [as given in eqn. (6.9)] of its characteristic equation be positive if $a_0 > 0$. If this condition is not met, the system is unstable and number of sign changes of the terms of the first column of the Routh array corresponds to the number of roots of the characteristic equation in the right half of the s -plane.

The Routh criterion stated above and the Hurwitz criterion are equivalent, as is shown below.

Elements of first column of the Routh array can be interpreted in terms of Hurwitz determinants as follows:

$$b_1 = \frac{a_1 a_2 - a_0 a_3}{a_1} = \frac{\begin{vmatrix} a_1 & a_0 \\ a_3 & a_2 \end{vmatrix}}{a_1} = \frac{\Delta_2}{\Delta_1}$$



You have either reached a page that is unavailable for viewing or reached your viewing limit for this book.



You have either reached a page that is unavailable for viewing or reached your viewing limit for this book.



You have either reached a page that is unavailable for viewing or reached your viewing limit for this book.



You have either reached a page that is unavailable for viewing or reached your viewing limit for this book.



You have either reached a page that is unavailable for viewing or reached your viewing limit for this book.



You have either reached a page that is unavailable for viewing or reached your viewing limit for this book.



You have either reached a page that is unavailable for viewing or reached your viewing limit for this book.

where

$$b_3 = \frac{288 - K}{10}$$

$$c_3 = \frac{(288 - K)(K + 32) - 100K\alpha}{b_3}$$

In order for the system to be stable the following three conditions should be satisfied.

$$K < 288$$

$$K\alpha > 0$$

$$(288 - K)(K + 32) - 100K\alpha > 0$$

If we choose $K = 200$

$$\alpha = \frac{88 \times 232}{100 \times 200} \approx 1$$

This choice gives system's velocity error constant as

$$K_v = \frac{K\alpha}{4 \times 2 \times 4} = \frac{K\alpha}{32} = 25/4$$

% velocity error = $4/25 \times 100 = 16$ (acceptable)

Observe that the controller transfer function becomes

$$G_c(s) = \frac{s+1}{s+4}$$

which as we shall see in Chapter 12 is a lead network.

6.5 RELATIVE STABILITY ANALYSIS

Once a system is shown to be stable, we proceed to determine its relative stability quantitatively by finding the settling time of the dominant roots of its characteristic equation. The settling time being inversely proportional to the real part of the dominant roots, the relative stability can be specified by requiring that all the roots of the characteristic equation be more negative than a certain value, *i.e.*, all the roots must lie to the left of the lines $s = -s_1$ ($s_1 > 0$). The characteristic equation of the system under study is then modified by shifting the origin of the s plane to $s = -\sigma_1$, *i.e.*, by the substitution

$$s = z - s_1$$

as illustrated in Fig. 6.6. If the new characteristic equation in z satisfies the Routh criterion, it implies that all the roots of the original characteristic equation are more negative than $-\sigma_1$.

Example 6.10 : Consider a third-order system with the characteristic equation

$$s^3 + 7s^2 + 25s + 39 = 0$$

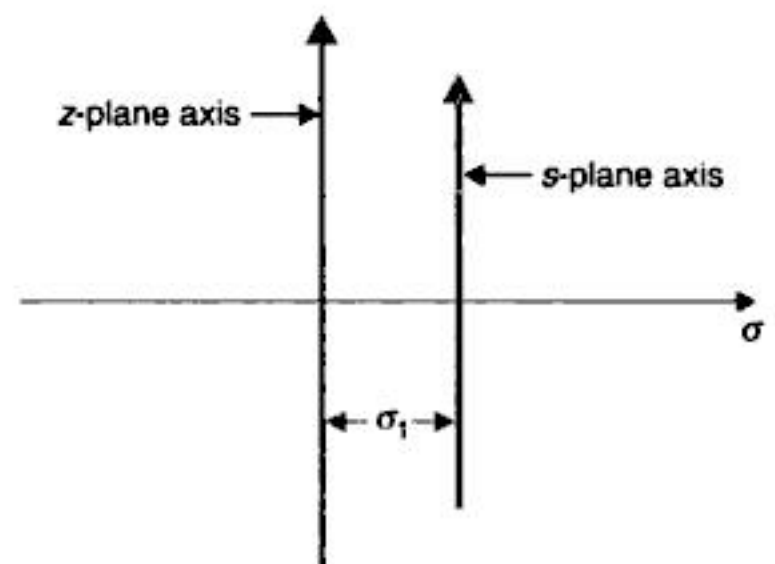


Fig. 6.6



You have either reached a page that is unavailable for viewing or reached your viewing limit for this book.



You have either reached a page that is unavailable for viewing or reached your viewing limit for this book.



You have either reached a page that is unavailable for viewing or reached your viewing limit for this book.

The Routh array is

$$\begin{array}{c|ccc}
 s^6 & 1 & 3 & 3 & 1 \\
 s^5 & 1 & 3 & 2 & \\
 s^4 & \varepsilon & 1 & 1 & \\
 s^3 & \frac{3\varepsilon - 1}{\varepsilon} & \frac{2\varepsilon - 1}{\varepsilon} & & \\
 s^2 & -2\varepsilon^2 + 4\varepsilon - 1 & 1 & & \\
 s^1 & \frac{4\varepsilon^2 - \varepsilon}{2\varepsilon^2 - 4\varepsilon + 1} & & & \\
 s^0 & 1 & & &
 \end{array}$$

As $\varepsilon \rightarrow 0$, the element of s^1 row tend to zero. This indicates that there are symmetrically located roots in the s -plane. We therefore need to examine the auxiliary polynomial to find out the possibility of the imaginary-axis roots. If no such roots exist, the usual procedure of replacing the all-zero row by coefficients of the derivative of the auxiliary polynomial is adopted. If the imaginary-axis roots are found to exist, the original polynomial is divided out by the auxiliary polynomial and test is performed on the remainder polynomial.

For the example under consideration, the auxiliary equation is (left $\varepsilon \rightarrow 0$ in s^2 -row)

$$s^2 + 1 = 0$$

yielding two roots on the imaginary axis. Dividing the original polynomial $q(s)$ by $(s^2 + 1)$, we get

$$q(s) = s^4 + s^3 + 2s^2 + 2s + 1$$

The Routh array for this polynomial is

$$\begin{array}{c|ccc}
 s^4 & 1 & 2 & 1 \\
 s^3 & 1 & 2 & \\
 s^2 & \varepsilon & 1 & \\
 s^1 & \frac{2\varepsilon - 1}{\varepsilon} & & \\
 s^0 & 1 & &
 \end{array}$$

As $\varepsilon \rightarrow 0$, there are two sign changes in the first-column elements. This indicates that there are two roots in the right s -plane.

6.7 STABILITY OF SYSTEMS MODELLED IN STATE VARIABLE FORM

We have seen in Section 2.7, that a single-input-single-output system can be expressed in state-variable form as (see eqns. 2.95(a), (b))

$$\dot{\mathbf{x}} = \mathbf{A}\mathbf{x} + \mathbf{b}u \quad \dots(6.10)$$

$$y = \mathbf{C}\mathbf{x} \quad \dots(6.11)$$

The system's characteristic equation is given by (eqn. 5.105)

$$|\lambda \mathbf{I} - \mathbf{A}| = 0$$



You have either reached a page that is unavailable for viewing or reached your viewing limit for this book.



You have either reached a page that is unavailable for viewing or reached your viewing limit for this book.



You have either reached a page that is unavailable for viewing or reached your viewing limit for this book.

- (a) Using the Routh criterion, calculate the range of values of K for the system to be stable.
 (b) Check if for $K = 1$, all these roots of the characteristic equation of the above system have damping factor greater than 0.5.

Note. Part (b) requires actual determination of the roots.

- 6.10** Determine whether the largest time constant of the characteristic equation given below is greater than, less than, or equal to 1.0 sec.

$$s^3 + 4s^2 + 6s + 4 = 0.$$

- 6.11** A feedback system has an open-loop transfer function of

$$G(s)H(s) = \frac{Ke^{-s}}{s(s^2 + 5s + 9)}$$

Determine by use of the Routh criterion, the maximum value of K for the closed-loop system to be stable.

[Hint : For low frequencies $e^{-s} \approx (1 - s)$]

- 6.12** A process is represented by the following state equations

$$\dot{x}_1 = x_1 - 4x_2$$

$$\dot{x}_2 = 8x_1 + u$$

The process dynamics is modified by state feedback

$$u = -k_1x_1 - k_2x_2$$

where k_1 and k_2 are real constants. Sketch the region of (k_1, k_2) for the system to be stable.

- 6.13** Determine the range of values of K ($K > 0$) such that the characteristic equation

$$s^3 + 3(k + 1)s^2 + (7K + 5)s + (4K + 7) = 0$$

has roots more negative than $s = -1$.



You have either reached a page that is unavailable for viewing or reached your viewing limit for this book.



You have either reached a page that is unavailable for viewing or reached your viewing limit for this book.



You have either reached a page that is unavailable for viewing or reached your viewing limit for this book.

(2) $K = a^2/4$, the roots are real and equal in value, i.e., $s_1 = s_2 = -a/2$.

(3) $a^2/4 < K < \infty$, the roots are complex conjugate with real part $= -a/2$, i.e., unvarying real part.

The root locus with varying K is plotted in Fig. 7.2. These loci given the following information about the system behaviour.

1. The root locus plot has two branches starting at the two open-loop poles ($s = 0$, and $s = -a$) for $K = 0$,

2. As K is increased from 0 to $a^2/4$, the roots move towards the point $(-a/2, 0)$ from opposite directions. Both the roots lie on the negative real axis which corresponds to an overdamped system. The two roots meet at $s = -a/2$ for $K = a^2/4$. This point corresponds to a critically-damped system. As K is increased further ($K > a^2/4$), the roots break away from the real axis, become complex conjugate and since the real part of both the roots remains fixed at $-a/2$, the roots move along the line $\sigma = -a/2$ and the system becomes underdamped.

3. For $K > a^2/4$, the real parts of the roots are fixed, therefore the settling time is nearly constant.

The root locus shown in Fig. 7.2 has been drawn by the direct solution of the characteristic equation. This procedure becomes highly tedious for higher-order systems. Evans developed a graphical technique by use of which the root locus for third-and higher-order systems can be constructed as easily as for a second order system. The characteristic equation of any system is given by

$$\Delta(s) = 0 \quad \dots(7.4)$$

where $\Delta(s)$ is the determinant of the signal flow graph of the system and is given by eqn. (2.86) which is reproduced below:

$$\Delta(s) = 1 - \sum_m P_{m1} + \sum_m P_{m2} - \sum_m P_{m3} + \dots$$

where P_{mr} = gain product of m th possible combination of r non-touching loops of the graph. Thus, the characteristic equation can always be written in the form

$$1 + P(s) = 0 \quad \dots(7.5)$$

For the single-loop system shown in Fig. 7.3

$$P(s) = G(s)H(s)$$

where $G(s)H(s)$ is the open-loop transfer function in block diagram terminology or loop transmittance in signal flow graph terminology.

From eqn. (7.5) it is seen that the roots of the characteristic equation (i.e., the closed-loop poles of the system) occur only for those values of s , where

$$P(s) = -1 \quad \dots(7.6)$$

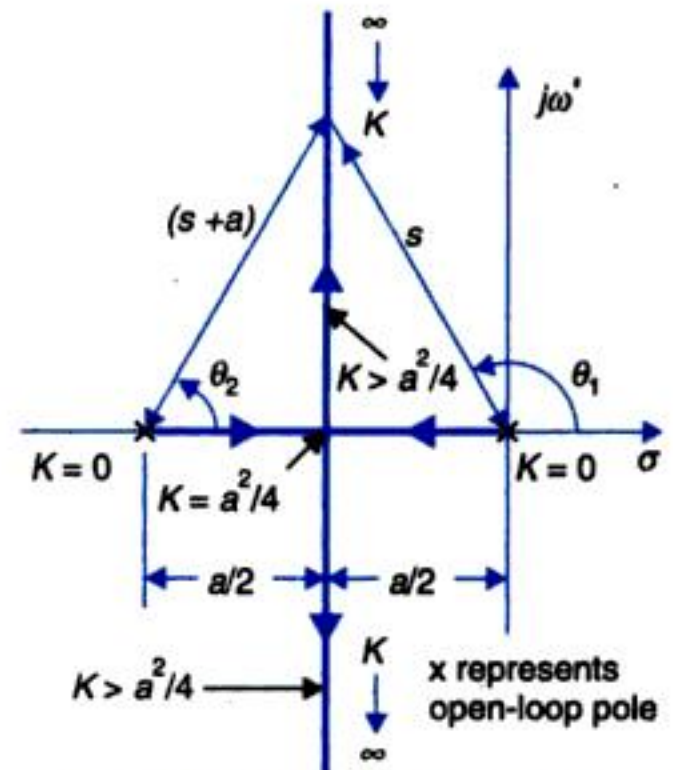


Fig. 7.2. Root loci of $s^2 + as + K = 0$ as a function of K .

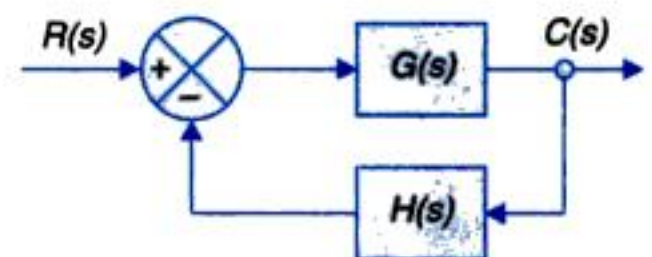


Fig. 7.3. Single-loop feedback system.



You have either reached a page that is unavailable for viewing or reached your viewing limit for this book.



You have either reached a page that is unavailable for viewing or reached your viewing limit for this book.



You have either reached a page that is unavailable for viewing or reached your viewing limit for this book.

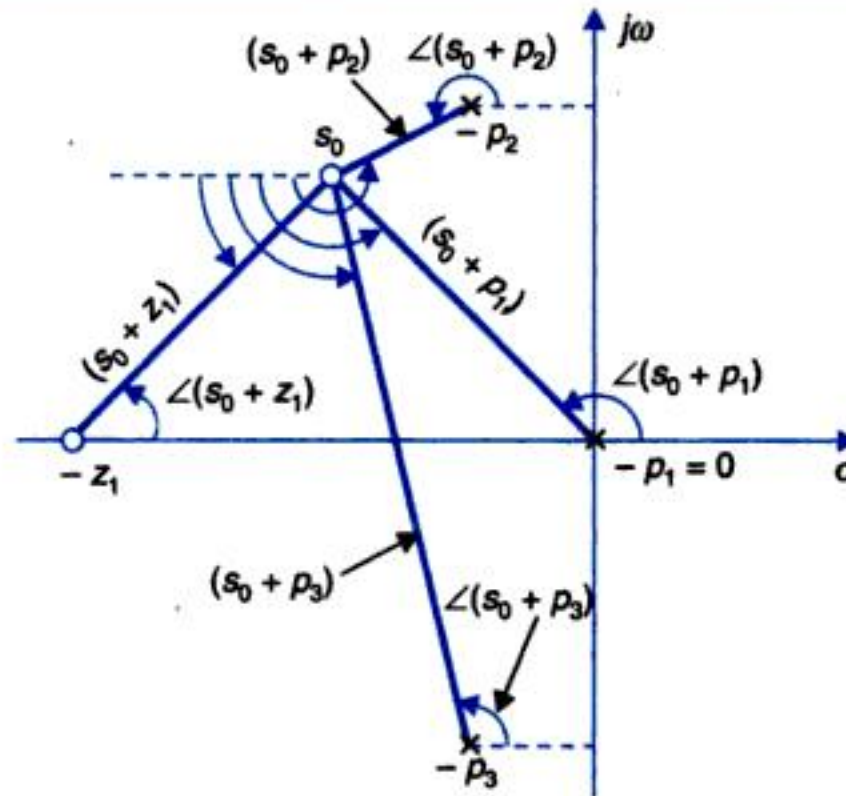


Fig. 7.5. Determining a point on root locus.
x represents a pole; 0 represents a zero.

Further, approximate root locus sketch, as obtained by the rules discussed below, is very useful in visualizing the effects, of variation of system gain K , the effects of shifting pole-zero locations and of bringing in a new set of poles and zeros. Actual root locus plot can then be obtained by MATLAB software; Appendix III.

Construction Rules

Rule 1 : The root locus is symmetrical about the real axis (σ -axis)

We know that the roots of the characteristic equation are either real or complex conjugate or combinations of both. Therefore their locus must be symmetrical about the σ -axis of the s -plane.

Rule 2 : As K increases from zero to infinity, each branch of the root locus originates from an open-loop pole with $K = 0$ and terminates either on an open-loop zero or on infinity with $K = \infty$. The number of branches terminating on infinity equals the number of open-loop poles minus zeros.

The characteristic eqn. (7.14) can be written as

$$\prod_{j=1}^n (s + p_j) + K \prod_{i=1}^m (s + z_i) = 0$$

When $K = 0$, this equation has roots at $-p_j$ ($j = 1, 2, \dots, n$) which are the open-loop poles. The root locus branches therefore start at the open-loop poles.

The same characteristic equation can also be written as

$$\frac{1}{K} \prod_{j=1}^n (s + p_j) + \prod_{i=1}^m (s + z_i) = 0$$

As K tends to infinity, the first term of the characteristic equation vanishes and the roots are located at $-z_i$ ($i = 1, 2, \dots, m$) which are the open-loop zeros of the system. Therefore m branches of the root locus terminate on the open-loop zeros.



You have either reached a page that is unavailable for viewing or reached your viewing limit for this book.



You have either reached a page that is unavailable for viewing or reached your viewing limit for this book.



You have either reached a page that is unavailable for viewing or reached your viewing limit for this book.



You have either reached a page that is unavailable for viewing or reached your viewing limit for this book.

double root at such a point. As the gain K is further increased, the root locus branches break away from the real axis to give a complex conjugate pair of roots. The point which represents a double root is known as *breakaway point* (determination of the breakaway point is discussed in the next rule). The branches which represent complex roots are known as *complex-root branches*.

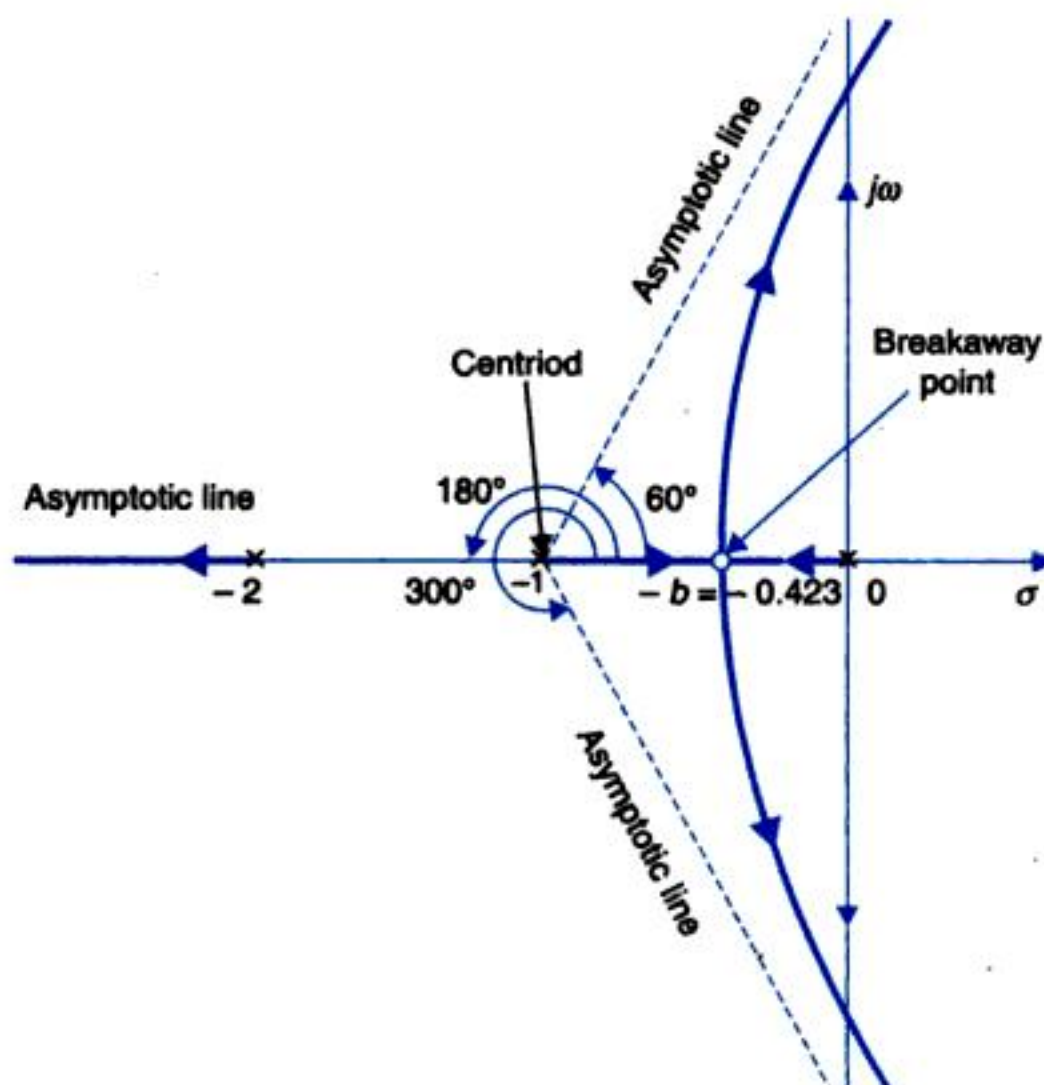


Fig. 7.9. Root locus plot of the equation $1 + K/s(s + 1)(s + 2) = 0$.

In Fig. 7.9, the two real-root branches originating from the open-loop poles $s = 0$ and $s = -1$ approaches each other, breakaway at the point $-b$ and then one branch moves to infinity along 60° asymptote and the other moves to infinity along 300° asymptote. The third branch being a real-root branch coincides with the 180° asymptote.

Rule 6 : The breakaway points (points at which multiple roots of the characteristic equation occur) of the root locus are the solutions of $dK/ds = 0$.

Assume that the characteristic equation $1 + G(s)H(s) = 0$ has a multiple root at $s = -b$ of multiplicity r . The

$$1 + G(s)H(s) = (s + b)^r A_1(s) \quad \dots(7.25)$$

where $A_1(s)$ does not contain the factor $(s + b)$.

Differentiating eqn. (7.25) with respect to s we have

$$\frac{d}{ds} [G(s)H(s)] = (s + b)^{r-1} [rA_1(s) + (s + b)A_1'(s)]$$

where $A_1'(s)$ represents the derivative of $A_1(s)$.



You have either reached a page that is unavailable for viewing or reached your viewing limit for this book.



You have either reached a page that is unavailable for viewing or reached your viewing limit for this book.



You have either reached a page that is unavailable for viewing or reached your viewing limit for this book.

the roots of which are found to be at $s = -2$ and $s = -2 \pm j2.45$.

Therefore, there is one breakaway point on the real axis at $s = -2$ and two complex conjugate breakaway points at $s = -2 \pm j2.45$. The root locus plot is sketched in Fig. 7.12.

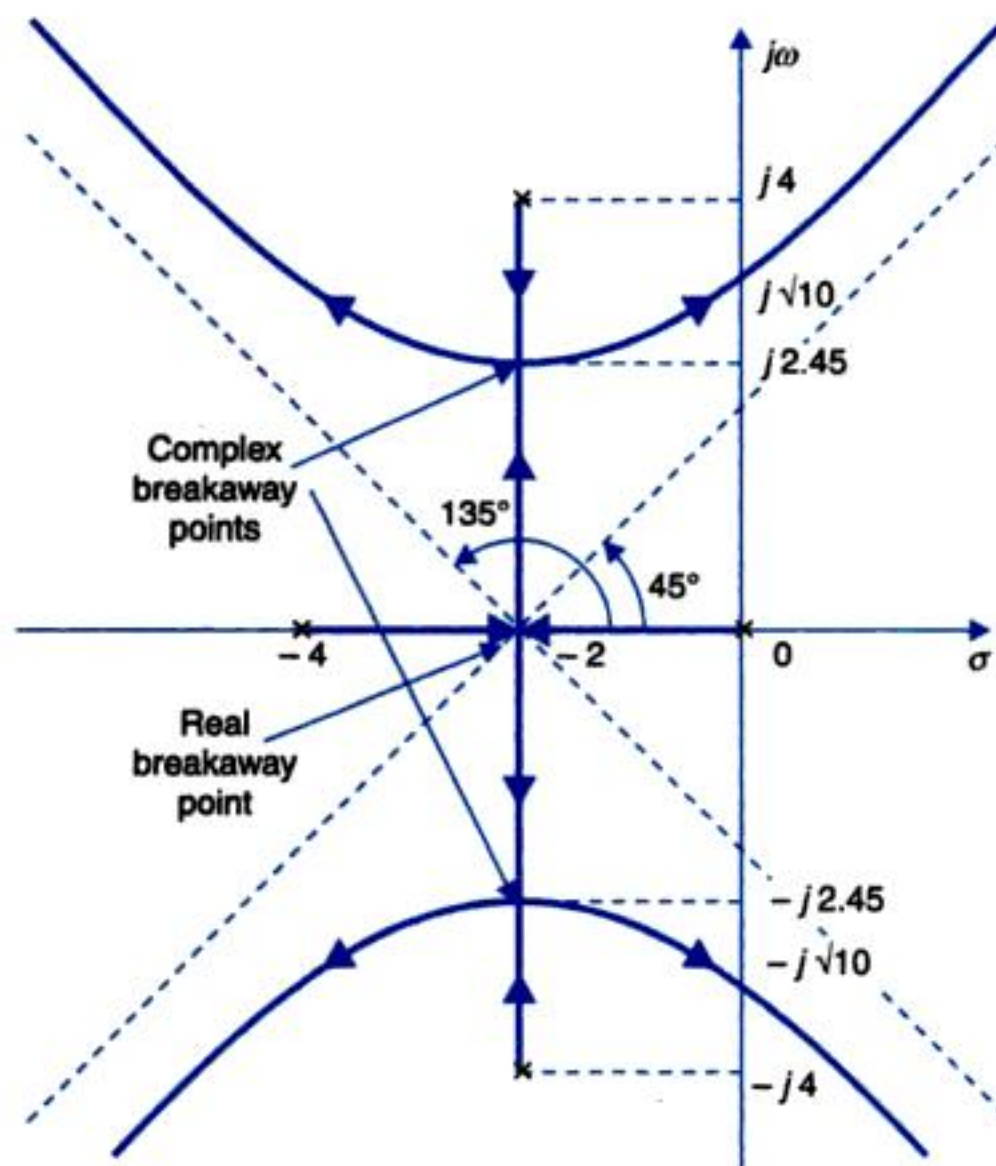


Fig. 7.12. Root locus plot with complex breakaway points.

Breakaway Directions of Root Locus Branches

The root locus branches must approach or leave the breakaway point on the real axis at an angle of $\pm 180^\circ/r$, where r is the number of root locus branches approaching or leaving the point.

The above statement can easily be verified by considering the root locus of Fig. 7.9. It is seen that two root locus branches approach the breakaway point and therefore according to the above statement, the root locus branches must leave the real axis breakaway point at an angle of $\pm 90^\circ$.

Take a point at an angle of 90° to the real axis and very close to the breakaway point. It can be shown by the angle criterion that the point lies on the root locus.

Rule 7 : The angle of departure from an open-loop pole is given by

$$\phi_p = \pm 180^\circ (2q + 1) + \phi ; q = 0, 1, 2, \dots \quad \dots(7.32)$$

where ϕ is the net angle contribution, at this pole, of all other open-loop poles and zeros.

Similarly the angle of arrival at an open-loop zeros is given by

$$\phi_z = \pm 180^\circ (2q + 1) - \phi ; q = 0, 1, 2, \dots$$



You have either reached a page that is unavailable for viewing or reached your viewing limit for this book.



You have either reached a page that is unavailable for viewing or reached your viewing limit for this book.



You have either reached a page that is unavailable for viewing or reached your viewing limit for this book.



You have either reached a page that is unavailable for viewing or reached your viewing limit for this book.



You have either reached a page that is unavailable for viewing or reached your viewing limit for this book.



You have either reached a page that is unavailable for viewing or reached your viewing limit for this book.



You have either reached a page that is unavailable for viewing or reached your viewing limit for this book.

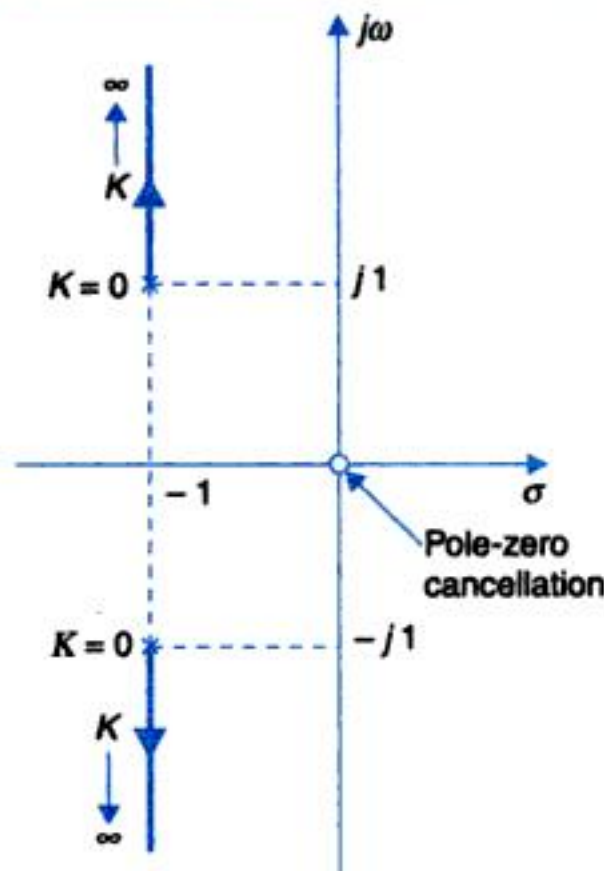


Fig. 7.16. Root locus plot of characteristic equation $(s^2 + 2s + 2 + K) = 0$.

Example 7.7 : An autonomous guided vehicle (AGV) is used to carry payloads to various destinations by an on-board computer. The vehicle having four wheels is powered by two dc servomotors of identical ratings, the two back wheels being free. Each of the motors is independently controlled by a PID scheme.

The basic block diagram of the control scheme is given in Fig. 7.16, wherein the motor is provided with an internal feedback loop.

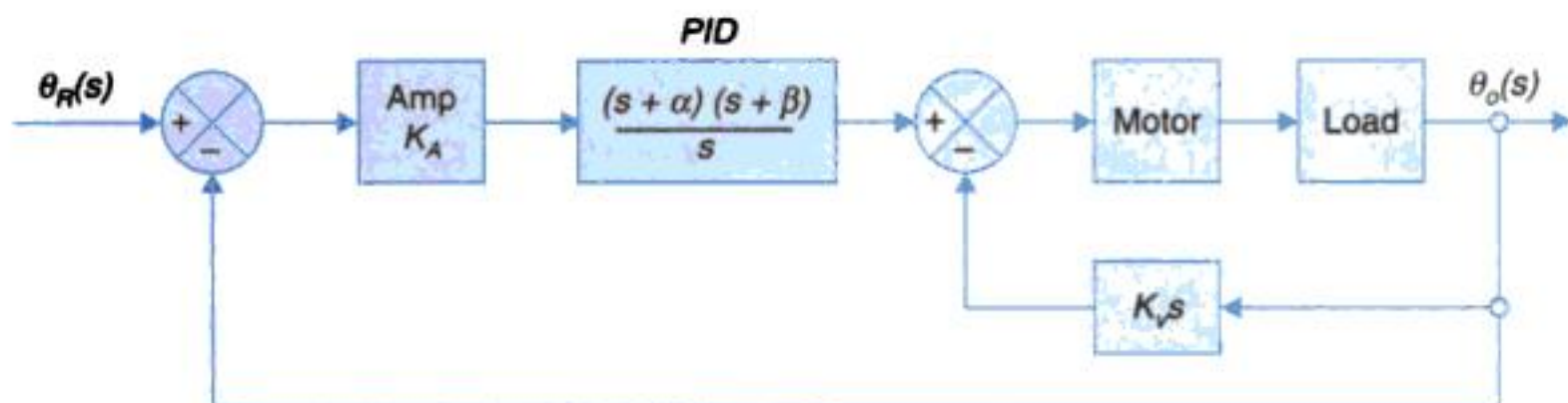


Fig. 7.16

The values of various constants are:

1. PID controller $\alpha = 100, \beta = 275$
2. Motor $K_T = K_b = 0.066 \text{ Nm/A}, R_a = 2.32 \Omega$
 $J_m = 0.0002 \text{ kg m}^2$

Motor inductance and viscous friction can be neglected.

3. Load inertia $J_L = 0.002 \text{ kg m}^2$; directly coupled to motor.
4. Tachometer constant $K_v = 11 \text{ V/rad(s)}$



You have either reached a page that is unavailable for viewing or reached your viewing limit for this book.



You have either reached a page that is unavailable for viewing or reached your viewing limit for this book.



You have either reached a page that is unavailable for viewing or reached your viewing limit for this book.

The above information is confirmed by the root locus plot of Fig. 7.19 obtained by means of MATLAB Control Tool.

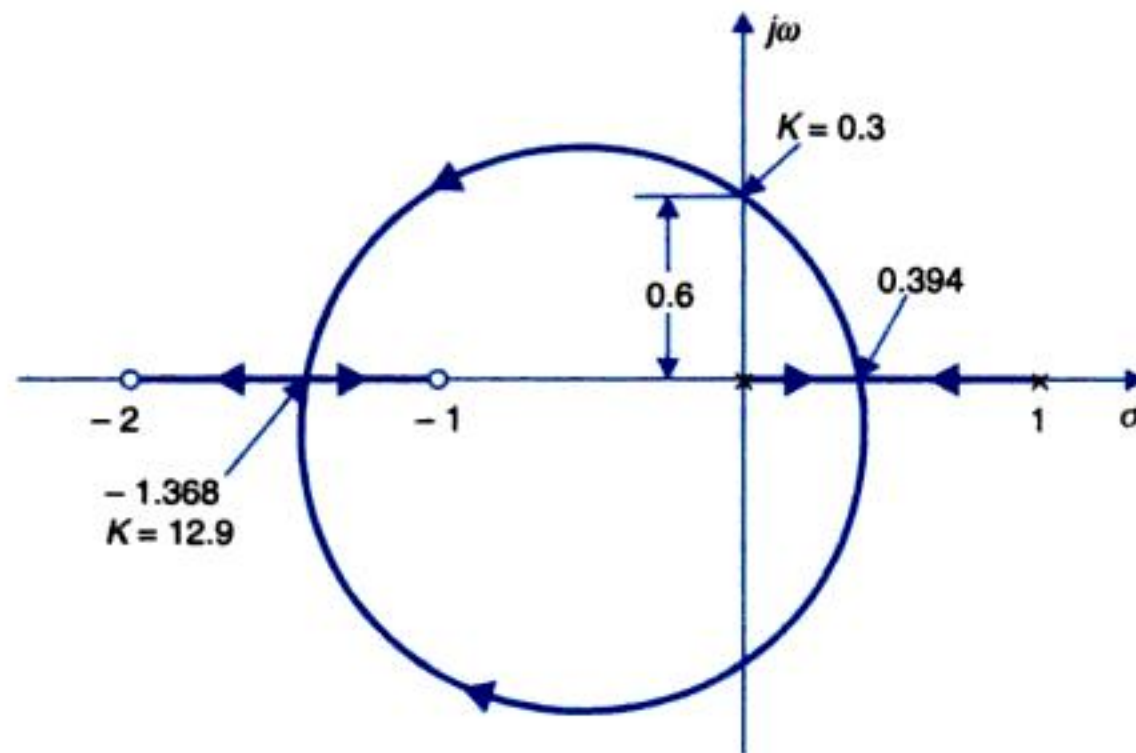


Fig. 7.19

Example 7.9 : A unity feedback control system has an open-loop transfer function of

$$G(s) = \frac{K(s^4/3)}{s^2(s+12)}$$

Plot the root locus. Find the value of K for which all the roots are equal. What is the value of these roots ?

Solution.

Poles : $s = 0, 0, -12$

Zeros : $s = -4/3$

$$-\sigma_A = \frac{-12 + 4/3}{3 - 1} = -16/3$$

$$\phi_A = \frac{\pm 180^\circ(2q + 1)}{3 - 1} = \pm 90^\circ$$

$$K = \frac{s^2 + 24s}{(s + 4/3)} + \frac{s^2(s + 12)}{(s + 4/3)} = 0$$

or $-3s(s + 8)(s + 4/3) + s^2(s + 12) = 0$ or $s(s + 4)^2 = 0$

$$s = 0, s = -4, -4$$

Breakaway point is at $s = -4$

Equal roots (3 nos) are at $s = -4$

$$K(s = -4) = \frac{4 \times 4 \times 8}{(4 - 4/3)} = \frac{128 \times 3}{8} = 48$$



You have either reached a page that is unavailable for viewing or reached your viewing limit for this book.



You have either reached a page that is unavailable for viewing or reached your viewing limit for this book.



You have either reached a page that is unavailable for viewing or reached your viewing limit for this book.

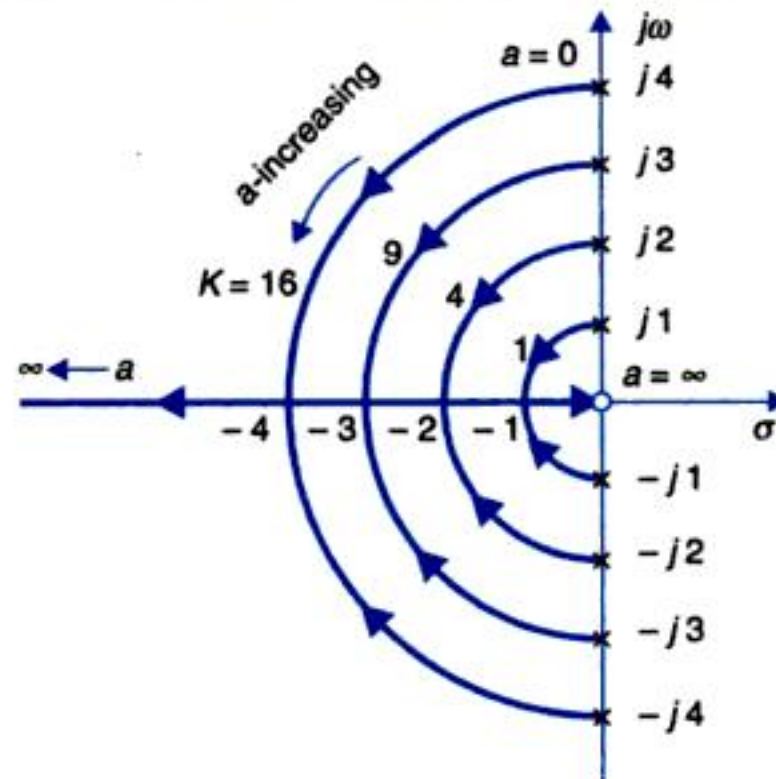


Fig. 7.23. Root contours of the system shown in Fig. 7.1.

Example 7.11 : Consider the feedback control system with an open-loop transfer function

$$G(s)H(s) = \frac{K}{s(s+1)(s+\alpha)}$$

in which the open-loop gain and the pole $s = -\alpha$ are both regarded as variable.

The characteristic equation of the system is

$$1 + \frac{K}{s(s+1)(s+\alpha)} = 0 \quad \text{or} \quad s^2(s+1) + \alpha(s+1)s + K = 0 \quad \dots(7.38)$$

It can be manipulated into the form below where α appears as a root locus parameter

$$1 + \frac{\alpha s(s+1)}{s^2(s+1) + K} = 0 \quad \dots(7.39)$$

Though eqn. (7.39) is in the form that root locus with respect to the parameter α can be drawn, however, we cannot proceed with it without determining its open-loop poles from the reduced characteristic equation

$$s^2(s+1) + K = 0$$

where K is a variable. The reduced characteristic equation can be obtained from the complete characteristic eqn. (7.38) by putting $\alpha = 0$. The reduced characteristic equation can be rewritten as

$$1 + \frac{K}{s^2(s+1)} = 0 \quad \dots(7.40)$$

The root locus of the reduced characteristic equation with K as a variable parameter is plotted in Fig. 7.24(a). The three roots of eqn. (7.40) for a particular value of K contribute the open-loop poles of eqn. (7.39).

The root contours for various values of K with varying α are drawn in Fig. 7.24(b). The value of α at which the root contours will cross the $j\omega$ -axis into the left half s -plane and the system will become stable is obtained by application of the Routh criterion to the characteristic equation (7.38) as given below:



You have either reached a page that is unavailable for viewing or reached your viewing limit for this book.



You have either reached a page that is unavailable for viewing or reached your viewing limit for this book.



You have either reached a page that is unavailable for viewing or reached your viewing limit for this book.

This method is applied here to analyze the system of Fig. 7.26. This system shows an arrangement of controlling the thickness of a steel plate produced by a rolling mill. A voltage signal corresponding to the desired thickness is the reference input to the system. A thickness gauge provides a feedback voltage signal proportional to the actual thickness of the plate. The error voltage actuates the motor which positions the rolls.

The open-loop transfer function of the system is given by

$$G(s)H(s) = \frac{K_1}{s(\tau_m s + 1)} \quad \dots(7.46)$$

where for the sake of simplicity, we assume a single dominant time constant in the loop, probably that of the motor.

In the transfer function given by eqn. (7.46), we have ignored the fact that a finite time must elapse before a change in thickness of steel plates between rolls reaches the point of measurement at the gauge.

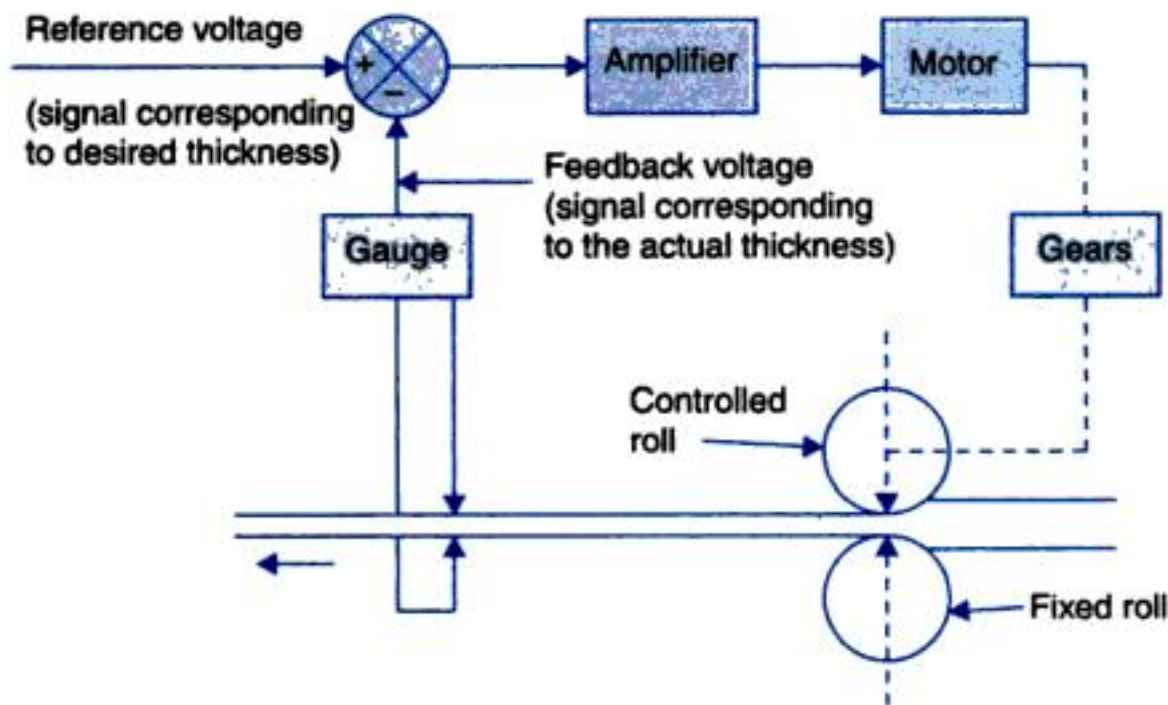


Fig. 7.26. A feedback system with transportation lag.

If this delay in transportation of signal is assumed to be T sec, then the open-loop transfer function of the system becomes.

$$G(s)H(s) = K_1 e^{-sT} / [s(\tau_m s + 1)]$$

The above equation may be rearranged in the following form

$$G(s)H(s) = K e^{-sT} / [s(s + \alpha)] \quad \dots(7.47)$$

Assuming the transportation lag to be small, we use the approximating $e^{-sT} = (1 - sT)$. Equation (7.47) can now be rearrange in the form

$$G(s)H(s) = \frac{-K(s - 1/T)}{s(s + \alpha)}$$

The characteristic equation becomes

$$1 - K(s - 1/T) / [s(s + \alpha)] = 1 - P(s) = 0 \quad \dots(7.48)$$



You have either reached a page that is unavailable for viewing or reached your viewing limit for this book.



You have either reached a page that is unavailable for viewing or reached your viewing limit for this book.



You have either reached a page that is unavailable for viewing or reached your viewing limit for this book.

The characteristic eqn. (7.54) can be written as

$$q(s) = A(s) + K B(s) = K_1 \prod_{k=1}^n (s + r_k) = 0 \quad \dots(7.55)$$

where $-r_k$ ($k = 1, 2, \dots, n$) are the roots of the characteristic equation. In eqn. (7.55) K_1 is given by

$$\begin{aligned} K_1 &= 1 \text{ if } n > m \\ &= 1 + K \text{ if } n = m \end{aligned}$$

Taking logarithm of each side eqn. (7.55), we get

$$\ln q(s) = \ln K_1 + \sum_{k=1}^n \ln (s + r_k) \quad \dots(7.56)$$

Differentiating eqn. (7.55) and (7.56) with respect to the parameter K , we have

$$\frac{\partial q(s) / \partial K}{q(s)} = \frac{B(s)}{q(s)} = K_1^{-1} \frac{\partial K_1}{\partial K} - \sum_{k=1}^n \frac{\partial(-r_k) / \partial K}{(s + r_k)} \quad \dots(7.57)$$

Each side of eqn. (7.57) must have the same residue at any pole. Taking the residue of both the sides at the pole $s = -r_k$, we have

$$\frac{\partial(-r_k)}{\partial K} = - (s + r_k) \frac{B(s)}{q(s)} \Big|_{s=-r_k} = - \frac{B(-r_k)}{q'(-r_k)} \quad \dots(7.58)$$

where

$$q'(-r_k) = \frac{dq(s)}{ds} \Big|_{s=-r_k}$$

In taking the residue above it has been assumed that the root $-r_k$ is a nonrepeated root of the characteristic equation.

It follows from eqn. (7.54) that

$$B(-r_k) = - \frac{A(-r_k)}{K}$$

Therefore we can write eqn. (7.58) as

$$S_K^{-r_k} = \frac{\partial(-r_k)}{\partial K / K} = \frac{A(-r_k)}{q'(-r_k)} \quad \dots(7.59)$$

The sensitivity of the roots $s = -r_k$ can thus be computed from the expression* given in eqn. (7.59).

The transfer function sensitivity and sensitivities of the roots of the characteristic equation can be correlated as follows.

The transfer function can be expressed as

$$T(s) = \frac{K_2 \prod_{i=1}^{m'} (s + z_i)}{\prod_{k=1}^n (s + r_k)} \quad \dots(7.60)$$

*The derivation of this expression is from Horowitz. Reproduced with permission.



You have either reached a page that is unavailable for viewing or reached your viewing limit for this book.



You have either reached a page that is unavailable for viewing or reached your viewing limit for this book.



You have either reached a page that is unavailable for viewing or reached your viewing limit for this book.

With the switch S closed, draw the root locus plot of the system with α as a varying parameter. Show that the complex-root branches are part of a circle. From the root locus plot, determine the value of α such that the resulting system has a damping ratio of 0.5. For this value of α , find the overall transfer function in factored form.

7.5. The block diagram of a control system is shown in Fig. P-7.5. Draw the root locus plot of the system with α as varying parameter.

(a) Determine the steady-state error to the unit-ramp input, damping ratio and settling time for the system without derivative feedback, i.e.,

$$\alpha = 0$$

(b) Discuss the effect of derivative feedback on transient as well as steady-state behaviour of the system assuming $\alpha = 0.2$.

(c) Determine the value of α for the system to be critically damped.

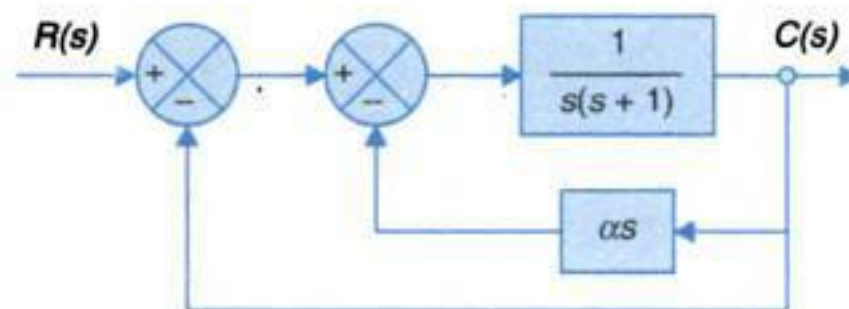


Fig. P-7.5

7.6. A unity feedback system has an open-loop transfer function

$$G(s) = K/s^2(s + 2)$$

(a) By sketching a root locus plot, show that the system is unstable for all values of K .

(b) Add a zero at $s = -a$ ($0 \leq a < 2$) and show that the addition of zero stabilizes the system.

(c) If $a = 1$, sketch the root locus plot and determine approximately the value of K which gives the greatest damping ratio for the oscillatory mode. Find also the value of this damping ratio and the corresponding undamped natural frequency.

7.7. Open-loop transfer function of a unity feedback system is

$$G(s) = K/(s + 2)^3$$

Sketch the root locus plot and determine the following:

(a) Static loop sensitivity for which the root locus crosses the $j\omega$ -axis and the corresponding frequency of sustained oscillations.

(b) The position error constant corresponding to a damping ratio of 0.5. Also determine the peak overshoot, time to peak overshoot and settling time considering the effect of dominant poles only.

(Note : The static loop sensitivity is defined to be the gain in pole-zero form.)

7.8. The characteristic equation of a feedback control system is

$$s^4 + 3s^3 + 12s^2 + (K - 16)s + K = 0$$

Sketch the root locus plot for $0 \leq K < \infty$ and show that the system is conditionally stable (stable for only a range of gain K). Determine the range of gain for which the system is stable.

7.9. Find the roots of the following polynomial by use of the root locus method.

$$3s^4 + 10s^3 + 21s^2 + 24s + 30 = 0$$

7.10. Figure P-7.10. shows an arrangement of controlling the thickness of steel plates. A signal proportional to the desired steel thickness is the reference input and a signal proportional to the



You have either reached a page that is unavailable for viewing or reached your viewing limit for this book.



You have either reached a page that is unavailable for viewing or reached your viewing limit for this book.



You have either reached a page that is unavailable for viewing or reached your viewing limit for this book.

8

FREQUENCY RESPONSE ANALYSIS

8.1 INTRODUCTION

Various standard test signals used to study the performance of control systems were discussed in Chapter 5. While the sinusoidal test signal was introduced there, the discussion on the same was postponed till this chapter which is fully devoted to it on account of its importance in control engineering. Consider a linear system with a sinusoidal input

$$r(t) = A \sin \omega t$$

Under steady-state, the system output as well as the signals at all other points in the system are sinusoidal. The steady-state output may be written as

$$c(t) = B \sin (\omega t + \phi)$$

The magnitude and phase relationship between the sinusoidal input and the steady-state output of a system is termed the *frequency response*. In linear time-invariant systems, the frequency response is independent of the amplitude and phase of the input signal.

The frequency response test on a system or a component is normally performed by keeping the amplitude A fixed and determining B and ϕ for a suitable range of frequencies. Signal generators and precise measuring instruments are readily available for various ranges of frequencies and amplitudes. The ease and accuracy of measurements are some of the advantages of the frequency response method. Wherever it is not possible to obtain the form of the transfer function of a system through analytical techniques, the necessary information to compute its transfer function can be extracted by performing the frequency response test on the system. The step response test can also be performed easily but the extraction of transfer function from the step response data is quite a laborious procedure. For systems with very large time constants, the frequency response test is cumbersome to perform as the time required for the output to reach steady-state for each frequency of the test signal is excessively long. Therefore, the frequency response test is not recommended for systems with very large time constants.



You have either reached a page that is unavailable for viewing or reached your viewing limit for this book.



You have either reached a page that is unavailable for viewing or reached your viewing limit for this book.



You have either reached a page that is unavailable for viewing or reached your viewing limit for this book.

$0 < \zeta \leq 1/\sqrt{2}$, and the resonant frequency ω_r of the frequency response is indicative of its natural frequency for a given ζ and hence indicative of its speed of response (as $t_s = 4/\zeta\omega_n$). M_r and ω_r of the frequency response could thus be used as performance indices for a second-order system.

Re-examining Fig. 8.2, we notice that for $\omega > \omega_r$, M decreases monotonically. The frequency at which M has a value* of $1/\sqrt{2}$ is of special significance and is called the *cut-off frequency* ω_c . The signal frequencies above cut-off are greatly attenuated in passing through a system.

For feedback control systems, the range of frequencies over which M is equal to or greater than $1/\sqrt{2}$ is defined as *bandwidth* ω_b . Control systems being lowpass filters (at zero frequency, $M = 1$), the bandwidth ω_b is equal to cut-off frequency ω_c . The definition of the bandwidth is depicted on typical frequency response of a feedback control system in Fig. 8.3a.

In general, the bandwidth of a control system indicates the noise-filtering characteristic of the system. Also, bandwidth gives a measure of the transient response properties as observed below.

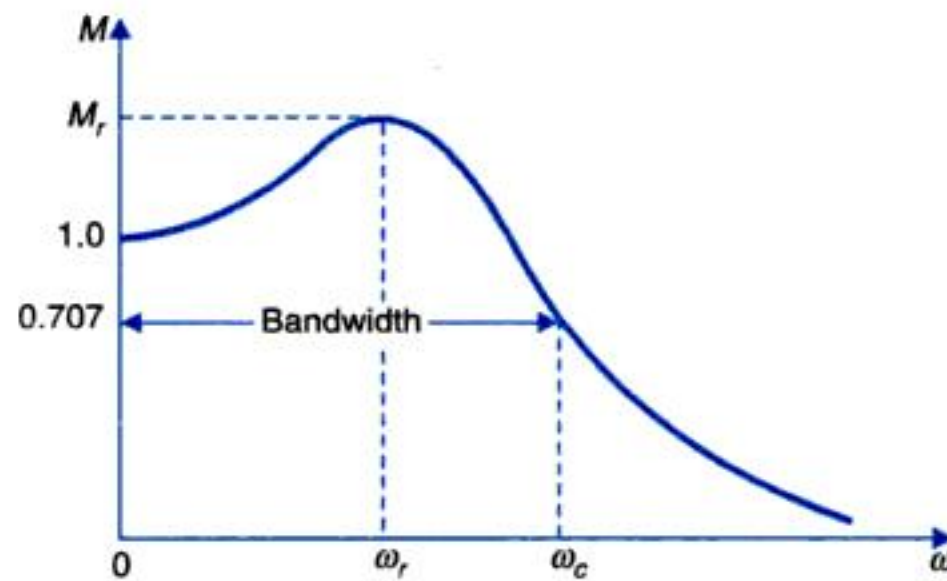


Fig. 8.3. (a) Typical magnification curve of a feedback control system.

The normalized bandwidth $u_b = \omega_b/\omega_n$ of the second-order system under consideration can be readily determined as follows:

$$M = \frac{1}{\sqrt{[(1 - u_b^2)^2 + (2\zeta u_b)^2]}} = \frac{1}{\sqrt{2}}$$

$$u_b^4 - 2(1 - 2\zeta^2)u_b^2 - 1 = 0$$

or

Solving for u_b we get

$$u_b = [1 - 2\zeta^2 + \sqrt{(2 - 4\zeta^2 + 4\zeta^4)}]^{1/2} \quad \dots(8.6)$$

As the bandwidth must be a positive real quantity, the negative sign in quadratic solution and the negative sign in taking the square-root have been discarded.

We observe from eqn. (8.6) that the normalized bandwidth is a function of damping only; u_b versus ζ is plotted in Fig. 8.3(b).

* This value corresponds to -3db point on the Bode plot of $T(j\omega)$ of the second-order system under consideration. Bode plots are dealt with in later part of this chapter.



You have either reached a page that is unavailable for viewing or reached your viewing limit for this book.



You have either reached a page that is unavailable for viewing or reached your viewing limit for this book.



You have either reached a page that is unavailable for viewing or reached your viewing limit for this book.

This transfer function may be rearranged as

$$G(j\omega) = \frac{-T}{1 + \omega^2 T^2} - j \frac{1}{\omega(1 + \omega^2 T^2)} \quad \dots(8.14)$$

From eqn. (8.14) we get

$$\lim_{\omega \rightarrow 0} G(j\omega) = -T - j\infty = \infty \angle -90^\circ$$

$$\lim_{\omega \rightarrow \infty} G(j\omega) = -0 - j0 = 0 \angle -180^\circ$$

The general shape of the polar plot of this transfer function is shown in Fig. 8.8. The plot is asymptotic to the vertical line passing through the point $(-T, 0)$.

The major advantage of the polar plot lies in stability study of systems. N. Nyquist (in 1932) related the stability of a system to the form of these plots. Because of his work, the polar plots are commonly referred to as *Nyquist plots*.

The general shapes of the polar plots of some important transfer functions are given in Table 8.1.

From the polar plots of Table 8.1, following observations are made:

(i) Addition of a nonzero pole to a transfer function results in further rotation of the polar plot through an angle of -90° as $\omega \rightarrow \infty$.

(ii) Addition of a pole at the origin to a transfer function rotates the polar plot at zero and infinite frequencies by a further angle of -90° .

The effect of addition of a zero to a transfer function is to rotate the high frequency portion of the polar plot by 90° in counter-clockwise direction.

Inverse Polar Plots

The inverse polar plot of $G(j\omega)$ is a graph of $1/G(j\omega)$ as function of ω . For example, for the RC filter shown in Fig. 8.6.

$$\begin{aligned} \frac{1}{G(j\omega)} &= G^{-1}(j\omega) \\ &= 1 + j\omega T = \sqrt{(1 + \omega^2 T^2)} \angle \tan^{-1} \omega T \end{aligned}$$

The corresponding inverse polar plot is shown in Fig. 8.9.

It will be seen later in Chapter 9 that the inverse polar plots are useful in applying M -criterion and are also valuable in stability study of nonunity feedback systems.

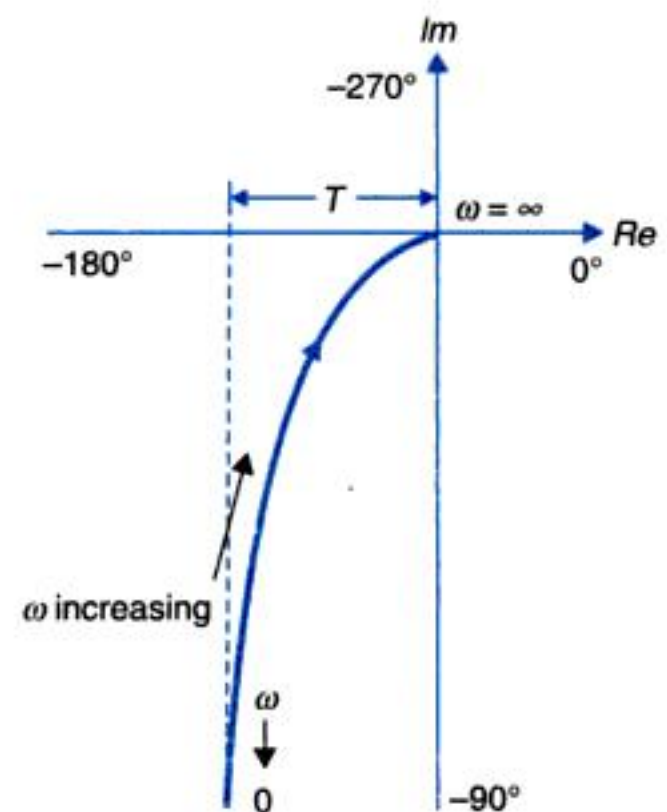


Fig. 8.8. Polar plot of $1/j\omega(1 + j\omega T)$

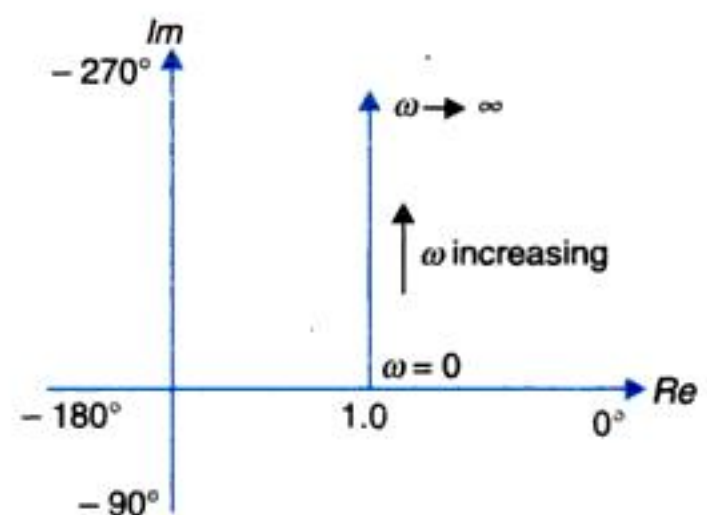


Fig. 8.9. Inverse polar plot of $1/(1 + j\omega T)$.



You have either reached a page that is unavailable for viewing or reached your viewing limit for this book.



You have either reached a page that is unavailable for viewing or reached your viewing limit for this book.



You have either reached a page that is unavailable for viewing or reached your viewing limit for this book.



You have either reached a page that is unavailable for viewing or reached your viewing limit for this book.



You have either reached a page that is unavailable for viewing or reached your viewing limit for this book.



You have either reached a page that is unavailable for viewing or reached your viewing limit for this book.



You have either reached a page that is unavailable for viewing or reached your viewing limit for this book.



You have either reached a page that is unavailable for viewing or reached your viewing limit for this book.



You have either reached a page that is unavailable for viewing or reached your viewing limit for this book.



You have either reached a page that is unavailable for viewing or reached your viewing limit for this book.



You have either reached a page that is unavailable for viewing or reached your viewing limit for this book.



You have either reached a page that is unavailable for viewing or reached your viewing limit for this book.



You have either reached a page that is unavailable for viewing or reached your viewing limit for this book.



You have either reached a page that is unavailable for viewing or reached your viewing limit for this book.



You have either reached a page that is unavailable for viewing or reached your viewing limit for this book.

As an illustration, let us derive the transfer function of the system whose experimental log-magnitude and phase-angle curves are shown in Fig. 8.21. First of all, the asymptotes are drawn on the experimentally determined curve as shown.

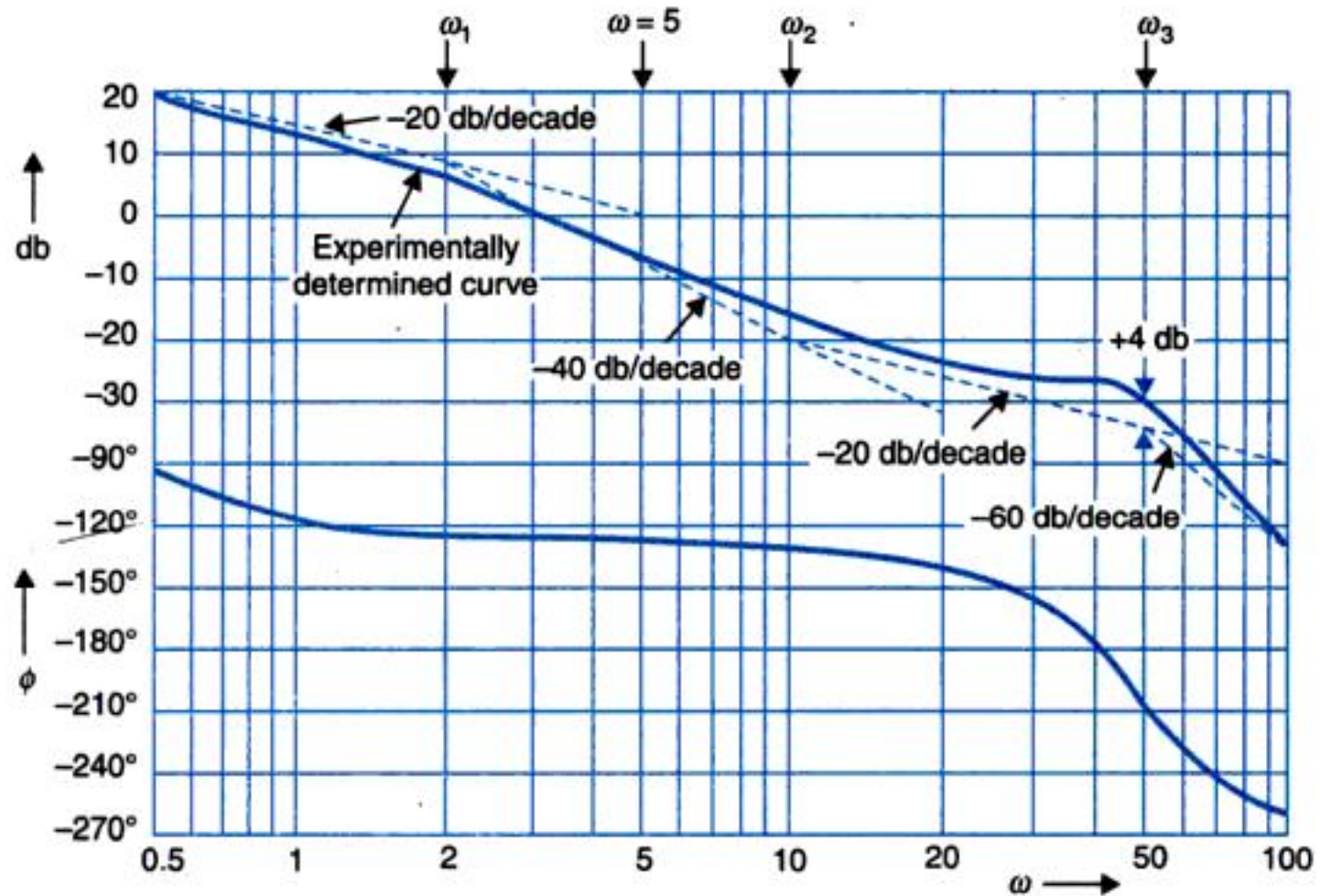


Fig. 8.21. Experimentally obtained log-magnitude and phase characteristics.

The low frequency asymptote has a slope of -20 dB/decade and when extended, intersects the 0 dB axis at $\omega = 5$. Therefore the asymptote is a plot of the factor $5/(j\omega)$. The corner frequencies are found to be located at $\omega_1 = 2$, $\omega_2 = 10$ and $\omega_3 = 50$. At the first corner frequency, the slope of the curve changes by -20 dB/decade and at the second corner frequency, it changes by $+20$ dB/decade. Therefore the transfer function has the factors $1/(1 + j\omega/2)$ and $(1 + j\omega/10)$ corresponding to these corner frequencies. At $\omega = \omega_3$, the curve changes by a slope of -40 dB/decade. At this frequency the error between actual and approximate plots is $+4$ dB. Therefore, the transfer function has a quadratic factor

$$\frac{1}{1 + j2\zeta(\omega/50) + (j\omega/50)^2}$$

where $\zeta = 0.3$, as obtained from the error graph of Fig. 8.15, corresponding to the error $+4$ dB.

Thus the transfer function of the system becomes

$$G(j\omega) = \frac{5(1 + j\omega/10)}{j\omega(1 + j\omega/2)[1 + j0.6(\omega/50) + (j\omega/50)^2]}$$

From the experimental phase angle curve shown in Fig. 8.21, it is seen that the phase angle at very high frequencies is -270° which is equal to $-90^\circ (q - p) = -90^\circ (4 - 1)$. Therefore the Bode plot represents a minimum-phase transfer function.

8.7 LOG-MAGNITUDE VERSUS PHASE PLOTS

In the previous sections, we considered polar plots and Bode plots as the graphical representations of the frequency response. An alternative approach to the frequency response



You have either reached a page that is unavailable for viewing or reached your viewing limit for this book.



You have either reached a page that is unavailable for viewing or reached your viewing limit for this book.



You have either reached a page that is unavailable for viewing or reached your viewing limit for this book.



You have either reached a page that is unavailable for viewing or reached your viewing limit for this book.



You have either reached a page that is unavailable for viewing or reached your viewing limit for this book.



You have either reached a page that is unavailable for viewing or reached your viewing limit for this book.



You have either reached a page that is unavailable for viewing or reached your viewing limit for this book.



You have either reached a page that is unavailable for viewing or reached your viewing limit for this book.



You have either reached a page that is unavailable for viewing or reached your viewing limit for this book.



You have either reached a page that is unavailable for viewing or reached your viewing limit for this book.



You have either reached a page that is unavailable for viewing or reached your viewing limit for this book.



You have either reached a page that is unavailable for viewing or reached your viewing limit for this book.



You have either reached a page that is unavailable for viewing or reached your viewing limit for this book.



You have either reached a page that is unavailable for viewing or reached your viewing limit for this book.



You have either reached a page that is unavailable for viewing or reached your viewing limit for this book.



You have either reached a page that is unavailable for viewing or reached your viewing limit for this book.



You have either reached a page that is unavailable for viewing or reached your viewing limit for this book.



You have either reached a page that is unavailable for viewing or reached your viewing limit for this book.



You have either reached a page that is unavailable for viewing or reached your viewing limit for this book.



You have either reached a page that is unavailable for viewing or reached your viewing limit for this book.

$$N = P - Z$$

$$-1 = 0 - Z \quad \text{or} \quad Z = 1$$

The system is therefore unstable for $K > \frac{1}{2}$. It would be stable for $K < \frac{1}{2}$, when

$$N = 0, P = 0 \Rightarrow Z = 0.$$

Example 9.7 : Sketch the Nyquist plot and determine there from the stability of the following open-loop transfer function of unity feedback control systems.

$$(i) GH(s) = \frac{K(s+2)}{s^2(s+1)} \quad (ii) GH(s) = \frac{K}{s(s^2 + s + 4)}$$

If the system is conditionally stable, find the range of K for which the system is stable.

Solution.

$$(i) \quad GH(j\omega) = \frac{(K/2)(1 + j\omega/2)}{(j\omega)^2(1 + j\omega/4)}$$

The Nyquist contour is the same as in Fig. 9.13(a). Following standard steps the Nyquist plot is sketched in Fig. 9.15.

It easily concluded from the Nyquist plot that the system is absolutely stable.

$$(ii) \quad GH(j\omega) = \frac{K}{j\omega(4 - \omega^2 + j\omega)}$$

Real axis crossing of Nyquist plot at

$$GH(j\omega) = \frac{-K[\omega + j(4 - \omega^2)]}{\omega[\omega^2 + (4 - \omega^2)^2]}$$

Equating imaginary part to zero

$$4 - \omega^2 = 0 \quad \text{or} \quad \omega^2 = 4 \quad \text{or} \quad \omega = \pm 2$$

$$|GH(j\omega)|_{\omega^2=4} = -K/4$$

So the Nyquist plot crosses the axis of reals at $\omega = \pm 2$ with an intercept of $-K/4$. The plot is sketched in Fig. 9.16.

From the Nyquist plot

$$K/4 > 1 \quad \text{or} \quad K > 4$$

For this value of K

$$N = P - Z$$

$$-2 = 0 - Z \quad \text{or} \quad Z = 2$$

So the system is unstable. It can be shown to be stable for

$$K < 4$$

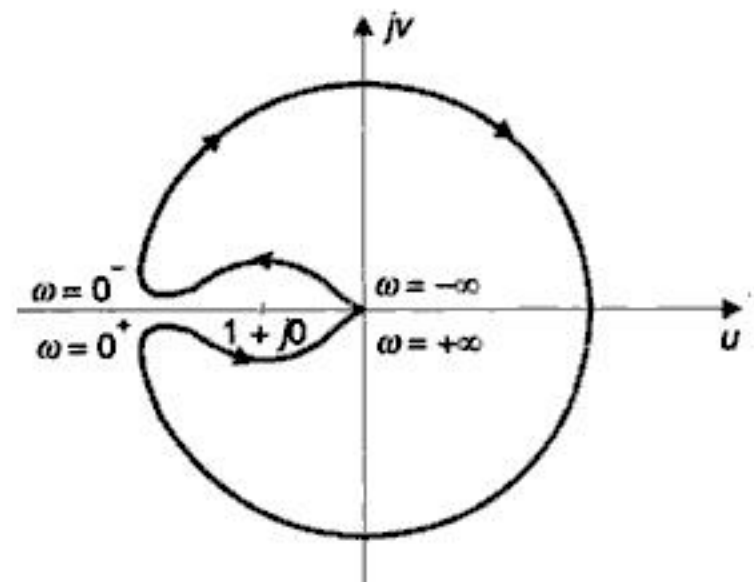


Fig. 9.15

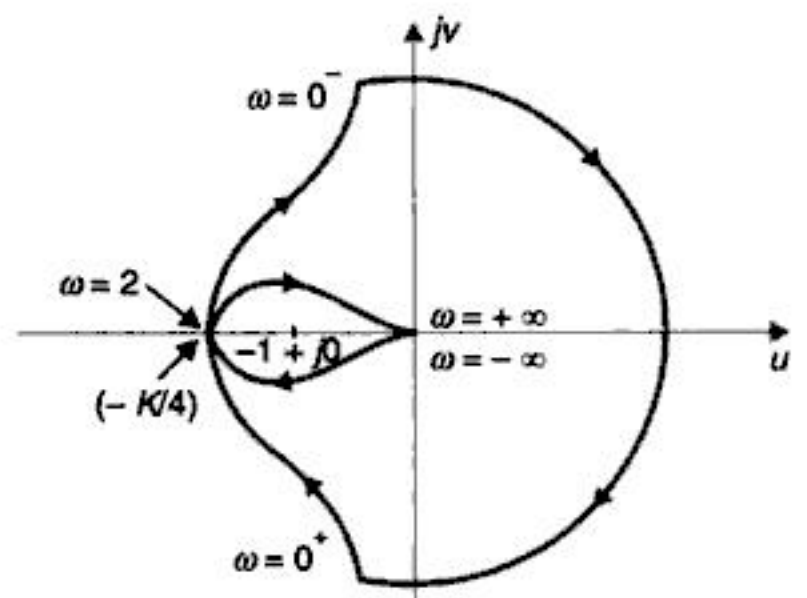


Fig. 9.16



You have either reached a page that is unavailable for viewing or reached your viewing limit for this book.



You have either reached a page that is unavailable for viewing or reached your viewing limit for this book.



You have either reached a page that is unavailable for viewing or reached your viewing limit for this book.



You have either reached a page that is unavailable for viewing or reached your viewing limit for this book.



You have either reached a page that is unavailable for viewing or reached your viewing limit for this book.

In decibels the increase in gain for $G(j\omega)H(j\omega)$ -plot to pass through $(-1 + j0)$ is given by

$$GM = -20 \log a \text{ db}$$

Since a is less than 1 for stable systems, $\log a$ is negative and hence GM is positive.

In the example considered earlier in this section if $T_1 = 1$, $T_2 = 0.5$, then for $K = 0.75$, the gain margin is given by

$$GM = \left[\frac{KT_1T_2}{T_1 + T_2} \right]^{-1} = 4$$

In decibels, the gain margin is given by

$$GM = 20 \log 4 = 12 \text{ db}$$

This value of gain margin indicates that the system gain may be increased by a factor of 4 before the stability limit is reached.

Phase margin. The frequency at which $|G(j\omega)H(j\omega)| = 1$ is called the *gain cross-over frequency*. It is given by the intersection of the $G(j\omega)H(j\omega)$ -plot and a unit circle centred at the origin as shown in Fig. 9.20. At this frequency, the phase angle $\angle G(j\omega_1)H(j\omega_1)$ is equal to $(-180^\circ + \phi)$. If an additional phase-lag equal to ϕ is introduced at the gain cross-over frequency, the phase angle $\angle G(j\omega_1)H(j\omega_1)$ will become -180° , while the magnitude remains unity. The $G(j\omega)H(j\omega)$ -plot will then pass through $(-1 + j0)$ point, driving the system to the verge of instability. This additional phase-lag ϕ is known as the *phase margin (PM)*.

The phase margin is thus defined as the amount of additional phase-lag at the gain cross-over frequency required to bring the system to the verge of instability. From Fig. 9.20 it is seen that the phase margin is measured positively in counter-clockwise direction from the negative real axis. The *phase margin is always positive for stable feedback systems*.

The value of phase margin for any system can be computed from

$$\text{Phase margin } \phi = \angle G(j\omega)H(j\omega)|_{\omega=\omega_1} + 180^\circ \quad \dots(9.17)$$

where the angle at ω_1 , the gain cross-over frequency, is measured negatively.

Gain margin (GM) and phase margin (PM) are frequently used for frequency response specifications by designers. It is important to note once again that these measures of stability are valid for open-loop stable systems only. A large gain margin or a large phase margin indicates a very stable feedback system but usually a very sluggish one. A GM close to unity or a PM close to zero corresponds to a highly oscillatory system. Usually a GM of about 6 db or a PM of $30\text{--}35^\circ$ results in a reasonably good degree of relative stability. In most practical systems a good gain margin automatically guarantees a good phase margin and vice versa. However, the cases where the specification on one does not necessarily satisfy the other, also exist as shown in Figs. 9.22 and 9.23.

In a second-order system with $G(j\omega)H(j\omega) = K/j\omega(j\omega T + 1)$ whose polar plot is shown in Fig. 9.24. GM always remains fixed at infinite value as the plot always reaches the real axis at the origin, while the PM reduces continuously with increasing system gain. In this case, as shall be seen below, PM is the correct measure of relative stability.

Usually it is the phase margin which is specified as a measure of system performance in design.



You have either reached a page that is unavailable for viewing or reached your viewing limit for this book.



You have either reached a page that is unavailable for viewing or reached your viewing limit for this book.



You have either reached a page that is unavailable for viewing or reached your viewing limit for this book.



You have either reached a page that is unavailable for viewing or reached your viewing limit for this book.



You have either reached a page that is unavailable for viewing or reached your viewing limit for this book.



You have either reached a page that is unavailable for viewing or reached your viewing limit for this book.



You have either reached a page that is unavailable for viewing or reached your viewing limit for this book.



You have either reached a page that is unavailable for viewing or reached your viewing limit for this book.



You have either reached a page that is unavailable for viewing or reached your viewing limit for this book.



You have either reached a page that is unavailable for viewing or reached your viewing limit for this book.



You have either reached a page that is unavailable for viewing or reached your viewing limit for this book.



You have either reached a page that is unavailable for viewing or reached your viewing limit for this book.



You have either reached a page that is unavailable for viewing or reached your viewing limit for this book.



You have either reached a page that is unavailable for viewing or reached your viewing limit for this book.



You have either reached a page that is unavailable for viewing or reached your viewing limit for this book.



You have either reached a page that is unavailable for viewing or reached your viewing limit for this book.



You have either reached a page that is unavailable for viewing or reached your viewing limit for this book.

The Nichols chart is very useful for determining the closed-loop frequency response from that of the open-loop. This is accomplished by superimposing the log-magnitude versus phase angle plot of $G(j\omega)$ on Nichols chart. The intersections of the log-magnitude versus phase angle plot and constant- M and $-\alpha$ contours give the magnitude M and phase angle α of the closed-loop frequency response at different frequency points.

Gain adjustments

When a control system is found to be unstable or has poor transient response, the first step is to check if its performance can be modified by adjustment of gain. This adjustment is usually based on a desirable value of M_r . While this adjustment can also be carried out by means of constant- M circles, we shall present here how this is done by means of the Nichols chart which is more convenient and is commonly used.

Gain adjustment by the Nichols chart. The determination of K for specified resonant peak or specified gain and phase margins carried out very conveniently on Nichols chart. For this purpose the log-magnitude versus phase angle [db vs $\angle G(j\omega)$] plot is superimposed on the Nichols chart. Since the gain adjustment has no effect on the phase angle, the db vs $\angle G(j\omega)$ plot merely moves vertically up for increase in gain and down for decrease in gain. The vertical location of the plot is adjusted till it is tangent to the desired M -curve. The db-shift determines the adjustment in gain required to meet the specified M_r . Phase margin or gain margin adjustments are similarly carried out on the Nichols chart. The following example illustrates the procedure for gain adjustment.

Example 9.15 : Let us reconsider the system discussed in Example 9.7. The system has an open-loop transfer function

$$G(j\omega) = \frac{10}{j\omega(j0.1\omega + 1)(j0.05\omega + 1)}$$

The db- $\angle G(j\omega)$ plot for this $G(j\omega)$ is shown in Fig. 9.38. (It is important to note that this plot is conveniently drawn by obtaining the log-magnitude and phase angle data for various values of frequency from the Bode plot of $G(j\omega)$ shown in Fig. 9.27). From Fig. 9.39, it is found that

$$GM = +12 \text{ db}; PM = +33^\circ$$

Gain adjustment for desired GM or PM. Suppose it is desired to find the open-loop gain for (i) a GM of 20 db, (ii) a PM of 24° .

(i) A GM of 20 db is obtained if the plot of Fig. 9.38 is shifted downwards by $(20 - 12) = 8$ db. The system gain is therefore changed by -8 db or decreased by a factor of 2.5.

(ii) A PM of 24° is obtained if the plot of Fig. 9.38 is raised upwards by 3.5 db or the system gain is increased by a factor of 1.5.

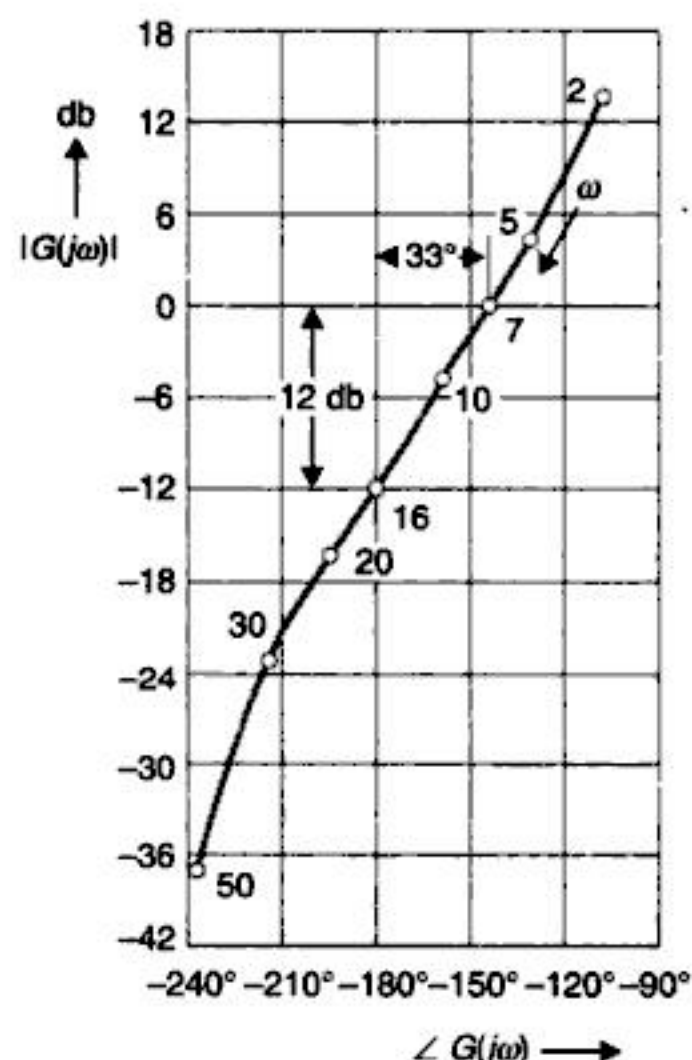


Fig. 9.38. Determination of GM and PM.



You have either reached a page that is unavailable for viewing or reached your viewing limit for this book.



You have either reached a page that is unavailable for viewing or reached your viewing limit for this book.



You have either reached a page that is unavailable for viewing or reached your viewing limit for this book.



You have either reached a page that is unavailable for viewing or reached your viewing limit for this book.



You have either reached a page that is unavailable for viewing or reached your viewing limit for this book.



You have either reached a page that is unavailable for viewing or reached your viewing limit for this book.



You have either reached a page that is unavailable for viewing or reached your viewing limit for this book.



You have either reached a page that is unavailable for viewing or reached your viewing limit for this book.



You have either reached a page that is unavailable for viewing or reached your viewing limit for this book.



You have either reached a page that is unavailable for viewing or reached your viewing limit for this book.



You have either reached a page that is unavailable for viewing or reached your viewing limit for this book.

A Design Example

Consider the system of Fig. 10.2 which has an open-loop transfer function

$$G(s) = \frac{5K_A}{s(s/2 + 1)(s/6 + 1)} \quad \dots(10.1)$$

From eqn. (10.1), K_v the velocity error constant of the system is given by

$$K_v = \lim_{s \rightarrow 0} sG(s) = 5K_A \quad \dots(10.2)$$

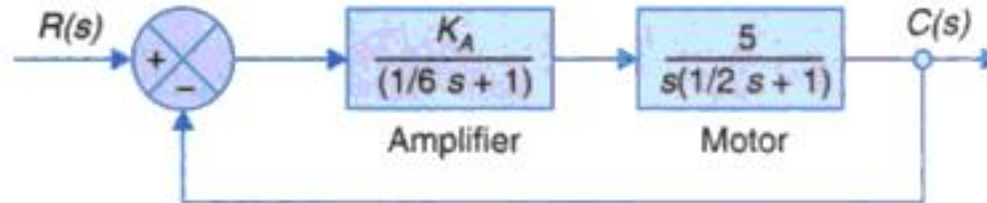


Fig. 10.2. A position control system.

For $K_A = 1$ (i.e., $K_v = 5$) the steady-state error to unit velocity input ($e_{ss} = 1/K_v$) is 0.2, which may be assumed to be an acceptable value.

From eqn. (10.1), we have

$$G(s) = \frac{60K_A}{s(s+2)(s+6)} = \frac{K}{s(s+2)(s+6)} \quad \dots(10.3)$$

The root locus plot of the uncompensated system appears in Fig. 10.3. Corresponding to the value $K = 60$ (i.e., $K_v = 5$) on the root locus plot, the dominant pair of root is found to be

$$s_{1,2} = -0.3 \pm j2.8$$

For this root pair, the damping ratio ζ is 0.105 and the undamped natural frequency ω_n is 2.85. The settling time ($= 4/\zeta\omega_n$) for the response is therefore about 13.36 sec.

From the above investigation of the uncompensated system, it is seen that the system has poor relative stability and large settling time.

Assume that the specifications on the transient performance are

$$\zeta = 0.6 ;$$

$$\text{settling time} < 4 \text{ sec.}$$

A line corresponding to $\zeta = 0.6$ is shown in Fig. 10.3. The intersection of this line with root locus branch determines the value of K which yields the specified ζ . From Fig. 10.3 we find that

$$K = 10.5 [K_v = 10.5/(2 \times 6) = 0.875, \text{ i.e., } K_A = 0.175];$$

$$\omega_n = 1.26 ;$$

$$\text{Settling time} = 5.3 \text{ sec;}$$

$$e_{ss} = 1.14.$$

Thus the reduction in gain satisfies the specification on ζ but the steady state error increases well beyond the tolerable of 0.2 and further the settling time specification is not fully satisfied. Therefore we conclude that our purpose is not served by mere given adjustment.



You have either reached a page that is unavailable for viewing or reached your viewing limit for this book.



You have either reached a page that is unavailable for viewing or reached your viewing limit for this book.



You have either reached a page that is unavailable for viewing or reached your viewing limit for this book.



You have either reached a page that is unavailable for viewing or reached your viewing limit for this book.



You have either reached a page that is unavailable for viewing or reached your viewing limit for this book.

in passing through the network whereby the signal to noise ratio is improved, in contrast to the lead network. A typical choice of β is 10.

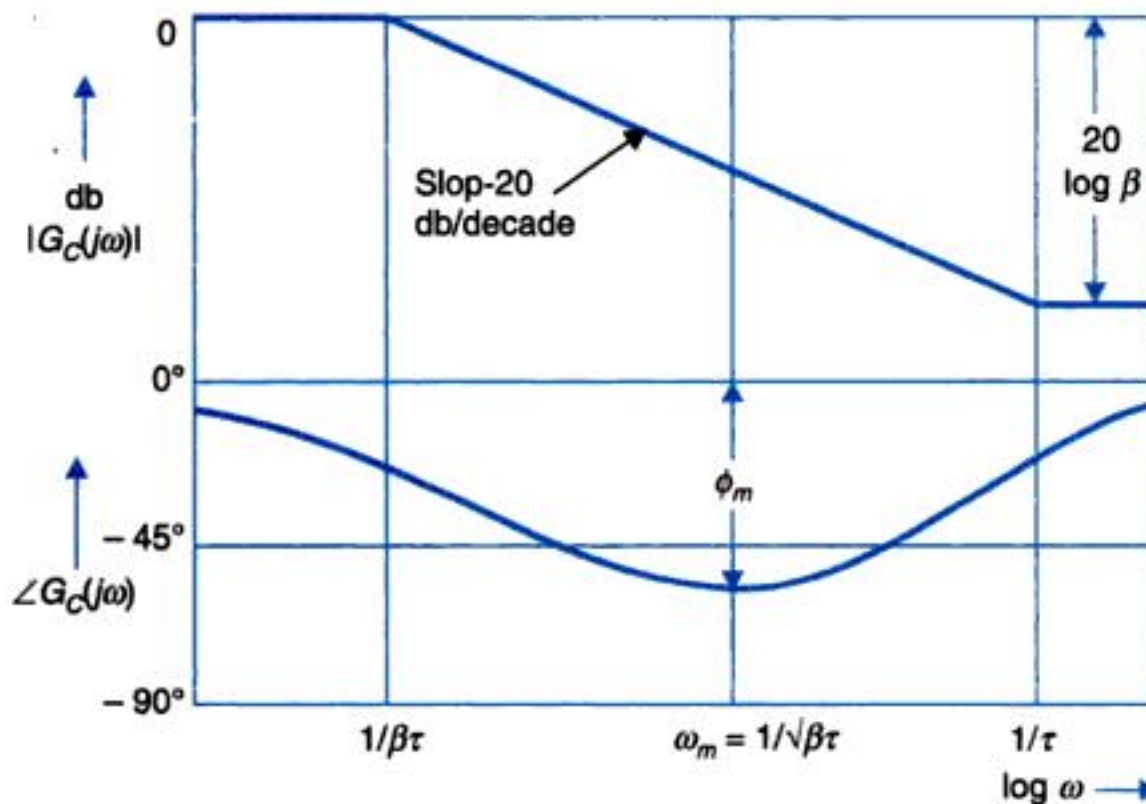


Fig. 10.14. Bode plot of phase-lag network.

Lag-lead Compensator*

As discussed earlier, the lag-lead compensator is a combination of a lag compensator and a lead compensator. The lag-section has one real pole and one real zero with the pole to the right of zero. The lead-section also has one real pole and one real zero but the zero is to the right of the pole. The general form of this compensator is

$$G_c(s) = \underbrace{\left(\frac{s + 1/\tau_1}{s + 1/\beta\tau_1} \right)}_{\text{Lag section}} \underbrace{\left(\frac{s + 1/\tau_2}{s + 1/\alpha\tau_2} \right)}_{\text{Lead section}}; \beta > 1, \alpha < 1 \quad \dots(10.21)$$

The eqn. (10.21) can be realized by a single electric lag-lead network shown in Fig. 10.15. From this figure, the transfer function of the network is given by

$$\begin{aligned} \frac{E_o(s)}{E_i(s)} &= \left[\frac{R_2 + 1/sC_2}{R_2 + \frac{1}{sC_2} + \frac{R_1/sC_1}{R_1 + 1/sC_1}} \right] \\ &= \left[\frac{\left(s + \frac{1}{R_1C_1} \right) \left(s + \frac{1}{R_2C_2} \right)}{s^2 + \left(\frac{1}{R_1C_1} + \frac{1}{R_2C_1} + \frac{1}{R_2C_2} \right) s + \frac{1}{R_1R_2C_1C_2}} \right] \quad \dots(10.22) \end{aligned}$$

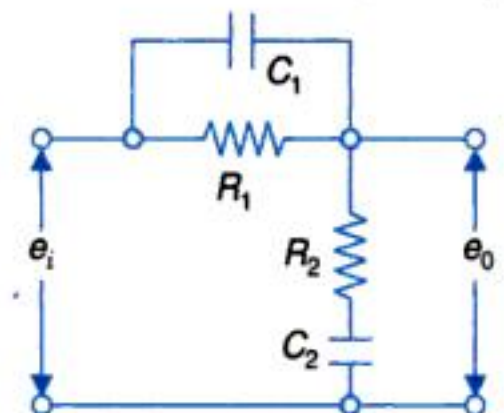


Fig. 10.15. Electric lag-lead network.

*When the forward path transfer function has complex poles close to the $j\omega$ -axis, phase lead, phase-lag or phase lag-lead networks are not effective. In such cases compensation may be achieved by Bridged- T networks.



You have either reached a page that is unavailable for viewing or reached your viewing limit for this book.



You have either reached a page that is unavailable for viewing or reached your viewing limit for this book.



You have either reached a page that is unavailable for viewing or reached your viewing limit for this book.

compensation wherein the compensating zero is placed exactly in the open-loop pole location completely cancelling the effect of this pole. In case the uncompensated system does not have any open-loop pole in the region below desired closed-loop poles, the dominance condition must be checked by locating the real axis closed-loop pole created by the compensating zero.

Example 10.2: A type-2 system with an open-loop transfer function

$$G_f(s) = \frac{K}{s^2(s+15)}$$

is to be compensated to meet the specifications in Example 10.1.

Following the procedure of the previous example, the desired dominant roots are found to lie at $s_d = -1 \pm j2$ (Fig. 10.22). The angle contribution required from a lead compensator is

$$\phi = \pm 180^\circ - \angle G_f(s_d) = \pm 180^\circ - (-2 \times 117^\circ - 75^\circ) = 129^\circ$$

The large value of ϕ here is an indication that a double lead network is appropriate. Each section of a double lead network has then to contribute an angle of 64.5° at s_d .

Let us locate the compensator zero at $s = -1.7$, i.e., in the region below the desired dominant closed-loop pole location and just to the left of the open-loop pole at $s = -1.5$. Join the compensator zero to s_d and locate the compensator pole by making an angle $\phi = 64.5^\circ$ as shown in Fig. 10.22. The location of the pole is found to be at -19.8 .

The open-loop transfer function of the compensated system becomes

$$G(s) = \frac{8.30(s+17)^2}{s^2(s+15)(s+19.8)^2}$$

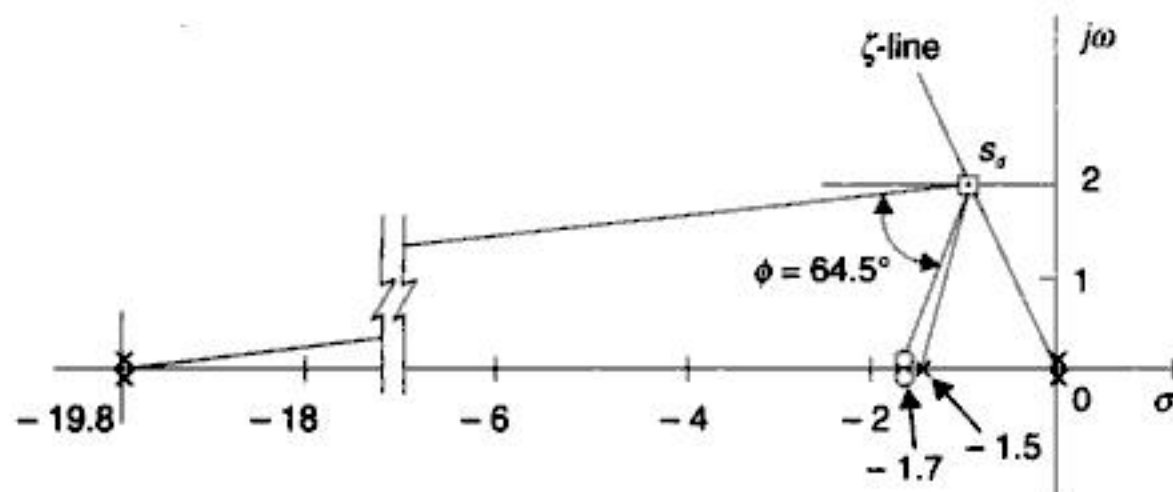


Fig. 10.22. Design of double lead compensator.

By locating the closed-loop poles of the compensated system, it can be easily verified that one closed-loop pole is located very close to the open-loop zero at -1.7 (contributed by the compensating zero) and therefore makes negligible contribution to system dynamics, while the other closed-loop poles are located far to the left of -1 and hence the dominance of the desired closed-loop poles ($-1 \pm j2$) is preserved.

Example 10.3: Consider a type-1 system with an open-loop transfer function of

$$G_f(s) = \frac{K}{s(s+1)(s+4)}$$



You have either reached a page that is unavailable for viewing or reached your viewing limit for this book.



You have either reached a page that is unavailable for viewing or reached your viewing limit for this book.



You have either reached a page that is unavailable for viewing or reached your viewing limit for this book.

This additional integration reduces the steady state error; type -0 steady state step input error is reduced to zero and ramp input error is limited to a finite value ; type-1 ramp input error is also reduced to zero.

PI controller design proceeds conveniently by root locus technique. All the poles (including additional pole at $s = 0$) of $G'(s)$ are located on the s -plane. The transient response specifications lead to the location of s_d , the desired root location. The compensating zero $s = -\alpha$ is located so that the angle criterion at s_d is met. The root locus gain can then be computed at s_d but this does not affect the steady-state error.

The zero of PI controller appears in the closed-loop transfer function which impairs the transient response which was computed on dominant pole pair basis ; see Section 5.6. This problem is more intense in PI controller than in lead network compensation.

Prefilter

To cancel out the closed-loop zero a prefilter

$$G_p(s) = \frac{1}{s + \alpha}$$

is introduced as shown in Fig. 10.26 of the complete compensated system

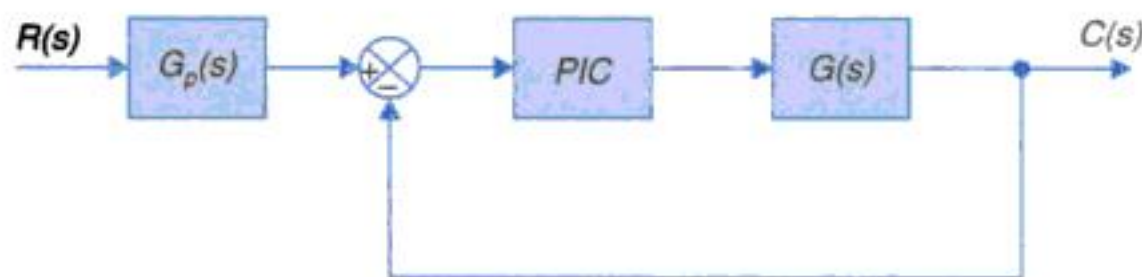


Fig. 10.26. PI compensated system.

The procedure enunciated above is illustrated below through two examples.

Example 10.5: A unity negative feedback system has an open-loop transfer function of

$$G(s) = \frac{K}{(s + 4)}$$

Consider a cascade compensator

$$G_c(s) = \frac{s + \alpha}{s}$$

(a) Select the values of K and α to achieve

(i) Peak overshoot of about 20%.

and (ii) Settling time (2% basis) ≈ 1 sec

(b) For the values of K and α found in part (a) calculate the unit ramp input steady-state error.

Solution. In this simple example we can proceed analytically. Compensated forward path transfer function is

$$G_c(s) G(s) = \frac{K(s + \alpha)}{s(s + 4)} \quad \dots(i)$$



You have either reached a page that is unavailable for viewing or reached your viewing limit for this book.



You have either reached a page that is unavailable for viewing or reached your viewing limit for this book.



You have either reached a page that is unavailable for viewing or reached your viewing limit for this book.



You have either reached a page that is unavailable for viewing or reached your viewing limit for this book.



You have either reached a page that is unavailable for viewing or reached your viewing limit for this book.



You have either reached a page that is unavailable for viewing or reached your viewing limit for this book.



You have either reached a page that is unavailable for viewing or reached your viewing limit for this book.



You have either reached a page that is unavailable for viewing or reached your viewing limit for this book.



You have either reached a page that is unavailable for viewing or reached your viewing limit for this book.



You have either reached a page that is unavailable for viewing or reached your viewing limit for this book.



You have either reached a page that is unavailable for viewing or reached your viewing limit for this book.



You have either reached a page that is unavailable for viewing or reached your viewing limit for this book.



You have either reached a page that is unavailable for viewing or reached your viewing limit for this book.



You have either reached a page that is unavailable for viewing or reached your viewing limit for this book.



You have either reached a page that is unavailable for viewing or reached your viewing limit for this book.



You have either reached a page that is unavailable for viewing or reached your viewing limit for this book.



You have either reached a page that is unavailable for viewing or reached your viewing limit for this book.



You have either reached a page that is unavailable for viewing or reached your viewing limit for this book.



You have either reached a page that is unavailable for viewing or reached your viewing limit for this book.



You have either reached a page that is unavailable for viewing or reached your viewing limit for this book.



You have either reached a page that is unavailable for viewing or reached your viewing limit for this book.



You have either reached a page that is unavailable for viewing or reached your viewing limit for this book.



You have either reached a page that is unavailable for viewing or reached your viewing limit for this book.



You have either reached a page that is unavailable for viewing or reached your viewing limit for this book.



You have either reached a page that is unavailable for viewing or reached your viewing limit for this book.



You have either reached a page that is unavailable for viewing or reached your viewing limit for this book.



You have either reached a page that is unavailable for viewing or reached your viewing limit for this book.



You have either reached a page that is unavailable for viewing or reached your viewing limit for this book.



You have either reached a page that is unavailable for viewing or reached your viewing limit for this book.



You have either reached a page that is unavailable for viewing or reached your viewing limit for this book.



You have either reached a page that is unavailable for viewing or reached your viewing limit for this book.



You have either reached a page that is unavailable for viewing or reached your viewing limit for this book.



You have either reached a page that is unavailable for viewing or reached your viewing limit for this book.



You have either reached a page that is unavailable for viewing or reached your viewing limit for this book.



You have either reached a page that is unavailable for viewing or reached your viewing limit for this book.



You have either reached a page that is unavailable for viewing or reached your viewing limit for this book.



You have either reached a page that is unavailable for viewing or reached your viewing limit for this book.



You have either reached a page that is unavailable for viewing or reached your viewing limit for this book.



You have either reached a page that is unavailable for viewing or reached your viewing limit for this book.



You have either reached a page that is unavailable for viewing or reached your viewing limit for this book.



You have either reached a page that is unavailable for viewing or reached your viewing limit for this book.



You have either reached a page that is unavailable for viewing or reached your viewing limit for this book.



You have either reached a page that is unavailable for viewing or reached your viewing limit for this book.



You have either reached a page that is unavailable for viewing or reached your viewing limit for this book.



You have either reached a page that is unavailable for viewing or reached your viewing limit for this book.



You have either reached a page that is unavailable for viewing or reached your viewing limit for this book.



You have either reached a page that is unavailable for viewing or reached your viewing limit for this book.



You have either reached a page that is unavailable for viewing or reached your viewing limit for this book.



You have either reached a page that is unavailable for viewing or reached your viewing limit for this book.



You have either reached a page that is unavailable for viewing or reached your viewing limit for this book.



You have either reached a page that is unavailable for viewing or reached your viewing limit for this book.



You have either reached a page that is unavailable for viewing or reached your viewing limit for this book.



You have either reached a page that is unavailable for viewing or reached your viewing limit for this book.



You have either reached a page that is unavailable for viewing or reached your viewing limit for this book.



You have either reached a page that is unavailable for viewing or reached your viewing limit for this book.



You have either reached a page that is unavailable for viewing or reached your viewing limit for this book.



You have either reached a page that is unavailable for viewing or reached your viewing limit for this book.



You have either reached a page that is unavailable for viewing or reached your viewing limit for this book.



You have either reached a page that is unavailable for viewing or reached your viewing limit for this book.



You have either reached a page that is unavailable for viewing or reached your viewing limit for this book.



You have either reached a page that is unavailable for viewing or reached your viewing limit for this book.



You have either reached a page that is unavailable for viewing or reached your viewing limit for this book.



You have either reached a page that is unavailable for viewing or reached your viewing limit for this book.



You have either reached a page that is unavailable for viewing or reached your viewing limit for this book.



You have either reached a page that is unavailable for viewing or reached your viewing limit for this book.



You have either reached a page that is unavailable for viewing or reached your viewing limit for this book.



You have either reached a page that is unavailable for viewing or reached your viewing limit for this book.



You have either reached a page that is unavailable for viewing or reached your viewing limit for this book.



You have either reached a page that is unavailable for viewing or reached your viewing limit for this book.



You have either reached a page that is unavailable for viewing or reached your viewing limit for this book.



You have either reached a page that is unavailable for viewing or reached your viewing limit for this book.



You have either reached a page that is unavailable for viewing or reached your viewing limit for this book.



You have either reached a page that is unavailable for viewing or reached your viewing limit for this book.



You have either reached a page that is unavailable for viewing or reached your viewing limit for this book.



You have either reached a page that is unavailable for viewing or reached your viewing limit for this book.



You have either reached a page that is unavailable for viewing or reached your viewing limit for this book.



You have either reached a page that is unavailable for viewing or reached your viewing limit for this book.



You have either reached a page that is unavailable for viewing or reached your viewing limit for this book.



You have either reached a page that is unavailable for viewing or reached your viewing limit for this book.



You have either reached a page that is unavailable for viewing or reached your viewing limit for this book.



You have either reached a page that is unavailable for viewing or reached your viewing limit for this book.



You have either reached a page that is unavailable for viewing or reached your viewing limit for this book.



You have either reached a page that is unavailable for viewing or reached your viewing limit for this book.



You have either reached a page that is unavailable for viewing or reached your viewing limit for this book.



You have either reached a page that is unavailable for viewing or reached your viewing limit for this book.



You have either reached a page that is unavailable for viewing or reached your viewing limit for this book.



You have either reached a page that is unavailable for viewing or reached your viewing limit for this book.



You have either reached a page that is unavailable for viewing or reached your viewing limit for this book.



You have either reached a page that is unavailable for viewing or reached your viewing limit for this book.



You have either reached a page that is unavailable for viewing or reached your viewing limit for this book.



You have either reached a page that is unavailable for viewing or reached your viewing limit for this book.



You have either reached a page that is unavailable for viewing or reached your viewing limit for this book.



You have either reached a page that is unavailable for viewing or reached your viewing limit for this book.



You have either reached a page that is unavailable for viewing or reached your viewing limit for this book.



You have either reached a page that is unavailable for viewing or reached your viewing limit for this book.



You have either reached a page that is unavailable for viewing or reached your viewing limit for this book.



You have either reached a page that is unavailable for viewing or reached your viewing limit for this book.



You have either reached a page that is unavailable for viewing or reached your viewing limit for this book.



You have either reached a page that is unavailable for viewing or reached your viewing limit for this book.



You have either reached a page that is unavailable for viewing or reached your viewing limit for this book.



You have either reached a page that is unavailable for viewing or reached your viewing limit for this book.



You have either reached a page that is unavailable for viewing or reached your viewing limit for this book.



You have either reached a page that is unavailable for viewing or reached your viewing limit for this book.



You have either reached a page that is unavailable for viewing or reached your viewing limit for this book.



You have either reached a page that is unavailable for viewing or reached your viewing limit for this book.



You have either reached a page that is unavailable for viewing or reached your viewing limit for this book.



You have either reached a page that is unavailable for viewing or reached your viewing limit for this book.

Then

$$\mathbf{AB} = \begin{bmatrix} 0 & 1 \\ -1 & -2 \end{bmatrix} \begin{bmatrix} 1 \\ -1 \end{bmatrix} = \begin{bmatrix} -1 \\ 1 \end{bmatrix}$$

The composite matrix defined in eqn. (12.90) is given by

$$\mathbf{Q}_c = [\mathbf{B} : \mathbf{AB}] = \begin{bmatrix} 1 & -1 \\ -1 & 1 \end{bmatrix}$$

The rank of r of this matrix is 1. The system is therefore not completely controllable. One state of the system is uncontrollable (r out of n states are controllable).

By the methods discussed in Section 12.3, the given differential equation can be transformed to the following controllable phase variable model:

$$\begin{bmatrix} \dot{x}_1 \\ \dot{x}_2 \end{bmatrix} = \begin{bmatrix} 0 & -1 \\ -1 & 2 \end{bmatrix} \begin{bmatrix} x_1 \\ x_2 \end{bmatrix} + \begin{bmatrix} 0 \\ 1 \end{bmatrix} u$$

$$y = [1 \quad 1] \begin{bmatrix} x_1 \\ x_2 \end{bmatrix}$$

Thus state controllability depends on how the state variables are defined for a given system.

Observability

Consider the state model of an n th order single-output linear time-invariant system,

$$\begin{aligned} \dot{\mathbf{x}} &= \mathbf{Ax} + \mathbf{Bu} \\ y &= \mathbf{Cx} \end{aligned}$$

The state equation may be transformed to the canonical form by the linear transformation $\mathbf{x} = \mathbf{Mv}$. The resulting state and output equations are

$$\dot{\mathbf{v}} = \mathbf{Av} + \tilde{\mathbf{B}}u \quad \dots(12.95a)$$

$$\begin{aligned} y &= \tilde{\mathbf{C}}\mathbf{v} \\ &= \tilde{c}_1 v_1 + \tilde{c}_2 v_2 + \dots + \tilde{c}_n v_n \end{aligned} \quad \dots(12.95b)$$

Since diagonalization decouples the states, no state now contains any information regarding any other state, *i.e.*, each state must be independently observable. It therefore follows that for a state to be observed through the output y , its corresponding coefficient in eqn. (12.95b) should be nonzero.

If any particular \tilde{c}_i is zero, the corresponding v_i can have any value without its effect showing up in the output y . Thus the necessary (it is also sufficient) condition for complete state observability is that none of the \tilde{c}_i 's (*i.e.*, none of the elements of $\tilde{\mathbf{C}} = \mathbf{CM}$) should be zero.

The result may be extended to the case of multi-input-multi-output systems where the output vector, after canonical transformation is given by

$$\begin{bmatrix} y_1 \\ y_2 \\ \vdots \\ y_p \end{bmatrix} = \begin{bmatrix} \tilde{c}_{11} & \tilde{c}_{12} & \cdots & \tilde{c}_{1n} \\ \tilde{c}_{21} & \tilde{c}_{22} & \cdots & \tilde{c}_{2n} \\ \vdots & \vdots & \ddots & \vdots \\ \tilde{c}_{p1} & \tilde{c}_{p2} & \cdots & \tilde{c}_{pn} \end{bmatrix} \begin{bmatrix} v_1 \\ v_2 \\ \vdots \\ v_n \end{bmatrix}$$



You have either reached a page that is unavailable for viewing or reached your viewing limit for this book.



You have either reached a page that is unavailable for viewing or reached your viewing limit for this book.



You have either reached a page that is unavailable for viewing or reached your viewing limit for this book.



You have either reached a page that is unavailable for viewing or reached your viewing limit for this book.



You have either reached a page that is unavailable for viewing or reached your viewing limit for this book.



You have either reached a page that is unavailable for viewing or reached your viewing limit for this book.



You have either reached a page that is unavailable for viewing or reached your viewing limit for this book.



You have either reached a page that is unavailable for viewing or reached your viewing limit for this book.



You have either reached a page that is unavailable for viewing or reached your viewing limit for this book.



You have either reached a page that is unavailable for viewing or reached your viewing limit for this book.



You have either reached a page that is unavailable for viewing or reached your viewing limit for this book.



You have either reached a page that is unavailable for viewing or reached your viewing limit for this book.



You have either reached a page that is unavailable for viewing or reached your viewing limit for this book.



You have either reached a page that is unavailable for viewing or reached your viewing limit for this book.



You have either reached a page that is unavailable for viewing or reached your viewing limit for this book.



You have either reached a page that is unavailable for viewing or reached your viewing limit for this book.

so that

$$a_{11}g(x_1) > 0$$

$$a_{11} = \frac{a_{22}}{3} g(x_1) \quad \dots(vii)$$

$$a_{22} > 0$$

The first of these conditions is satisfied when the other two are met with, because

$$\frac{a_{22}}{3} g^2(x_1) > 0$$

We can therefore choose a_{22} to be any positive constant.

Thus

$$\nabla V = \begin{bmatrix} \frac{1}{3} a_{22} g(x_1) x_1 \\ a_{22} x_2 \end{bmatrix} \quad \dots(viii)$$

$$\dot{V} = -\frac{1}{3} a_{22} x_1^2 g^2(x_1) - a_{22} x_2^2$$

It may also be noticed that the gradient vector in (viii) meets the curl conditions (13.19).

The Liapunov function can now be obtained by taking the line integral of the gradient vector along the path defined in eqn. (13.17). Thus

$$\begin{aligned} V &= \frac{1}{3} a_{22} \int_0^{x_1} g(x_1) x_1 dx_1 + a_{22} \int_0^{x_2} x_2 dx \\ &= \frac{1}{3} a_{22} \int_0^{x_1} g(x_1) x_1 dx_1 + \frac{1}{2} a_{22} x_2^2 \quad \dots(x) \end{aligned}$$

If $g(x_1) > 0$, i.e. $f(x_1) = g(x_1)x_1$ lies in first and third quadrants, V is positive definite. Under this condition the system is asymptotically stable.

Also if

$$\lim_{x_1 \rightarrow \infty} \int_0^{x_1} g(x_1) x_1 dx_1 \rightarrow \infty$$

the system would be asymptotically stable in-the-large.

Example 13.6: A simple mass, spring and viscous friction system is shown in Fig. 13.9.

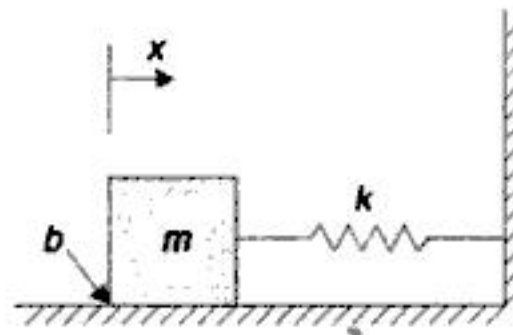


Fig. 13.9

Show that the system is stable.

Solution:

The differential equation governing the system is

$$m\ddot{x} + b\dot{x} + kx = 0$$



You have either reached a page that is unavailable for viewing or reached your viewing limit for this book.



You have either reached a page that is unavailable for viewing or reached your viewing limit for this book.



You have either reached a page that is unavailable for viewing or reached your viewing limit for this book.



You have either reached a page that is unavailable for viewing or reached your viewing limit for this book.



You have either reached a page that is unavailable for viewing or reached your viewing limit for this book.



You have either reached a page that is unavailable for viewing or reached your viewing limit for this book.



You have either reached a page that is unavailable for viewing or reached your viewing limit for this book.



You have either reached a page that is unavailable for viewing or reached your viewing limit for this book.



You have either reached a page that is unavailable for viewing or reached your viewing limit for this book.



You have either reached a page that is unavailable for viewing or reached your viewing limit for this book.



You have either reached a page that is unavailable for viewing or reached your viewing limit for this book.



You have either reached a page that is unavailable for viewing or reached your viewing limit for this book.



You have either reached a page that is unavailable for viewing or reached your viewing limit for this book.



You have either reached a page that is unavailable for viewing or reached your viewing limit for this book.



You have either reached a page that is unavailable for viewing or reached your viewing limit for this book.



You have either reached a page that is unavailable for viewing or reached your viewing limit for this book.



You have either reached a page that is unavailable for viewing or reached your viewing limit for this book.



You have either reached a page that is unavailable for viewing or reached your viewing limit for this book.



You have either reached a page that is unavailable for viewing or reached your viewing limit for this book.



You have either reached a page that is unavailable for viewing or reached your viewing limit for this book.



You have either reached a page that is unavailable for viewing or reached your viewing limit for this book.



You have either reached a page that is unavailable for viewing or reached your viewing limit for this book.



You have either reached a page that is unavailable for viewing or reached your viewing limit for this book.



You have either reached a page that is unavailable for viewing or reached your viewing limit for this book.



You have either reached a page that is unavailable for viewing or reached your viewing limit for this book.



You have either reached a page that is unavailable for viewing or reached your viewing limit for this book.



You have either reached a page that is unavailable for viewing or reached your viewing limit for this book.



You have either reached a page that is unavailable for viewing or reached your viewing limit for this book.



You have either reached a page that is unavailable for viewing or reached your viewing limit for this book.



You have either reached a page that is unavailable for viewing or reached your viewing limit for this book.



You have either reached a page that is unavailable for viewing or reached your viewing limit for this book.



You have either reached a page that is unavailable for viewing or reached your viewing limit for this book.



You have either reached a page that is unavailable for viewing or reached your viewing limit for this book.



You have either reached a page that is unavailable for viewing or reached your viewing limit for this book.



You have either reached a page that is unavailable for viewing or reached your viewing limit for this book.



You have either reached a page that is unavailable for viewing or reached your viewing limit for this book.



You have either reached a page that is unavailable for viewing or reached your viewing limit for this book.



You have either reached a page that is unavailable for viewing or reached your viewing limit for this book.



You have either reached a page that is unavailable for viewing or reached your viewing limit for this book.



You have either reached a page that is unavailable for viewing or reached your viewing limit for this book.



You have either reached a page that is unavailable for viewing or reached your viewing limit for this book.



You have either reached a page that is unavailable for viewing or reached your viewing limit for this book.



You have either reached a page that is unavailable for viewing or reached your viewing limit for this book.



You have either reached a page that is unavailable for viewing or reached your viewing limit for this book.



You have either reached a page that is unavailable for viewing or reached your viewing limit for this book.



You have either reached a page that is unavailable for viewing or reached your viewing limit for this book.

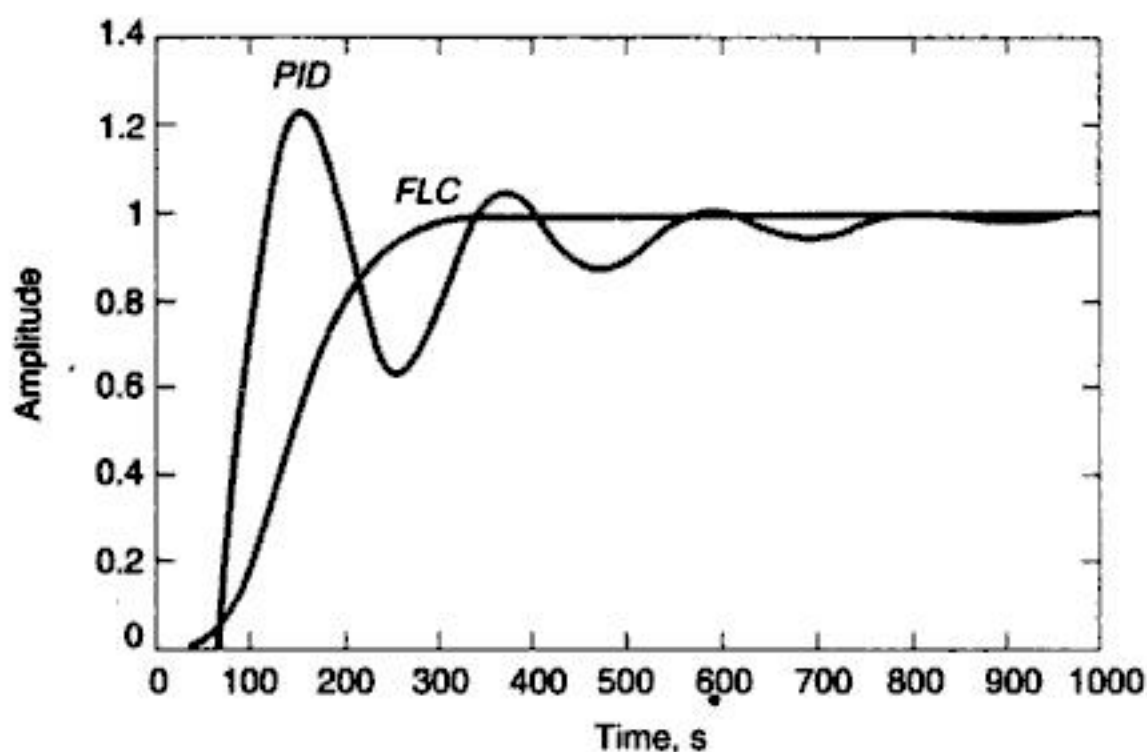


Fig. 15.25. Step input response : *FLC Vs PID*.

15.4 NEURAL NETWORKS

Artificial neural networks have emerged from the studies of how brain performs. The human brain is made up of many millions of individual processing elements, called *neurons*, that are highly interconnected. A schematic diagram of a single biological neuron is shown in Fig. 15.26. Information from the outputs of the other neurons, in the form of electrical pulses, are received by the cell at connections called *synapses*. The synapses connect to the cell inputs, or *space dendrites*, and the single output of the neuron appears at the *axon*. An electrical pulse is sent down the axon when the total input stimuli from all of the dendrites exceeds a certain threshold.

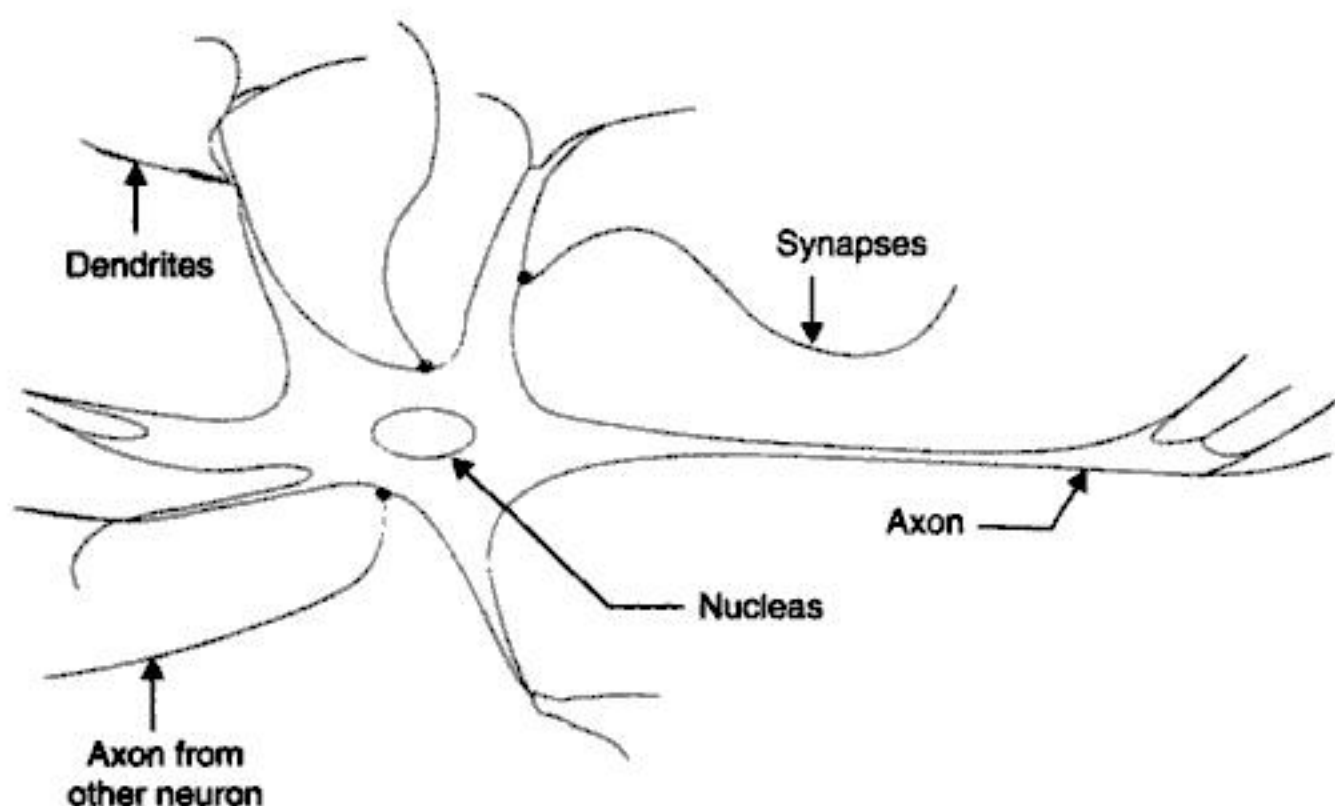


Fig. 15.26. A biological neuron.



You have either reached a page that is unavailable for viewing or reached your viewing limit for this book.



You have either reached a page that is unavailable for viewing or reached your viewing limit for this book.



You have either reached a page that is unavailable for viewing or reached your viewing limit for this book.



You have either reached a page that is unavailable for viewing or reached your viewing limit for this book.



You have either reached a page that is unavailable for viewing or reached your viewing limit for this book.



You have either reached a page that is unavailable for viewing or reached your viewing limit for this book.



You have either reached a page that is unavailable for viewing or reached your viewing limit for this book.



You have either reached a page that is unavailable for viewing or reached your viewing limit for this book.



You have either reached a page that is unavailable for viewing or reached your viewing limit for this book.



You have either reached a page that is unavailable for viewing or reached your viewing limit for this book.



You have either reached a page that is unavailable for viewing or reached your viewing limit for this book.



You have either reached a page that is unavailable for viewing or reached your viewing limit for this book.



You have either reached a page that is unavailable for viewing or reached your viewing limit for this book.



You have either reached a page that is unavailable for viewing or reached your viewing limit for this book.



You have either reached a page that is unavailable for viewing or reached your viewing limit for this book.



You have either reached a page that is unavailable for viewing or reached your viewing limit for this book.



You have either reached a page that is unavailable for viewing or reached your viewing limit for this book.



You have either reached a page that is unavailable for viewing or reached your viewing limit for this book.



You have either reached a page that is unavailable for viewing or reached your viewing limit for this book.



You have either reached a page that is unavailable for viewing or reached your viewing limit for this book.



You have either reached a page that is unavailable for viewing or reached your viewing limit for this book.



You have either reached a page that is unavailable for viewing or reached your viewing limit for this book.



You have either reached a page that is unavailable for viewing or reached your viewing limit for this book.



You have either reached a page that is unavailable for viewing or reached your viewing limit for this book.



You have either reached a page that is unavailable for viewing or reached your viewing limit for this book.



You have either reached a page that is unavailable for viewing or reached your viewing limit for this book.



You have either reached a page that is unavailable for viewing or reached your viewing limit for this book.



You have either reached a page that is unavailable for viewing or reached your viewing limit for this book.



You have either reached a page that is unavailable for viewing or reached your viewing limit for this book.



You have either reached a page that is unavailable for viewing or reached your viewing limit for this book.



You have either reached a page that is unavailable for viewing or reached your viewing limit for this book.



You have either reached a page that is unavailable for viewing or reached your viewing limit for this book.



You have either reached a page that is unavailable for viewing or reached your viewing limit for this book.



You have either reached a page that is unavailable for viewing or reached your viewing limit for this book.



You have either reached a page that is unavailable for viewing or reached your viewing limit for this book.



You have either reached a page that is unavailable for viewing or reached your viewing limit for this book.



You have either reached a page that is unavailable for viewing or reached your viewing limit for this book.



You have either reached a page that is unavailable for viewing or reached your viewing limit for this book.



You have either reached a page that is unavailable for viewing or reached your viewing limit for this book.



You have either reached a page that is unavailable for viewing or reached your viewing limit for this book.



You have either reached a page that is unavailable for viewing or reached your viewing limit for this book.



You have either reached a page that is unavailable for viewing or reached your viewing limit for this book.



You have either reached a page that is unavailable for viewing or reached your viewing limit for this book.



You have either reached a page that is unavailable for viewing or reached your viewing limit for this book.



You have either reached a page that is unavailable for viewing or reached your viewing limit for this book.



You have either reached a page that is unavailable for viewing or reached your viewing limit for this book.



You have either reached a page that is unavailable for viewing or reached your viewing limit for this book.

INDEX

- Absolutely stable, [275](#)
- Ac position control system, [151](#)
- Ac servomotor, [138](#)
 - incremental transfer function, [141](#)
- Ac tachometer, [141](#)
- Accelerometer, mechanical, [28](#)
- Across variable, [24](#)
- Adaptive control, [715](#)
 - MIT rule, [717](#)
- Adding zero, effect of, [214](#)
- All-pass system function, [366](#)
- Analogous quantities, [42](#)
- Analogous systems, [35](#)
- Analogy, force (torque)-voltage, [36](#)
 - force (torque)-current, [36](#)
- Approximation of, higher-order systems by lower order, [248](#)
- Armature control, dc motor, [49](#)
- Artificial neuron model, [749](#)
- Asymptotic stability, [643](#)
 - in-the-large, [644](#)
 - in-the-small, [644](#)
- Automatic control system, [4](#)
 - history and development of, [7](#)
 - general block diagram, [5](#)
- Autonomous system, [642](#)

- Bellman's dynamic programming, [688-691, 694-696](#)
- Bandwidth, effect of feedback, [99](#)
- Bandwidth, [350, 351](#)
- Barbalat's Lemma, [721](#)
- Bilinear transformation, [553](#)

- Block diagram algebra, [54](#)
 - closed-loop, [55](#)
 - reduction rules, [58-59](#)
 - summing or differencing point, [54](#)
 - take-off point, [54](#)
- Block diagram, [24](#)
 - cause-effect form, [24](#)
- Bode plots, [355](#)
 - complex conjugate poles, [360](#)
 - corner frequency (break frequency), [357](#)
 - db error normalized, first-order-factor, [358](#)
 - db error normalized, second-order factor, [361](#)
 - decade, [357](#)
 - decibel, [356](#)
 - general construction procedure, [362](#)
 - octave, [357](#)
 - pole or zero on real axis, [360](#)
 - typical factors of $G(j\omega)$, [358](#)
- Break frequency, [357](#)
- Brushless dc motor, [136](#)
- Bush form or companion form, [587](#)

- Caley-Hamilton theorem, [611](#)
- Canonical state model, [592](#)
- Canonical variables, [599](#)
- Cascade compensation, frequency domain, [459](#)
 - lag, [466](#)
 - lag-lead, [470](#)
 - lead, [460](#)
 - translation of specifications, [459](#)
- Cascade compensation, time domain, [440](#)
 - cancellation, [444](#)



You have either reached a page that is unavailable for viewing or reached your viewing limit for this book.

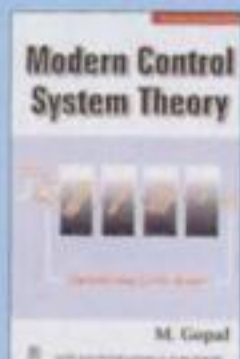


You have either reached a page that is unavailable for viewing or reached your viewing limit for this book.

Control Systems Engineering

FOURTH EDITION

IJ. NAGRATH • M. GOPAL



ISBN 81-224-0503-7
Rs. 220.00

Modern Control System Theory (M. Gopal)

The book covers mainly two areas of modern control theory, namely; system theory, and multivariable and optimal control. Practical control problems from various engineering disciplines have been drawn to illustrate the potential concepts. Most of the theoretical results have been presented in a manner suitable for digital computer programming along with necessary algorithms for numerical computations.



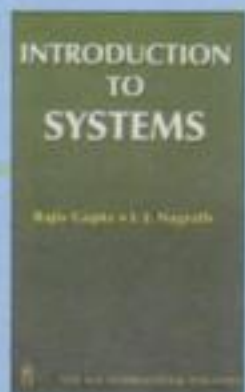
ISBN 0-85226-308-2
Rs. 220.00

Digital Control Engineering (M. Gopal)

The book presents control theory that is relevant to the analysis and design of Computer-Controlled Systems.

It also includes:

- Computer-aided-design package.
- Discusses basic characteristics of stepping motors and their associated drives.
- Three case studies on microprocessor-based control.



ISBN 81-224-1599-7
Rs. 250.00

Introduction to Systems. (Rajiv Gupta, I.J. Nagrath)

Designed for an introductory course encompassing a wide variety of systems-physical, nonphysical and combination there of.

The salient features of the book are:

- Stress throughout on systems approach and systems thinking
- Modeling of all types of systems, a commonality of approach
- Analytico-qualitative approach for social systems
- Coverage extended to man-machines systems, expert systems, MIS, e-commerce, systems reliability

ISBN 81-224-1775-2



9 788122 417753



PUBLISHING FOR ONE WORLD

NEW AGE INTERNATIONAL (P) LIMITED, PUBLISHERS

(formerly Wiley Eastern Ltd.)

New Delhi • Bangalore • Chennai • Cochin • Guwahati • Hyderabad
Jalandhar • Kolkata • Lucknow • Mumbai • Ranchi

Visit us at www.newagepublishers.com